



HAL
open science

Methodology to identify the key variables driving the techno-economic feasibility of Trigeneration – Thermal Storage systems

Mexitli Eva Sandoval Reyes

► **To cite this version:**

Mexitli Eva Sandoval Reyes. Methodology to identify the key variables driving the techno-economic feasibility of Trigeneration – Thermal Storage systems. Chemical and Process Engineering. Ecole nationale supérieure Mines-Télécom Atlantique; Instituto superior técnico (Lisbonne), 2020. English. NNT : 2020IMTA0182 . tel-03035014

HAL Id: tel-03035014

<https://theses.hal.science/tel-03035014>

Submitted on 2 Dec 2020

HAL is a multi-disciplinary open access archive for the deposit and dissemination of scientific research documents, whether they are published or not. The documents may come from teaching and research institutions in France or abroad, or from public or private research centers.

L'archive ouverte pluridisciplinaire **HAL**, est destinée au dépôt et à la diffusion de documents scientifiques de niveau recherche, publiés ou non, émanant des établissements d'enseignement et de recherche français ou étrangers, des laboratoires publics ou privés.

THESE DE DOCTORAT DE

L'ÉCOLE NATIONALE SUPÉRIEURE MINES-TÉLÉCOM
ATLANTIQUE BRETAGNE PAYS DE LA LOIRE - IMT ATLANTIQUE

ET INSTITUTO SUPERIOR TÉCNICO, LISBOA, PORTUGAL

ECOLE DOCTORALE N° 602
Sciences pour l'Ingénieur
Spécialité : Energétique, Thermique et Combustion

Par

Mexitli Eva SANDOVAL REYES

Methodology to identify the key variables driving the techno-economic feasibility of Trigenération – Thermal Storage systems

Thèse présentée et soutenue à Lisbonne, le 9 mars 2020

Unité de recherche : GEPEA UMR CNRS 6144

Thèse N° : 2020IMTA0182

Rapporteurs avant soutenance :

Patrícia Carla GAMA PINTO PEREIRA DA SILVA, Professeur adjoint Université de Coimbra
Luís Miguel PIRES NEVES, Professeur Coordinateur Institut Politechnique de Leiria

Composition du Jury :

Président : Paulo FERRÃO, Professeur IST, Université de Lisbonne
Examineurs : Massimo SANTARELLI, Professeur Politechnic de Turin
Patrícia Carla GAMA PINTO PEREIRA DA SILVA, Professeur adjoint Université de Coimbra
Luís Miguel PIRES NEVES, Professeur Coordinateur Institut Politechnique de Leiria

Directeurs de Thèse : Bruno LACARRIERE, Professeur IMT Atlantique
Co-encadrant de Thèse : Carlos SANTOS, Professeur IST, Université de Lisbonne

Invité(s)
Tania SOUSA, Professeur adjoint IST, Université de Lisbonne

*To my beloved family,
because they are and always will be my North Star.*

*To my brother Tenoch,
because he is still the most inspiring engineer I know.*

*To the reader,
because his/her time makes this work meaningful.*

*“The important thing is not to stop questioning.
Curiosity has its own reason for existence.
One cannot help but be in awe
when he contemplates the mysteries of eternity,
of life, of the marvelous structure of reality.
It is enough if one tries merely to comprehend
a little of this mystery each day.*

— Old Man's Advice to Youth: 'Never Lose a Holy Curiosity.'
LIFE Magazine (2 May 1955) p. 64”
— Albert Einstein

ACKNOWLEDGMENTS

I would like to express my deepest gratitude to my supervisors Dr. Bruno Lacarrière, and Dr. Carlos Silva (mentioned in alphabetical order), as well as Dr. Pierrick Haurant. Their guidance and their scientific rigor contributed greatly to this thesis, but especially to my professional and personal learnings. I was very lucky to share this path with the three of them. Their combined support is the perfect balance.

I would also like to acknowledge Dr. Miguel Heleno and Alan Valenzuela for their support during my stay in the Lawrence Berkeley National Laboratory, California, US.

I thank from the bottom of my heart to Tenoch Sandoval-Reyes, Monica Eskander, João Pires, and Aurora Villanueva for their academic collaboration. I have greatly enjoyed working with them and hopefully it will continue in the future.

I would like to extend my gratitude to Rui Pereira and João Patricio from the Project “Campus Sustentável”, as well as, Diana Neves, from the at the IST for their help to get the data used in this thesis.

In the personal sphere, I greatly thank the endless support and encouragement from my parents and siblings, from Richard, and from my friends Jorge, Erika, Liz, Vanessa, Max, Gabriel, Kai, Monica, Mina, Laura, Felix, Ian, Joana, André, Filip, Sandra, Maria, Helena, Marcelina, Andreia, Guillermo, Ângelo, Lumango, and Cristian. Life is much better with them.

Finally, I would like to acknowledge the Erasmus Mundus Joint Doctorate SELECT+ program Environomical Pathways for Sustainable Energy Services funded with support from the Education, Audiovisual, and Culture Executive Agency (EACEA) (Nr 2012-0034) of the European Commission. Also, the funding provided by the Fundação para a Ciência e a Tecnologia, Portugal [Project IN+ strategic, ID/EEA/50009/2013] is highly recognized. Moreover, I would like to acknowledge the InnoEnergy PhD School for providing financial support for an additional international education within the area of business management and innovation, as well as my stay in the Berkeley Lab.

This publication reflects the views only of the author(s), and the funders cannot be held responsible for any use, which may be made of the information contained therein.

INDEX

ACKNOWLEDGMENTS.....	v
INDEX	vii
LIST OF FIGURES.....	xi
LIST OF TABLES.....	xv
ACRONYMS	xvii
ABBREVIATIONS	xix
SYMBOLS AND NOMENCLATURE	xxi
RÉSUMÉ LONG (Français).....	xxv
LONG ABSTRACT (English).....	xxxi
1 INTRODUCTION.....	1
1.1 Context.....	1
1.2 Combined thermal and power energy systems	1
1.2.1 Cogeneration	2
1.2.2 Trigeneration	3
1.2.3 Trigeneration with Thermal Storage	3
1.3 Market framework	5
1.3.1 Size of the thermal sector.....	5
1.3.2 Current status of CHP market.....	7
1.3.3 Relevant sectors for combined thermal and power energy systems.....	8
1.3.4 Key success factors for combined thermal and power energy systems	12
1.3.5 Perspective for thermal storage.....	13
1.4 Motivation.....	14
1.5 Hypothesis and Research questions.....	16
1.6 Outline of the thesis	16
2 LITERATURE REVIEW.....	19
2.1 Combined thermal and power energy systems	19
2.2 Relevant variables for the feasibility analysis	21
2.2.1 Energy prices.....	23
2.2.2 Energy loads.....	25
2.3 Computational tools to simulate energy system	27
2.4 Modeling and optimization of combined thermal and power energy systems	30

2.4.1	Optimization algorithms for combined thermal and power energy systems.....	31
2.4.2	The general structure of the optimization model.....	33
2.4.3	PYOMO – CPLEX : a computational alternative.....	35
2.5	Sensitivity analysis.....	36
2.6	Position of the thesis.....	40
3	METHODOLOGY.....	43
3.1	General methodology.....	43
3.2	Phase I: Exploratory study of the CCHP-TS feasibility.....	44
3.2.1	Full factorial DoE.....	44
3.2.2	Modeling and optimization in DER-CAM.....	45
3.2.3	Data analysis.....	47
3.3	Phase II: Sensitivity analysis of the CCHP-TS feasibility.....	53
3.3.1	Modeling and optimization solutions adapted to SA implementation.....	53
3.3.2	Sensitivity analysis – theoretical background.....	56
3.3.3	Global sensitivity analysis methods.....	57
3.3.4	Sampling methods.....	66
3.3.5	Global sensitivity analysis vs. full factorial DoE.....	69
3.4	Case study: A university campus.....	71
4	PHASE I: Exploratory study of the CCHP-TS feasibility.....	75
4.1	Sampling of scenarios from the case study.....	76
4.2	Energy system optimization: DER-CAM.....	77
4.3	Data analysis: Clustering.....	84
4.4	Results interpretation.....	91
4.4.1	Analysis of generation means for each energy carrier.....	92
4.4.2	Analysis of the energy flows within the CCHP-TS system.....	95
4.4.3	Analysis of the percentage of savings.....	97
4.4.4	Summary of results.....	102
4.5	Hypothesis regarding the impact of energy prices.....	103
4.5.1	Problem statement.....	103
4.5.2	Creating a hypothesis.....	104
4.5.3	Testing the hypothesis.....	104
4.6	Conclusions of the section.....	108
5	PHASE II: Sensitivity analysis of the CCHP-TS feasibility.....	109
5.1	Introduction.....	109
5.2	Morris – Derivative based approach.....	110

5.3	VARS – Variogram based approach	117
5.4	Sobol – Variance based approach	123
5.5	General conclusion of the sensitivity analysis	127
5.6	Overall comparison of the three SA methods.....	129
5.7	Isolines of the variables.....	131
6	CONCLUSIONS AND FUTURE WORK.....	137
6.1	General conclusions.....	137
6.2	Conclusions from the methodology	141
6.3	Future work	142
	REFERENCES.....	145
	ANNEX I. Consolidated output data from DERCAM.....	165
	ANNEX II. Equation used in MATLAB to extract information from DER-CAM reports.....	173
	ANNEX III. Multi-criteria Decision Making ELECTRE 1S	183
	ANNEX IV. Adaptation of DER-CAM model into Python	187

LIST OF FIGURES

Figure 1 Méthodologie générale de cette thèse	xxvi
Figure 2 General methodology of this thesis	xxxii
Figure 3 Comparison of a trigeneration-thermal storage system vs. a conventional system, while meeting the annual loads $L_n \forall n=\{E: \text{electricity}, H:\text{heating}, C:\text{cooling}\}$.4	
Figure 4 Estimated European heat market in 2010 including residential and service sector (Adapted from Persson, 2015 [26]).....	5
Figure 5 Cooling demand total (top) and per capita (bottom) for selected countries in 2000 and 2017 (image adapted from [28])	6
Figure 6 CHP electricity generation [TWh] and CHP share in the gross electricity generation for European countries in 2017 [31]	7
Figure 7 Share of type of useful thermal energy (by temperature) for the industry of EU27 in 2009 [27]	8
Figure 8 Industrial sectors that require thermal energy in Peta-Joules [PJ] (by temperature) for EU27 in 2009 [27].....	9
Figure 9 Useful heat demand for Iron & steel, and non-metallic minerals (high temperature) and chemical (for low temperature). EU27 in 2009 [27]	10
Figure 10 Breakdown of useful energy demand for the service sector in EU-27 for 2009	11
Figure 11 Household energy use (by end use) around the world [27].....	11
Figure 12 Useful energy demand for the residential sector in EU-27 for 2009.....	12
Figure 13 Subtropical desert places (adapted from the Global Solar Atlas [40])	15
Figure 14 Household electricity price worldwide in 2016, by region (published by Statista Research Department [64])	24
Figure 15 Wholesale natural gas prices worldwide in 2018, by region (data from the International Gas Union [65])	24
Figure 16 European energy prices 2017 [66]	25
Figure 17 Electric energy demand depending on the dimension of the case study...26	
Figure 18 General methodology of this thesis	44
Figure 19 Difference of percentage of savings reported by DER-CAM and the Python-PYOMO-CPLEX tool for 30 scenarios.....	56
Figure 20 VARS is based on pairs of points at the response surface. Adapted from Razavi, 2016 [161]	64
Figure 21 Image taken from Razavi, 2016 [111]. At left, the profile of three different response surfaces $f_1(x)$, $f_2(x)$, and $f_3(x)$. At right, their respective directional variograms.	65
Figure 22 STAR-based sampling with $k=2$ independent variables and $r=2$ STAR-centers [111]	66

Figure 23 (a) Optimal LHS with low correlated factors and optimal space-filling (distribution of samples), (b) Sampling with good space-filling only, (c) LHS with very poor space-filling and highly correlated factors	67
Figure 24 Doubling procedure of PLHS with $k=2$ variables (a) Initial LHS with $r=3$ samples, (b) Dividing initial sample domain into 6 intervals with equal marginal probability	68
Figure 25 Load duration curves (left) and the normalized hourly pattern of the Electricity, Heating and Cooling loads for the IST Alameda Campus, expressed in hourly basis	72
Figure 26 Comparison of a trigeneration-thermal storage system vs. a conventional system, while meeting the annual loads $L_n \forall n=\{E: \text{electricity}, H:\text{heating}, C:\text{cooling}\}$	75
Figure 27 Refined methodology of Phase I	76
Figure 28 Example of one scenario out of the 600 possible, as part of the full factorial design of experiments.	77
Figure 29 Simulation data obtained from the full factorial design of experiments, using DER-CAM (example of $SS4=6.6$)	81
Figure 30 CHP Technology Mix Histogram (example of $SS4=6.6$) and its relationship with levels E, H, C, and percentage of savings.	83
Figure 31 Graphical explanation of the set of criteria for the MCDM ELECTRE 1S method	87
Figure 32 Clusters across the axis of annual loads E, H, C (example for $SS4=6.6$)..	90
Figure 33 Ternary diagram for the distribution of the percentage of Grid, Boiler, Absorption, and Heat Scrap across dominance rates (rE, rH, rC) and SS rates....	93
Figure 34 Ternary diagram for the distribution of E4E, E4C, E4CS, H4H, H4C and H4CS across dominance rates (rE, rH, rC) and SS rates.	96
Figure 35 Ternary diagrams of SS2, SS3 and SS4 for the distribution of the percentage of savings across dominance rates (rE, rH, rC)	98
Figure 36 Boxplots comparing rE, rH, rC , and the percentage of savings for each cluster across the spark spread rates SS2-SS3-SS4.....	100
Figure 37 Ternary diagrams of SS1 for the distribution of the percentage of savings across dominance rates (rE, rH, rC)	101
Figure 38 Boxplots comparing rE, rH, rC , and the percentage of savings for each cluster across the spark spread rate $SS1 = 3.0$	101
Figure 39 Average percentage of savings for each cluster across spark spread rates SS2-SS3-SS4.	103
Figure 40 Isolines for the price of electricity [\$/kWh]	106
Figure 41 Isolines for the price of natural gas	107
Figure 42 Morris sensitivity indexes for the ranges 0 to 10 GWh/y (top), 0 to 100 GWh/y (middle), and 0 to 1000 GWh/y (bottom). Each range shows the analysis for the amount of savings (left) and the percentage of savings (right)	112

Figure 43 Morris sensitivity indexes for the ranges 0 to 5 GWh/y, 5 to 10 GWh/y, and 10 to 40 GWh/y. Each range shows the analysis for the amount of savings (left) and the percentage of savings (right).....	115
Figure 44 Morris sensitivity indexes for the ranges 40 to 70 GWh/y, and 70 to 100 GWh/y. Each range shows the analysis for the amount of savings (left) and the percentage of savings (right)	116
Figure 45 Variogram of variables for the amount of savings (top), zoom (bottom) ..	119
Figure 46 Response surface (amount of savings) vs. the raw data corresponding to the four seed points for variables pE , pNG , E , H , and C	120
Figure 47 Variogram of variables for the percentage of savings (top), zoom (bottom).....	121
Figure 48 Response surface (percentage of savings) vs. the raw data corresponding to the four seed points for variables pE , pNG , E , H , and C	122
Figure 49 Sobol SA indexes for amount of savings.....	124
Figure 50 Sobol SA indexes for percentage of savings.....	125
Figure 51 Three dimensional charts of the average amount and percentage of savings (left and right respectively), across pE , pNG , and E	127
Figure 52 Isolines of $pNG-E-H-C$ across the electricity price [pE] for the amount of savings (top); and addition of the isoline $pNG=0.075$, $E=40$, $H=70$, $C=65$ (bottom).....	132
Figure 53 Isolines of $pNG-E-H-C$ across the electricity price [pE] for the percentage of savings	133
Figure 54 Isolines of $pE-E-H-C$ across the natural gas price [pNG] for the amount and percentage of savings (top and bottom respectively)	133
Figure 55 Isolines of $pE-pNG-H-C$ across the annual electricity load [E] for the amount and percentage of savings (top and bottom respectively)	134
Figure 56 Isolines of $pE-pNG-E-C$ across the annual heating load [H] for the amount and percentage of savings (top and bottom respectively)	135
Figure 57 Isolines of $pE-pNG-E-H$ across the annual cooling load [C] for the amount and percentage of savings (top and bottom respectively)	136
Figure 58 Ternary diagrams of SS1, SS2, SS3, and SS4 for the distribution of the percentage of savings across dominance rates (rE , rH , rC). Taken from subsection 4.4.3.	138
Figure 59 Graphical explanation of Heat for Cooling (H4C) and Heat for Cooling Storage (H4CS).....	179
Figure 60 Behavior of partial concordance Index [$c_{jai, ak}$], depending on the value of q_i , p_i and Ω_i	184

LIST OF TABLES

Table 1 Papers studying combined thermal and power energy systems.....	20
Table 2 General characteristics of the computational tools [79]–[81], [86], [87]	28
Table 3 Specific characteristics of the computational tools [79]–[87]	29
Table 4 Papers using optimization algorithms to assess the feasibility of combined thermal and power energy systems.....	32
Table 5 Types of sensitivity analysis methods used in energy analysis	37
Table 6 Types of clustering: Inputs and outputs.....	48
Table 7 Comparison of clustering types	49
Table 8 Comparison of GSA methods against OAT, and full factorial DoE	70
Table 9 Energy prices used in DERCAM	78
Table 10 Technological settings for the reference scenario in DERCAM.....	78
Table 11 Technological settings for the CCHP-TS scenario (CHP prime movers)....	78
Table 12 Technological settings for the CCHP-TS scenario (absorption chiller)	79
Table 13 Technological settings for the CCHP-TS scenario (thermal storage)	79
Table 14 Other settings used in DERCAM.....	79
Table 15 General information of the energy analysis for the scenarios belonging to the different SS rates.....	80
Table 16 Set of criteria for the MCDM ELECTRE 1S method	86
Table 17 Enlarged performance table (example of SS4=6.6).....	88
Table 18 Concordance matrix and outranking relations (example of SS4=6.6)	89
Table 19 Discordance matrix (example of SS4=6.6). Note: one means veto condition.	90
Table 20 Prices of electricity and natural gas (in cents of EUR / kWh) for the spark spread rates in chapter 4.....	104
Table 21 Feasible combinations by fixing price of electricity and spark spread rate.....	105
Table 22 Feasible combinations by fixing price of natural gas and spark spread rate	107
Table 23 First point of the 20 routes for the Morris SA	111
Table 24 Seed point for VARS SA	118
Table 25 Raw data obtained from DER-CAM report (part 1).....	173
Table 26 Raw data obtained from DER-CAM report (part 2).....	174
Table 27 Electricity and Heat produced by the CHP and scrapped.....	174
Table 28 Energy scrap produced by the CHP	175
Table 29 Source proportion per type of energy	175

Table 30 Source proportion for the whole system	176
Table 31 Source proportion for the whole system	178
Table 32 Source proportion for the whole system	180

ACRONYMS

BBD	Box-Behnken Design of experiments
CCD	Central Composite Design of experiments
CCHP	Combined Heating, Cooling, and Power (Trigeneration). Also referred by some authors as CHCP
CHP	Combined Heating and Power (Cogeneration)
COP	Coefficient of performance
CT	Combustion turbine
CTDB	Combustion Turbine Duct Burner
DER-CAM	Distributed Energy Resources Customer Adoption Model
DHC	District Heating and Cooling
DoE	Design of experiments
EU	European Union
GA	Genetic algorithms
GAMS	General Algebraic Modeling System (software)
GDP	Gross domestic product
GSA	Global sensitivity analysis
ICE	Internal combustion engine
IEA	International Energy Agency
IPCC	Intergovernmental Panel on Climate Change
JRC	Joint Research Centre (Europe)
LBNL	Lawrence Berkeley National Laboratory
LHS	Latin Hypercube Sampling
MCDM	Multi-Criteria Decision-Making
MILP	Mixed integer linear programming
MINLP	Mixed integer non-linear programming

OAT	“One-at-a-time” sensitivity analysis
OECD	Organization for Economic Co-operation and Development
SA	Sensitivity analysis
SS	Spark Spread
TS	Thermal Storage
VARIS	Variogram Analysis of Response Surfaces

ABBREVIATIONS

Abs	Absorption chiller
C#	Cluster number # (in k-Means application)
CStg	Cold storage
E4C	Electricity produced by the CHP and used to cover cooling loads
E4CS	Electricity produced by the CHP and used to produce cold that will be stored
E4E	Electricity produced by the CHP and used to cover electric loads
HStg	Heat storage
H4CS	Heat produced by the CHP and used to produce cold that will be stored
H4C	Heat produced by the CHP and used to cover cooling loads
H4H	Heat produced by the CHP and used to cover heating loads
pSav	Percentage of savings
VCchiller	Vapor-compression chiller

SYMBOLS AND NOMENCLATURE

Nomenclature

C	Annual size of the cooling load (in terms of energy) [GWh/y]
$\text{Cooling}_{\text{Absorption}}(t)$	Cooling produced with an Absorption chiller, in hourly basis [kW]
$\text{Cooling}_{\text{Electric}}(t)$	Cooling produced with vapor-compression chiller, in hourly basis [kW]
$\text{dim}(h)$	No. of levels, where $h=\{h_1, \dots, h_j, \dots, h_n\}$ are the levels (in VARS SA)
$d_n(t)$	Hourly load pattern of the n energy carrier, where $n=\{E: \text{electricity}, H: \text{heating}, C: \text{cooling}\}$ [-/h]
E	Annual size of the electric load (in terms of energy) [GWh/y]
EE_i	Elementary effects of the variable i (in Morris SA)
$\text{Electricity}_{\text{CHP}}(t)$	Electricity produced by CHP, expressed in hourly basis [kW]
$\text{Electricity}_{\text{Grid}}(t)$	Electricity imported from the national grid, expressed in hourly basis [kW]
$\text{Electricity}_{\text{CHP}}^{\text{CS}}(t)$	Electricity produced by CHP and used to produce Cooling and store it, expressed in hourly basis [kW]
$\text{Electricity}_{\text{CHP}}^{\text{LC}}(t)$	Electricity produced by CHP and used to supply Cooling load, expressed in hourly basis [kW]
$\text{Electricity}_{\text{CHP}}^{\text{LE}}(t)$	Electricity produced by CHP and used to supply Electric load, expressed in hourly basis [kW]
$\text{Energy}_{\text{CHP}}(t)$	Total energy produced by CHP, expressed in hourly basis [kW], including Electricity and Heat
H	Annual size of the heating load (in terms of energy) [GWh/y]
$\text{Heating}_{\text{Boiler}}(t)$	Heating produced by a boiler, expressed in hourly basis [kW]

Heating _{CHP} (t)	Heating produced by CHP, expressed in hourly basis [kW] NOTE: This is useful heat. Non-useful heat is the one that is produced and not consumed
Heat _{CHP} ^{CS} (t)	Heat produced by CHP and used to produce Cooling and store it, expressed in hourly basis [kW]
Heat _{CHP} ^{LC} (t)	Heat produced by CHP and used to supply Cooling load, expressed in hourly basis [kW]
Heat _{CHP} ^{LH} (t)	Heat produced by CHP and used to supply Heating load, expressed in hourly basis [kW]
L _n (t)	Hourly energy load of <i>n</i> carrier [kW], where <i>n</i> ={E: electricity , H: heating , C: cooling }
n	Number of seed point (in VARS SA)
p	Number of levels (in Morris SA)
pE	Price of the electricity from the national grid [\$/kWh]
pNG	Price of the natural gas from the national grid [\$/kWh]
R	Range
r	Number of seed point (in Morris SA)
r _n	Dominance rates of <i>n</i> carrier [-], where <i>n</i> ={E: electricity , H: heating , C: cooling }
S1	Individual effects (in Morris SA)
S2	Interaction effects (in Morris SA)
ST	Total effects (in Morris SA)

Greek letters

$\gamma(h_i)$	Directional variogram of variable i (in VARS SA)
Δ	Resolution or size of the step (in Morris SA)
Δh	Resolution or size of the step (in VARS SA)
μ	Mean of the distribution of the elementary effects $EE_i \sim F_i$ (in Morris SA)
μ^*	Mean of the distribution of the absolute values of the elementary effects $ EE_i \sim G_i$ (in Morris SA)
σ	Standard deviation of the distribution of elementary effects $EE_i \sim F_i$ (in Morris SA)

RÉSUMÉ LONG (Français)

Mots clés: Systèmes de trigénération couplés à du stockage thermique, faisabilité technico-économique, demandes en énergies, prix de l'énergie, analyse de sensibilité.

Les systèmes de trigénération couplés à du stockage thermique (CCHP-TS) contribuent à la production distribuée d'énergie et à la réduction des émissions de gaz à effet de serre. Ils sont conçus pour découpler la production et la consommation de chauffage, de froid et d'électricité. Néanmoins, il est important d'évaluer leur faisabilité technico-économique pour assurer une mise en œuvre à long terme. Par ailleurs, la détermination et la caractérisation des variables influentes sont essentielles pour identifier les domaines d'application les plus viables. Potentiellement, cela peut stimuler l'intérêt des chefs de projet, des investisseurs et des décideurs politiques, encourageant ainsi l'adoption de cette technologie.

Plusieurs auteurs suggèrent que les prix et les demandes en énergies (électricité, chaleur et froid) sont des variables importantes de la faisabilité technico-économique des systèmes combinés d'énergie thermique et électrique. Ils ont notamment utilisé le ratio Spark Spread (SS) qui est le rapport entre le prix de l'électricité du réseau et du combustible de cogénération. Cependant, seules quelques études, telles que celles de Hajabdollahi [1], et Cardona et al. [2], évaluent l'influence combinée des prix et de la demande en énergies. De plus, ces travaux présentent certaines limites dans leur modèle. Ainsi, Hajabdollahi étudie les charges mensuellement uniquement alors qu'une résolution temporelle plus courte de la demande est nécessaire pour plus de précision pour une analyse de faisabilité. Quant à Cardona et al., ils analysent les prix et les charges sur une base horaire, mais le modèle qu'ils proposent n'optimise que la stratégie d'opération et non la conception (puissances installées des systèmes) qu'ils supposent définie a priori.

La littérature mettant en avant les prix de l'énergie et les niveaux de demandes comme variables importantes, ce travail propose et analyse deux hypothèses : 1) Il existe un couplage entre les prix de l'énergie et la variabilité des demandes en énergies qui influe techniquement et économiquement sur la faisabilité des systèmes

CCHP-TS; 2) Les prix de l'énergie (électricité et gaz naturel) doivent être considérés séparément plutôt que d'utiliser seulement le ratio Spark Spread (SS).

Le travail repose sur une méthodologie divisée en deux phases, présentées sur la Figure 1.

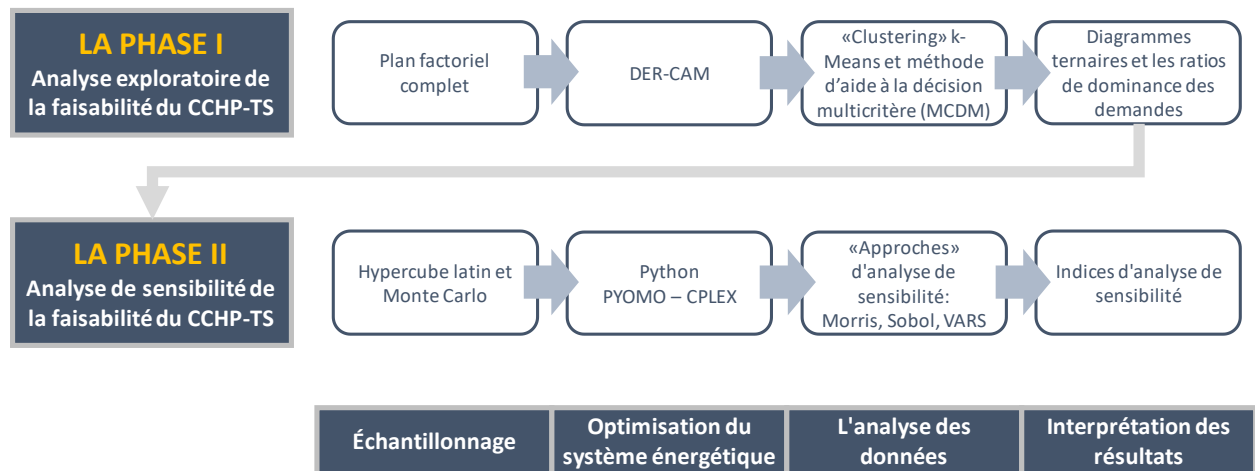


Figure 1 Méthodologie générale de cette thèse

La première phase est une analyse exploratoire visant à démontrer que le modèle utilisé de CCHP-TS est pertinent et sensible aux variables d'analyse (prix et demandes énergétiques). Pour ce faire, nous utilisons l'outil DER-CAM et son modèle pour optimiser le système énergétique. La méthode d'analyse de sensibilité, quant à elle, met en œuvre un plan factoriel complet, en raison de sa simplicité, de sa capacité d'analyse globale et de la possibilité d'identifier les effets d'interaction. Après avoir effectué les simulations, les données sont analysées à l'aide d'une nouvelle combinaison de la méthode de «clustering» k-Means et d'une méthode d'aide à la décision multicritère (MCDM). Les enseignements tirés de cette première phase permettent de définir la méthodologie de la seconde phase et de proposer un modèle de simulation et d'optimisation pertinent et sensible aux variables d'analyse.

La seconde phase propose donc une analyse de sensibilité rigoureuse qui permet de plus une comparaison de trois «approches»: Morris («aproche» basée sur la dérivé), Sobol («aproche» basée sur la variance) et VARS («aproche» basée sur le variogramme). Chacune de ces méthodes est associée à différentes méthodes d'échantillonnage (Hypercube latin et Monte Carlo). Concernant la simulation et l'optimisation du système énergétique, DER-CAM est un outil limité pour effectuer le nombre de simulations nécessaires à une analyse de sensibilité globale. Par

conséquent, pour la deuxième phase, un modèle adapté de simulation et d'optimisation de systèmes CCHP-TS (développés en langage Python) est proposé. Le modèle est basé sur les bilans énergétiques et utilise la méthode MILP comme algorithme d'optimisation. En Python, cette approche MILP est mise en oeuvre à l'aide de la bibliothèque d'optimisation PYOMO et du solveur CPLEX. Cette combinaison puissante est une alternative aux logiciels commerciaux tels que GAMS, qui est couramment utilisé dans ce type de travaux. Par ailleurs, les prix de l'électricité et du gaz naturel sont étudiés de façon découplée, au lieu de les consolider dans le ratio Spark Spread.

Trois aspects montrent l'importance d'effectuer une analyse de sensibilité globale dans la deuxième phase, au lieu de conserver les résultats obtenus avec le plan factoriel complet pendant la première phase: 1) Le plan factoriel complet est une méthode guidée par le modèle utilisé, tandis que l'analyse de sensibilité globale est indépendante de celui-ci. Ces dernières reposent sur une exploration globale de l'espace contrairement aux méthodes guidées par un modèle 2) La précision du plan factoriel complet repose sur la dispersion de l'échantillon, tandis que l'analyse de sensibilité globale garantit un échantillonnage aléatoire et dispersé sur toute la plage des variables. 3) Le plan factoriel complet permet principalement l'identification d'effets individuels des paramètres et d'interaction possibles, tandis que les méthodes d'analyse de sensibilité globale, telles que Sobol, sont également utiles pour classer et quantifier la sensibilité relative des paramètres. La mise en oeuvre complémentaire des trois méthodes d'analyse de sensibilité globales de cette deuxième phase a ainsi renforcé l'analyse de faisabilité technico-économique.

Les résultats de cette analyse de sensibilité identifient cinq variables importantes à prendre en compte dans l'analyse de faisabilité, ainsi que les effets de leurs interactions. Ces variables sont: le prix de l'électricité [pE], le prix du gaz naturel [pNG], la demande électrique [E], la demande en chauffage [H] et la demande en froid [C]. L'ordre d'importance diffère selon que l'indicateur de performance économique utilisé soit absolu (montant d'économies réalisées [\$]) ou relatif (pourcentage d'économies réalisées [%]). Ci-dessous, la description des résultats et la réponse aux deux hypothèses formulées.

HYPOTHÈSE 1

Oui, il existe un couplage entre les prix de l'énergie et les demandes énergétiques qui influe sur la faisabilité des systèmes de trigénération couplés à du stockage thermique. Les effets de ce couplage dépendent de l'indicateur de performance économique considérée.

Concernant leur impact sur le montant d'économies réalisées, le prix de l'électricité (pE), le prix du gaz (pNG) et la demande en électricité (E) sont, de loin, les variables les plus importantes, tandis que les effets des demandes en chaleur et en froid (H et C respectivement) semblent relativement négligeables. Les principaux effets d'interaction impliquent la demande électrique et les prix de l'énergie (E - pNG et E - pE). En d'autres termes, avoir une demande électrique importante est en faveur d'un système CCHP-TS, d'autant plus que le prix du gaz sera faible et celui de l'électricité élevé, et inversement. Il est par ailleurs montré que, pour des valeurs pE et pNG déterminées, une augmentation des demandes améliore le montant des économies réalisées par la mise en oeuvre de ce type de systèmes. Enfin, il est important de mentionner que le prix du gaz pNG est une variable singulière qui a des effets d'interaction avec toutes les autres.

Concernant les effets d'économies relatives réalisées, les prix de l'énergie pE et pNG apparaissent comme les variables les plus importantes. La demande en électricité E reste plus influente que H et C , mais devient moins impactante que sur les économies absolues. Cela tient au fait que pour l'indicateur du montant d'économies, il existe un lien direct entre l'argent économisé et la demande E , tandis que le pourcentage d'économies tient compte des proportions plutôt que du montant total. Néanmoins, il est à noter que lorsque les économies relatives sont utilisées comme indicateur de faisabilité, l'influence des trois demandes (E , H et C) est légèrement plus équilibrée que lorsque la faisabilité est étudiée via le montant des économies. Le prix du gaz pNG est ici aussi la seule variable qui a des effets d'interaction avec toutes les autres dont certains aspects attirent l'attention. Le couplage pNG - pE est notablement plus fort que dans le cas d'un montant absolu d'économies, ce qui suggère que le ratio Spark Spread pourrait être plus pertinent pour analyser les économies relatives que les économies absolues. Cependant, on constate que les demandes énergétiques ont des effets d'interaction presque exclusivement avec le pNG . Par conséquent, la importance de E , H et C n'est fortement liée qu'au prix du gaz naturel.

HYPOTHÈSE 2

Concernant l'intérêt d'étudier séparément les prix de l'énergie, on peut dire que les deux paramètres pE et pNG, sont importants individuellement quelle que soit l'indicateur de performance économique utilisé (montant absolu ou pourcentage d'économies réalisées). De plus, ils sont clairement liés, directement ou indirectement. Cependant, la principale différence entre les deux est que pNG interagit avec toutes les autres variables, indiquant une influence plus large. En ce qui concerne spécifiquement le pourcentage d'économies, les demandes énergétiques interagissent presque exclusivement avec le pNG. De plus, bien que le pE ait également de forts effets d'interaction avec le pNG, il est montré que contrairement à la règle générale établie par les organismes gouvernementaux internationaux, le seuil du ratio Spark Spread pourrait être inférieur à la valeur usuelle (SS=3) en fonction du prix du gaz naturel. Il est donc recommandé d'analyser séparément les prix de l'énergie pour évaluer la faisabilité des systèmes de trigénération couplés à du stockage thermique

Au-delà des résultats techniques, la contribution de cette thèse comprend l'adaptation d'un modèle de pas de temps horaire des systèmes CCHP-TS dans un langage de programmation qui permet une analyse de sensibilité agile. De plus, la mise en œuvre des trois méthodes d'analyse de sensibilité a permis d'identifier leurs avantages et leurs limites. Cette complémentarité a ainsi renforcé l'analyse de faisabilité technico-économique des systèmes de trigénération couplés à du stockage thermique.

LONG ABSTRACT (English)

Key words: Trigeneration systems with thermal storage, techno-economic feasibility, energy loads, energy prices, sensitivity analysis.

Trigeneration systems with thermal storage (CCHP-TS) contribute to the distributed generation of energy and the reduction of greenhouse gas emissions. They are designed to decouple the production and consumption of heating, cooling and electricity. Nevertheless, it is important to assess their techno-economic feasibility to ensure long-term implementation. Moreover, determining and characterizing the influential variables is essential to identify the most viable application fields. Potentially, this could foster the interest of project managers, investors, and policymakers, therefore encouraging the adoption of this technology.

Several authors suggest that energy prices and loads are important variables for the techno-economic feasibility of combined thermal and power energy systems. Particularly they have explored the Spark Spread rate, a ratio between the price of electricity from the grid and the price of CHP fuel. However, just a few studies, such as Hajabdollahi [1], and Cardona et al. [2], assess the prices and loads together. Moreover, they present some limitations in their analysis. Hajabdollahi study the loads in monthly basis, but a smaller time-step in the loads is important because it gives more precision to the feasibility analysis. As for Cardona et al., they analyze prices and loads in hourly basis, but the model they propose only optimizes the operation strategy, while the design (installed capacity of the equipment) is an assumption.

As the literature reveals that energy prices and loads size are important variables, this study aims to take a university campus as case study and analyze two hypotheses proposed: 1) There is a combination of energy prices and the size of the annual energy loads that makes techno-economically feasible a CCHP-TS system; 2) The energy prices (electricity and natural gas) should be considered separately instead of consolidating them into the spark spread rate (SS).

The analysis is divided into two phases, exhibited the general methodology of Figure 18.

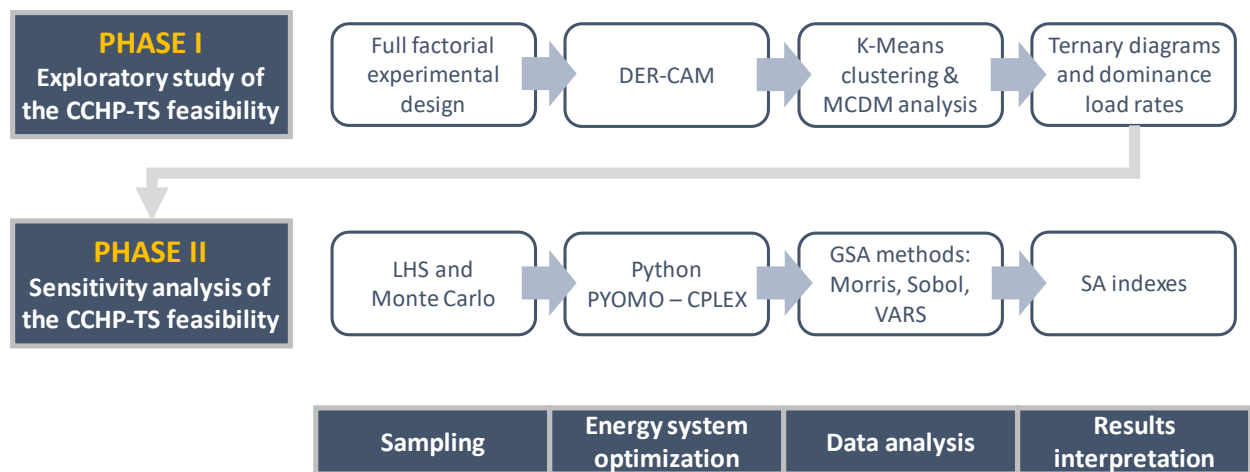


Figure 2 General methodology of this thesis

The first one is an exploratory study aiming to demonstrate that the model for CCHP-TS is relevant and sensitive to the variables of analysis (energy prices and loads). To take advantage of the computational tools, we use DER-CAM and its embedded model to optimize the energy system. As for the sensitivity analysis method, it implements a full factorial design of experiments, due to its simplicity, ability to analyze globally, and the possibility of identifying interaction effects. Once the simulations are conducted, the data gets analyzed using a novel combination of k-Means clustering and multicriteria decision making (MCDM). The learnings from this first phase are the cornerstone for the second one, because the objective is to demonstrate that the model is relevant and sensitive to the variables of analysis.

The second is a in depth sensitivity analysis and the comparison of three approaches: Morris (derivative-based approach), Sobol (variance-based approach), and VARS (variogram-based approach). Each of them incorporates their corresponding sampling methods (LHS and Monte Carlo). Regarding the energy system optimization, DER-CAM is a limited tool to perform the amount of simulations required for a global sensitivity analysis. Therefore, for the second phase, we adapted the model of a CCHP-TS system into the programming language Python. The model is based on energy balances and uses MILP as optimization algorithm. In Python, the MILP model is solved using the optimization library PYOMO and the solver CPLEX. This combination is a powerful alternative to commercial software such as GAMS, which is commonly used in this context. In addition, it is worth mentioning that at this

stage, electricity and natural gas prices are studied separately, rather than consolidating them into Spark Spread.

Three aspects exhibit the importance of conducting a global sensitivity analysis in the second phase, instead of keeping the results obtained with the full factorial design of experiments during the first phase: 1) The factorial design of experiments is a model-based method, while global sensitivity analysis is model-free. Model-free methods are not related to any local reference at the model. In other words, while a model-free method takes the samples randomly, a model-based method takes them based on a specific starting point or indication given by the user. 2) The accuracy of the factorial design of experiments relies on the sample dispersion, while the global sensitivity analysis ensures a random and dispersed sampling across the range of the variables. 3) The factorial design of experiments is primarily for screening purposes and provides an idea of the individual and interaction effects of the parameters, while global sensitivity analysis methods, such as Sobol, are useful also for ranking and quantifying the relative sensitivity of the parameters. In general, the complementary implementation of the three global sensitivity analysis methods in this second phase thereby reinforced the techno-economic feasibility analysis.

The results of the sensitivity analysis rank five variables from the least to the most relevant, as well as their interaction effects. The variables are: the electricity price [pE], the natural gas price [pNG], the annual size of electric loads [E], the annual size of heating loads [H], and the annual size of cooling loads [C] (Note that E, H, and C are expressed in energy). The order of relevance relies on the measure used for the techno-economic performance of the CCHP-TS system. It can be amount of savings [\$] or the percentage of savings [%]. Below the description of the results and the answer to the two hypotheses formulated.

HYPOTHESIS 1

Yes, there are combination of energy prices and size of the energy loads that make a Trigeneration – Thermal Storage feasible. The optimal combination depends on the metric considered.

When talking about the **amount of savings**, pE , pNG , and E are, by far, the most relevant variables. While H and C seem comparatively unimportant. The main

interaction effects are between the electricity load and the energy prices ($E - pNG$ and $E - pE$). In other words, having a large E is good, but it should be along with a small pNG and high pE . Vice versa it is also true. It was show that, for determined pE and pNG , an increase of the loads rises the amount of savings. Finally, it is good to mention that pNG is a singular variable that has interaction effects with all the others.

When talking about the **percentage of savings**, the energy prices pE , and pNG are the most relevant variables. E is still more influential than H and C , but it becomes less influential compared with its analysis for the amount of savings. That is because, when measuring the amount of savings, there is a direct link between the money saved and the size of E . But when measuring percentage of savings, it considers the proportions, rather than the total amount. Nevertheless, an important remark is that in the percentage of savings, the influence of the three loads (E , H , and C) is slightly more equilibrated than in the amount of savings. On the other hand, pNG is again the only variable that has interaction effects with all the others, but some aspects draw attention. The index $pNG - pE$ is notably bigger compared with its analogous in the amount of savings, suggesting that the Spark Spread rate (SS) could be relevant for the relative savings. However, that resolution becomes weak when noticing that the energy loads have interaction effects almost exclusively with pNG . Therefore, the relevance of E , H , and C is strongly linked only to the price of natural gas.

HYPOTHESIS 2

Concerning the interest of studying the **energy prices** separately, it can be said that both, pE and pNG , are relevant individually regardless of the output measure (amount or percentage of savings). Also, they are clearly tied, either directly or indirectly. However, the main difference between them is that, in either output (amount or percentage of savings), pNG keeps interaction effects with all the other variables, indicating that its influence is wider. Specifically talking about the percentage of savings, the energy loads interact almost exclusively with pNG . Moreover, although pE also has a strong interaction effects with pNG , it is shown that contrary to the general rule established by international governmental organisms, the spark spread threshold could be lower than three depending on the price of natural gas. Therefore,

it is recommendable to analyze separately the energy prices while assessing the feasibility of Trigeneration systems with Thermal Storage.

Beyond the technical results, the contribution of this thesis includes adapting an hourly time-step model of the CCHP-TS systems into a programming language that allows an agile sensitivity analysis. Additionally, the implementation of the three sensitivity analysis methods allowed identifying their advantages and limitations. Moreover, this complementarity thereby reinforced the techno-economic feasibility analysis of the Trigeneration systems with Thermal Storage.

1 INTRODUCTION

1.1 Context

Throughout the years, several authors have suggested that there is a relationship between the energy consumption and the economic growth of a region [3]–[8]. With regards to the environmental impact of the energy consumption, the IPCC report [9] indicates that half of the anthropogenic CO₂ emissions between 1750 and 2011 have occurred in the last 40 years. From those, 40% were kept in the atmosphere and 60% were removed and stored on land (plants and soils) and ocean, causing ocean acidification. The report also identified the energy sector as the largest contributor to the greenhouse gas emissions. Burning coal, natural gas, and oil for electricity and heat production represented 25% of the emissions in 2010, while fuel extraction, refining, processing, and transportation represented another 10%. Therefore, reducing energy demand is one of the most important mitigation strategies proposed by the IPCC report [9].

Given the dependency between energy consumption and economic growth and the impact of energy consumption in climate change, one of the major challenges faced by society today is how to promote the economic growth of developing regions like Africa, southeast Asia, middle east and Latin America without increasing the emissions of greenhouse gases. The only way to solve this challenge is by promoting the efficient use of energy demand and supply it using the most efficient generation technologies and renewable resources.

1.2 Combined thermal and power energy systems

Around the globe, society requires electrical and thermal energy to cover their needs in the building sector and industry (which together account from almost 60% of the total final energy consumption [10]). Typically, they are produced

separately, but a combined thermal and power energy system can generate both using the same fuel.

There are several advantages in using combined thermal and power energy systems: 1) improving the energy efficiency and reducing emissions; 2) enabling the use of local renewable and residual thermal energy; 3) increasing the security of energy supply by decentralizing its production; 4) reducing the transmission and distribution losses because such decentralized systems are closer to the location of the demand; and 5) generating cost-savings for the energy consumer ([11], [12]). In general, combined heat and power generation technologies contribute to a low-carbon and resilient local energy system.

The combined generation of heat and power may have different approaches. The following sections 1.2.1, 1.2.2, and 1.2.3 provide a more detailed insight.

1.2.1 Cogeneration

Combined Heating and Power (CHP), also known as cogeneration, is a process that generates simultaneously heat and electrical energy from a single fuel. The fuel could be either fossil or non-fossil.

According to the CODE2 [13], CHP can save up to 25% of the primary energy compared to the separate production of both outputs. The increase of this number depends on the carbon intensity of the electricity from the grid [14], and the efficiency of the CHP. The Fraunhofer Institute reports an overall CHP efficiency up to 93% [15].

In general, CHP can significantly reduce greenhouse gases emissions in residential, industry, and tertiary sectors, by lowering fuel demand and transmission losses [16]. The latter happens because it produces the energy closer to the consumer.

In 2012, the EU published the Energy Efficiency Directive (EED) 2012/27/EU that replaced the 2004/8/EC, to promote the use of CHP. Specifically, the EED talks about cogeneration in its Art. 14 and annexes I, II, VIII, IX, and X. The method to calculate the CHP efficiency is detailed in the Annexes I and II [17].

As part of the Directive 2012/27/EU, in 2015, all EU members assessed the potential for high-efficiency CHP and DHC, to promote the joint generation of electricity and useful heat. In Portugal [18], [19], the transposition of the Directive 2004/8/EC was through the Decree-Law n°. 23/2010, and later, in 2015, the Decree-Law n°. 68-A/15 transposed the Directive 2012/27/EU. Portugal has mainly used CHP for industrial purposes. However, the Decree-Law n°. 68-A/15 [20] introduced changes to the regulation that made more difficult for the CHP owners to access to supports such as the *remuneration according to a reference tariff* and the *bonus per efficiency*. Potentially, this has had a negative impact in the CHP for Portugal.

1.2.2 Trigeneration

Combined Heating, Cooling and Power (CCHP), also known as trigeneration, is a system that includes CHP and additional technologies, such as heat pumps or absorption cooling systems, to produce cooling from the heat and electricity generated by the CHP. These systems can reach overall efficiencies as high as 90%, depending on the configuration [21].

1.2.3 Trigeneration with Thermal Storage

In CHP and CCHP systems, the production of electricity, heat, and cold are coupled, but this is not necessarily true for the consumption. A solution is to install Thermal Storage (TS) units that decouple the heat and cold supply from the electricity one [22]. Additionally, this helps to shave peaks of demand [23], and reduce operation cost, primary energy use and emissions [24], [25]. This type of system is then called Trigeneration – Thermal Storage (CCHP-TS) and it is a specific configuration of the Combined Thermal and Power Energy Systems.

There are already successful examples of application of this approach. In Denmark, it has been proven that using thermal storage within DHC networks, helps to manage intermittency from wind and solar PV, by optimizing the

operation of thermo-electric equipment like heat pumps, electric boilers and CHP [11].

Figure 3 illustrates an example of the configuration for a CCHP-TS system (right) and compares it with a conventional energy system, called reference design (left). The latter uses electricity from the grid to meet the annual electric and cooling loads (through a vapor-compression chiller) and uses a natural gas boiler to meet the annual heating loads.

The CCHP-TS system uses grid and boiler just as auxiliary units. The main supply of energy comes from the CHP unit, that produces electricity and heat. Both energy vectors can be used directly to cover their loads, or they can be used to produce cold (through an electrical and/or absorption chiller respectively). The cold, like the heat, can be directly used to cover cooling and heating demand, or they can be stored using sensible thermal storage systems (hot-water tanks or cold-water tanks).

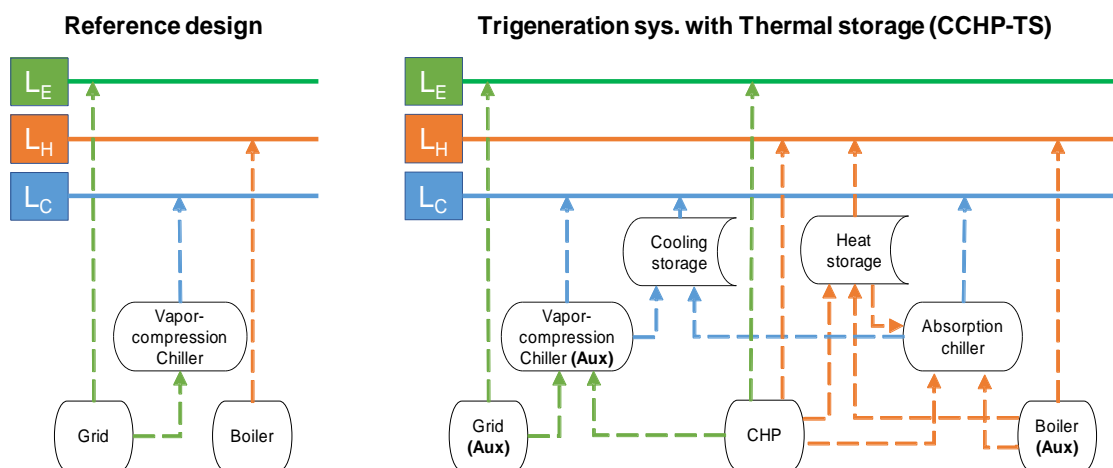


Figure 3 Comparison of a trigeneration-thermal storage system vs. a conventional system, while meeting the annual loads $L_n \forall n=\{E: \text{electricity}, H: \text{heating}, C: \text{cooling}\}$

NOTE: Energy Supply (dotted lines) and Energy Loads (solid lines)

1.3 Market framework

1.3.1 Size of the thermal sector

Only in Europe, the heating and cooling represent about 50% of the final energy consumption. From that, 84% is still generated from fossil fuels and only 16% from renewable energy [11].

The heat demand in the EU28 in 2010 reached approximately 4,306 PWh (Peta-Watt hour) [26]. From that, only 12% was covered with district heating, other 12% with electricity, and 66% with natural gas, oil, and coal products. According to Persson [26], the demand of heat depends on factors such as: the climate, the levels of building insulation, the energy services available and desired, as well as the level of comfort.

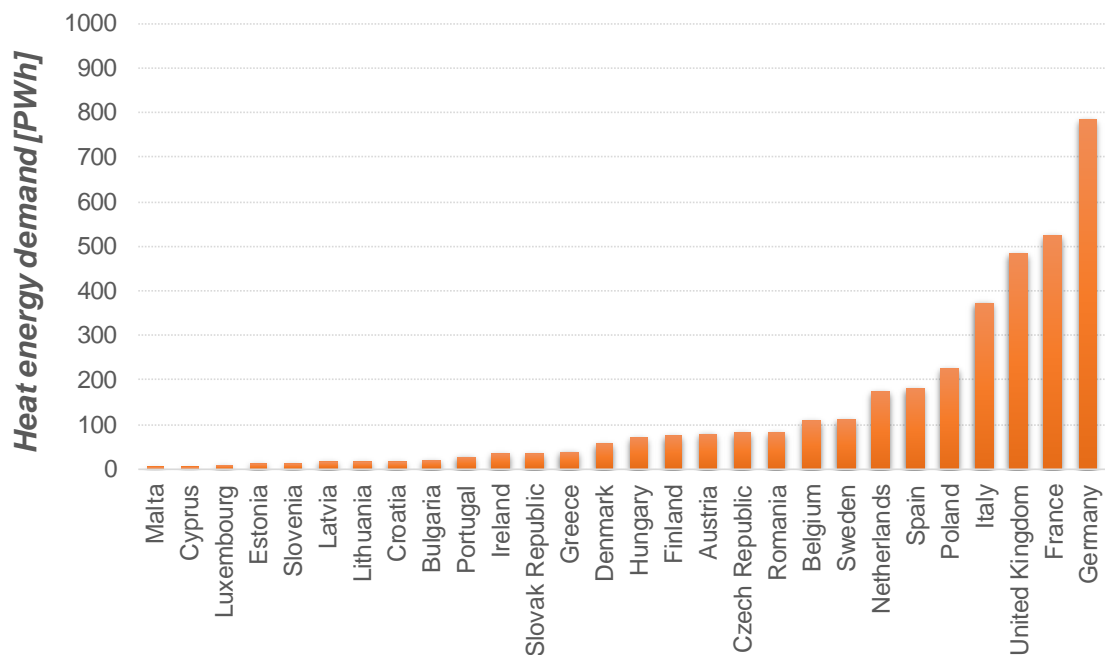


Figure 4 Estimated European heat market in 2010 including residential and service sector (Adapted from Persson, 2015 [26])

It is worth mentioning that the largest heat demand in the European markets are located in Germany, France, the United Kingdom, Italy, Poland, Spain, and the Netherlands (Figure 4). The reason is that, according to the JRC [27], the heat demand of those countries is representative in the three main sectors (industrial, residential, and services).

Regarding the cooling demand, Figure 5 presents an estimate for selected countries in 2000 and 2017 across the world. The increase of the total cooling demand (top of Figure 5) shows that the market is growing around the world. Also, it is evident that Asia is taking relevance, especially with the market growth in China and India. The demand per capita (bottom of Figure 5) shows that countries such as the US consume significantly more than others [28]. Therefore, if other countries follow the same trend, the cooling demand could grow exponentially.

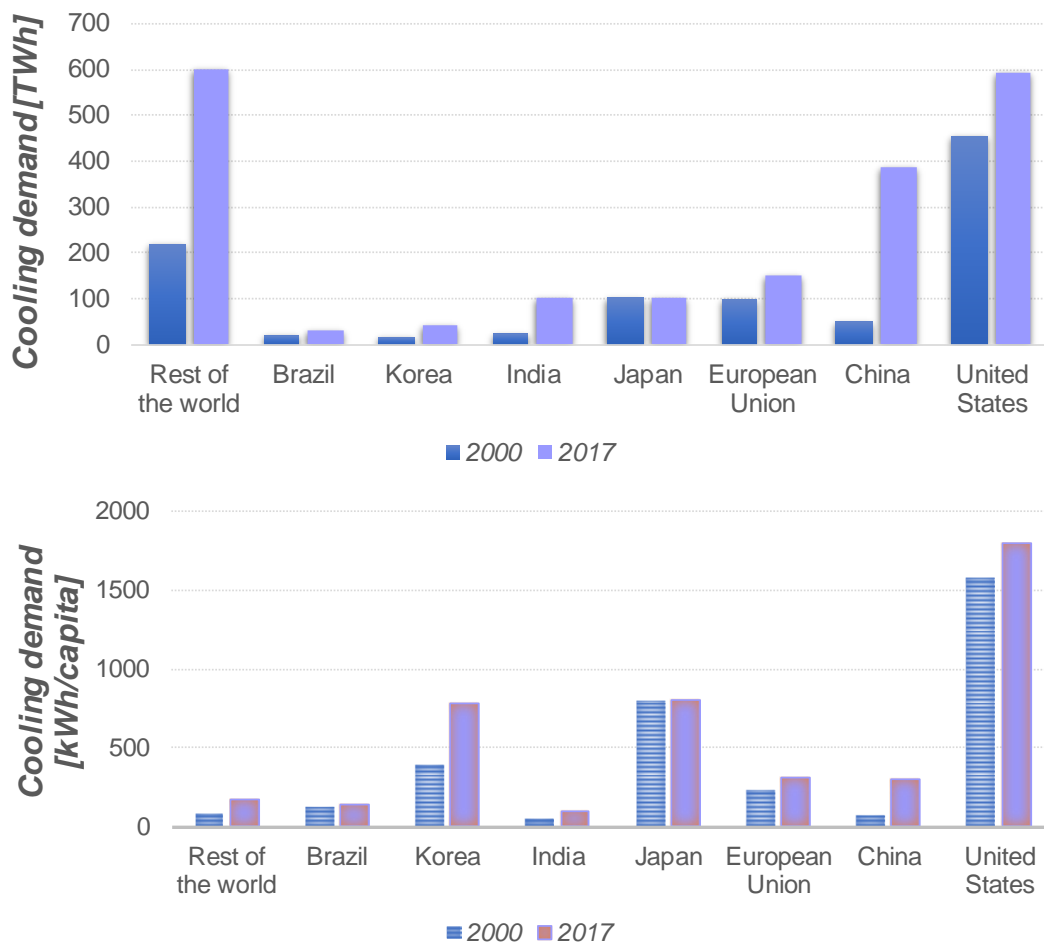


Figure 5 Cooling demand total (top) and per capita (bottom) for selected countries in 2000 and 2017 (image adapted from [28])

1.3.2 Current status of CHP market

As mentioned at the beginning of the section 1.2, a combined thermal and power energy system produces electricity and thermal energy from the same fuel. That increases its efficiency dramatically. Typically, the total efficiency of a CHP system is between 77% and 83% [29], however, in some systems, it can reach up to 90% [30].

Worldwide, CHP accounts for 10% of the electricity production [12]. But most of the contribution comes from countries with focused governmental policies.

Figure 6 shows the CHP electricity generation and its share for the European countries in 2017. The blue line indicates the European average CHP share in the gross electricity production. It was 11.3% in 2017 [31]. Countries such as Denmark, Latvia, and the Netherlands have the largest share of CHP electricity production. Whilst Germany and Italy are leading the absolute electricity generation.

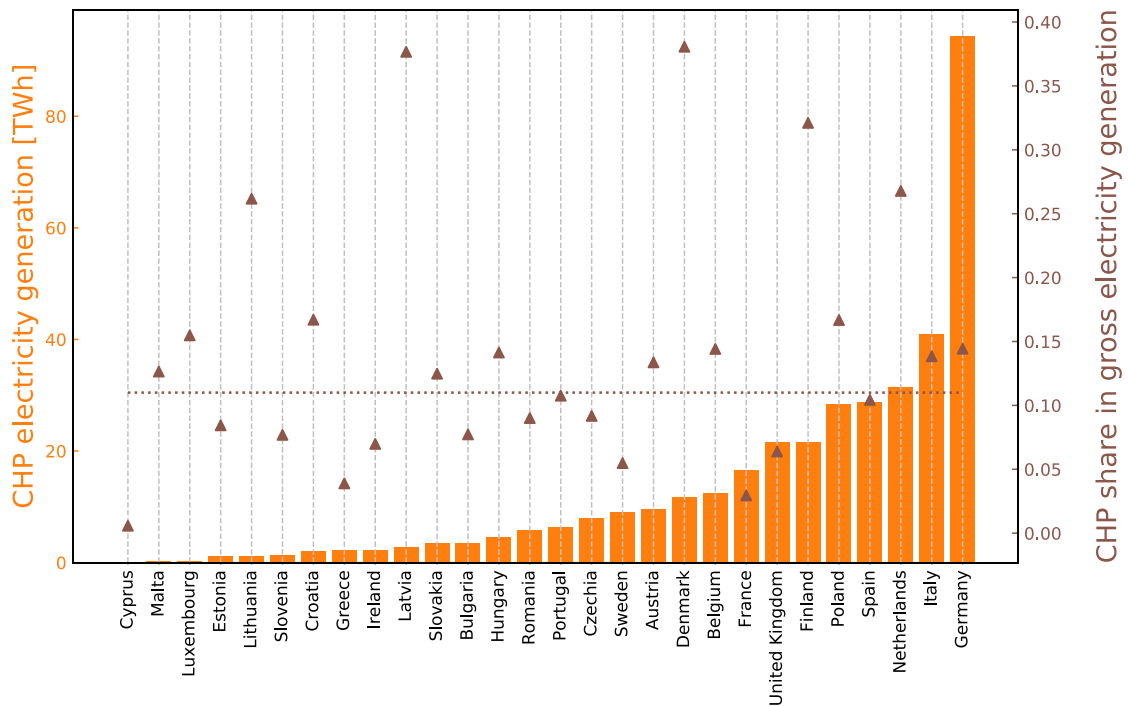


Figure 6 CHP electricity generation [TWh] and CHP share in the gross electricity generation for European countries in 2017 [31]

On the other hand, in recent years, the Asia-Pacific region has fostered CHP systems installation in new industrial facilities. China and India were leading this path in 2012 with 13% and 5% of their electricity production respectively [32], [33]. In 2017, CHP was already accounting for 20% of the total electricity production in China [34].

1.3.3 Relevant sectors for combined thermal and power energy systems

Combined thermal and power energy systems can be used mainly in three different sectors: industry, services, and households, in the form of district heating and cooling (DHC) [30].

Industry

For the OECD countries, the industry represents 25% of the total final energy consumption, only behind the transport (37%).

The industry is the application *par excellence* of the CHP technology, as it usually requires high temperature thermal energy. Until 2007, this represented 80% of the installed capacity of CHP worldwide [30]. In the European context, 55% of the industry in 2009 had high temperature energy requirements (Figure 7).

TOTAL USEFUL HEAT DEMAND FOR THE INDUSTRY (EU-27 IN 2009)

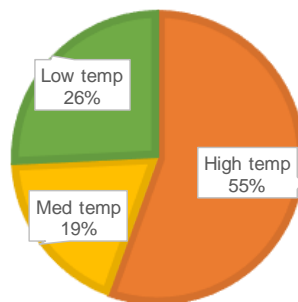


Figure 7 Share of type of useful thermal energy (by temperature) for the industry of EU27 in 2009 [27]

The typical industrial sectors using CHP are metallurgy, mining, chemical, petrochemical, food processing, pulp & paper, etc. The common characteristic among all is their high needs of thermal energy, usually in high temperatures.

Figure 8 shows the European industrial sectors that required thermal energy in 2009. The most representative ones for high temperature are Iron & steel, and non-metallic minerals. For low temperature, it is the chemical sector. Figure 9 illustrates that the Germany, Italy, Spain, and France concentrate the highest thermal demand due to these sectors, therefore, they are the largest industrial markets for CHP.

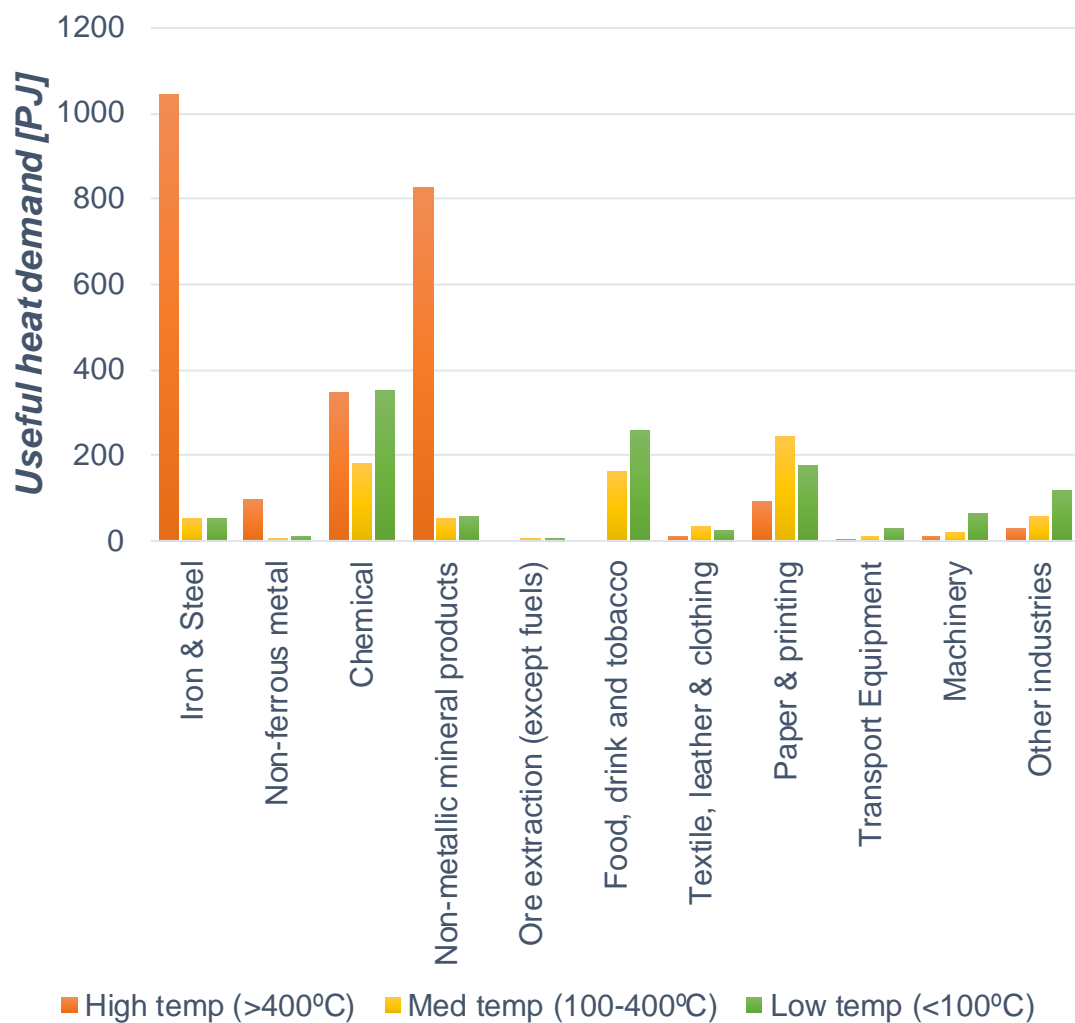


Figure 8 Industrial sectors that require thermal energy in Peta-Joules [PJ] (by temperature) for EU27 in 2009 [27]

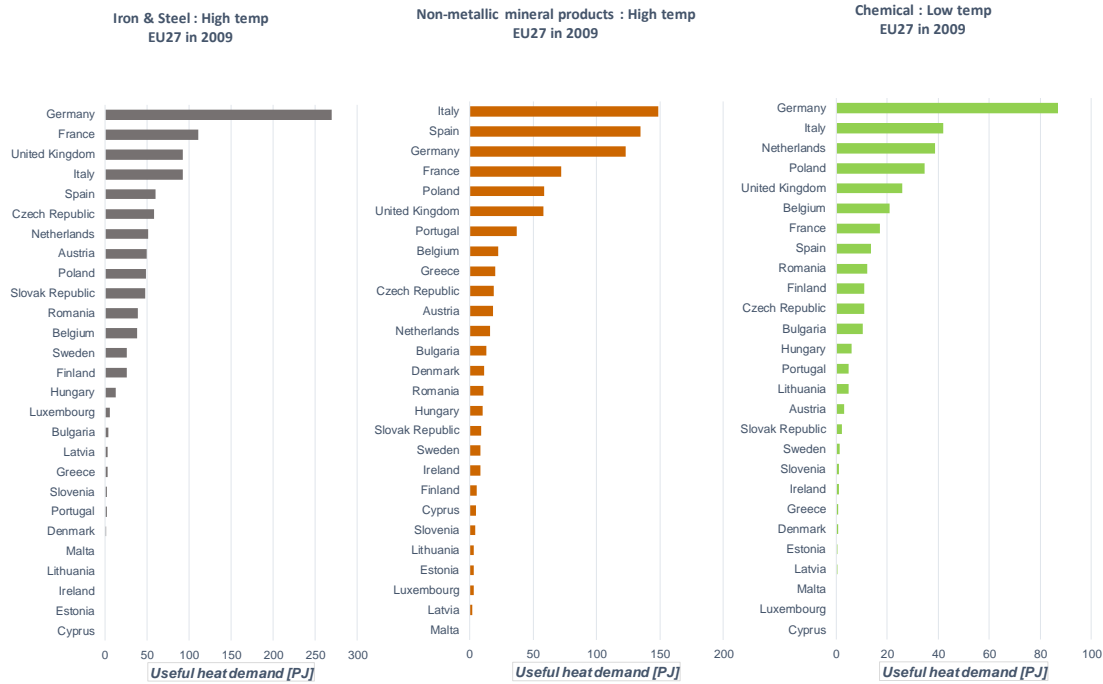


Figure 9 Useful heat demand for Iron & steel, and non-metallic minerals (high temperature) and chemical (for low temperature). EU27 in 2009 [27]

Services

For the OECD countries, the sector of services represents more than 70% of their GDP and 13% of their total final energy consumption. A significant share of this energy consumption, around 50%, is for heating and cooling, in order to provide thermal comfort for the building users (offices, schools, hospitals, shopping centers, etc.) Figure 10 shows that Germany, France, UK, and Italy concentrate the highest thermal demand in the service sector. CHP is used in this sector through the connection of the buildings to district heating (and cooling) networks or with the direct installation of CHP units in the facilities, like in the case of hospitals.

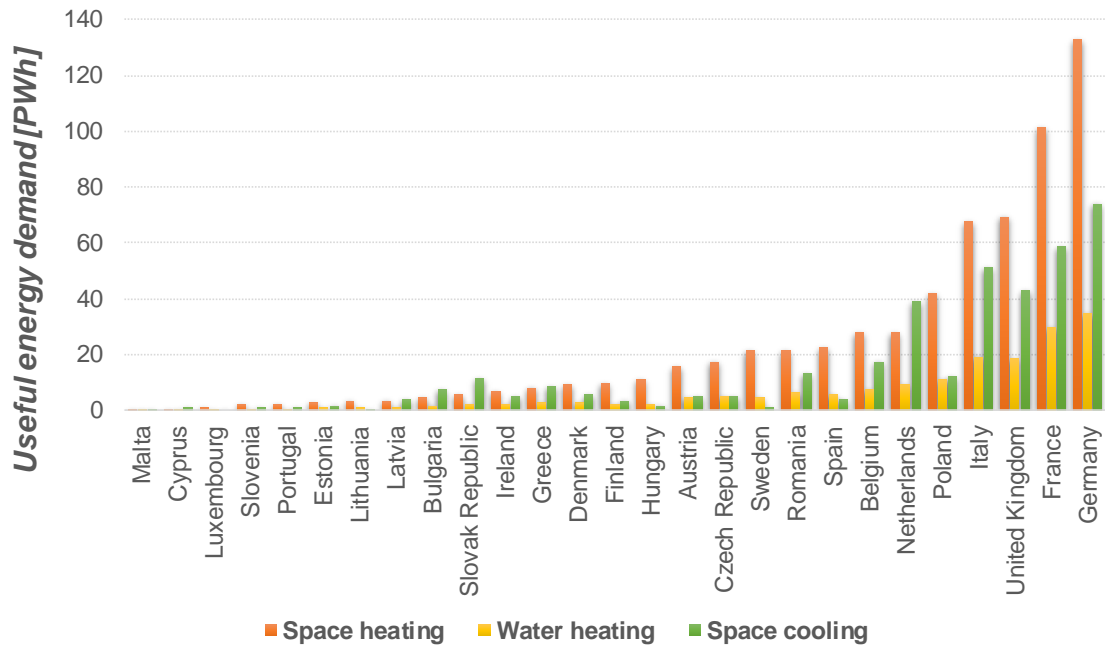


Figure 10 Breakdown of useful energy demand for the service sector in EU-27 for 2009

Households

For the OECD countries, the sector of households represents 21% of their total final energy consumption. And within the households, space heating consumes the most (Figure 11), in general with at least 50% of the share.

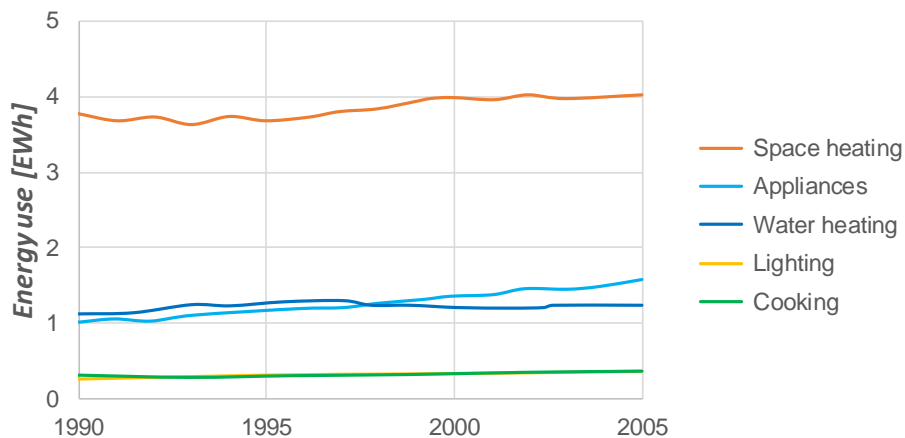


Figure 11 Household energy use (by end use) around the world [27]

As for the delivery of heating, hot water and cooling services to households, it is usually done through District Heating and Cooling (DHC) networks. These networks deliver hot water or cold water through a network of insulated pipes, from a central point of generation to the end user [35]. The generation can be done through a combined thermal and power energy system.

In Europe, the countries that have the largest energy demand for households are Germany, France, United Kingdom, Italy, and Poland (Figure 12).

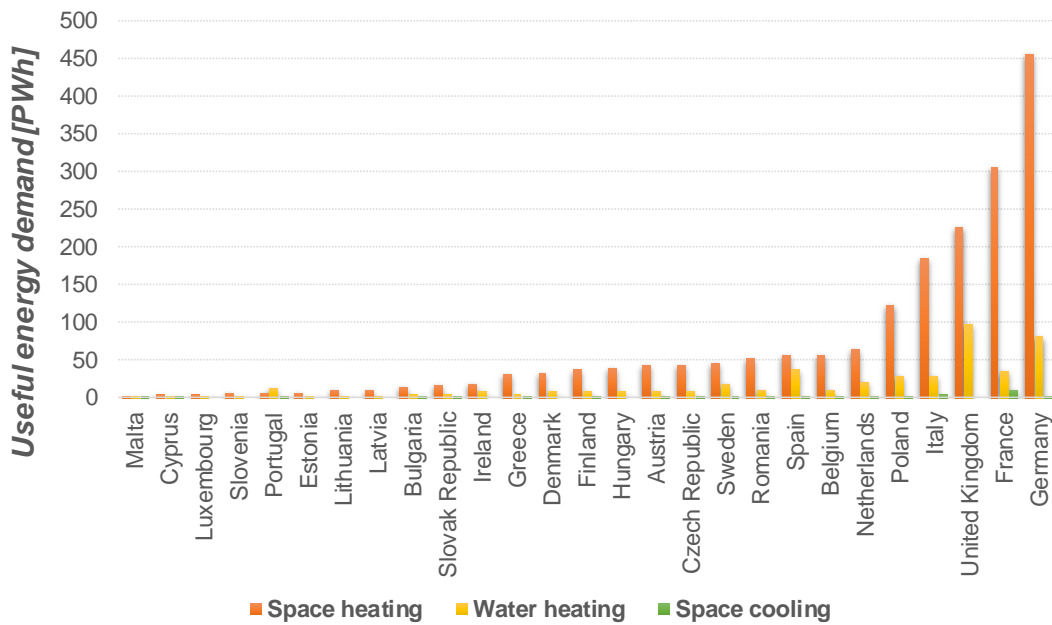


Figure 12 Useful energy demand for the residential sector in EU-27 for 2009

1.3.4 Key success factors for combined thermal and power energy systems

Figure 6 exhibits the countries that currently present a large penetration of CHP in the power generation. However, there are multiple factors influencing it. As stated by Persson [26], the climate, architectural characteristics, and cultural context are important because they determine the level of demand. However, Galindo Fernández [11] presented a list of key factors determining the success of the technology. They include governmental interest to reduce CO₂ emissions, a liberalized thermal energy market with low regulation, predictability of prices

and urban planning, and tax incentives. This statement is backed-up by multiple governmental reports ([12], [30]) that highlight case studies with different policies in place: building regulations and interconnection standards, feed-in-tariffs, green certificates, emission trading, and installed capacity grants. Galindo Fernández also identified some factors in terms of the market characteristics: competitive prices, local energy resources, possibility of economies of scale, and operation flexibility.

1.3.5 Perspective for thermal storage

There are three types of thermal energy storage technologies: sensible, latent and thermochemical. The first includes tank, pit, borehole, and aquifer. The second refers to phase change materials, and the third uses reversible chemical reactions.

According to the Department for Business Energy & Industrial Strategy in the UK [36], the cheapest are the pits and boreholes with a cost of 0.3-0.8 £/kWh. While the thermochemical storage can go up to 400 £/kWh. The report highlights that for any thermal storage technology, the cost decreases with the economies of scale, in other word, the size of the installation. Regarding the operation and maintenance cost, they are almost negligible.

The technology with the largest penetration is the water tank (sensible thermal storage). Although its price is not the lowest (25-180 £/kWh). It has an efficiency of 50-90% and the sector that mainly use it is the residential. However, it is also found on district heating and some commercial applications. They are generally coupled with solar thermal power systems (solar receivers), heat pumps, CHP, biomass, district heating, and solar PV (to transform the surplus of electricity into thermal energy). This technology foresees low chances of cost reduction. Mainly because the technology is already mature. In contrast, phase change materials and reversible chemical reactions have large probability to reduce their cost, but the forecast is uncertain.

Finally, the time-of-use tariffs are among the most relevant measures fostering the implementation of thermal storage technologies. This incentivize the consumption of energy at off-peak times and therefore the storing it.

1.4 Motivation

Cogeneration and trigeneration systems, with or without thermal storage, can contribute to the distributed generation of energy and reduce greenhouse gas emissions [12], [13], [16], [37], [38]. Still, and despite the maturity of the technology and its efficiency, its dissemination is still limited to some geographical areas and the potential of implementation is far from being exploited.

As identified, the barriers are mostly in the economic and regulatory domain, so the techno-economic assessment of this type of systems is vital to demonstrate the sustainability of its implementation and disseminate its use.

Research until now has targeted mostly their operational performance and feasibility. Regarding the techno-economic feasibility, several authors have established that the energy prices are important variables when assessing the systems. Their analysis is mostly focused on the impact of the Spark Spread rate (SS), which has been widely used across the scientific and industrial community as the economic indicator to evaluate the feasibility of implementation of this type of systems.

The spark spread, expressing the ratio between the cost of electricity from the grid and the CHP fuel (usually natural gas), is a variable that influences the economic feasibility of the systems. Still, many other variables also impact, such as the type of loads and its size, the individual prices of electricity and fuels (natural gas), rather than consolidated in the SS rate.

This thesis proposes a methodology to perform a systematic techno-economic analysis of the CCHP-TS systems. The objective is identifying the conditions that determine the feasibility of their implementation. In particular, the aim of this study is to identify and quantify the importance of five different variables while

evaluating the feasibility of trigeneration systems with thermal storage: the price of electricity [pE], the price of natural gas [pNG], the size of the annual energy loads of electricity [E], heating [H], and cooling [C].

Finding the set of values for these variables that make the CCHP-TS systems feasible could foster the interest of project managers, investors, and policymakers, and therefore encourage the adoption of this technology. Thus, it would be possible to also characterize the potential niche markets for its implementation. As an example, trigeneration systems with thermal storage are conceived to supply electricity, heating, and cooling in a decoupled manner. A potential market for this type of systems are the regions with sub-tropical desert climates (using the Köppen classification [39]). Those are the regions with the most intense solar radiation, according to the Global Solar Atlas [40], and potentially with the largest cooling demand (Figure 13). One of the objectives of this thesis is to explore the relevance of the size of energy demand, that indeed varies with the geography of the place.

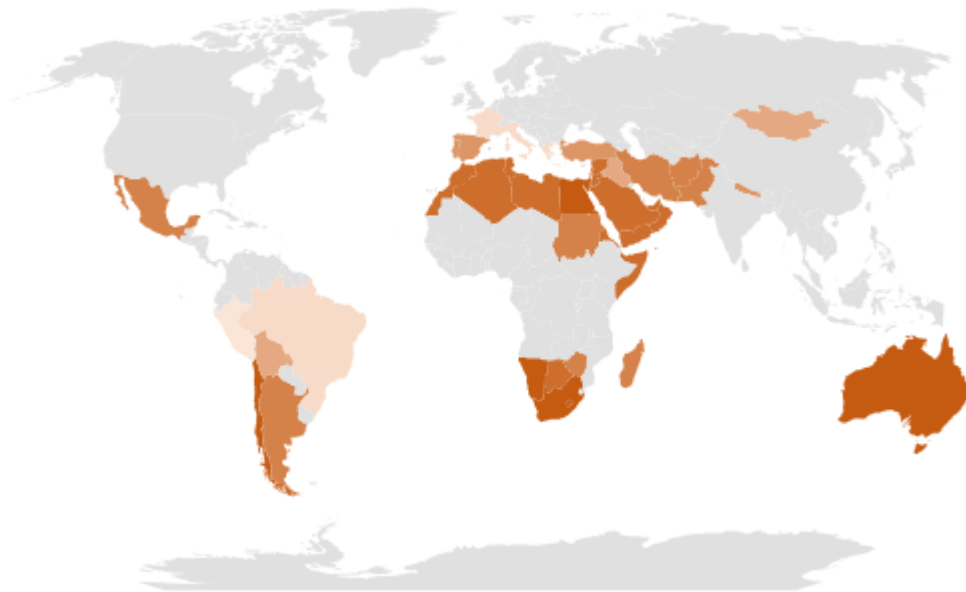


Figure 13 Subtropical desert places (adapted from the Global Solar Atlas [40])

1.5 Hypothesis and Research questions

Overall, this work aims to give answer to the following hypotheses:

1. There is a combination of energy prices (pE and pNG) and size of the energy loads (E, H, C) that make a Trigeneration – Thermal Storage feasible,
2. The energy prices should be considered separately, instead of consolidating them into the spark spread rate (SS).

Therefore, the main research question for this thesis is: What are the key variables and their combination that make more feasible the usage of Trigeneration – Thermal Storage?

The reader should note that the variables $E, H,$ and C are in this work expressed in terms of energy, instead of power.

Beyond the technical questioning presented above in the form of hypotheses and a research question, the development of the thesis required the implementation of different tools and approaches to give answer to these premises. Then, another objective of this work is to analyze and contrast the different steps taken at the methodology of the thesis. Finally, it is worthy to highlight that this work is developed using a university campus as a case study, as it is a representative profile of a combination of multiple energy services profiles (education, offices, etc.).

1.6 Outline of the thesis

This thesis is divided in six chapters. Chapter 1 introduces the context of the study, as well as the potential market and relevant sectors for a combined thermal and power energy system. It also outlines the motivation of the thesis and poses the hypotheses and research questions.

Chapter 2 reviews the state of the art of the feasibility analysis for combined thermal and power energy systems. It discusses the relevant variables that different authors have studied, the existent computational tools used to simulate these energy systems, the optimization algorithms typically implemented, as well as the general structure of the model used. Then, the chapter introduces an alternative to the existent computational tools. Finally, the chapter concludes with a discussion contrasting the typical sensitivity analysis methods used for the research in energy context and used for combined thermal and power energy systems.

Chapter 3 explains the general methodology of the work, which has been divided into two phases: the first is an exploratory analysis of the CCHP-TS model, and the second a deep sensitivity analysis of the feasibility study, combined with a comparison of three GSA approaches.

Chapter 4 corresponds to the first phase of the work. The objective is to demonstrate that the model for the CCHP-TS systems is relevant and sensitive to the variables of analysis (energy prices and loads). It combines tools such as full factorial design of experiments (DoE), DER-CAM simulation tool, k-Means clustering, and multicriteria decision making (MCDM). The results are shown in ternary diagrams and using load dominance rates.

Chapter 5 corresponds to the second phase of the work. It is a rigorous sensitivity analysis and compares three approaches: Morris, Sobol, and VARS. In this phase, thousands of simulations were required. Therefore, we needed to increase the simulation efficiency. For that, the CCHP-TS model was adapted into the programming language Python, using the optimization library PYOMO and the solver CPLEX.

Finally, chapter 6 outlines the overall conclusions of the thesis.

2 LITERATURE REVIEW

This chapter examines the state-of-art of the combined thermal and power energy systems. It summarizes how different authors assess their feasibility and the main features considered. It specially outlines which variables have been studied as main drivers. After that, it presents a review of the computational tools which use simulation to assist in the design, operation strategy and assessment of a CCHP-TS system. Among them, it highlights DER-CAM, a tool that comprises an optimization algorithm to maximize the benefits. Next section analyses those models which aim to optimize the design, and the operation strategy of combined thermal and power energy systems. Lastly, the chapter presents a review of works on the sensitivity analysis in the energy context.

The afore mentioned allows to conclude the chapter explaining the contributions of this thesis.

2.1 Combined thermal and power energy systems

Table 1 provides a list of journal papers studying the combined thermal and power energy systems. It indicates the type of system, the technologies studied (CHP, CCHP, or CCHP-TS), and the type of feasibility assessment (economically, environmentally, energetically, etc.). The assessment of a systems implies 1) determining the best design (installed capacity) and operation strategy of the proposed technologies, and 2) quantifying the benefits. This requires evaluating a model either analytically or through a simulation software. The evaluation is carried out through a parametric analysis or using an optimization algorithm.

The subsection 2.4.1 deepen the analysis of the optimization algorithms of these works.

	CHP	CCHP	CCHP-TS	Multi-objective	Economic	Environmental	Energetic	Energy	Analytics – Parametric	Analytics – Optimization	Simulation - Parametric	Simulation - Optimization	Others	Characteristics of case study	Energy prices	Fuel mix at grid generation	Type of prime mover	Energy loads / Energy load ratios	Peak loads	Fraction of energy produced with CHP	Efficiency of diverse equipment	Other characteristics of the equipment	Offices	Hotel	Hospital / Outpatient	Restaurant	Supermarket / Retail / Mall	Apartment / Residential bldg	Airport	District heating	Generic	Timestep for loads (F / A / S / M / D / H) ?
	Tech			Assmnt.			Solution type						Variables in sensitivity analysis						Case study													
Mago, 2007 [41]	*				*	*				*				*	*				*			*										A
Fumo, 2010 [42]	*					*		*												*										*	F	
Fumo, 2009 [43]	*			*	*	*		*												*		*									A	
Wang, 2011 [44]	*				*	*	*	*									*			*			*								H	
Li, 2008 [45]	*			*					*								*						*	*							S-H	
Wu, 2012 [46]	*		*	*	*	*		*						*			*												*		F	
Hajabdollahi, 2015 [1]	*			*					*					*		*	*												*		F	
Knizley, 2015 [47]	*			*				*									*					*	*	*	*	*					M	
Li, 2016 [48]	*	*	*	*	*	*	*						*	*		*						*	*				*				S-H	
Sundberg, 2001 [49]	*			*						*				*	*	*	*			*	*							*			S-H	
Hajabdollahi, 2015 [50]		*		*					*								*					*									M	
Memon, 2017 [51]	*			*				*						*	*	*	*			*							*				F	
Cardona, 2006 [2], [52]		*		*	*	*				*				*	*	*	*										*				H	

Table 1 Papers studying combined thermal and power energy systems
KEY for Loads: Fixed (F); seasonal (S); annual (A); monthly (M); daily (D); hourly (H).

These works can be sort into different categories depending on the variables the authors approach, the case studies used, and the timestep considered for the energy loads.

Regarding the case studies, there are several papers focusing on offices, hotels, and residential buildings. Others study district heating or different high energy intensity buildings such as hospitals, restaurants, supermarkets, and airports.

On the other hand, the timestep for the loads is interesting because the smaller it is, the higher the precision of the feasibility analysis. Table 1 shows that only Cardona [2], [52], Wang [44], Li [45], Li [48], and Sundberg [49] conduct it hourly. But the last three only analyze a typical day per season (S-H), instead of each month or day of the year, as Cardona [2], [52], and Wang [44] do it.

Finally, Table 1 also displays the variables that different authors have studied, considering them relevant to assess the feasibility of combined thermal and power energy systems. It is evident that most of them focus on energy prices and energy loads. But only Wu [46], Hajabdollahi [1], Memon [51], and Cardona [2], [52] analyze them together. And from those, only Cardona [2], [52] considers loads with hourly timestep. The following section 2.2 extends the analysis of the variables that different authors have studied.

2.2 Relevant variables for the feasibility analysis

The feasibility of combined thermal and power energy systems can be evaluated based on energy savings or cost savings. For the latter, the ratio between the cost of electricity and the CHP fuel, called spark spread rate (SS), has been identified as the key variable. Many authors have studied this variable. Some examples are Smith et al. [53] in the US context, Kavvadias et al. [54] and Fonseca et al. [55] in the European context, Tooukian et al. [53]–[57] in the Canadian context, and Chan et al. analyzing four cities (Qingdao, New York, Hong Kong, and Dubai) [57]. Moreover, some international governmental organisms have established as a general rule that the technology is economically feasible when the SS rate is higher than three [13]. In other words, the systems are likely to be feasible when the fuel is three or more times cheaper than the electricity from the grid. The physical understanding of this rule can be

explained by the electrical efficiency of the older thermal power plants, which is around 33% [58]. Intuitively the CHP is feasible if it has a better cost efficiency. Then, the SS threshold of three is inversely related with the electrical efficiency of thermal power plants [59].

Other key variables have been proposed in the literature to explain the feasibility of combined thermal and power energy systems. For example, to evaluate the primary energy savings generated by the CCHP system, Wang et al. [44] studied the influence of performance from different equipment. They found that the most sensitive parameter belongs to the electric generation at the separate production system, that is, the electric efficiency of the grid. Fumo et al [43] showed the relevance of the electrical efficiency of CHP and found that an increase of it reduces the primary energy used more than proportionally. The Midwest CHP Application Center [60] highlighted the importance of having a large number of CHP operating hours (greater than 3,000 hours/year). Mago et al. [41] evaluated the CCHP system based on the reduction of pollutants and identified the interest of the fuel mix used to generate electricity at the grid of each region. Then they propose that the CCHP system avoids more emissions in regions where electricity from the grid comes mainly from fossil fuels, especially coal.

In recent years, some authors have suggested that the size of energy loads also plays an important role to evaluate the feasibility of combined thermal and power energy systems. Authors such as Cardona et al. [52], Wang et al. [44], Mago et al. [41] and Fumo et al. [42] assessed the energy reduction generated by these systems, using respectively load rates (Heating/Electricity, Cooling/Electricity or Heating/Cooling), load rates vs. CHP production rates, and the fraction of electricity, heating and cooling loads covered by the CCHP. Similarly, Memon et al. [51], Wu et al. [46], Knizley et al. [47] and Hajabdollahi [1] used measures related to load size to assess the cost reduction of CHP or CCHP systems. Memon et al. [51] analyzed the net present value and payback period for using a trigeneration system in residential buildings. The authors found that the economic feasibility improves with the rise of fuel prices and load factors. They defined the heating and cooling load factors as the fraction of time the products are required in a year. Their parametric study included a variation between 0.2–

0.5 in the heating load factor and 0.4–0.75 in the cooling load factor. Wu et al. [46] applied Mixed Integer Nonlinear Programming (MINLP) to optimize the operation strategy of a micro-CCHP, conducting a screening analysis over a small range of SS and the size of electric and heating loads. They concluded that the operation strategy of a micro-CCHP is affected by load size (in instant energy, or power) and SS. For their part, Knizley et al. [47] proposed that the economic savings of a CHP system can be guaranteed when the ratio between electricity and heating loads of a building is less than three. Six out of eight case studies verify the hypothesis, using an SS=2.77. Finally, Hajabdollahi [1] studied the influence of load rates over the selection of the optimal prime mover for a Trigeneration system with Organic Rankine Cycle. The author concluded that, at given constant loads during the whole year, the gas turbine is convenient when heating loads are high, and the diesel engine is more suitable for high electric and heating loads.

The literature review indicates that energy prices and loads size are two interesting variables for the techno-economic assessment. Subsections 2.2.1 and 2.2.2 provide a context regarding their ranges of interest.

2.2.1 Energy prices

The last section introduced the spark spread as a relevant term for the feasibility of combined thermal and power energy systems. It was coined in the UK during the late 1990's in the context of trading and hedging opportunities [61]. And nowadays, this metric is widely used in the financial energy markets to quantify the profitability of buying fuel and selling electricity [62].

In the scientific context, authors such as Smith et al. [53] and Kavvadias et al. [54] proposed steady state equations to determine the minimum spark spread rate based on the efficiency of the CHP (electric and thermal), costs and loads.

The spark spread rate (SS) comprises the price of electricity and fuel (natural gas, for the purposes of the thesis). Therefore, it is relevant to explore their status worldwide. Figure 14 outlines that the largest electricity prices are paid in Europe and North America, while the lowest are in the Sub-Saharan Africa.

Sadly, these low prices in the sub-Saharan Africa have driven to bankruptcy to a number of power utility companies and obliged the state to subsidy part of the electrification costs [63]. Regarding the price of natural gas, Figure 15 shows that the largest prices are paid in Asia-Pacific and Europe, whereas the lowest are in the Former Soviet Union, Middle East, and North America. The low prices in the latter regions are related to the natural gas deposit they have available.

Household electricity price per region (2016)

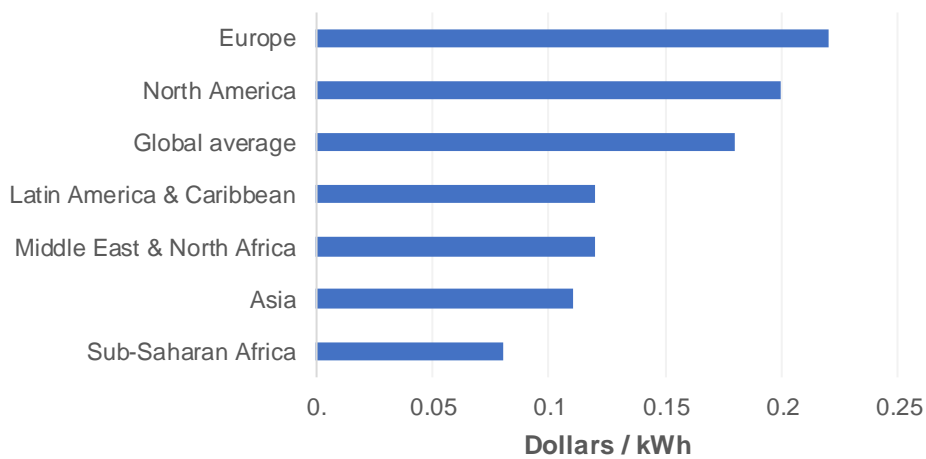


Figure 14 Household electricity price worldwide in 2016, by region (published by Statista Research Department [64])

Wholesale gas price per region (2018)
[Dollar per MMBTU]

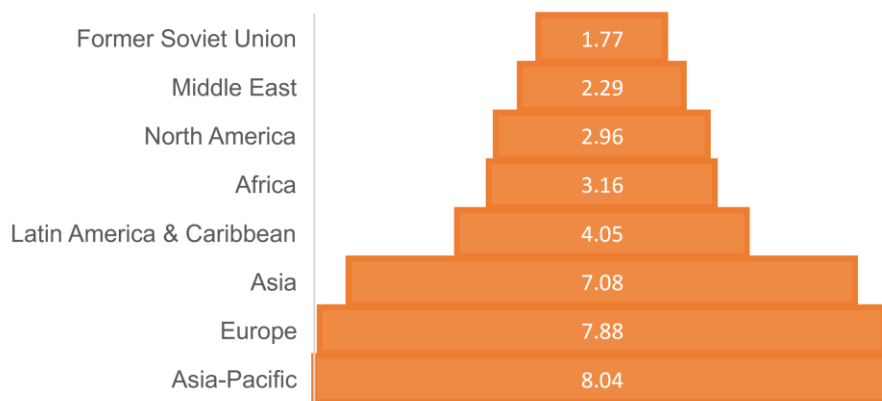


Figure 15 Wholesale natural gas prices worldwide in 2018, by region (data from the International Gas Union [65])

Europe, in average, has the largest electricity prices available, but also one of the highest prices of natural gas. Therefore, the interest of buying fuel and selling electricity is not straight forward. Then, it is crucial to conduct a feasibility analysis for combined thermal and power energy systems as detailed as possible.

Figure 16 shows the prices of electricity and natural gas for different European countries in 2017, according to Eurostat [66]. In the household context, the prices of electricity and natural gas present a strong linear correlation. However, in the industrial context, the prices are more independent.

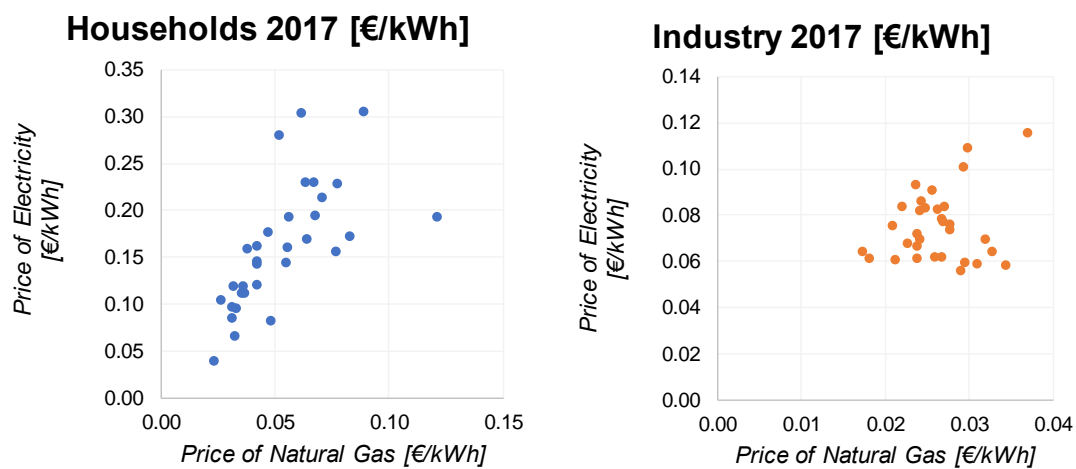


Figure 16 European energy prices 2017 [66]

It worth highlighting that the information of this section is based in average values. However, studying the average values of prices is a good approximation even for energy market with volatile prices, such as Europe. The reason is that empirically, the spot prices for these commodities display mean reversion [67], [68]. In other words, the price will tend to move to the average price over time. Given the above-mentioned, this work considers simply the average prices of energy, rather than the spot prices.

2.2.2 Energy loads

Combined thermal and power energy systems are recommended by multiple institutional reports [13], [30], [60], [69]–[72] as a sustainability measure.

This subsection provides some references of the possible cases for implementation, as well as their range of energy loads. Figure 17 describes these ranges depending on the dimensions of analysis.



Figure 17 Electric energy demand depending on the dimension of the case study

At a household level: According to the World Bank and the IEA statistics in 2014, the worldwide average electric consumption per capita was 3.13 MWh/y [73]. Moreover, the United Nations published that worldwide, the number of members per household ranges from three to six persons [74]. Therefore, an average household worldwide, consumes between 9.39 and 18.78 MWh/y.

At block and neighborhood level: It is possible to take the example of some of the most energy intensive squares in Manhattan, New York [75], that can go up to 80.2 GWh/y of electricity, 70 GWh/y for space heating and 12 GWh/y for space cooling.

At buildings level: There are some high intensity buildings in terms of energy consumption, such as airports, hotels, hospitals, university campi, etc. For hotels, Wang et al. [44, Fig. 4,5,6.a] studied a 5-stars hotel with electricity, heat and cooling demand of approximately 1.5, 2.4 and 3.9 GWh/y respectively. Regarding University campi, there are examples such as the IST Alameda Campus [76], which demand is approximately 2.4, 0.6 and 1 GWh/y, respectively for electricity, heat and cooling, but there are some other examples of larger demand; such as the West Campus of the University of Illinois, in Chicago [77] that has an CHP installed capacity of 21 MW_e, being able to produce up to 147 GWh/y. Talking about airports, according to the examples provided by Cardona et al. [52, Fig. 1,2], their energy consumption can go from 20 GWh/y to more than 150 GWh/y, such as the Malpensa Airport in Milan,

whose electricity, heat and cooling demand are approximately 151, 129.3 and 102.5 GWh/y. However, there are larger airports such as Heathrow, that is 17 times larger in area than Malpensa and serves 3.5 times the number of passengers than in Milan.

At a regional level: A reasonable energy demand size for region could start in 500 GWh/y. This would be assuming a region with 160,000 inhabitants, and considering 3.13 MWh/y as the electric consumption per capita, as given above [73]. In terms of technical viability, Wu et al. [78] found, as part of their literature review, that CCHP systems could be as large as 300MW when supplying energy to districts.

2.3 Computational tools to simulate energy system

Some computational tools assisting the design, operation and feasibility assessment of distributed energy generation are in Table 2 and Table 3 [79]–[87]. All tools analyzed assess the techno-economic feasibility (Assmnt.), and some also the environmental one. Most of them running easily in Windows platform, while others require GAMS programming language to run.

A very important aspect is the solution method which can be run either by scenarios or optimization. The first reside on the idea that the user tests different setups and manually distinguishes the most appropriate. In contrast, software with optimization capabilities such as DER-CAM, BALMOREL, COMPOSE, TIMES/MARKAL, and HOMER use algorithms to get the proper type, size and operation schedule of technologies. From the five aforesaid, only DER-CAM, and COMPOSE are free access. But the second is mostly designed to assess single project, rather than microgrids (Table 3). A microgrid is usually more complex than a single project, because it is a local energy grid with control capability and able to operate autonomously from the traditional grid [88].

Software	Institution	Platform required to run	Comments
DER-CAM	LBNL, US	Web-based Windows	Written in GAMS and uses MILP as optimization algorithm.
Energy PLAN	Aalborg University, Denmark	Windows	
Energy PRO	EMD International A/S, Denmark	Windows	
LEAP	Stockholm Environment Institute, Sweden	Windows	
BALMOREL	Different institutions in Baltic countries	GAMS	-Any user can modify the tool to suit specific requirements (open source). -BALMOREL is free, but GAMS is not. -Depending on the situation, the optimization algorithms used are LP (linear programming), QP (quadratic programming), MILP (Mixed Integer Linear Programming), MIQCP (mixed integer quadratic programming), or RMIP (relaxed mixed integer programming).
COMPOSE	Aalborg University, Denmark	Windows	-It is a parametric linear programming model. -It integrates MILP model generation and solving. It works with any solver (Gurobi, CPLEX, COINMP, etc.). -It has Monte Carlo risk assessment. -It interacts with energyPRO, EnergyPLAN, and RETScreen
BCHP Screening Tool	Oak Ridge National Lab, US		
RETScreen	NRCAN, Canada	Excel / Windows	
TIMES/MARKAL	IEA-ETSAP (international)	Windows	It runs with GAMS and a solver.
HOMER	NREL, US	Windows	It is designed for stand-alone systems.

Table 2 General characteristics of the computational tools [79]–[81], [86], [87]

	Multi-objective	Economic	Environmental	Optimization	Scenarios	Single plant/equipment analysis	Microgrid	Bottom-up approach	Top-down approach	CHP	Boiler	Absorption chiller	Heat storage	Cold storage	Allow variation of the electricity price?	Free access? (P) - partial free access	Simulation time step (m / H / D / M / Y)	Time span for planification	No. of papers referring it (since 2005 until Dec 1 st , 2019)
	Assmnt.	Sol.	Case	Apch.	Technologies	Other charac.													
DER-CAM [86]	*	*	*	*		*	*			*	*	*	*	*	*	*	H	1y	397
Energy PLAN		*	*		*	*	*			*	*	*	*	*	*	*	H	1y	1220
EnergyPRO		*			*	*	*			*	*	*	*	*	*		m	40y	521
LEAP		*			*	*	*	*	*	*	*	*	*	*		P	Y	any	712
BALMOREL [87]		*		*		*	*			*	*	*	*	*			H	50y	1160
COMPOSE [83]		*		*		*	*			*	*	*	*	*	*	*	H	any	17
BCHP Screening Tool		*			*	*	*			*	*	*	*	*		*	H	1y	68
RETScreen [84]		*			*	*	*			*	*	*	*	*		P	M	50y	3750
TIMES / MARKAL		*	*	*		*	P	*	*	*	*	*	*	*			H	50y	147
HOMER [82], [85]		*		*		*	*			*	*	*	*	*	*		m	1y	16000

Table 3 Specific characteristics of the computational tools [79]–[87]

KEY: Partially (P); by minute (m); hourly (H), daily (D), monthly (M); yearly (Y); years (y).
NOTE: The last column reports the number of papers that appear by searching in Google Scholar the keywords: “name of the software” + simulation. For LEAP: simulation + LEAP + “Long-range Energy Alternatives Planning system”. For COMPOSE: simulation + COMPOSE + “Compare Options for Sustainable Energy”. For HOMER: simulation + model + HOMER + energy + software.

There are other six relevant characteristics of a software tool that this thesis evaluates. 1) The approach it uses (Apch.): Mostly all tools use a bottom-up approach, where the user builds the case study by taking small pieces of information and constructing the subsystem-level as accurate as possible. 2) The technologies it can simulate: Modeling a CCHP-TS system requires at least the use of CHP, boiler, absorption chiller, and heat and cold storage. All tools,

except EnergyPLAN, RETScreen, and Homer have them available. 3) The possibility to vary the price of electricity: That is relevant for markets with time-varying price, such as Europe. Only DER-CAM, Energy PLAN, EnergyPRO, COMPOSE, and HOMER have that feature. 4) The time step during the simulation: That determines the precision of the loads, and the smaller the time step in the loads, the higher the precision of the feasibility analysis and operation strategy. Any tool with hourly or by the minute time step is preferable. 5) the planification timespan: One year would be enough for operative and financial purposes, but the user must verify that the installation costs consider the time value of money. 6) The adoption of the tool over the scientific community: This is related to the relevance of the tool, as well as the documentation and support available. We quantify it in the last column of Table 3, reporting the number of papers referring to the software tool. That could include papers that use it to conduct an analysis, or papers that only mention its name.

After the analysis in this section, it is possible to state that DER-CAM offers some comparative strengths over the others computational resources optimizing the design and operation strategy of a microgrid. DER-CAM is a free access tool that follows a bottom-up approach and includes all the technologies required to simulate a CCHP-TS system. It allows for an energy price variation. Its planification time span is one-year, and the simulation time-step is in hourly basis. Moreover, the documentation available is detailed enough to understand and analyze the methods used and the assumptions done. The subsection 3.2.2 describes its characteristic in detail.

2.4 Modeling and optimization of combined thermal and power energy systems

Until this point, it has been discussed that the assessment of combined thermal and power energy systems is done either analytically or through computational

tool to simulate. Moreover, the section 2.3 emphasized the importance of using computational tool that provide the optimal solution.

This section presents a review of the optimization algorithms that different authors have used. Afterwards, it explains the general mathematical model to optimize a trigeneration systems with thermal storage. And finally, it presents a free computational solution to modeling and optimization.

2.4.1 Optimization algorithms for combined thermal and power energy systems

A model is a set of mathematical expressions that describe a system. An analytical model is based on Physics laws and a parametrical one is based on the characterization of experimental data. Once the model is formulated, it can be used to simulate or optimize.

To assess the feasibility of combined thermal and power energy systems, authors such as Cardona et al. [89] and Angrisani et al. [90] collect data through experimental pilot plants. This is the basis to build a parametric model. While Cardona et al. [89] provides the detailed experimental measurement methodology, Angrisani et al. [90] reports the results of a case study in Frignano, Italy. They even formulate a set of expressions comparing the operational cost, PES (primary energy savings) and CO₂ emissions with the conventional scenario. On the other hand, Mago et al. [41], Fumo et al. [42], Wang et al. [44], and Knizley et al. [47] are authors who develop analytical models to simulate in steady-state. The first three assess the energy and emission reduction, and the other assesses the cost reduction.

However, the object of interest for this section and Table 4 are authors that design analytical models to optimize. Wu et al. [46], Hajabdollahi [1], and Hajabdollahi [50] develop models for steady-state. They implement a multi-objective MINLP, Genetic Algorithms (GA) and Particle Swarm Optimization (PSO) respectively as optimization algorithms for the cost reduction. However, there are other authors that work with dynamic models. These capture the behavior of the systems across the different hours of the year. For example,

Cardona et al. [2], [52] and Li et al. [91] dynamically assess the energy reduction for CCHP systems using LP and GA. While H. Li et al. [92], C.Z. Li et al. [45], and Sundberg [49] dynamically assess the cost reduction using GA, MINLP, and MILP respectively. Similarly, computational tools, such as DER-CAM, BALMOREL, and COMPOSE, base their dynamic analysis in MILP.

As side comment, the LP optimization used by Cardona [2], [52] is possible because it is a simpler model without integer variables. The model already proposes the design of the system (installed and functional capacity of the equipment) and simply optimizes the operation strategy. Then, the authors calculate the marginal cost of each configuration and conducts a LP for each hour of the year.

	LP	MILP	MINLP	PSO	GA	Comments
Li, 2008 [45]			*			Linearize the non-linear items. And uses the barrier method and branch & bound.
Wu, 2012 [46]			*			Multi-objective MINLP calculated hierarchically through the lexicographically stratified method.
Hajabdollahi, 2015 [1]					*	Real Parameter Genetic Algorithm (RPGA).
Sundberg, 2001 [49]		*				MILP with Branch & Bound in the software MODEST.
Hajabdollahi, 2015 [50]				*	*	
Cardona, 2006 [2]	*					Linear programming with a code in Visual Basic.
Li, 2019 [91]					*	It uses quantum genetic algorithm (QGA) and simple genetic algorithm (SGA)
H. Li, 2006 [92]					*	
DER-CAM [86]		*				Uses GAMS
BALMOREL [87]		*				Uses GAMS
COMPOSE [83]		*				

Table 4 Papers using optimization algorithms to assess the feasibility of combined thermal and power energy systems

From the table above, it can be said that MILP and GA are the most often used optimization methods [93]. Although metaheuristic methods, such as GA, produce good solution quickly, the optimality is impossible to guarantee [94]. In contrast, MILP find optimal solutions, but they require the simplification of non-linear behaviors embedded in the energy scheduling optimization [93]. In any case, mathematical methods, such as MILP, are a good first choice [95]. It is due to their simplicity that allows gaining insight in the structure of the problem, and because there is a wider amount of solvers available [95], [96].

2.4.2 The general structure of the optimization model

All the models mentioned in subsection 2.4.1, are based on energy balances. And, independently from the optimization algorithm used, the general structure of the model is as follows:

Objective function: Minimizing cost, emissions, or energy consumption.

Constraints

- Equality Constraints
 - The demand of the three energy vectors is fully covered (electricity, heat, and cold).
 - The heat produced by each CHP units is tied to its electricity production (considering the corresponding efficiencies).
 - The state-of-charge of the thermal storage at each hour is tied to its state-of-charge on the previous hour: inputs and outputs (considering the decays of energy corresponding to its storage)
- Inequality Constraints
 - The electricity production of all CHP units does not exceed their installed capacity, but it is larger than a minimum production level. It also considers the efficiency of the equipment.

- The amount of active CHP units each hour does not exceed the CHP units installed.
- The Installed capacity of units such as boiler, vapor-compression chiller, absorption chiller, and thermal storage, is not exceeded (considering the corresponding efficiencies).
- The state-of-charge of the thermal storage does not go lower than a minimum level. This is a technological constraint.
- The input and output of the thermal storage do not exceed the maximum charge and discharge rate.
- A restriction to avoid an input and an output from the thermal storage within the same hour (timestep). That would not make sense in terms of optimal management of energy.

The variables of the model are divided into three types:

- ✓ Non-negative integer variables
 - To determine the installed capacity of units such as boiler, vapor-compression chiller, absorption chiller, and thermal storage.
 - To determine the number of CHP units installed, and how many are active at the time t .
- ✓ Non-negative real variables
 - To quantify the electricity imported from the grid at the time t .
 - To quantify the electricity and heat produced by the CHP and boiler, at the time t .
 - To quantify the electricity and heat consumed by the vapor-compression and absorption chiller at the time t .
 - To quantify the state-of-charge, input and output of the thermal storage at the time t .

✓ Binary variables

- To activate the fixed capital cost of units such as boiler, vapor-compression chiller, absorption chiller, and thermal storage, when their installed capacity is over zero.
- To avoid having an input and output of the thermal storage within the same hour.

2.4.3 PYOMO – CPLEX : a computational alternative

The section 2.3 provided a list of computational tools assisting the design, operation and feasibility assessment of distributed energy generation. At least three of them have been written in GAMS. Which is a commercial software system combining mathematical algebra and computer programming to solve optimization problems [97].

As an alternative to GAMS, the combination of PYOMO – CPLEX has the capability to solve MILP problems, appropriate for the feasibility assessment of CCHP-TS systems.

PYOMO [98], [99] is a Python-based open-source software package supporting optimization capabilities. It is an effective framework to develop Python scripts, and includes optimization solvers for stochastic programming, dynamic optimization with differential algebraic equations, and mathematical programming with equilibrium conditions. It allows the formulation of complex model, even as object-oriented, allowing a variety of modelling components: sets, scalar and multidimensional parameters, decision variables, objectives, constraints, equations, etc.

The functionality of PYOMO is usually associated with algebraic modelling languages (AML) that support the analysis of mathematical models with a high-level language. An AML does not solve the problems directly. Instead, it calls external algorithms (solvers), to obtain a solution [100]. Then PYOMO provides a general interface for the solver, such as CBC, CPLEX, FortMP, Gurobi, MINOS, IPOPT, SNOPT, KNITRO, and LGO.

Among them, the IBM ILOG CPLEX Optimization Studio [101] is a recognized solver in the industrial and academic contexts. CPLEX is suitable to solve MILP problems, that are much harder to solve than LPs, and uses the Branch & Bound (B&B) algorithm [102]. This is a systematic search over the possible combinations of the discrete variables (as if they were branches of a tree). Moreover, it uses linear or quadratic programming relaxations to find bounds on the solution. The B&B search stops when every partial solution in the tree has been either branched or terminated, or when the gap between the upper and lower bounds becomes smaller than a certain threshold [103].

2.5 Sensitivity analysis

Sections 2.1 and 2.2 have explored the variables that different authors have studied, considering them relevant to assess the feasibility of combined thermal and power energy systems. This section aims to show 1) how the authors of Table 1 have conducted their variables analysis and, 2) how other authors in the field of energy analysis have done it in different contexts. The following paragraphs, along with Table 5 give the insights.

Across the literature, there are different ways to assess the impact of the parameters or variables within an output function. The simplest way is to vary one parameter around an initial baseline value and measure the impact on the output. That is called “**one-at-a-time**” (OAT) sensitivity analysis [49], [104] and normally it is made locally. The disadvantages of OAT include that it is time consuming when parameters are numerous, it does not capture non-linear and interactions effects (when the effect of one factor depends on the value of another one), and it becomes a non-explorative method at high dimensional space. The latter is the result of the curse of dimensionality, and it means that the more parameters, the lower the size of the hyperspace that is explored, converging to zero [105], [106].

Paper	Application	Approach							Comments	
		OAT (parametric analysis)	Sets of parameters	Derivative-based SA (GSA)	RSA (GSA)	Variance-Based SA (GSA)	VARS (GSA)	Factorial DoE		Others
Jaxa-Rozen, 2018 [104]	Generic			*		*			*	Random forests and extra-Trees compared with Sobol and Morris.
Razavi, 2016 [110], [111]	Hydrological modeling			*		*	*			VARS is compared with Sobol and Morris as reference.
Sarrazin 2016 [112]				*	*	*				Analysis with Morris, RSA, and Sobol.
Garcia Sanchez, 2014 [113]	Building thermal energy model			*						Morris method with first and second-order sensitivity analysis.
Shen, 2013 [115]						*				FAST, with uncertainty analysis based on the Monte Carlo with LHS.
Spitz, 2012 [114]						*				Analysis with Sobol.
Knizley, 2015 [47]	Feasibility of CHP		*							
Sundberg, 2001 [49]								*		Full factorial design of experiments with runs at two levels.
Memon, 2017 [51]	Feasibility of CCHP	*								
Mago, 2007 [41]		*								
Fumo, 2010 [42]		*								
Fumo, 2009 [43]		*								
Wang, 2011 [44]		*								
Li, 2008 [45]		*								
Wu, 2012 [46]		*								
Hajabdollahi, 2015 [1]		*								
Cardona, 2006 [2]		*								
Hajabdollahi, 2015 [50]	Feasibility of CCHP-TS		*							Varies the case study in three different climates.
Li, 2016 [48]			*							Fuzzy logic analysis w/weighting method for different set of factors.

Table 5 Types of sensitivity analysis methods used in energy analysis

Another alternative is to build scenarios with **different sets of parameters**. This is suitable for the analysis of major changes, but neither does it captures non-linear and interactions effects [49].

Most of the papers assessing the feasibility of combined thermal and power energy systems belong to the two categories above [1], [2], [50], [51], [41]–[48].

A more rigorous alternative is to use a **global sensitivity analysis (GSA) method**. It evaluates the importance of each input over the model output by exploring each parameter across the domain of all the other inputs. Yet, using GSA methods is not a fully deployed practice in the scientific community. Saltelli et al. found that less than 40% of papers of the energy field use GSA methods [107]. In 2013, Wei et al. [108] conducted a review which concluded that the main GSA methods used for energy analysis are: screening-based, variance-based, regression, and meta-model based approaches. Similarly, Song et al. [109] presented a pie chart reflecting that Morris, Sobol, and FAST were the most popular GSA methods used between the years 1996 and 2013 for water resources and environmental sciences. Table 5 consolidates a number of papers that take Morris and Sobol as regular reference methods [104], [110]–[112], or use them separately [113], [114]. Similarly, there are specific cases using FAST [115], RSA [112] and VARS [110], [111].

Apart from the GSA methods, there are other “unconventional” methods to assess sensitivity analysis. For example, Jaxa-Rozen suggests using **decision tree-based ensemble methods** (random forests and extra-trees) applied to sensitivity analysis problems [104]. The method of extra-tree performs favorably compared to Morris. But that is not the case against Sobol, because decision tree-based methods only return the relative importance of the inputs, rather than their direct effect on the output variance. Finally, another option is to use **design of experiment (DOE) methods** for sensitivity analysis purposes [116]. That is the case of Sundberg et al. [49] which assess the economic feasibility of a CCHP system by varying 25 factors using a full factorial design of experiments with runs at two levels. Besides, there are different experimental design methods: full factorial, central composite design (CCD), Box-Behnken design (BBD), among others. Rakic et al. [117] conducted a comparative analysis of them for a

pharmaceutical application and found that the three-level full factorial design and CCD created significantly better models than the two-level full factorial design and BBD. They also highlighted that CCD requires less samples than three-level full factorial design, but that also means that the latter has more degrees of freedom. This is helpful to create more reliable models, especially when experimental errors are present. Additionally, the National Institute of Standards and Technology (NIST) [118] shows a table indicating that when there are five factors or more, it is better to use a DoE such as factorial design for screening purposes.

In summary, the factorial DoE seems an adequate alternative to the popular OAT and the rigorous GSA. It ensures the best choice of sample points within a space, it is simpler than GSA methods, but at the same time corrects the main drawback of OAT regarding its local analysis. Additionally, it gives an idea of the interaction effects between parameters because it changes several factors simultaneously.

Altogether, this section revealed that most of the authors conducting sensitivity analysis for combined thermal and power energy systems, use a simple parametric analysis (OAT) [1], [2], [41]–[46], [51]. As for the use of global sensitivity analysis methods (GSA), it is rare for this application although it is extensively used in the energy analysis context. Morris and Sobol are the most popular GSA methods across the literature. However, VARS is also an interesting and novel approach that characterizes the variation of the model at different points and scales.

Morris is a derivative-based or screening-based method, ideal to identify the significant factors for the output, without quantifying it exactly. It aims to deal with many input factors while keeping a small number of samples. As a drawback, while it helps to recognize that interaction effects among parameters exist, it does not identify them precisely. Unless the second order sensitivity index is calculated [113], but that in turn makes the method computationally expensive. On the other hand, derivative-based approaches, similar to OAT, suffer the curse

of dimensionality and becomes a non-explorative method at a high dimensional space [105].

Sobol is a variance-based method ideal for risk assessment, but it is computationally expensive [119]. It assesses how much the variance of the output depends on the uncertain input factors and decomposes it accordingly. Moreover, it identifies non-linearities and non-additive properties of the model, quantifying the interaction effects among parameters. According to Saltelli et al. [120], Sobol method is superior than FAST on the capacity to easily compute high-order indexes. Moreover, this method does not suffer the curse of dimensionality.

VARS (Variogram Analysis of Response Surfaces) [110], [111] is a new GSA method proposed by Razavi in 2016. It arises as an alternative to Morris and Sobol. VARS is computationally less expensive than Sobol, but it explores the full range of the input factors. It uses an anisotropic variogram concept to characterize the variation of the model at different points and scales. Thus, it allows raking the relevant variables at different points of the range.

2.6 Position of the thesis

Chapter 2 is devoted to exhibiting the state of art for the feasibility assessment of combined thermal and power energy systems. Likewise, it highlights the importance of energy prices and energy loads as relevant variables.

The first and most evident remark across chapter 2 is the lack of studies on the technological combination of Trigeration and Thermal Storage. Moreover, the ones studying it (Hajabdollahi [1], Li et al. [48], and Cardona et al. [2] from Table 1) have a dearth in the joined analysis of energy prices and loads as relevant variables. Hajabdollahi study, both, energy prices and loads, but the loads are in monthly basis. As explained in section 2.1, a smaller time-step in the loads is important because it gives more precision to the feasibility analysis. This higher precision is a must for context like the European, where the interest of buying

fuel and selling electricity is not straight forward due to the large energy prices (see the last paragraph of subsection 2.2.1). Regarding Li et al., they do not study neither energy prices nor loads. As for Cardona et al., they analyze both in hourly basis, but the model they propose only optimizes the operation strategy, while the design (installed capacity of the equipment) is an assumption.

The second remark from subsection 2.2.2 is that university campi, depending on the place and climate, are suitable application for combined thermal and power energy systems. The reason is that they are high energy intensity buildings. Moreover, several institutional and industrial reports present them as a usual application of CHP [69]–[72]. Therefore, the analysis of their load profiles seems promising.

The last remark is the high relevance of the economic feasibility. Most of the papers assess it, and all governmental organizations take it as parameter to invest in this kind of projects.

Said the above, this thesis aims to study the techno-economic feasibility of Trigeneration-Thermal Storage systems (CCHP-TS). The focus is the attribute relevance analysis for energy prices and size of the energy loads. All this, taking a university campus as case study.

3 METHODOLOGY

3.1 General methodology

The methodology is divided in two phases, presented in Figure 18.

The first phase (developed in chapter 4) corresponds to an exploratory analysis to examine the relevance of the CCHP-TS model, its feasibility, and its sensitivity to the selected variables (energy prices and loads). To do so, DER-CAM and its embedded model is used. As for the sensitivity analysis method, full factorial DoE is used due to its simplicity, capacity to analyze globally, and possibility to identify interaction effects. Once the simulations are conducted, clustering is implemented to analyze the data and get the pertinent conclusions. The learnings from this phase are cornerstone for the second one, because the objective is to demonstrate that the model developed in DER-CAM is sensitive to the variables of analysis.

The second phase (developed in chapter 5) is a deep sensitivity analysis of the feasibility study, combined with a comparison of three GSA approaches: Morris, Sobol, and VARS. Each of them uses their corresponding sampling methods (LHS, and Monte Carlo). To understand the relevance of a sensitivity analysis, subsection 3.3.5 highlights how a study with GSA complements the insights obtained by a full factorial DoE. Regarding the energy system optimization, as DER-CAM is not adapted to conduct global sensitivity analysis (developed further in subsection 3.2.2.1), it is proposed an adapted model of a CCHP-TS system developed in Python. The model is based on energy balances and uses the MILP algorithm for the optimization step. As seen in the subsection 2.4.1, MILP is the most appropriate method for this type of application. The implementation is done by using the library PYOMO and the solver CPLEX to optimize.

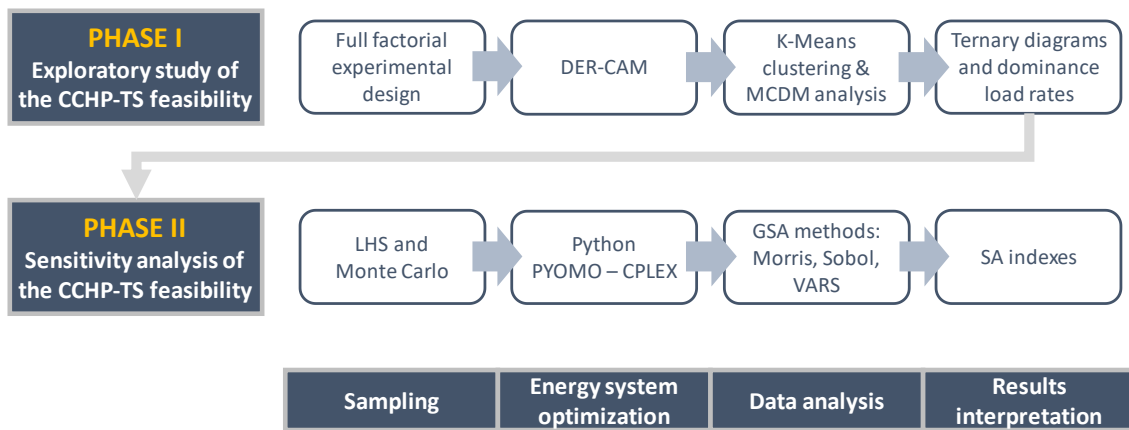


Figure 18 General methodology of this thesis

3.2 Phase I: Exploratory study of the CCHP-TS feasibility

3.2.1 Full factorial DoE

Design of experiments (DoE) is a branch of statistics [121], [122] with the objective of obtaining the maximum information from the minimum number of experiments. Conduct an ideal DoE should include: 1) designing the experimental space to include the critical ranges of the inputs of a model; 2) varying the inputs to study their individual and interaction effects; 3) designing the experiment to account the variability due to external factors (operators, raw materials, or processes). The latter mainly applies to experiments, rather than simulations.

There are different DoE methods: one-at-a-time (OAT) that explore the factors one by one, but does not identify interaction effects; orthogonal design of experiments, such as Taguchi, that reduces experimental runs at a loss in experimental resolution and do not find interaction effects; and factorial DoE, that explores all the factors at the same time and recognizes interactions effects.

Full factorial DoE [122], [123] is an design of experiments method studying the effect of the input factors over the model. It explores every possible combination of factors and their levels. The method requires n^k runs, where k is the number of factors, and n the number of levels. Full factorial DoE is an expensive method; therefore, it is recommendable when a reduced number of features are studied.

When there is a previous knowledge of the system, it is possible to reduce the samples, by conducting a fractional factorial DoE, although the full factorial DoE is more useful in terms of the information. Another alternative is to conduct it with a low resolution full factorial DoE to identify the main effects, and then a high-resolution one [122].

In this work, a full factorial DoE is conducted, aiming to examine a wide range of the variables. The results of this exploratory phase provide the direction to increase the resolution in following steps.

3.2.2 Modeling and optimization in DER-CAM

3.2.2.1 About DER-CAM

DER-CAM (Distributed Energy Resources Customer Adoption Model) is a tool created by the Lawrence Berkeley National Laboratory (LBNL) in 2000. Its purpose is the simulation of buildings or multi-energy microgrids finding their optimal design and operation strategy (best combination of technology) to supply energetic needs.

DER-CAM is written in GAMS but runs either in a Web-based environment or in the Windows platform. The solvers included in GAMS allow to use a Mixed Integer Linear Programming algorithm (MILP) to minimize the total annual cost, or the CO₂ emissions, or both.

DER-CAM has been typically used in the context of microgrids [124], [125] supporting the investment and planning of energy services such as space heating and cooling, hot water, and electricity for appliances. Additionally, it includes modules for thermal storage [126], demand response, ancillary grid services [127] and multi-node modeling approach [128]. All these features have made DER-CAM the chosen tool for a number of publications with different purposes: assessing the feasibility of distributed energy generation [129], [130]; combining the distributed generation with energy conservation measures [131]; analyzing the performance of the electrical distribution circuit for microgrids

[132]; and even studying the integration of communication technologies and information models for the integration and interoperability of distributed energy generation systems [133].

A significant drawback of DER-CAM is the impossibility to conduct sensitivity analysis in an efficient manner. DER-CAM, in its current state, requires running scenarios time and again, modifying the user's variable of interest. Moreover, once the results are obtained, the calculation of the sensitivity analysis indexes must be done separately. In other words, DER-CAM does not have any sensitivity analysis capability.

3.2.2.2 How DER-CAM works?

Last subsection mentioned that DER-CAM minimizes total annual cost and/or CO₂ emissions. To do that, a reference scenario is required. The total annual cost and CO₂ emissions of the reference scenario are calculated and then compared with the proposed scenario. In this thesis, the reference scenario (shown in Figure 3) uses electricity from the grid to meet the annual electric and cooling loads (through a vapor-compression chiller) and uses a natural gas boiler to meet the annual heating loads.

Then, the four key inputs of the model in DER-CAM are: the end-use energy loads (electricity, heating, and cooling), based on hourly information and typical days per month (week, weekend and peak days); the tariff structures of electricity and other fuels; the characteristics of the pool of technologies available (installed capacities, investment and maintenance costs and efficiencies); and the total annual cost and CO₂ emissions of the reference scenario.

Notice that the first and second input (energy loads and prices) are based on the combinations proposed with the full factorial DoE, as per the methodology anticipated in this thesis.

On the other hand, the outputs of the model, after simulating all the combinations proposed by the full factorial DoE, are: the corresponding total annual cost and

CO₂ emissions, the optimal combination of technologies and their installed capacity (design of the system), the hourly schedule for each technology (operation strategy), and the hourly consumption per type of energy vector and fuel.

Analyzing and extracting insights from the output of DER-CAM requires data analysis techniques that will be introduced in subsection 3.2.3.

3.2.3 Data analysis

Data analysis [134] is the process of evaluating data to get useful insight and support decision-making. It implements analytical and statistical tools aiming to inspect, clean, transform and model.

Given the number of scenarios explored in this work, the use of data analysis tools, such as clustering, is essential. It aims to understand the effects of the variables, as well as the coupling effects, over the feasibility of the system.

3.2.3.1 Data clustering

Clustering is a part of the exploratory data analysis, used for pattern recognition, image analysis, information retrieval, data compression, machine learning, etc.

Clustering methods are a solution to segregate the data in relevant categories, based on a concept of similarity or proximity among them [135]. Several studies of the energy fields have used them, ranging from social studies [136] to the assessment of renewable energy [137], [138] and analysis of energy loads [135]. For example, Grigoras et al. [137] uses k-Means clustering algorithm for data mining on renewable energy generation in Romania, based on the analysis of different variables such as installed capacity, level voltage, type of renewable technology and geographical location. The results are useful to take decision regarding retrofitting substations and upgrading or redesigning transmission and distribution lines.

There are four types of clustering commonly used: centroid, density, distribution, and connectivity [139]. Table 6 indicates inputs and outputs, as well as the

characteristic methods for each type. The centroid clustering relies on iterating to find the coordinate for the centroid of each cluster and gathering the surrounding points. For this method, the analyst must decide the number of clusters in advance and the method could form forced clusters to comply with this number. In contrast, the density clustering identifies the areas with the higher concentration of points and the clusters are formed based on the distance between them. Setting up the desired is of key importance because it should be large enough to perceive the difference between clusters, and small enough to group the similar points. On the other hand, the distribution clustering works by proposing a density distribution for each cluster (the analyst must decide the number of clusters in advance). The process iterates until finding the distributions that best represent the data. A particularity of this method is that instead of determining that a point A belongs to cluster 1 (hard clustering), it quantifies the probability of point A belonging to cluster 1 or cluster 2 (soft clustering). Lastly, the connectivity clustering is characterized by the hierarchies represented with dendrograms. It uses a bottom-up approach where each point starts with its own cluster, but along the process similar points get merged.

	Inputs	Output	Characteristic method
Centroid clustering	No. of clusters	Clusters	k-Means
	Max no. of iterations		
	Converging tolerance		
Density clustering	Max distance between points	Clusters	DBSCAN
	Min points for cluster		
Distribution clustering	No. of clusters	Probability property of each clusters (μ, σ).	Gaussian mixtures
	Convergence setpoint	Proportion of points mainly described by each cluster.	
Connectivity clustering	No. of clusters OR Distance threshold (maximum distance between clusters)	Clusters	Hierarchical method

Table 6 Types of clustering: Inputs and outputs

Table 7 consolidates the characteristics of their corresponding methods [140]–[142]. Each column relates to one feature, either positive or negative (indicated by a sign).

	Kind of clusters	(+) Calculates no. clusters?	(+) Limit variance within clusters?	(+) Identify outliers?	(+) Identify clusters that are next to each other?	(+) Identifies clusters with arbitrary shapes? (non-convex or non-isotropic)	(+) Scales well in large samples?	(-) Computational cost	(-) Curse of dimensionality	(-) Is it a stochastic process?	(-) Large differences in cluster density?
kMeans	H	No‡	No‡	No	Yes▲	No	Yes	Low	Yes	Yes	No
DBSCAN	H	Yes	Yes	Yes	No	Yes	Yes	Low	Yes	Yes	Yes
Gaussian mixtures	S	No	No	Yes♦	Yes♦	No	No	Low	Yes	Yes	Yes
Ward hierarchical	H	No*	No	Yes*	n.a.	n.a.	Yes	High	Yes	n.f.	Yes

Table 7 Comparison of clustering types

KEY general: non-applicable (n.a.); not found (n.f.)

KEY for Type of clustering : Hard (H); Soft (S).

* When the analyst provides the distance threshold alternatively to the number of clusters.

♦ Analyzing the probabilities provided by the soft clustering.

▲ It depends on the accuracy of the method to determine the number of clusters.

‡ It is possible to solve this by implementing a method to estimate the optimal number of clusters.

Among the four methods shown in Table 7, k-Means has some advantages over the others. It is well known for being easy to implement as an exploratory method in data analysis and data mining. It is computationally more efficient (low memory consumption [143]) than the Ward hierarchical method. It scales well in

large samples, compared to the Gaussian mixture method. And, contrary to DBSCAN, it avoids large differences in cluster density. Moreover, k-Means can identify clusters that are next to each other.

One drawback that k-Means and other methods share is its stochastic nature. In the case of DBSCAN, the results depend on the starting point considered. For k-Means and Gaussian mixtures, they depend on the random proposal during the first iteration (place of centroids and characteristics of the clusters respectively). A practical countermeasure is to repeat the clustering several times and ensure that the solution does not change dramatically. To do that, it is helpful to use an inexpensive method in terms of computational resources.

It is good to mention that some of the disadvantages of k-Means can be offset by using a pre-assessment method. The objective is to determine the optimal number of clusters and include measures to restrict the variance within clusters.

The k-Means method is selected for the analysis proposed in this work.

3.2.3.2 k-Means

The algorithm k-means [135], [144], [145] is the most popular unsupervised clustering tool used in scientific and industrial applications [146]. It is a heuristic clustering analysis method from the field of machine learning and data mining [140]. Its function is to segregate m data observations, $X = (x_i)_{i \in [1, m]} = (x_1, x_2, \dots, x_m)$ characterized by a set of p parameters, in k clusters; where each $x_i \in X$ is a real vector of length p : $\forall i \in [1, m], x_i = (v_{x_i,1}, v_{x_i,2}, \dots, v_{x_i,p})$, corresponding to the number of parameters contained. K-Means algorithm aims to distribute these m observations into K subsets $S = \{s_j\}_{j \in [1, K]} = \{s_1, s_2, \dots, s_K\}$, mainly characterized by their clusters centroids μ_j . The set of centroids $\{\mu\}$ is iteratively determined following the objective of minimizing the global sum of distances between them and the corresponding observations of the all the subsets. In other words, the objective is to minimize the sum of square distance (SSD) between each observation x_i and its corresponding μ_j ; these centroids

do not necessarily coincide with any observations, although they live in the same space X .

$$\min SSD = \min \sum_{j=1}^{k \text{ clusters}} \sum_{x_i \in \text{Cluster } j} \|x_i - \mu_j\|^2 \quad \text{Eq. 1}$$

The distances $\|x_i - \mu_j\|$ between the observation $x_i \in S_j$, and the centroid μ_j of subset S_j can be Euclidian, Manhattan or others. In our case, Euclidian distance has been used:

$$d(x_i, \mu_j) = \|x_i - \mu_j\|_2 = \sqrt{\sum_{l=1}^p (v_{x_i,l} - v_{\mu_j,l})^2} \quad \text{Eq. 2}$$

The three key parameters required for k-Means are:

1. The number of clusters desired
2. The maximum number of iterations
3. The tolerance to declare convergence between iterations, measured by either the relative decrease in the objective function or centroids moving less than the tolerance

Choosing the desired number of subsets or clusters k that are used to segregate the data is not trivial. There should be a balance between minimizing the cluster dispersion (making elements of a cluster alike) and maximizing inter-cluster dispersion (making clusters different enough from each other). For example, a larger k minimizes the cluster dispersion because it encourages having small clusters with more similar elements within them. However, a larger k could also cause that those small clusters have similar properties, that could allow to aggregate them in a single cluster.

If k is based on the knowledge of the data behavior [147], there are different approaches to determine it. Some authors compare the variance within groups vs. the variance between the groups, making sure that the latter is larger [148]; other use the silhouette and the Calinski–Harabasz criteria [149]; others like Ramos [135] conclude that none of the possible methods get the best result for

all datasets. In section 3.2.3.3, we propose a methodology to determine the optimal number of clusters.

3.2.3.3 Proposed methodology: ELECTRE 1S determining the number of clusters in k-Means

In k-Means, the number of clusters k is the key parameter to determine. The higher k , the smaller and the denser the clusters are, increasing the similarity of the points that constitute each cluster. On another hand, each cluster must highlight a specific behavior so that inter-cluster dissimilarity and distance must be maximized. A good cluster formation is when clusters are very dense, but also very far from each other. Finally, it seems relevant to minimize the number of clusters in order to draw general rules and conclusions that are applicable to many situations. These three targets are conflicting so that compromise must be found. To sort out these conflict targets, Multi Criteria Decision Making (MCDM) is used in this work to determine k . One of the most well-known families in MCDM is ELECTRE and its variations can be used in choice, ranking or sorting decision-making problems. The theoretical background of MCDM ELECTRE 1S is described in Annex III.

In this work, each data point corresponds to one DER-CAM simulation, consolidating a vector of different outputs, called segregation parameters. These segregation parameters describe important design and operation results. They include the percentage of cost savings obtained with the CCHP-TS system, the production means for each energy carrier (i.e. if the electricity comes from the national grid or is produced in-house) and the energy flows within a CCHP-TS system (i.e. if the heat produced by the CHP is used to cover the heating load, or it is devoted producing cooling through the usage of Absorption chiller).

Then, these data points are classified with k-means using different values of k (number of clusters). These different values of k give origin to several clustering alternatives that are discriminated pair by pair with MCDM ELECTRE 1S. Last, it is selected the clustering alternative (depending on the k value) that minimizes

the cluster dispersion and maximizes the inter-cluster dispersion. All these steps are followed and explained thoroughly in section 4.3.

3.3 Phase II: Sensitivity analysis of the CCHP-TS feasibility

3.3.1 Modeling and optimization solutions adapted to SA implementation

DER-CAM is appropriate for the energy system optimization in the Phase I due to its interface, making the implementation of the tests easier. However, as explained in subsection 3.2.2.1, it is not designed to conduct many simulations (on the order of thousands), which is required to perform a global sensitivity analysis study in Phase II.

Therefore, a faster and adapted model has been designed in collaboration with the group developing DER-CAM in the Lawrence Berkeley National Laboratory. This new tool keeps the good representation of the systems given by DER-CAM, because it uses the same thermo-dynamical and economical logic (described in section 2.4.2). The difference is that it is coded in the Python programming language, using the PYOMO library and the CPLEX solver to optimize (see subsection 2.4.3 further detail). The main advantages of this Python-PYOMO-CPLEX tool over DER-CAM is that it works without human-machine interface and aims to perform faster thousands of simulations.

The main equations governing the model, are the objective function that minimizes the total annual cost (Eq. 3), and the equality constraints to cover the energy loads at each hourly timestep t (Eq. 4, Eq. 5, and Eq. 6). These are explained below, and the full model is given in Annex IV.

$$\begin{aligned}
 \text{MIN Annual Cost} & & \text{Eq. 3} \\
 &= \text{Grid(Cost)} + \text{CHP(Cost)} + \text{Boiler(Cost)} + \text{Abs(Cost)} \\
 &\quad + \text{VCchiller(Cost)} + \text{CStg(Cost)} + \text{HStg(Cost)}
 \end{aligned}$$

The total annual cost (Eq. 3) is the sum of all cost related to importing electricity from the grid, producing energy with the CHP, using the boiler, absorption chiller (*Abs*), vapor-compression chiller (*VCchiller*), and cold and heat storage (*CStg* and *HStg* respectively). The costs also include the investment and maintenance cost of the technologies, considering their lifetime and the interest rate of the investment.

When the objective function is minimizing the cost, it includes the investment and s -- it is not obvious... say it includes investment....

$$eGrid_t + \sum_u eCHP_{u,t} - eVCchiller_t = E_t \quad \text{Eq. 4}$$

The constraint to cover the electric demand each hour t (Eq. 4) sums the electricity imported from the grid ($eGrid_t$), the electricity produced by the CHP type u at the timestep t ($\sum_u eCHP_{u,t}$) and subtracts the electricity used by the vapor-compression chiller ($eVCchiller_t$). All this is equal to the loads of electricity at the timestep t (E_t).

$$Hboiler_t + \sum_u HCHP_{u,t} - Habs_t - hHStgIn_t + \left(\varphi_{discharge}^{HStg}\right) hHStgOut_t = H_t \quad \text{Eq. 5}$$

The constraint to cover the heating demand each hour t (Eq. 5) sums the heat produced by the boiler ($Hboiler_t$), the heat produced by the CHP type u at the timestep t ($\sum_u HCHP_{u,t}$), subtracts the heat used by the absorption chiller ($Habs_t$), subtracts also the heat stored in the heat storage ($hHStgIn_t$) and sums the heat taken from the heat storage at the time t ($hHStgOut_t$). This latter is multiplied by a factor $\varphi_{discharge}^{HStg}$ to consider the losses of discharge (due to heat transfer with pipes, equipment, etc.). All the before mentioned equal the loads of heating at the timestep t (H_t).

$$\left(\frac{COP_{Abs}}{COP_{VCchiller}}\right) Habs_t + eVCchiller_t - eCStgIn_t + \left(\varphi_{discharge}^{CStg}\right) eCStgOut_t = \frac{C_t}{COP_{VCchiller}} \quad \text{Eq. 6}$$

The constraint to cover the cooling demand each hour t (Eq. 6) is expressed in terms of the electricity required by a vapor-compression chiller to produce the cold. The objective is to have a standard unit measuring the cold produced by technologies that use different energy drivers. Then, Eq. 6 is the sum of the cold produced by the absorption chiller ($COP_{Abs} * H_{abs_t}$) divided by the COP of the vapor-compression chiller ($COP_{VCchiller}$) to have the term expressed in electricity required to cover the cooling; plus the electricity used by the vapor-compression chiller ($e_{VCchiller_t}$); minus the electricity required to produce the cold stored in the cold storage at time t (e_{CStgIn_t}); plus the avoided cooling consumption (transformed into electricity) by taking cold out of the cold storage at time t ($e_{CStgOut_t}$), multiplied by the factor $\varphi_{discharge}^{CStg}$ to consider the losses of discharge. All the above mentioned equal the loads of cooling at the timestep t divided by the COP of the vapor-compression chiller to express it in electricity required to cover the cooling ($\frac{C_t}{COP_{VCchiller}}$). Note that the cold storage stores thermal energy, but its equations are expressed in terms of the electricity required by a vapor-compression chiller to produce the cold.

On the other hand, we tested the good correspondence between the Python-PYOMO-CPLEX tool and DER-CAM, by running 30 different scenarios in both and comparing the results given by each of the tool.

The input data corresponding to the scenarios was the same for Python-PYOMO-CPLEX tool and DER-CAM. However, an important setting for the branch and bound method (B&B) in CPLEX, explained in section 2.4.3, is the *relative MIP gap tolerance*. This is the relative tolerance on the gap between the best integer objective and the objective of the best node remaining (Eq. 7) [103]. The smaller this number, the more accurate the solution will be, but the time to obtain the solution is larger. In the case of this code, the *relative MIP gap tolerance* = 0.02, and the average solution time is 1 hour per simulation.

$$\text{relative MIP gap tolerance} \leq \frac{|\text{Best integer solution} - \text{Best B\&B solution}|}{(1e10^{-10})|\text{Best integer solution}|} \quad \text{Eq. 7}$$

As an illustration of the test results, the Figure 19 shows that for all the cases, the difference between both tools regarding the percentage of savings is less

than 1%, showing the good correspondence between DER-CAM and the Python-PYOMO-CPLEX tool.

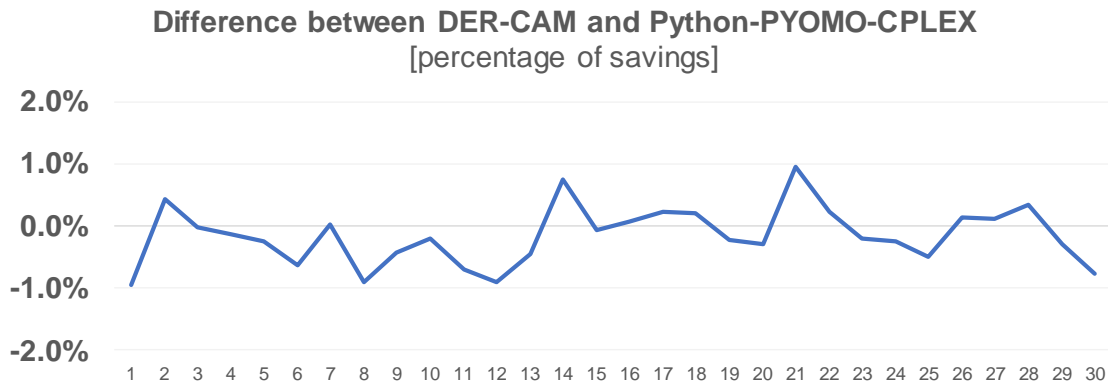


Figure 19 Difference of percentage of savings reported by DER-CAM and the Python-PYOMO-CPLEX tool for 30 scenarios

Other advantages of the Python-PYOMO-CPLEX tool in comparison with DER-CAM, is: 1) PYOMO allows using an object-oriented approach, which gives scalability to the model; 2) The model includes only the modules of interest (CCHP-TS), therefore, it is smaller and more controllable (DER-CAM has several default settings that are difficult to control). 3) All the parameters of interest can be tracked, and simulation can be performed in a more agile way.

3.3.2 Sensitivity analysis – theoretical background

A sensitivity analysis (SA) assesses the uncertainty of a dependent function given the change of its independent parameters [150]. It is commonly used to identify the most influential variables and quantify their effects. In the field of building energy analysis [108], it is useful for building design [113]–[115], calibration of energy models [151], building retrofit [152], building stock [153], impact of climate change on buildings [154], etc. As introduced in section 2.5, SA methods can be local or global.

Local SA uses the first and second order partial derivatives to find the change of the response function $Y=f(x_1, \dots, x_k)$, while varying $x_i \forall i=1, \dots, k$, around one point of the domain Ω in the k -dimensional space.

In a two-dimension space this gives:

$$S_{x_1} = \left. \frac{dY}{dx_1} \right|_{x_1^* x_2^*} \quad \text{Change of } Y \text{ given the change in } x_1, \text{ at the point } (x_1^*, x_2^*) \quad \text{Eq. 8}$$

$$S_{x_2} = \left. \frac{dY}{dx_2} \right|_{x_1^* x_2^*} \quad \text{Change of } Y \text{ given the change in } x_2, \text{ at the point } (x_1^*, x_2^*) \quad \text{Eq. 9}$$

$$S_{x_{1,2}} = \left. \frac{dY}{dx_1 dx_2} \right|_{x_1^* x_2^*} \quad \text{Change of } Y \text{ given the interaction between } x_1 \text{ and } x_2, \text{ at the point } (x_1^*, x_2^*) \quad \text{Eq. 10}$$

On the other hand, global sensitivity analysis (GSA) methods quantify the influence of the model's parameters x_i over Y across its whole domain of uncertainty Ω .

3.3.3 Global sensitivity analysis methods

Across the literature, Morris and Sobol are the most popular GSA methods, even used as benchmark [104], [110]–[114]. While VARS [110], [111], [155] is a novel approach, based on a variogram analysis, that characterizes the variation of the model at different points and scales.

3.3.3.1 Morris – Derivative based approach

Morris [108], [111], [119], [156], [157] is a screening-based or derivative-based approach. Its objective is determining which parameters have (a) negligible effects, (b) linear and additive, or (c) nonlinear effects or interactions with other factors. Note that Morris captures interaction effects, but it cannot separate them from nonlinearities [105].

This method is used when there is no interest in knowing quantitatively the sensitivity of each variable but instead, it is a qualitative way to identify the influential variables at a low simulation cost [119], [120], [158]. It is also good to mention that Morris becomes a non-explorative method at high dimensional space due to the curse of dimensionality. In other words, when the number of

parameters increase, the size of the hyperspace explored converges to zero and the sensitivity analysis becomes less relevant [105].

The Morris method aggregates the local sensitivity (partial derivatives), creating a global distribution of derivatives for each independent parameter $F_i \left(\frac{dY}{dx_i} \right)$. The distribution $F_i \sim N(\mu_i, \sigma_i)$ is a normal distribution of the elementary effects of the variable i (Eq. 11, Eq. 12, and Eq. 14). While $G_i \sim N(\mu_i^*, \sigma_i)$ is a normal distribution of the absolute values of the elementary effects (Eq. 11, Eq. 13, and Eq. 14). Each elementary effect EE_i corresponds to the change of Y , given the variation of the variable $x_i \forall i=1, \dots, k$ at certain point (partial derivative). The axis of each variable is divided into p different levels. And Δ corresponds to the sampling step in the scale $[0,1]$, independently of the distribution of each input. The p is an even number, usually suggested as $p=4$ [119], [157]. And a convenient choice of Δ , to guarantee an equal probability in the sampling level, is $\Delta=p/[2(p-1)]$ [119]. Finally, r is the number of independent random samples of EE_i .

$$EE_i = \frac{[Y(x_1, x_2, \dots, x_i + \Delta, \dots, x_k) - Y(x_1, x_2, \dots, x_i, \dots, x_k)]}{\Delta} \quad \text{Eq. 11}$$

$$\mu_i = \frac{1}{r} \sum_{m=1}^r EE_i \quad \text{Eq. 12}$$

$$\mu_i^* = \frac{1}{r} \sum_{m=1}^r |EE_i| \quad \text{Eq. 13}$$

$$\sigma_i^2 = \frac{1}{r-1} \sum_{m=1}^r (EE_i - \mu_i)^2 \quad \text{Eq. 14}$$

To obtain the r random samples within the uncertainty domain, Morris [156] proposes the design of r trajectories, establishing for each a starting point and allowing the k independent variables vary one by one, in steps of Δ . The

establishment of the starting point is random, as well as the order to vary the parameters and their direction. In 2007, Campolongo proposed a sampling strategy that maximizes the dispersion of the r trajectories within the domain Ω [119], [157]. But in 2014, Sohier et al. [158], [159] demonstrated that using the Latin Hypercube Sampling (LHS) to determine the starting point of the route gives a uniform cover of the domain. Moreover, LHS is the most used method due to its stratification properties [108].

The SA indexes obtained out of the Morris method correspond to Eq. 12, Eq. 13, and Eq. 14. They are:

1. μ : Mean of the distribution of the elementary effects $EE_i \sim F_i$.
2. σ : Standard deviation of the distribution of elementary effects $EE_i \sim F_i$.
3. μ^* : Mean of the distribution of the absolute values of the elementary effects $|EE_i| \sim G_i$.

For the interpretation of the indexes, the reader should know that Morris in 1991 [119], [156] proposed μ to assess the overall influence of a variable on the output, while σ estimates the impact of non-linearity or the interaction effects. Therefore, a large σ means that the influence of the variable strongly depends on the choice of the sample (non-linear effect) and/or the values of the other variables (interaction effects). On the other hand, similar μ and σ means that there are small non-linear and/or interaction behavior. Finally, a small σ means that the variable has an approximately linear behavior [119]. Morris suggests representing results in a plane (μ, σ) . And Garcia Sanchez et al. [113] added a line $\mu = \sigma$ to this plane, to recognize easily the factors that are linear and monotonic from the ones that are non-monotonic, non-linear or have interaction effects. Morris also recommends analyzing μ and σ together, to avoid error type II during the interpretation process. The error type II in statistics, specifically in hypothesis testing, refers to the false positive. In this case, it is when the method fails to identify an influent factor [157]. This happens with non-monotonic variables that have positive and negative elementary effects which cancel each other when accounted in μ . As an alternative solution, Campolongo et al. [119], [157] proposed in 2007 using μ^* , that prevents this type of error. Therefore, when

μ^* has different magnitude than μ , it means that the variable has a non-monotonic effect. Therefore, μ^* becomes a good estimator of the total sensitivity index, measuring the overall effect of a variable on the output (including the interactions effects) [119].

3.3.3.2 Sobol – Variance based approach

Sobol [108], [111], [119] is a variance-based approach. It recognizes that the response function Y can be described by a probability density function $F(Y)$ and its associated variance $V(Y)$. Then, the challenge is to separate the effect of each parameter x_i .

Sobol proposes decomposing the variance $V(Y)$ of the function $F(Y)$. This is called the high-dimensional model representation decomposition, ANOVA-HDMR (Eq. 15).

$$V(Y) = \sum_i V_i + \sum_i \sum_{j>i} V_{ij} + \dots + V_{12\dots k} \quad \text{Eq. 15}$$

Where V_i is the variance of the function only due to the change in variable i (Eq. 16). It is also called first-order variance or main effect contribution of i .

$$V_i = V[E(Y|X_i)] \quad \text{Eq. 16}$$

V_{ij} is the variance of the function due to the interaction between variable i and j (Eq. 17). It is also called second-order variance or interaction effects between i and j . Variables i and j interact, for example, when a value of i is exclusively associated to another of j . The interaction exists when the first order variance V_i and V_j cannot fully explain the effect of X_i and X_j over Y .

$$V_{ij} = V[E(Y|X_i, X_j)] - V[E(Y|X_i)] - V[E(Y|X_j)] \quad \text{Eq. 17}$$

Similarly, there is third, fourth, and n -order variance.

To calculate the sensitivity indices corresponding to each term of the ANOVA-HDMR decomposition (Eq. 18), divide both sides of Eq. 15 by $V(Y)$.

$$\sum_i S_i + \sum_i \sum_{j>i} S_{ij} + \dots + S_{12\dots k} = 1 \quad \text{Eq. 18}$$

Then, for example the sensitivity analysis index of the main effect contribution for variable i is (Eq. 19),

$$S_i = \frac{V_i}{V(Y)} = \frac{V[E(Y|X_i)]}{V(Y)} \quad \text{Eq. 19}$$

While the total effect index of the variable i accounts for the total contribution to the output variation due to factor X_i , therefore, it counts the first-order effect plus all higher-order effects due to interactions (Eq. 20).

$$S_{Ti} = S_i + \sum_{j>i} S_{ij} + \sum_{j>i} \sum_{l>j} S_{ijl} + \dots + S_{i2\dots k} \quad \text{Eq. 20}$$

For a given factor X_i , a significant difference between S_{Ti} and S_i indicates an important interaction involving that factor. In contrast, $S_i = S_{Ti}$ means that X_i is an additive factor within the model [105]. On the other hand, the condition $S_{Ti} = 0$ is necessary and enough for X_i to be a noninfluential factor. It means that the factor can be fixed anywhere, without affecting the output (Factor Fixing). For practical terms, if $S_{Ti} \approx 0$, the analyst can fix X_i anywhere without affecting the output variance $V(Y)$ significantly and the approximation error made when this model simplification is carried out depends on the value S_{Ti} .

For this method, it is not rare to find negative value in the SA indexes. It is part of the numerical error due to estimations within the method. They are generally found in SA indexes close to zero (unimportant factors), and increasing the sample reduces the likelihood of these events [119].

According to Saltelli [119], some advantages of the variance-based methods are: 1) the sensitivity measure is model-free, 2) it is useful for parameters under uncertainty because it captures the influence of their full range of variation, and 3) it measures the interaction effects among parameters. Moreover, by definition, Sobol decomposes the output variance into terms attributed to different combinations of parameters. In counterpart, the disadvantage is their computational cost. On the other hand, the variance-based approach is useful

for: 1) Factor prioritization: identifying the most relevant parameter (or group of them) into the variance; 2) Factor fixing: identifying the non-relevant parameters; 3) Variance Cutting: guaranteeing that the output variance or uncertainty $V(Y)$ is below a given tolerance.

Numerical sampling procedure based on Monte-Carlo

The variance-based methods usually require special sampling methods [49].

In 2002, Saltelli [160] proposed a numerical procedure to calculate the sensitivity analysis indexes. The steps are the following:

1. Generate two matrices of data (A and B). Each with N random samples that contain the k independent variables. The order of magnitude of N is typically a few hundreds to a few thousands.

$$A = \begin{bmatrix} x_1^{(1)} & x_2^{(1)} & \dots & x_i^{(1)} & \dots & x_k^{(1)} \\ x_1^{(2)} & x_2^{(2)} & \dots & x_i^{(2)} & \dots & x_k^{(2)} \\ \vdots & \vdots & \ddots & \vdots & \ddots & \vdots \\ x_1^{(N-1)} & x_2^{(N-1)} & \dots & x_i^{(N-1)} & \dots & x_k^{(N-1)} \\ x_1^{(N)} & x_2^{(N)} & \dots & x_i^{(N)} & \dots & x_k^{(N)} \end{bmatrix} \quad \text{Eq. 21}$$

$$B = \begin{bmatrix} x_1^{(N+1)} & x_2^{(N+1)} & \dots & x_i^{(N+1)} & \dots & x_k^{(N+1)} \\ x_1^{(N+2)} & x_2^{(N+2)} & \dots & x_i^{(N+2)} & \dots & x_k^{(N+2)} \\ \vdots & \vdots & \ddots & \vdots & \ddots & \vdots \\ x_1^{(2N-1)} & x_2^{(2N-1)} & \dots & x_i^{(2N-1)} & \dots & x_k^{(2N-1)} \\ x_1^{(2N)} & x_2^{(2N)} & \dots & x_i^{(2N)} & \dots & x_k^{(2N)} \end{bmatrix} \quad \text{Eq. 22}$$

2. Define k matrices corresponding to each independent variable. Where C_i contains the columns of B , except the i^{th} column, that comes from A .

$$C_i = \begin{bmatrix} x_1^{(N+1)} & x_2^{(N+1)} & \dots & x_i^{(1)} & \dots & x_k^{(N+1)} \\ x_1^{(N+2)} & x_2^{(N+2)} & \dots & x_i^{(2)} & \dots & x_k^{(N+2)} \\ \vdots & \vdots & \ddots & \vdots & \ddots & \vdots \\ x_1^{(2N-1)} & x_2^{(2N-1)} & \dots & x_i^{(N-1)} & \dots & x_k^{(2N-1)} \\ x_1^{(2N)} & x_2^{(2N)} & \dots & x_i^{(N)} & \dots & x_k^{(2N)} \end{bmatrix} \quad \text{Eq. 23}$$

3. Compute the model output for all the input values in the sample matrices A , B and C_i , obtaining three vectors of model outputs of dimension $N \times 1$.

$$y_A = f(A) \quad \text{Eq. 24}$$

$$y_B = f(B) \quad \text{Eq. 25}$$

$$y_{C_i} = f(C_i) \quad \text{Eq. 26}$$

4. Calculate the first-order sensitivity index

$$S_i = \frac{V[E(Y|X_i)]}{V(Y)} = \frac{y_A \cdot y_{C_i} - f_0^2}{y_A \cdot y_A - f_0^2} = \frac{\frac{1}{N} \sum_{j=1}^N y_A^{(j)} y_{C_i}^{(j)} - f_0^2}{\frac{1}{N} \sum_{j=1}^N (y_A^{(j)})^2 - f_0^2} \quad \text{Eq. 27}$$

where...

$$f_0^2 = \left(\frac{1}{N} \sum_{j=1}^N y_A^{(j)} \right)^2 \quad \text{Eq. 28}$$

5. Calculate the total-effect indices

$$S_{T_i} = 1 - \frac{V[E(Y|X_{\sim i})]}{V(Y)} = 1 - \frac{y_B \cdot y_{C_i} - f_0^2}{y_A \cdot y_A - f_0^2} = 1 - \frac{\frac{1}{N} \sum_{j=1}^N y_B^{(j)} y_{C_i}^{(j)} - f_0^2}{\frac{1}{N} \sum_{j=1}^N (y_A^{(j)})^2 - f_0^2} \quad \text{Eq. 29}$$

The computational cost if this method is $N(k+2)$.

3.3.3.3 VARS – Variogram based approach

VARS [110], [111] stands for Variogram Analysis of Response Surface. The method considers the model output $Y=f(X_i) \forall i=1,\dots,k$. The k independent variables can vary within a continuous or discrete range. The method characterizes the spatial structure of Y and its variability.

Studying the shape of Y give information about its sensitivity, such as: 1) the degree on non-smooth or roughness at different points and scales (zoom-in or zoom-out); 2) Multimodality, that reflect the spatial order of the structure because the response values might not be randomly distributed.

VARS is built considering the distance between pairs of observations across the response surface Y (Figure 20) and characterizing it based on directional variograms and covariograms.

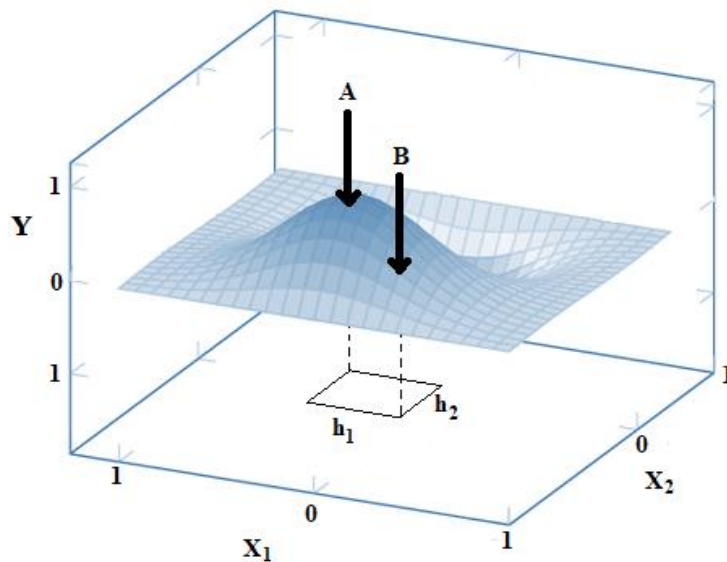


Figure 20 VARS is based on pairs of points at the response surface. Adapted from Razavi, 2016 [161]

A variogram $\gamma(h)$ measures the variance of change in the response surface Y between two points (A and B) separated by a distance $h=x^A-x^B$ (Eq. 30). The measure is taken at different distances $h=\{h_1,\dots,h_j,\dots,h_n\}$ for each independent variable X_i .

$$\gamma(h) = \frac{1}{2}V[Y(X_1 + h) - Y(X_1)] \quad \text{Eq. 30}$$

Directional variograms $\gamma(h_i)$ of variable X_i , are one-dimensional functions used to assess the sensitivity of the response surface Y in the direction of variable X_i when varying the distance h (Figure 21).

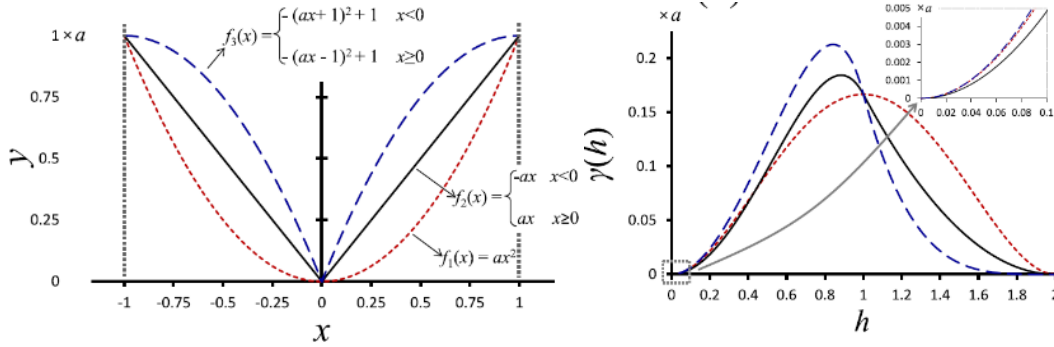


Figure 21 Image taken from Razavi, 2016 [111]. At left, the profile of three different response surfaces $f_1(x)$, $f_2(x)$, and $f_3(x)$. At right, their respective directional variograms.

Figure 21 (left) shows three different response surfaces Y , called $f_1(x)$, $f_2(x)$ and $f_3(x)$. The directional variograms (right), show the change of the response surfaces with respect to x , across the different values of h_i (scale). For $h < 1$, $f_3(x)$ is the most sensitive (blue curve). When $h = 1$, the three response surfaces are equally sensitive. And for $h > 1$, $f_1(x)$ is the most sensitive (red curve).

VARS uses a STAR-based sampling strategy [110], that allow sampling all across the full range of the k independent variables. The steps of the strategy are described below, and in parallel, the Figure 22 shows the example for $k = 2$ variables:

1. Scale all variables on the range zero to one. In Figure 22, there are $k = 2$ independent variables (x_1 and x_2).
2. Select the levels $h = \{h_1, \dots, h_j, \dots, h_n\}$ and the resolution $\Delta h = h_j - h_{j-1}$. Note that $dim(h)$ expresses the number of levels. For Figure 22, $\Delta h = 0.1$ and $dim(h) = 9$ for each variable.
3. Generate r STAR-center (using for example, LHS). The location of these centers are $x_j^* = \{x_{j,1}^*, \dots, x_{j,i}^*, \dots, x_{j,k}^*\}$ where $j = 1, \dots, r$. In Figure 22, there are $r = 2$ STAR-centers and they are marked with diamonds.

4. Generate cross sections for each STAR-center with equally spaced points Δh , along each k input (Figure 22). In Figure 22, each r STAR-center generate $dim(h)-1$ points, marked with circles.
5. Extract pairs and generate directional variograms, such as the ones in Figure 21.

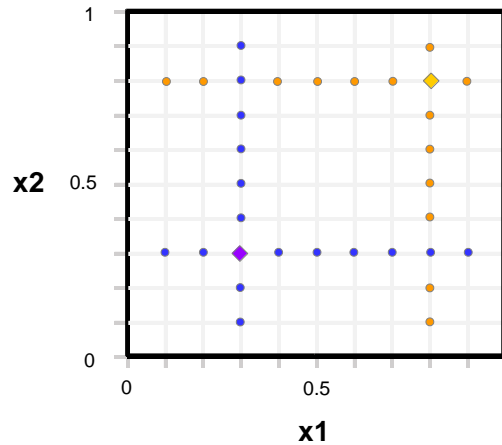


Figure 22 STAR-based sampling with $k=2$ independent variables and $r=2$ STAR-centers [111]

3.3.4 Sampling methods

The previous subsections explained that Latin Hypercube Sampling (LHS) are the sampling methods used by Morris and VARS, while Monte Carlo is used by Sobol. This section intends to give a theoretical background of them.

3.3.4.1 Latin Hypercube Sampling

Latin Hypercube (LHS) designs ensures that the sample points are uniformly scattered across the input space with minimal unsampled regions. It is well known for their flexibility to provide data for modeling techniques based on very different statistical assumptions, and to cover small or large design spaces (no constraints in terms of data density and location) [105], [162]. The objective functions are (1) maximizing the minimum interpoint distance among all possible pairs of sample points, and (2) minimizing the correlations (absolute value)

between all pairs of columns of the sample matrix. Figure 23 is an image taken from Sheikholeslami, 2017 [163] contrasting what a good LHS is.

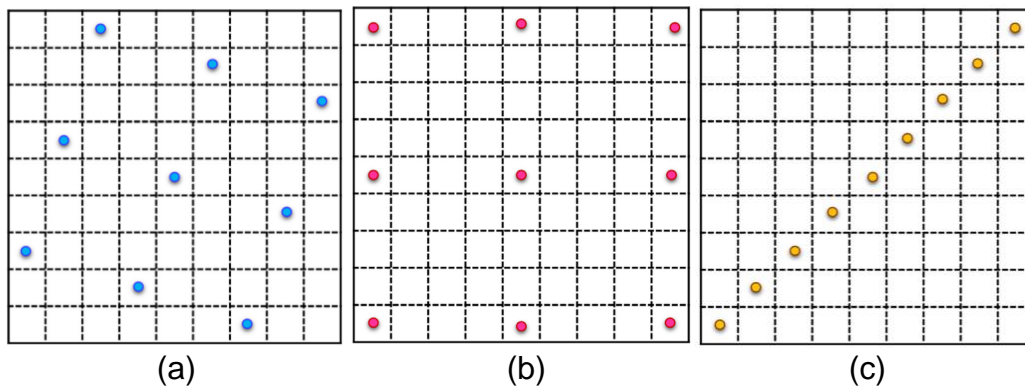


Figure 23 (a) Optimal LHS with low correlated factors and optimal space-filling (distribution of samples), (b) Sampling with good space-filling only, (c) LHS with very poor space-filling and highly correlated factors

Image taken from Sheikholeslami, 2017 [163]

The steps followed to generate r^* sampling points with the LHS, are:

- i. Divide the test range of each variable in r^* intervals. Note that the number of intervals must be equal for all the factors.
- ii. Generate r^* samples randomly, making sure that each column and row are selected just once.

One of its drawbacks of LHS is that the user needs to specify the sample size (r) prior to the associated sampling-based analysis, then, if the sample needs to be enlarged, the user needs to discard the previous sample, or generate a new sample by LHS, knowing that the union of the two samples will not be Latin Hypercube. For such cases, the alternative is to implement a Progressive Latin Hypercube (PLHS).

Progressive Latin Hypercube Sampling

The Progressive Latin Hypercube (PLHS) is a technique to extend an original LHS, in such a way that the result is still an LHS achieving the maximum stratification in any one-dimensional projection. The Figure 24, taken from Sheikholeslami, 2017 [163], describes the steps of PLHS.

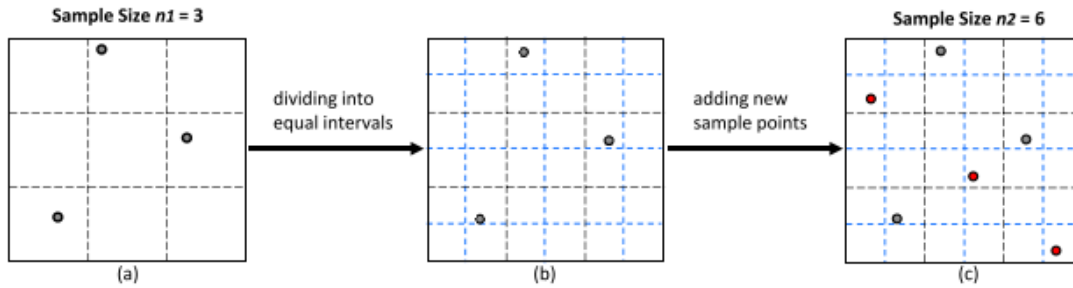


Figure 24 Doubling procedure of PLHS with $k=2$ variables (a) Initial LHS with $r=3$ samples, (b) Dividing initial sample domain into 6 intervals with equal marginal probability

Image taken from Sheikholeslami, 2017 [163]

3.3.4.2 Monte Carlo sampling

Monte Carlo [164], [165] is a computational algorithm based on random sampling and statistical analysis. It performs a numerical experiment taking N random samples from a system and obtains the statistical properties that describe them.

Some characteristics and conditions of the Monte Carlo algorithm, are:

1. The systems analyzed should be described by probability density functions (PDF),
2. Monte Carlo is suitable for continuous or discrete probability distribution,
3. The random samples are chosen by using a generator for random numbers. This picks numbers uniformly distributed on a unit interval that could pass tests for randomness.
4. The statistical error (variance) is function of the number of trials. And there are variance reduction techniques.

Monte Carlos is useful when it is not possible to use any other algorithm. For example, when the system has unknown or uncertain parameters, many coupled degrees of freedom, or complicated boundary conditions.

3.3.5 Global sensitivity analysis vs. full factorial DoE

As explained at the beginning of chapter 3, although OAT is very popular to assess the feasibility of combined thermal and power energy systems, it is a local method.

In contrast, full factorial DoE explores the global range of variables at lower simulation cost than the GSA methods. It is a simple method that gives a good understanding of the impact and interaction effects of parameters. Then, full factorial DoE is selected for first phase of the thesis due to its efficiency and acceptable accuracy.

For the second phase of the thesis the objective is to rank the important parameters and accurately measure their interaction effects. Then, it is proposed to conduct an in-depth sensitivity analysis using three GSA methods: Morris, Sobol, and VARS. The first two are well known methods typically used as reference across the literature, and the third is a novel approach that characterizes the variation of the model at different points and scales.

The main advantages of GSA methods over simply using a full factorial DoE, are explain below and shown in Table 8:

- GSA are robust model-free methods, also called sample-based [119], [166]–[168]. While full factorial DoE, in this work, has the characteristics of a model-based method.

Model-free methods are not related to any local reference at the model. They are recommended when the analyst does not have prior knowledge of the process model (relevant parameters, ranges, structure of the model, etc.) [169]. Therefore, typically they use space-filling designs, that intend to distribute uniformly the samples in the design space [170]. In contrast, a model-based method is tailored according to the process to maximize the information obtained with the samples (starting point, ranges to analyses, sampling according to the distribution of the parameters, etc.) [169].

Full-factorial and fractional factorial DoE are among the techniques that require proper space-filling [171]. Therefore, it is natural to conclude that

the are model-free methods. However, to implement them for this work, it is a precondition to define the discrete levels of analysis for each continuous variable. Then, the method becomes a model-based one.

- Full factorial DoE gives a sense of the individual and interaction effects of parameters, although the accuracy depends on its resolution and dispersion, in other words, the number and location of the levels studied in full factorial DoE. Contrary, GSA methods ensure a random and disperse sampling across the range (using sampling techniques such as LHC, Monte Carlo, etc.). Moreover, methods like Sobol are very robust in terms of resolution, due to the number of samples required.
- Full factorial DoE is mainly for screening purposes (determining the influential variables), but GSA methods such as Sobol are useful also for ranking and quantifying the relative sensitivity of the parameters.

In terms of simulations cost, GSA approaches such as Morris could be similar to the full factorial DoE [105]. However, that is not the case for Sobol.

	Scale of the method (L / G)	Simulation cost (low / mid / high)	Type of method (M / S)	Identifies interaction effects?	Quantifies interaction effects?	Application (S / R / Q)
OAT	L	Low	M			S
Full factorial DoE	G	Mid	M	*	*	S, R
Morris	G	Mid	S	*		S, R
Sobol	G	High	S	*		S, R, Q
VARs	G	Mid	S	*	*	S, R

Table 8 Comparison of GSA methods against OAT, and full factorial DoE

Key for Scale of the method : Local (L); Global (G).

KEY for Type of method : Model-based (M); Sampling-based (S).

KEY for Application : Screening (S); Ranking (R); Quantifying relative sensitivity (Q).

3.4 Case study: A university campus

To illustrate the implementation of the proposed methodology, the hourly load profiles of a University Campus are used as it corresponds to an example of a large set of buildings that reflect different use patterns.

This University Campus is the IST – Alameda Campus in Lisbon, Portugal. It is a typical university comprising 26 buildings including classrooms, labs, multiple cafeterias with cooking installations, sports facilities and a day nursery. The campus is used during weekdays by students, faculty members, researchers, and general staff. The activity is reduced during weekends and holidays (August, Christmas and New Year). The IST Alameda Campus has four main buildings that contribute to its energy demand. By 2015, the aggregated annual loads of them were 2.4 GWh/y of electricity [E], 0.63 GWh/y of heating [H], and 0.98 GWh/y of cooling [C]. This data comes from the energy analysis performed with EnergyPlus calibrated with real data as part of the Project *Campus Sustentável* at the IST – Alameda Campus [76].

The load duration curves and the normalized campus hourly patterns [d_n] of each n carrier (E: Electricity, H: Heating, C: Cooling) are represented in Figure 25. From the normalized campus hourly patterns (Figure 25, right), it is possible to observe the behavior of energy loads across the 8760 hours of the year and notice that they decay for the three energy carriers every weekend and during the first two weeks of August. During the weekdays, electricity load reaches its maximum during January-February, the minimum during the first two weeks of August and in general, the rest of the year is 60% of the maximum values; the heating has the highest values from December to February and cooling load spans from March to November, with the maximum from June to the end of August.

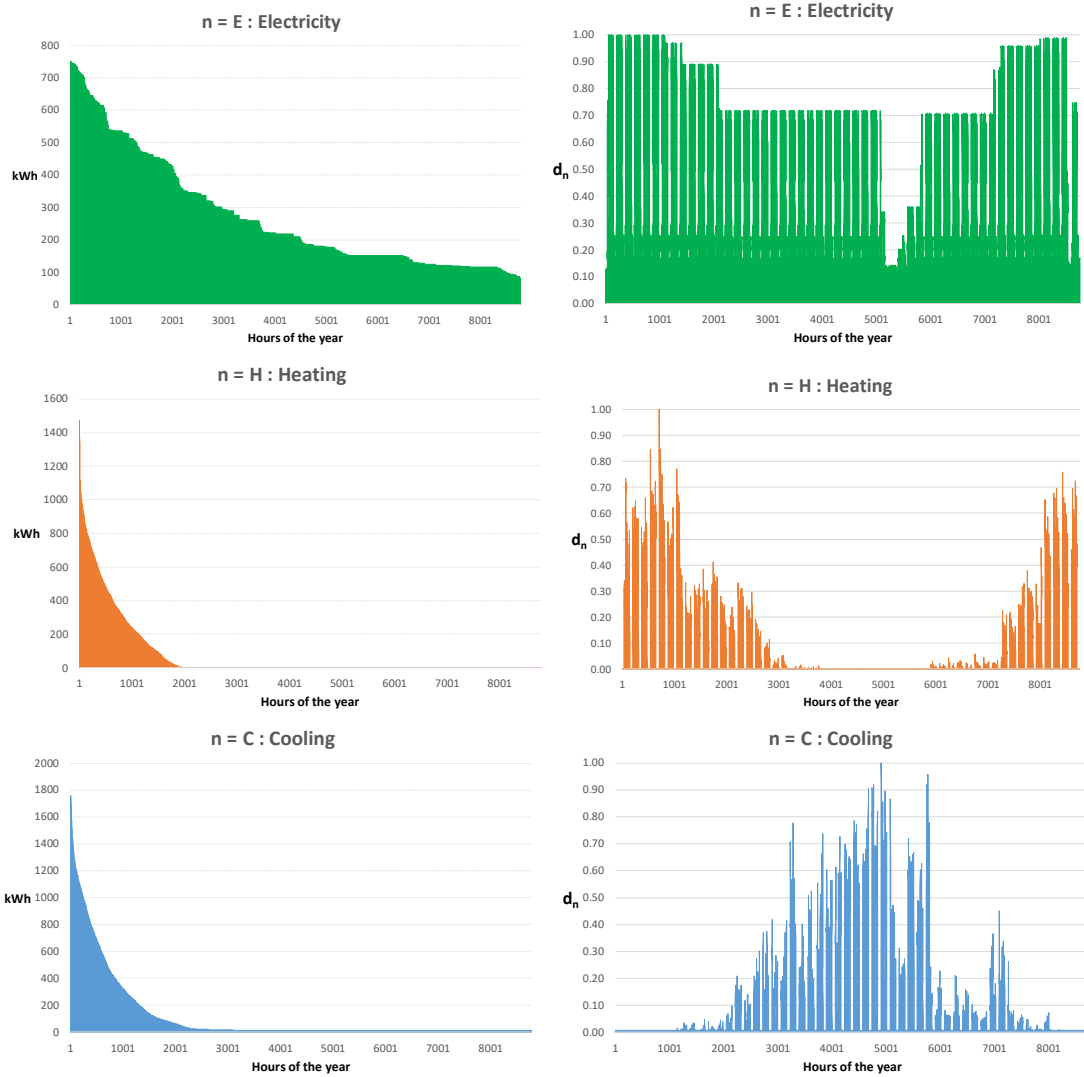


Figure 25 Load duration curves (left) and the normalized hourly pattern of the Electricity, Heating and Cooling loads for the IST Alameda Campus, expressed in hourly basis

The sections 4.1, 5.2, 5.3, and 5.4 of this thesis introduce the simulation of scenarios with different size of the annual energy load for each n carrier (E: Electricity, H: Heating, C: Cooling). Afterwards, a homothetic transformation is used to adapt these annual loads to the hourly load patterns $d_n(t)$ of the IST – Alameda Campus. The Eq. 31 allows obtaining the hourly energy load $L_n(t)$ corresponding to each carrier n . Note that the denominator 1×10^6 transforms the loads from GWh to kWh.

$$L_n(t) = \left(\frac{n}{1000000} \right) \frac{d_n(t)}{\sum_{t=1}^{8760} d_n(t)} \quad \text{Eq. 31}$$

The hourly energy load $L_n(t)$ are the ones introduced at the modeling and optimization tools, like DER-CAM and the Python-PYOMO-CPLEX tool. As mentioned in subsection 2.6, the hourly analysis of energy loads aims to provide more precision to the feasibility analysis.

4 PHASE I: Exploratory study of the CCHP-TS feasibility

This chapter corresponds to the first phase of the thesis. It is an exploratory analysis to examine the techno-economic relevance of the CCHP-TS model, as well as the impact of load size and energy prices.

In this phase, the energy prices are consolidated into the spark spread rate (SS) and the CCHP-TS model used is the one embedded in DER-CAM. The analysis is based on the percentage of cost savings obtained by using a Trigeneration systems with thermal storage, instead of the reference scenario (Figure 26).

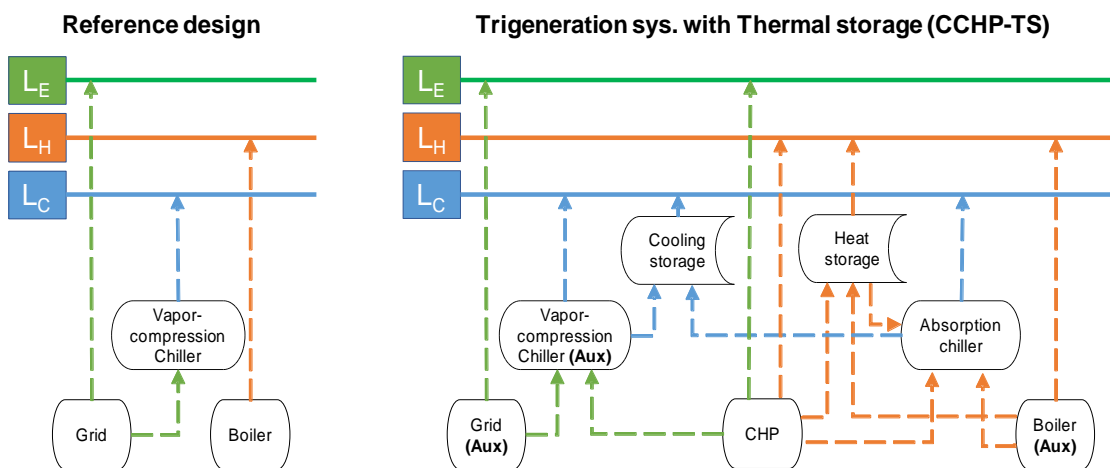


Figure 26 Comparison of a trigeneration-thermal storage system vs. a conventional system, while meeting the annual loads $L_n \forall n=\{E: \text{electricity}, H: \text{heating}, C: \text{cooling}\}$

NOTE: Energy Supply (dotted lines) and Energy Loads (solid lines)

The scheme in Figure 27 details the methodology of this phase. To start, a full factorial DoE aims to generate different scenarios of CCHP-TS based on different levels of electricity, heating, and cooling loads and spark spread rates. After that, the optimal system configuration for each scenario is obtained with DER-CAM. Once the results of all the simulations are obtained, it is essential to identify the functioning variables and segregate data implementing clustering. For the latter, the methodology presented in the Chapter 3 is used. Finally, the influence of the variables under different conditions is analyzed.

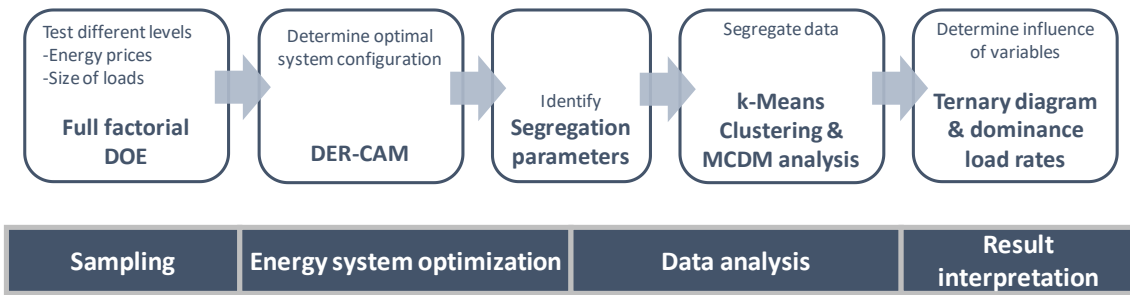


Figure 27 Refined methodology of Phase I

4.1 Sampling of scenarios from the case study

The analysis comes in two levels: Firstly, four Spark Spread rates (SS) are analyzed. Secondly, within each SS, to evaluate the impact of Electricity, Heating and Cooling loads, a set of scenarios are defined by varying the size of the three.

The levels of the annual energy load of each n carrier (where E: Electricity, H: Heating, C: Cooling) are selected in a logarithmical way, to test different orders of magnitude in terms of load size. The levels (in GWh/y) are $E = \{0.1, 1, 10, 100, 500, 1000\}$, $H = \{0.1, 1, 10, 100, 400\}$ and $C = \{0.1, 1, 10, 100, 500\}$. Some of these levels are arbitrarily big with the sole objective of widely explore the possible spectrum of annual energy loads, introduced in section 2.2.2. Regarding the Spark Spread rate, the four levels selected are $SS = \{3.0, 3.9, 5.4, 6.6\}$. These rates correspond to spark spread rates in different regions around the world (two in Europe, Africa, and US respectively) [86], [172], intending to emulate different conditions of electricity and natural gas prices. In this work, the electricity and natural gas tariffs are constant, independently of the day and time.

Then, a full factorial design of experiments is followed, testing the 600 scenarios resulting from the combination of 6 levels for electricity, 5 levels of heating, 5 levels of cooling and 4 levels of SS rate. Figure 28 shows the cube sketching all the possible combinations for the $SS=3.0$ and takes one as example.

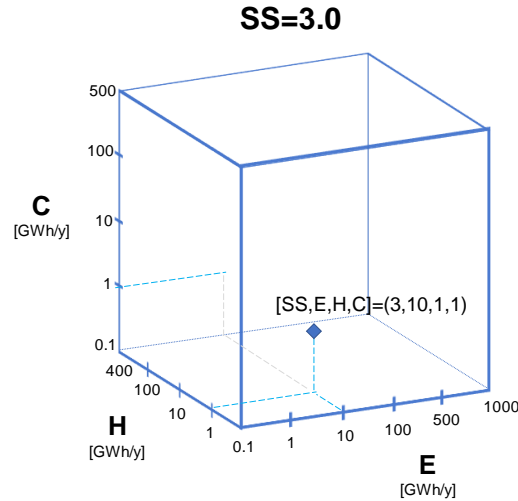


Figure 28 Example of one scenario out of the 600 possible, as part of the full factorial design of experiments.

These hourly energy loads are used as inputs of the optimization process done with DER-CAM and the scenario of using CCHP-TS is compared against the reference scenario (Figure 3).

4.2 Energy system optimization: DER-CAM

DER-CAM is configured to minimize the annual total cost, and it calculates the percentage of cost savings that are reached by using the CCHP-TS system compared to the reference scenario. The three key inputs are configured as follows:

- End-use energy loads $L_n(t)$ of electricity, heating, and cooling. They result from the E, H and C mentioned in section 3.4 and the use of Eq. 31. The loads $L_n(t)$ are in hourly basis and expressed as typical days per month (week, weekend and peak days);
- The tariff structures of electricity and fuel, listed in Table 9;
- The characteristics of the pool of technologies available to be chosen by DER-CAM. These are the installed capacities, efficiencies, emissions, variable and fixed cost of the technologies: absorption and vapor-

compression chiller, boiler, thermal storage and CHP generators–ICE (Internal Combustion Engines) ranging from 75kW to 5MW installed capacity, CT (Combustion Turbines) and CTDB (Combustion Turbine Duct Burner) ranging from 15MW to 25MW installed capacity. All this information is available on the DER-CAM default database. They are listed in Table 10 to Table 14.

Table 9 shows the energy prices corresponding to each spark spread level. They follow a fixed and constant tariff structure.

	SS1 = 3.0	SS2 = 3.9	SS3 = 5.4	SS4 = 6.6
Price of electricity [€ / kWh]	0.1223	0.1580	0.1030	0.1623
Price of natural gas [€ / kWh]	0.0404	0.0400	0.0190	0.0246

Table 9 Energy prices used in DERCAM

Table 10 shows the characteristics of the technologies used for the reference scenario. It is considered that the equipment belonging to the reference scenario is already installed, therefore, it does not show any installation cost.

	Efficiency [-]	Lifetime [y]
Vapor-compression chiller	COP = 0.1223	10
Boiler	$\eta = 0.0404$	10

Table 10 Technological settings for the reference scenario in DERCAM

Table 11, Table 12, and Table 13 show the characteristics of the technologies used for the CCHP-TS scenario.

Type	Installed capacity	Fixed capital cost [k€]	O&M variable cost [€ / kWh]	Electric efficiency [-]	Heat to Electricity rate [-]	Lifetime [years]
CT25	25 MW	31,191.78	0.00720	0.35970	1.05300	20
CTDB25	25 MW	31,831.72	0.00740	0.35970	1.05300	20
CT15	15 MW	22,783.32	0.00730	0.33250	1.20440	20
CTDB15	15 MW	23,272.36	0.00755	0.33250	1.20440	20
ICE5	5 MW	7,021.58	0.00875	0.41600	0.79740	20
ICE2.5	2.5 MW	5,005.66	0.01625	0.40400	0.78570	20
ICE1	1 MW	2,340.00	0.01950	0.36800	1.01940	20
ICE0.75	750 kW	2,047.72	0.02150	0.34500	1.16050	20
ICE0.25	250 kW	675.97	0.02500	0.27000	1.82970	15
ICE0.075	75 kW	225.80	0.02550	0.26000	2.00640	15

Table 11 Technological settings for the CCHP-TS scenario (CHP prime movers)

It is good to mention that in this work the CHP technology is considered modular. In other words, several units from Table 11, of the same or different type, could be joined to conform the optimal CHP installed capacity.

	Efficiency [-]	Variable capital cost [€ / kW inst]	O&M fixed cost [€ / month / kW inst]	Lifetime [years]
Absorption chiller	COP = 0.7	685	1.88	20

Table 12 Technological settings for the CCHP-TS scenario (absorption chiller)

	Charge / discharge efficiency [-]	Decay rate [h ⁻¹]	Max charge and discharge rate*	Min state of charge*	Variable capital cost [€ / kW inst]	Lifetime [years]
Heat Storage	0.9	0.0006	0.25	0	100	17
Cold Storage	0.9	0.0006	0.25	0	100	17

Table 13 Technological settings for the CCHP-TS scenario (thermal storage)

NOTE: (*) The maximum charge and discharge rate, as well as the minimum state of charge are expressed as a percentage of the installed capacity.

Table 14 reports the interest rate used to evaluate the project and the carbon intensity of the electricity from the grid. The latter takes as reference the average in Europe [14].

Interest rate [%]	5%
Carbon intensity of electricity from the grid [kg CO ₂ eq. / kWh]	0.447

Table 14 Other settings used in DERCAM

On the other hand, the outputs from DER-CAM are:

- The CCHP and Thermal Storage technologies selected, as well as their installed capacity;

Note: As explained in Table 11, the optimal CHP installed capacity is conformed in a modular way.

- The hourly production for each technology (CHP units, Absorption Chiller and Boiler) and/or import from the national grid, as well as hourly consumption for each type of energy (Electricity, Heat and Cooling);

- The monthly consumption of fuel (Natural Gas), as well as the allocation per technology (CHP and Boiler);
- The hourly energy stored at the Thermal Storage;
- The total annual cost and CO₂ emissions of the scenario proposed, as well as the percentage of cost savings and CO₂ reduction compared with the reference scenario.

The general results of the simulation in DER-CAM for the 600 scenarios are in Table 15 and show the results per Spark Spread rate. Notice that installing a CCHP-TS system is economically and environmentally feasible only for 419 out of the 600 scenarios. For the rest, it is either cheaper or less polluting to use the reference design of the energy system defined in Figure 3. Annex I show the consolidated output data for each feasible scenario within the four SS rates.

	SS1 = 3.0	SS2 =3.9	SS3 = 5.4	SS4 = 6.6
Number of Feasible scenarios (419 out of 600)	50 out of 150	118 out of 150	118 out of 150	133 out of 150
Maximum % cost savings	6.6%	21.8%	25.2%	42.9%
Average % cost savings	4.3%	12.1%	15.1%	26.7%
Minimum % cost savings	2.9%	1.1%	1.1%	1.6%

Table 15 General information of the energy analysis for the scenarios belonging to the different SS rates

Both, the number of feasible scenarios and the average percentage of savings, increase with the spark spread rate. A larger SS means a higher difference in price between the electricity imported from the grid and the fuel to run the CHP (natural gas for this paper). Therefore, a larger SS improves the economic advantage of producing electricity in-house with the CHP.

For the sake of explaining in detail the need of a further analysis and the different steps, the rest of section 4.2 and 4.3 are developing the example of SS4=6.6. However, the reader should note that the same analysis was followed with the other three SS rates. Section 4.4 analyze them all together again, allowing an effective comparison.

Having said this, Figure 29 and Figure 30 presents the DER-CAM results obtained with SS=6.6. They were a total of 150 simulations (six levels of E, five of H, five of C and one of SS). From those, only 133 showed that using a CCHP-TS system is economically and environmentally better than using the reference scenario, while for the other 17 simulations, the reference system is preferred.

Figure 29 shows the percentage of savings obtained for each of the 133 feasible scenarios, depending on the loads (E, H, and C). At a first glance, three different regions are perceived. Firstly, when electricity demand is higher (500 to 1000 GWh/y), savings are practically stable, no matter the value of heating and cooling demand. Secondly, when electricity demand is 100GWh/y, savings are quasi-stable across cooling demand variation, but they drop when heat demand reaches 400GWh/y. Thirdly, when electricity demand is from 0.1 to 10 GWh/y, savings are impacted by variations in any of the three carriers.

However, from Figure 29, it is not possible to detect why the scenarios have certain savings. For example, the two circled dots correspond to events with similar percentage of savings (16.2% and 16.4% respectively) and annual energy load alike (E1-H10-C100 and E1-H10-C500). However, the installed capacity of the CHP units and absorption chiller are completely different.

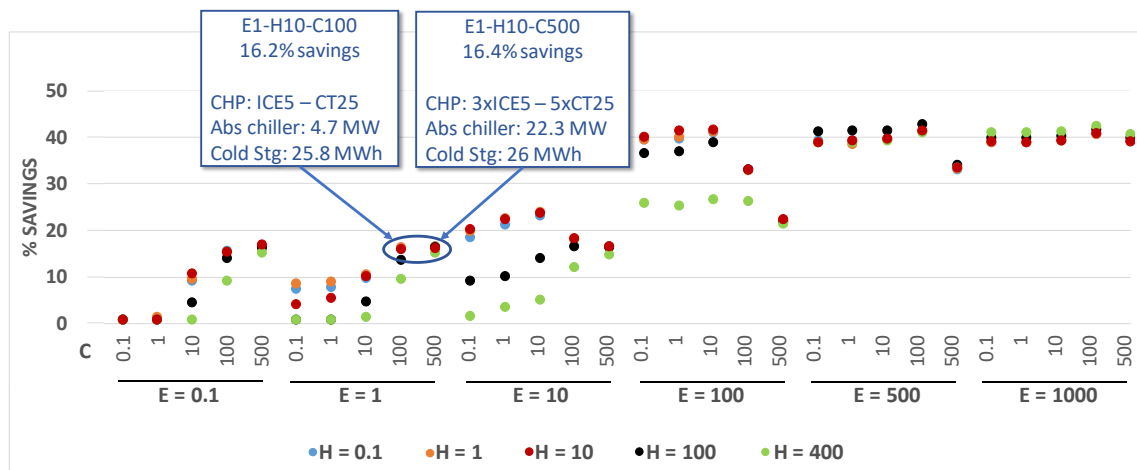


Figure 29 Simulation data obtained from the full factorial design of experiments, using DER-CAM (example of SS4=6.6)

KEY: ICE (Internal Combustion Engine), CT (Combustion Turbine), and CTDB (Combustion Turbine Duct Burner).

NOTE: The CHP technology is modular, as explained in Table 11. Then, the number before the type of prime movers indicates the number of units installed. As example, 4xICE5 – ICE2.5 denote the installation is four units of ICE of 5MW, and one ICE of 2.5MW.

On the other hand, Figure 30 shows a frequency histogram of CHP Technology Mix and displays the related ranges of energy loads levels and savings. In this chart also, is possible to perceive that the percentage of savings trend roughly follows the behavior of Electricity demand, particularly for high values of the load. Further, the installed capacity (increasing values along the X-axis) is influenced by Electricity demand. For example, the plateau of electricity demand 1000 GWh/y is between 225-275 MW installed capacity, the one of 500 GWh/y is located between 100-125 MW, the one for 100 GWh/y goes from 20-25 MW and finally, the one for 10 GWh/y is between 1.75-3.5 MW. On the other hand, there is a threshold of CHP installed capacity (25MW), where Internal Combustion Engines (ICE) technology is no longer the most economically feasible solution, and then combustion turbines (CT) start being used, adding small ICE units just to manage peak demand. This is related with the fact that CT configuration allows a better rate of heat production and higher electric production, but electric efficiency of CHP slightly decreases. This gives an understanding that the selection of the prime mover is influenced by the relative size of electricity and heating loads. Although it does not affect directly the percentage of savings obtained.

An important difference in savings can be noted when focusing on two cases having the same installed capacity (green box in the Figure 30) but using two different technical solutions (5xICE5 and CT25). As mentioned, this main difference is coherent with the electricity demand level in each case. However, one of the cases has a significant dispersion in savings, mainly driven by the dispersion bar observed in heat and cooling demand (associated to the boiler usage in case of heat). This example illustrates the potential coupling effects of different demands and justifies a deeper analysis of the possible interactions, which is done using clustering analysis.

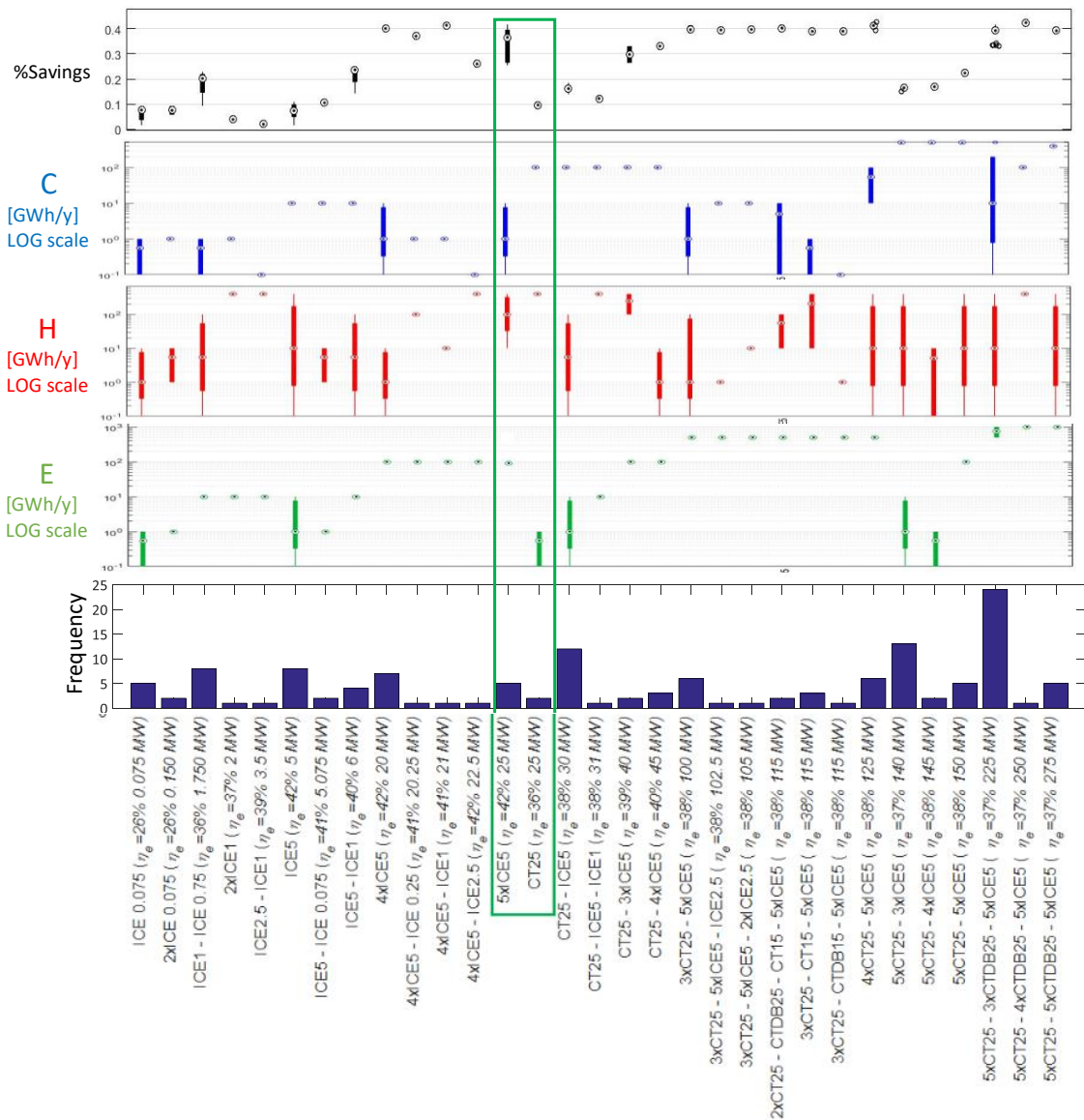


Figure 30 CHP Technology Mix Histogram (example of SS4=6.6) and its relationship with levels E, H, C, and percentage of savings.

KEY: ICE (Internal Combustion Engine), CT (Combustion Turbine), and CTDB (Combustion Turbine Duct Burner).

NOTE: The CHP technology is modular, as explained in Table 11. Then, the number before the type of prime movers indicates the number of units installed. As example, 4xICE5 – ICE2.5 denote the installation is four units of ICE of 5MW, and one ICE of 2.5MW.

It is difficult to see the actual influence of E, H and C from Figure 29 and Figure 30. A deeper data analysis, presented in the next section, aims to understand the coupling effect of loads on the percentage of savings. It includes Data segregation and clustering, based on segregation parameters, k-Means clustering method and Multi-Criteria Decision-Making type ELECTRE 1S.

4.3 Data analysis: Clustering

The Data Clustering objective is to understand the relation between energy demand and techno-economic feasibility of the system, analyzing the interaction among the driving parameters. Ten segregation parameters are selected, using MATLAB to automatize the extraction of information from DER-CAM reports (code in Annex II). Each scenario, obtained from the full factorial DoE, represents a data point that can be described as a vector with the following parameters:

- The percentage of cost savings obtained with the CCHP-TS system when compared to the reference system (heating covered with natural gas boilers and electricity and cooling covered using electricity from the grid);
- The generation means for each energy carrier (%Grid, %Boiler and %Absorption);
- The percentage of heat generated by the CHP units, that is not consumed (% heat scrap); and
- The energy flows within a CCHP-TS system (electricity for electricity (E4E), electricity for cooling (E4C), electricity for cooling storage (E4CS), heat for heating (H4H), heat for cooling (H4C), and heat for cooling storage (H4CS))

The production means for each energy carrier can be followed in Figure 26 and described by Eq. 32 to Eq. 34: electricity can be generated by the CHP or imported from the Grid, Heating can be produced by the CHP or a Boiler, and Cooling can be produced by an absorption chiller or the vapor-compression chiller.

Percentage of Electricity imported from the Grid Eq. 32

$$\% \text{ Grid} = \frac{\sum_t \text{Electricity}_{\text{Grid}}(t)}{(\sum_t \text{Electricity}_{\text{Grid}}(t) + \sum_t \text{Electricity}_{\text{CHP}}(t))}$$

Percentage of Heating produced with Boiler Eq. 33

$$\% \text{ Boiler} = \frac{\sum_t \text{Heating}_{\text{Boiler}}(t)}{(\sum_t \text{Heating}_{\text{Boiler}}(t) + \sum_t \text{Heating}_{\text{CHP}}(t))}$$

Percentage of Cooling produced with Absorption Chiller Eq. 34

$$\% \text{ Absorption} = \frac{\sum_t \text{Cooling}_{\text{Absorption}}(t)}{(\sum_t \text{Cooling}_{\text{Absorption}}(t) + \sum_t \text{Cooling}_{\text{Electric}}(t))}$$

The energy flows can be followed in Figure 3 and described by Eq. 35 to Eq. 40.

Part of the electricity generated by the CHP that is used to meet the electric load: Eq. 35

$$E4E = \frac{\text{Electricity}_{\text{CHP}}^{\text{LE}}(t)}{\text{Energy}_{\text{CHP}}(t)}$$

Part of the electricity generated by the CHP that is used to meet the cooling load through a vapor compression chiller: Eq. 36

$$E4C = \frac{\text{Electricity}_{\text{CHP}}^{\text{LC}}(t)}{\text{Energy}_{\text{CHP}}(t)}$$

Part of the electricity generated by the CHP that is used to supply the cooling storage: Eq. 37

$$E4CS = \frac{\text{Electricity}_{\text{CHP}}^{\text{CS}}(t)}{\text{Energy}_{\text{CHP}}(t)}$$

Part of the heat produced by the CHP that is used to meet the heating load: Eq. 38

$$H4H = \frac{\text{Heat}_{\text{CHP}}^{\text{LH}}(t)}{\text{Energy}_{\text{CHP}}(t)}$$

Part of the heat produced by the CHP that is used to meet the cooling load through an absorption chiller: Eq. 39

$$H4C = \frac{\text{Heat}_{\text{CHP}}^{\text{LC}}(t)}{\text{Energy}_{\text{CHP}}(t)}$$

Part of the heat generated by the CHP that is used to supply the cooling storage: Eq. 40

$$H4CS = \frac{\text{Heat}_{\text{CHP}}^{\text{CS}}(t)}{\text{Energy}_{\text{CHP}}(t)}$$

where,

The total energy generated by the CHP, expressed in hourly basis [kW] Eq. 41

$$\begin{aligned} & \text{Energy}_{\text{CHP}}(t) \\ &= \text{Electricity}_{\text{CHP}}^{\text{LE}}(t) + \text{Electricity}_{\text{CHP}}^{\text{LC}}(t) + \text{Electricity}_{\text{CHP}}^{\text{CS}}(t) + \text{Heat}_{\text{CHP}}^{\text{LH}}(t) + \text{Heat}_{\text{CHP}}^{\text{LC}}(t) + \text{Heat}_{\text{CHP}}^{\text{CS}}(t) \end{aligned}$$

Once the segregation parameters are established, the objective is to understand better the interaction among the segregation parameters. For this, k-Means algorithm from the scikit-learn module of Python is used. k-Means will cluster

the 600 simulations, each of them characterized by the ten segregation parameters mentioned above. The settings for k-Means to be used in this work, are:

- Number of clusters desired.
- Maximum number of iterations = 100,000 iterations
- Tolerance to declare convergence (relative to centroids) = 0.00000001

As mentioned in subsection 3.2.3.2, while performing the k-Means clustering method, an input parameter is the number of k desired clusters.

Therefore, the outranking approach of Multi Criteria Decision Making (MCDM) ELECTRE 1S [173], [174], is used to discriminate different alternatives (k number of cluster), as explained in section 3.2.3.3. Nineteen different values of $k \in [2,20]$ clusters are to be tested. Generating the set $A = \{ a_1: k = 2, a_2: k = 3, \dots, a_{19}: k = 20 \}$. These alternatives are discriminated pair by pair. A detailed theoretical explanation about MCDM ELECTRE 1S is provided in Annex III.

The use of MCDM aims finding the number of k clusters that meet the balance between minimizing the cluster dispersion (making elements of a cluster alike) and maximizing inter-cluster dispersion (making clusters different enough from each other). Therefore, six decision criteria are considered to evaluate the best alternative.

Objective	Criteria	Description
Minimize	g_1	Number of clusters k
	g_2	1 st quartile Q_1 of the intra-clusters distances
	g_3	2 nd quartile Q_2 of the intra-clusters distances
	g_4	3 rd quartile Q_3 of the intra-clusters distances
	g_5	Maximum M of the intra-clusters
Maximize	g_6	Mean inter-clusters distances

Table 16 Set of criteria for the MCDM ELECTRE 1S method

Table 16 and Figure 31 describes the criteria for MCDM. The criteria g_2 to g_5 evaluate the similarity of points inside each cluster through its intra-cluster

Euclidian distance. That is measured from the center of each cluster to its different quartiles, and afterwards an average of all the clusters is calculated : g_2 quantifies the size of a cluster's core (1st quartile), while g_3 and g_4 estimate the distance of peripheral points (2nd and 3rd quartile), and g_5 give the distances to the furthest point of the cluster. On the other hand, the criterion g_6 is based on the mean of the distances between the clusters' centroids. As note, the points located in the maximum and minimum distances within each cluster are excluded from these criteria, since they statistically bias the measures. Finally, g_1 indicates that number of clusters should be as less as possible, to reduce the number analysis points. As an additional constraint in the methodology framework, each cluster must have a minimum number of eight points for the alternative to eligible ($N_{\min} = 8$), since making statistics on less than eight points makes no sense.

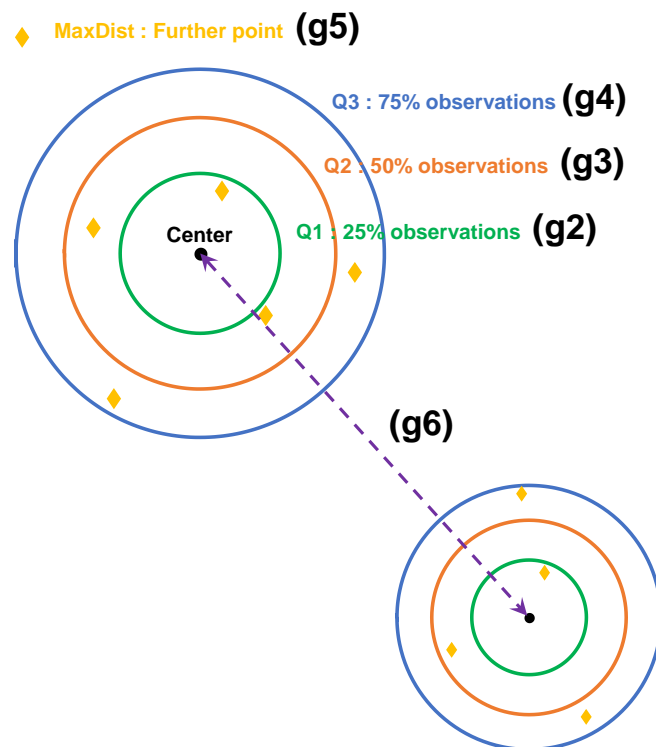


Figure 31 Graphical explanation of the set of criteria for the MCDM ELECTRE 1S method

Table 17 illustrates the MCDM performance table for the feasible scenarios from the simulations with $SS4=6.6$ (continuing with the example shown in Figure 29 and Figure 30).

Alternative [a_i]	Criteria [g_j]					
	g_1	g_2	g_3	g_4	g_5	g_6
	MINIMIZE				MAXIMIZE	
a_1	2	0.335	0.387	0.497	0.95	0.654
a_2	3	0.273	0.317	0.428	0.643	0.660
a_3	4	0.217	0.264	0.339	0.536	0.689
a_4	5	0.176	0.224	0.301	0.537	0.675
a_5	6	0.151	0.198	0.253	0.502	0.659
a_6	7	0.152	0.207	0.271	0.500	0.646
a_7	8	0.134	0.177	0.242	0.450	0.628
Weight [w_j]	0.2	0.15	0.15	0.15	0.15	0.2
Thresholds						
Indifference [q_j]	0	0	0	0	0	0
Preference [p_j]	1	0.0415	0.0394	0.0484	0.0367	0.01346
Veto [v_j]	7	0.122	0.1235	0.1749	0.3068	0.0311
Level of majority [s]	0.60					

Table 17 Enlarged performance table (example of $SS4=6.6$)

The performance table displays the seven alternatives that comply with the additional constraint of $N_{\min} = 8$. It specifies the partial concordance index for the six criteria g_i , their corresponding weights, thresholds of indifference, preference, and veto, as well as their majority level.

The weights have been determined with the intention of balancing and leaving no predominance among the criteria. The g_1 refers to the number of clusters, g_6 to the intercluster distance and g_2 to g_5 deal with the core size of the clusters. Therefore, the sum of weight of g_2 to g_5 balance the weight of the other criteria.

The thresholds allow making difference and drawing preferences between alternatives for driving decision. In that view, all the indifference thresholds are set to 0, considering that the smallest difference leads at least to a weak

preference of an alternative over another. It is been decided that the preference threshold for each criterion, correspond to the 1st quartile of all values $\Omega_j(a_k, a_i)$. In other words, 75% of the cases lead to a strict preference of one alternative over the other. That allows drawing strong preferences necessary for outranking relation. Note that $\Omega_j(a_k, a_i)$ is defined in Annex III and refers to the difference defining the advantage of alternative k over alternative i , considering criterion j . Regarding the veto thresholds, it corresponds to the 3rd quartile of advantages values. Therefore, 25 % of them lead to a veto situation. Finally, the majority level has been set to 60 %, which means that *it is necessary to have at least 60 % of the criteria total weights in concordance, to set an outranking relationship*. The level is quite high in order to increase the requirements of an outranking relation.

Given the information above, it is possible to calculate the concordance and discordance matrixes (Table 18 and Table 19), that allow to identify respectively if the concordance and non-veto conditions are fulfilled for each pair of alternatives.

The proper way to read the concordance matrix (Table 18) is from horizontal to vertical, for example, “The alternative a_5 of forming six clusters is at least as good as the alterative a_1 of forming two clusters, with a value of 0.8”. Then it is evident that alternatives a_5 and a_7 present concordance value bigger than the majority level in all the cases.

	a ₁	a ₂	a ₃	a ₄	a ₅	a ₆	a ₇
a ₁	1.	0.29	0.2	0.2	0.31	0.4	0.4
a ₂	0.8	1.	0.2	0.2	0.4	0.4	0.4
a ₃	0.8	0.8	1.	0.58	0.41	0.4	0.4
a ₄	0.8	0.8	0.6	1.	0.52	0.61	0.4
a ₅	0.8	0.78	0.60	0.60	1.	0.99	0.68
a ₆	0.69	0.6	0.6	0.6	0.5	1.	0.58
a ₇	0.6	0.6	0.6	0.6	0.6	0.6	1

Table 18 Concordance matrix and outranking relations (example of SS4=6.6)

However, from Table 19, a_7 is in veto situation with alternatives a_2 , a_3 , a_4 and a_5 , which means that it does not outrank these alternatives, even if exceeds the majority level in the concordance matrix.

	a_1	a_2	a_3	a_4	a_5	a_6	a_7
a_1	0	1	1	1	1	1	1
a_2	0	0	0	0	1	0	1
a_3	0	0	0	0	0	0	0
a_4	0	0	0	0	0	0	0
a_5	0	0	0	0	0	0	0
a_6	0	0	1	0	0	0	0
a_7	0	1	1	1	1	0	0

Table 19 Discordance matrix (example of $SS4=6.6$). Note: one means veto condition.

Thus a_5 , corresponding to six clusters, is the only alternative defeating all the others in concordance matrix (Table 18) and complies the non-veto condition expressed at the discordance matrix (Table 19). Then, for the simulations with $SS4=6.6$ (following the example in Figure 29 and Figure 30), the MCDM ELECTRE 1S suggests creating six clusters with K-Means.

The clusters group solutions according to similarities in the features before mentioned. Figure 32, shows the distribution of clusters across the axis of annual loads E, H, C for $SS4=6.6$. It illustrates that the solutions within each cluster share common characteristics regarding load size.

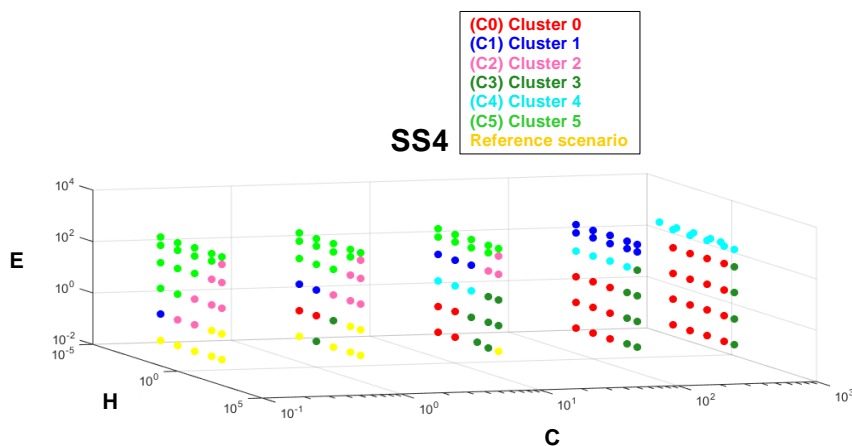


Figure 32 Clusters across the axis of annual loads E, H, C (example for $SS4=6.6$).

The implementation of the methodology for the rest spark spread rates suggests that the best alternative is to group the solutions into three clusters ($k=3$) for SS1 and six clusters ($k=6$) for SS2, SS3, and SS4. To ensure obtaining relevant clusters that segregate properly the techno-economic performance of scenarios, the segregation criterion in SS1 is the percentage of savings, while the other use the savings, in addition to the Grid, Boiler, Absorption, and energy flows.

4.4 Results interpretation

To delve deeper into the impacts of the spark spread rate and the size of loads, the analysis is structured as follows:

Analysis of generation mean for each energy carrier

Analysis of energy flows within the CCHP-TS system

Analysis of the percentage of savings

The results analysis in the following sections is in terms of the load dominance rates r_n (Eq. 42 to Eq. 44). They are parameters to measure the relative weight of the annual loads of electricity, heating, and cooling (E, H, and C respectively).

Dominance rate for annual electricity load Eq. 42

$$r_E = \frac{E}{E + H + C}$$

Dominance rate for annual heating load Eq. 43

$$r_H = \frac{H}{E + H + C}$$

Dominance rate of annual cooling load Eq. 44

$$r_C = \frac{C}{E + H + C}$$

The sum of these three dominance rates reflects the energy conservation ($r_E + r_H + r_C = 1$). Then, using them in ternary diagrams aims to show the behavior of the functioning variables and compare them among the spark spread rates.

Each vertex of the ternary diagrams represents dominance rates equal to 1 for each energy carrier. In other words, the left, right, and top vertices represent respectively Heat, Cooling, and Electricity load only. Each square in the diagram embodies a scenario, while the size reflects the value of the characterization variable. The colors identify the different clusters that are particularly relevant for the analysis of the percentage of savings. However, the color code keeps for all the section to facilitate tracking and analyzing the different simulations across all the functioning variables.

The following two subsections analyze the results for each functional variable. They focus on describing their behavior , across the load dominance and spark spread rates. The relevance relies on showing the operational and economic performance of the CCHP-TS system under different conditions.

4.4.1 Analysis of generation means for each energy carrier

This section aims to characterize the generation means for the energy carriers, given the dominance of loads and spark spread rates.

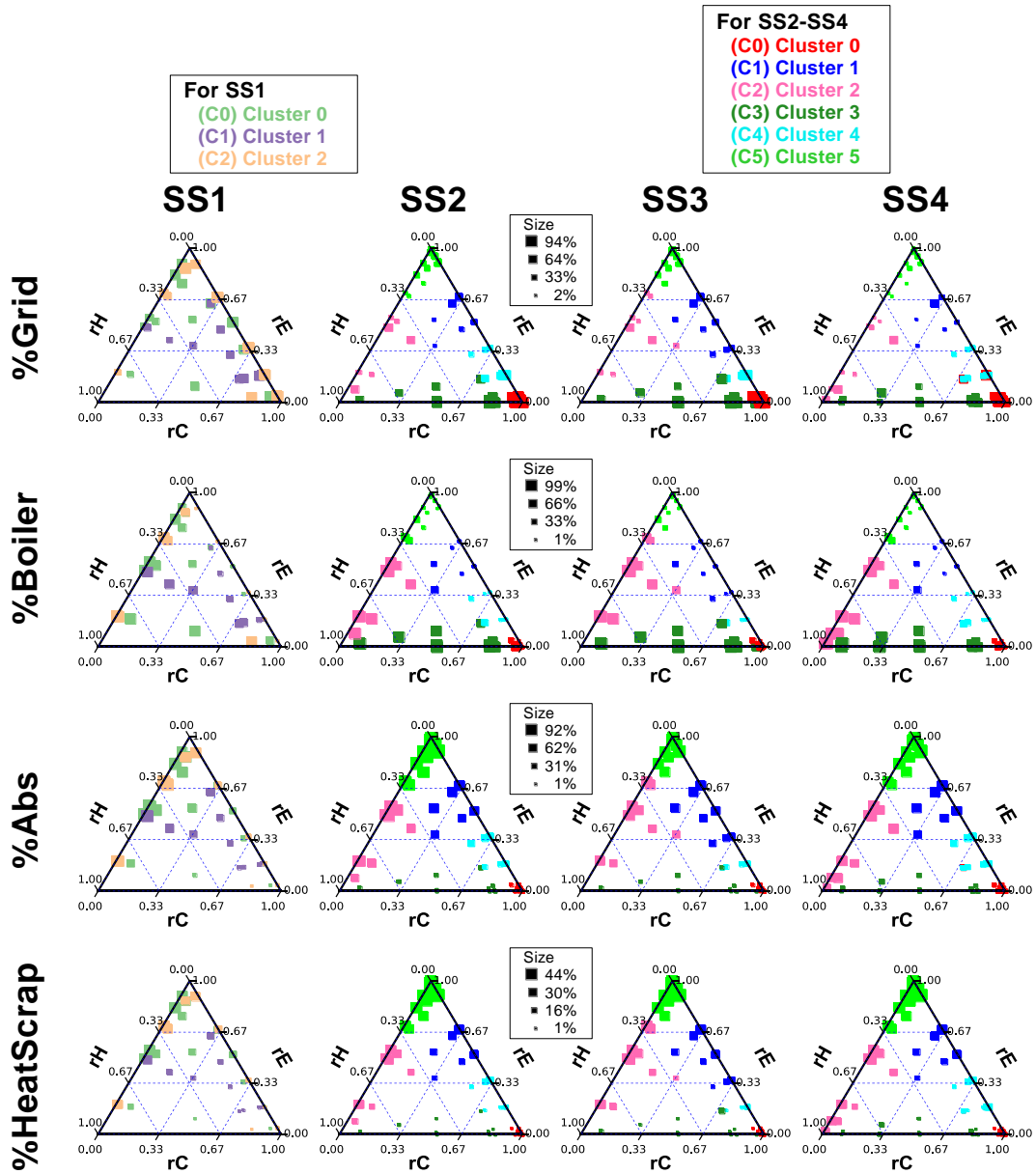


Figure 33 Ternary diagram for the distribution of the percentage of Grid, Boiler, Absorption, and Heat Scrap across dominance rates (r_E , r_H , r_C) and SS rates.

PERCENTAGE OF GRID

The percentage of the grid measures how much electricity is imported from the grid, apart from the electricity that results from the CHP units. This electricity can be used directly to meet electric load or to produce cooling through vapor compression chillers. The first line of diagrams of the Figure 33 presents the ternary diagrams in terms of percentage of the grid.

For all the spark spread and especially for $SS1=3$, the percentage of the grid reduces in two cases. First, when the heating load dominates because it does not need the grid to cover them. Second, when the dominance of loads is balanced (referring to the points in the middle of the diagrams). It suggests that a load balance promotes the usage of the CCHP-TS system, especially for SS1. For SS2-SS4 (when the spark spread rate is larger than 3), the percentage of the grid is small when the dominance of electric load is high. Therefore, this condition promotes the use of the CCHP-TS system.

In contrast, the percentage of the grid is high when cooling load dominates. It is because it is more convenient to use vapor compression chiller powered by the grid under these circumstances. There is more detail of this in the analysis corresponding to the percentage of absorption.

The analysis above points out that the behavior and trend of %Grid in SS1 is slightly different from SS2-SS4. In the latter, the use of CCHP-TS systems is especially feasible when electric load dominates.

PERCENTAGE OF BOILER

The percentage of Boiler (second line of diagrams in the Figure 33) measures how much heating is provided directly from a natural gas boiler. For all the SS rates, it is larger when the heating load dominates, r_H (Figure 33), while r_E , and r_C have no real influence. Therefore, heating load alone never justifies the use of CHP, and then Boiler is used as the generation unit. Note that the trend and average value (square size) are the same for all the SS rates, differing only in the number of feasible scenarios that reduce with the SS rate.

PERCENTAGE OF ABSORPTION AND HEAT SCRAP

The percentages of Absorption and Heat Scrap are large when electric loads dominate (Figure 33). Because when there is a surplus of heat produced by the CHP, the Absorption is used as much as possible, trying to reduce the Heat Scrap.

On the contrary, Absorption and Heat Scrap are small when cooling loads dominate. Because in those cases there is a preference for vapor-compression chiller due to the large difference in COP (4.5 for vapor-compression [175] and 0.8 for absorption [176]).

Subsection 4.4.3 analyze the percentage of savings for the clusters identified in Figure 33. The Figure 35 and Figure 37 represent the percentage of savings by the size of the squares. There, it is well shown that, especially for SS2-SS4, some of the clusters with the highest percentage of savings also have the largest percentages of Heat Scrap. This is important because it reflects that the Heat Scrap does not affect greatly the percentage of savings obtained. The reason is that from the economic point of view (and not strictly from the energy point of view), it is cheaper to produce electricity rather than buying it from the grid, even if it produces a surplus of heat.

The trends for the percentage of Absorption and Heat Scrap are the same for all the SS rates. The only difference is the number of feasible scenarios that reduce accompanying the SS rate.

4.4.2 Analysis of the energy flows within the CCHP-TS system

Regarding the energy flow variables (Figure 34), the main flows of CHP (electricity and heat) –E4E, E4C, H4H, and H4C– have the same trend and average value (square size) across the spark spread rates. In other words, they are equal for all SS rates, except that the number of feasible scenarios reduces. In contrast, the flows for the storage –E4CS and H4CS– are different in square size (average value) but follow the same trend across the different SS rates. Observe that none feasible solution includes heat storage. The reason is related to the marginal cost of storing heat, which is larger than the marginal cost of activating the boiler to produce the shortage of heat.

As expected, E4E grows with the electric dominance r_E , and H4H grows with the heating dominance r_H . While E4C and H4C grow with the cooling dominance r_C , but these are respectively more representative when Electric and Heating dominance is low.

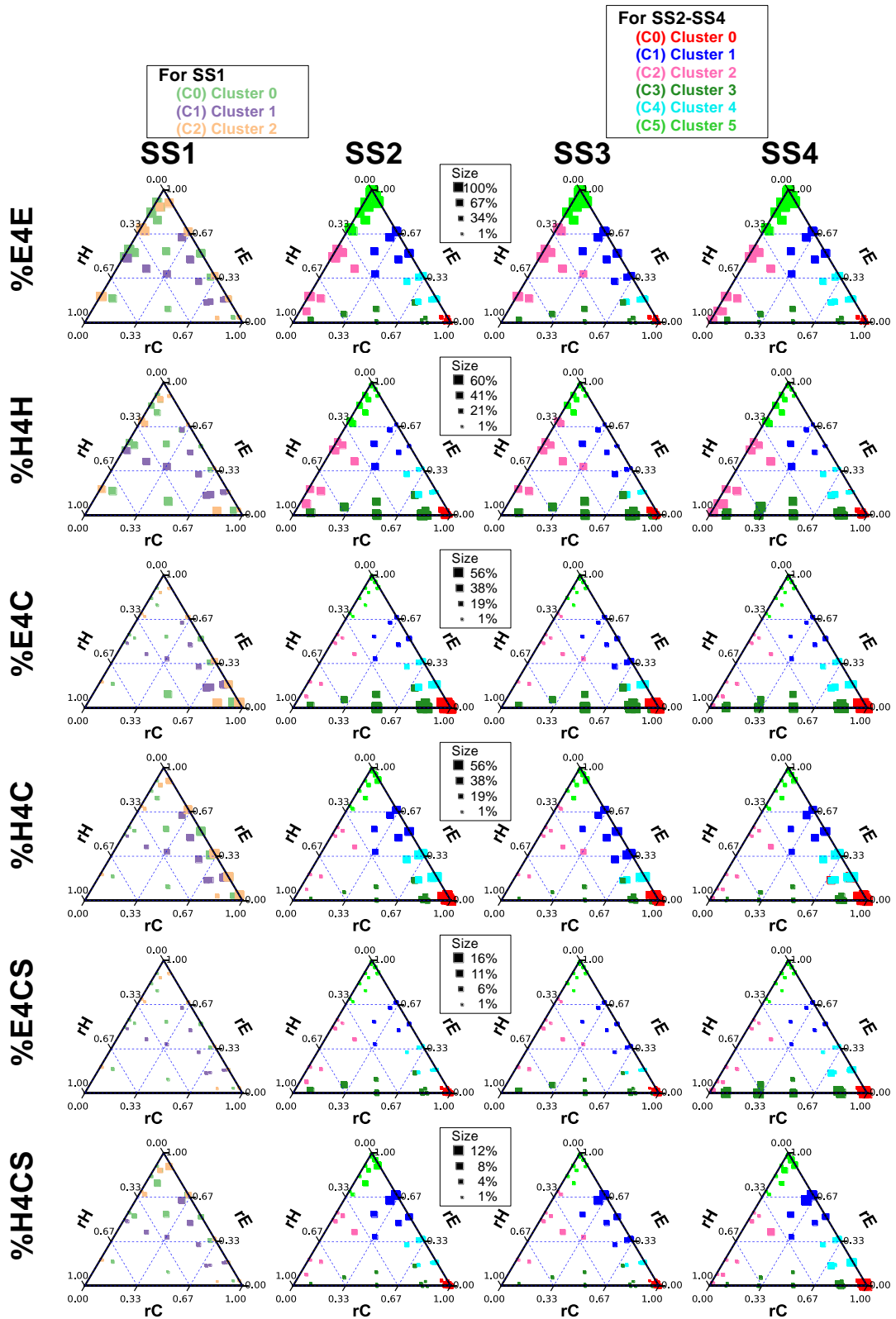


Figure 34 Ternary diagram for the distribution of E4E, E4C, E4CS, H4H, H4C and H4CS across dominance rates (r_E , r_H , r_C) and SS rates.

On the other hand, the Cooling Storage gives flexibility to the CCHP-TS systems because it decouples its production and consumption. The functioning variables E4CS and H4CS (Figure 34) indicate if the accumulated cooling is produced with electricity or heat respectively. In general, E4CS and H4CS are small, but they are slightly more representative for SS4=6.6. Because a high SS favors the use of CHP for electricity loads, leaving the heat as co-product and available to produce cooling and store it. E4CS is larger in clusters C0 and C3 (from SS2-SS4) because it is preferable using the vapor-compression chiller when cooling loads dominate (C0: $r_C=98\%$ and C3: $r_C=58\%$). On the other hand, H4CS exists when $r_E \gg r_H$, using heat from the CHP to produce cooling and store it. Therefore, Cooling Storage promotes the usage of Absorption and potentializes Trigeneration.

4.4.3 Analysis of the percentage of savings

This section analyzes the percentage of cost savings reached by using the CCHP-TS system compared to the reference design of the energy system. For better characterization, the analysis divides the cases when the spark spread is higher than three, and when it is equal to three.

THE CASES OF SS > 3

This section analyzes the feasible scenarios corresponding to SS2=3.9, SS3=5.4, and SS4=6.6. Note from Figure 35 that the three have the same number of clusters (six clusters). Moreover, these clusters have similar characteristics along the three SS rates. The following paragraph gives a brief outline of each cluster, making some references to the characterization variables of section 4.3.

Cluster C5 consolidates the scenarios where electric load dominates and use the CHP almost exclusively to cover it (high E4E and low %Grid). For scenarios in C1, electricity load dominates slightly more than cooling. Therefore, electricity from the CHP covers the corresponding load and the heat is used to produce

cooling (refer to the analysis of E4E, and H4C). Regarding C4, it is a cluster with a shared dominance between electricity and cooling demand, then it uses CHP electricity production to cover electric demand, and uses both, electricity and heat, to cover cooling demand (refer to the analysis of E4E, E4C, and H4C). As for C2 has a shared dominance between electricity and heat demand, therefore, uses CHP to cover these demands directly (refer to the analysis of E4E, and H4H). On the other hand, C0 consolidates scenarios where the cooling demand is very high and then it uses electricity and heat produced by the CHP to cover cooling demand (refer to the analysis of E4C, and H4C). Finally, C3 has a shared dominance between heat and cooling demand, so, it uses electricity to produce cooling and heat to cover the demand (refer to the analysis of H4H, and E4C).

Regarding the percentage of savings, indicated by the size of the squares at Figure 35, the smaller are at the bottom-left of the three diagrams ($r_H \rightarrow 1$) and the larger at the top ($r_E \rightarrow 1$). In other words, the dominance of the electric load favors the percentage of savings for the CCHP-TS systems. In contrast the dominance of heating loads disfavors it. Regarding the dominance of cooling, this diagram does not show that r_C governs the percentage of savings.

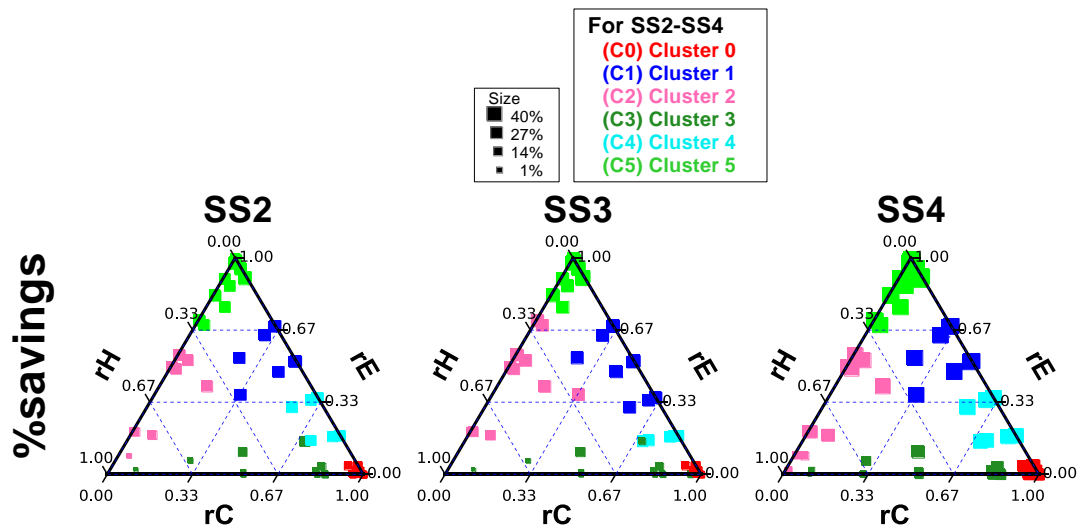


Figure 35 Ternary diagrams of SS2, SS3 and SS4 for the distribution of the percentage of savings across dominance rates (r_E , r_H , r_C)

NOTE: The percentage of savings are represented by the square size

On the other hand, the difference among SS2, SS3, and SS4 is that the percentage of savings increases with the spark spread rate (Table 15 and Figure 35) because a higher SS makes more feasible to produce electricity in-house.

Figure 36 shows boxplots for each cluster in terms of the percentage of savings and $r_E - r_H - r_C$. It allows confirming the remark from the ternary diagram of Figure 35. The clusters with the largest dominance of electric load have the largest average percentage of savings (C5: $r_E=92\%$ and $\%savings=39\%$; C1: $r_E=60\%$ and $\%savings=37\%$). The clusters with middle dominance of electric load have a middle average percentage of savings (C4: $r_E=22\%$ and $\%savings=33\%$; C2: $r_E=30\%$ and $\%savings=23\%$). Note that C2 has larger r_E than C4, but the latter has a better percentage of savings. This situation is related to the larger dominance of cooling load (r_C) in C4. The analysis of the percentage of absorption in section 4.4.1 shows that C4 uses more vapor-compression chiller than C2. Therefore, the trend established is still valid because the cooling load of C4 contributes to an increase in the electric load. Finally, the clusters with lower dominance of electric load have the lowest average percentage of savings (C0: $r_E=7\%$ and $\%sav=16\%$; C3: $r_E=3\%$ and $\%sav=11\%$). This pair of clusters is an excellent example of the low impact that the heating and cooling loads have over the percentage of savings when electric loads are not present. For the dominance of cooling loads, note that C0 and C3 have the largest r_C among all the clusters. Section 4.4.1 shows that they are covered mostly with a vapor-compression chiller. However, this transformation of cooling loads into electric one is not enough to drive savings up. On the other hand, the dominance of heating loads (r_H) also demonstrates a lack of relevance since both clusters have the same level of $\%savings$, although only C3 has larger heating loads.

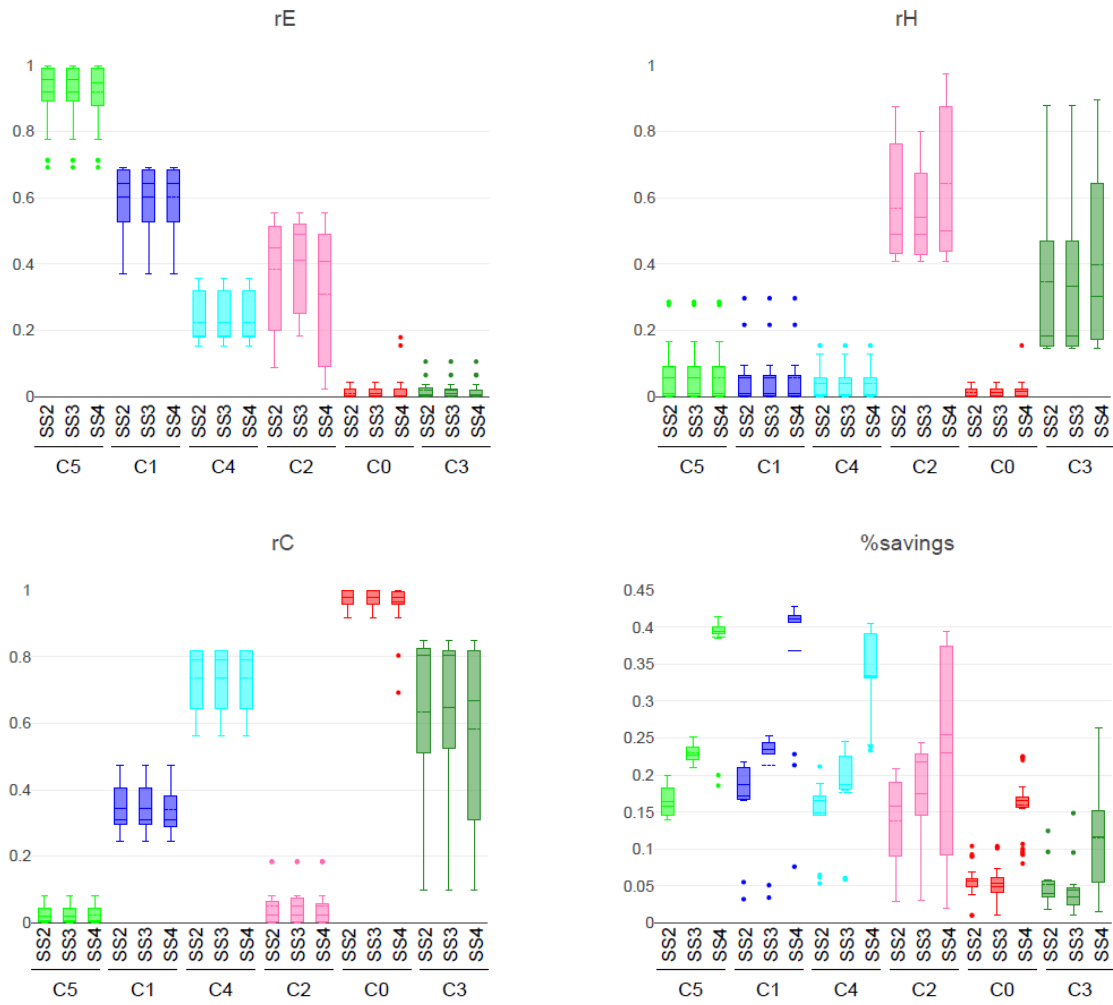


Figure 36 Boxplots comparing r_E , r_H , r_C , and the percentage of savings for each cluster across the spark spread rates SS2-SS3-SS4.

THE CASE OF SS=3

This section analyzes the 50 scenarios that are feasible with SS1=3. Note that the scenarios in SS1, different from SS2-SS3-SS4, have a lower percentage of savings and are segregated into three clusters only. The ternary diagram in Figure 37 shows them distributed according to their dominance load rates.

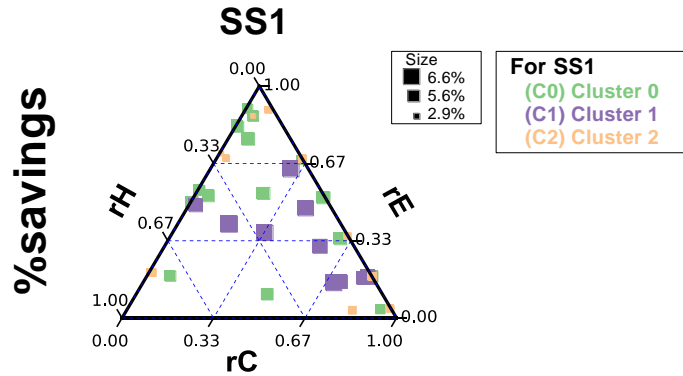


Figure 37 Ternary diagrams of SS1 for the distribution of the percentage of savings across dominance rates (r_E , r_H , r_C)

NOTE: The percentage of savings are represented by the square size

Cluster C1 consolidates the scenarios with the highest percentage of savings (bigger squares). It is in the middle-right of the ternary diagram, corresponding to a balance among the loads with a slight trend to a low dominance of heating.

Figure 38 presents the boxplots of dominance load rates and the percentage of savings for the three clusters. The charts show that C1, the cluster with the higher percentage of savings, is the only one where all the scenarios present the three loads, while the others could have the absence of heating or cooling loads. Although the boxplots show big ranges of variation for $r_E - r_H - r_C$, it is possible to infer that the higher percentage of savings in SS1=3 relates to the balance of Electric, Heating, and Cooling loads (as suggested as well per the ternary diagram in Figure 37).

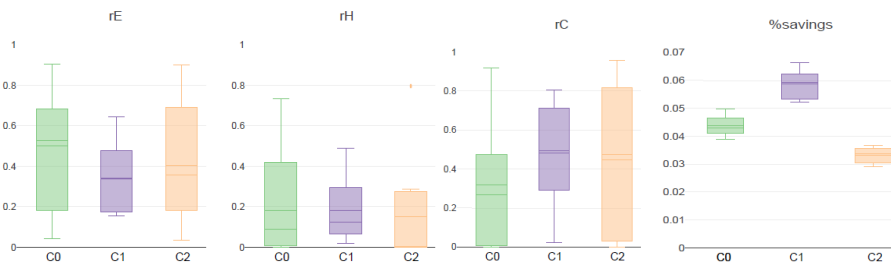


Figure 38 Boxplots comparing r_E , r_H , r_C , and the percentage of savings for each cluster across the spark spread rate SS1 = 3.0

The finding in this section regarding the relationship between the savings and the balance of loads is aligned with the study presented by Knizley et al. [47].

They use an SS rate=2.77 and propose that the monthly economic savings of a CHP system are likely to occur if electricity loads are not much larger than the heating loads. These authors measure it with the monthly PHR (power to heat ratio). They verified their hypothesis with seven out of eight case studies (buildings).

4.4.4 Summary of results

The proposed methodology allowed to analyze multiple optimal scenarios of trigeneration systems with thermal storage, bringing further insights on the rules of thumb for their design.

The results stemming from the analysis indicate that the techno-economic feasibility of a CCHP-TS system relies upon different combination of spark spread and the load dominance rates. For low spark spreads (SS=3), the loads should be balanced among the energy vectors. While for high spark spreads (SS>3), the savings are higher when the electricity load dominates.

The trend for the percentage of Boiler, Absorption and Heat Scrap are the same for all the SS rates, differing only in the number of feasible scenarios. In general, it is more profitable to use the boiler when heating loads dominate. Regarding absorption for cooling, it is only economically better when the cooling loads are relatively low. Furthermore, when electric loads dominate, it favors the use of Absorption and Cooling Storage (H4CS), because it reduces the Heat Scrap. This behavior is stronger with larger SS rates.

However, heat scrap does not affect the percentage of savings significantly. In other words, it is more profitable to oversize heat production and ensure that the CHP covers the electricity load.

Here, it is evident that the CCHP-TS is a flexible system because it supplies the energy (electricity, heating, and cooling) with different units. Moreover, the thermal storage improves this flexibility by decoupling the supply and demand.

The work developed in this chapter reveals that there is a two-level characterization. First, there is a threshold in the Spark Spread rate (SS)

influencing the techno-economic feasibility of a CCHP-TS system. And that threshold indicates how the size of the annual loads influence.

The work also reveals the importance of electricity loads for any spark spread rate, because the use of CCHP-TS is feasible when these exist or even dominate. In contrast, heating loads do not have the same relevance because the system could be feasible despite a high percentage of Heat Scrap. In general, when heating or cooling loads dominate, it is preferable to use the auxiliary units (boiler and vapor-compression chiller). However, the reader should notice that the existence (not dominance) of heating and cooling improves the environmental performance, by reducing the heat scrap [59].

4.5 Hypothesis regarding the impact of energy prices

4.5.1 Problem statement

Subsection 4.4.3 was devoted to analyzing the behavior of the percentage of cost savings. For the case of $SS > 3$, there are three spark spread rates (SS) to analyze. The simulations corresponding to each are classified within six different clusters. Those six clusters are comparable among the three spark spread rates, because they share similarities regarding their segregation parameters (read subsection 4.4.3). Figure 36 shows how the percentage of cost savings changes across the three SS rates for each cluster. Interestingly, this change is not linear. Taking the averages of the boxplot corresponding to the percentage of cost savings in Figure 36, we have the following pattern for each cluster (Figure 39).

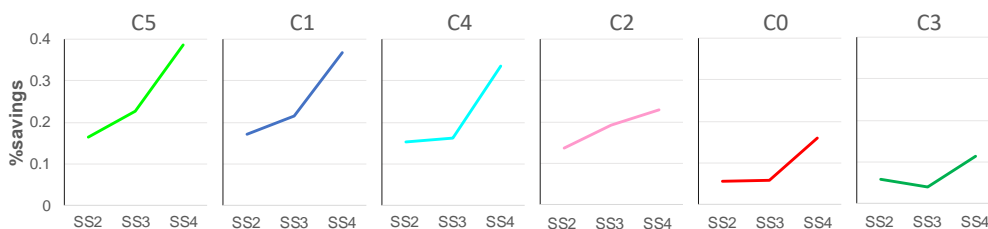


Figure 39 Average percentage of savings for each cluster across spark spread rates SS2-SS3-SS4.

KEY C0 – C5 correspond to the data of cluster 0, cluster 1, ..., cluster 5.

The patterns present a bow in the SS3, that in some cases even suggest lower savings for SS3 than for SS2. A possible way to explain this non-linear behavior is that each spark spread (SS2, SS3, and SS4) has different prices of electricity and natural gas (see Table 20).

	SS2	SS3	SS4
Spark spread	3.9	5.4	6.6
Price of electricity [pE]	15.8	10.3	16.23
Price of natural gas [pNG]	4.0	1.9	2.46

Table 20 Prices of electricity and natural gas (in cents of EUR / kWh) for the spark spread rates in chapter 4.

If the reader observes carefully, the price of electricity for SS2 and SS4 are close to 16 cents of EUR. While the one of SS2 is completely different (~10 cents).

4.5.2 Creating a hypothesis

In the diagram outlining the percentage of savings and the spark spread rate (Figure 39), exist isolines corresponding to each price of electricity. The behavior of those isolines respects the following trend: the larger the spark spread, the larger the percentage of savings. In the Figure 39, the line corresponding to the cluster 3 (C3) presents a bow, suggesting that the percentage of savings is lower for SS3 = 5.4, than for SS2 = 3.9. The reason might be that SS2 and SS4 belong to one isoline of electricity price, while SS3 belongs to a different one.

4.5.3 Testing the hypothesis

To prove the hypothesis, we are exploring the impact of varying one price at a time (parametric analysis). The steps below will follow the example of analyzing the price of electricity.

1. Determine the variable to analyze, E.g. price of electricity.

2. Fix the values to explored regarding the spark spread and the variable of analysis, E.g. spark spread and price of electricity.
3. Determine the values of the other variable, E.g. price of natural gas.

Note that from the combinations created (see Table 21), some of them are feasible to implement a CCHP-TS systems (white), some other are unfeasible (blue), and other are technically feasible although they do not exist in a real European context (gray).

		<i>Value of pNG</i>									
		SS									
		1.5	2.0	2.5	3.0	3.5	4.0	4.5	5.0	5.5	6.0
pE	0.28	0.19	0.14	0.11	0.09	0.08	0.07	0.06	0.06	0.05	0.05
	0.25	0.17	0.13	0.10	0.08	0.07	0.06	0.06	0.05	0.05	0.04
	0.22	0.15	0.11	0.09	0.07	0.06	0.06	0.05	0.04	0.04	0.04
	0.19	0.13	0.10	0.08	0.06	0.05	0.05	0.04	0.04	0.03	0.03
	0.16	0.11	0.08	0.06	0.05	0.05	0.04	0.04	0.03	0.03	0.03
	0.13	0.09	0.07	0.05	0.04	0.04	0.03	0.03	0.03	0.02	0.02
	0.10	0.07	0.05	0.04	0.03	0.03	0.03	0.02	0.02	0.02	0.02

Table 21 Feasible combinations by fixing price of electricity and spark spread rate.

KEY: Non-feasible scenarios (blue); Scenarios technically feasible, but non-existent at the European context (gray); Existent and feasible scenarios (white).

4. Simulate the different combinations in DER-CAM.
5. Build the isolines of the selected variable, E.g. price of electricity.

Isolines for the price of electricity

Figure 40 shows the isolines obtained after getting the percentage of savings for each combination of prices.

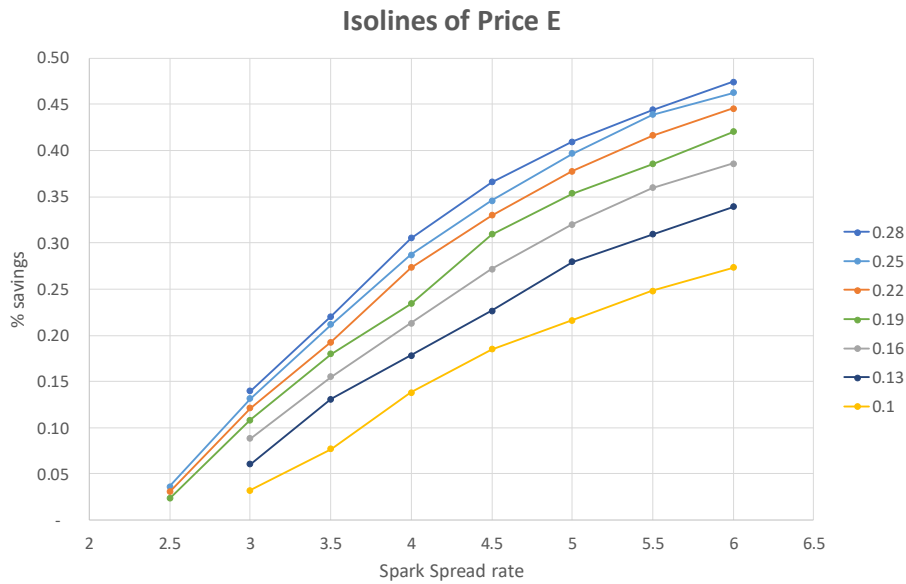


Figure 40 Isolines for the price of electricity [\$/kWh]

The Figure 40 confirms what was seen in the diagram outlying the percentage of savings and the spark spread rate (Figure 39), there are isolines corresponding to each price of electricity. The behavior of those isolines respects the following trend: the larger the spark spread, the larger the percentage of savings”.

Moreover, those isolines never cross each other, even if they become closer and closer. Therefore, it is possible to conclude that in Figure 39, SS3 belongs to a different isoline than SS2 and SS4. In fact, in the strict sense, SS2 and SS4 should belong to two different isolines.

Isolines for the price of natural gas

A similar hypothesis can be confirmed for gas prices. Once we already proved that there are isolines of electricity prices, it is interesting to test the following hypothesis as well:

Similarly, in the diagram outlying the percentage of savings and the spark spread rate (Figure 39), there are isolines corresponding to each price of natural gas.

Like in the Table 21, Table 22 shows the feasible scenarios for a CCHP-TS systems (white), the unfeasible ones (blue), and others that are technically feasible although they do not exist in a real European context (gray)

		Value of pE									
		SS									
		1.50	2.00	2.50	3.00	3.50	4.00	4.50	5.00	5.50	6.00
pNG	0.10	0.15	0.20	0.25	0.30	0.35	0.40	0.45	0.50	0.55	0.60
	0.08	0.12	0.16	0.20	0.24	0.28	0.32	0.36	0.40	0.44	0.48
	0.06	0.09	0.12	0.15	0.18	0.21	0.24	0.27	0.30	0.33	0.36
	0.04	0.06	0.08	0.10	0.12	0.14	0.16	0.18	0.20	0.22	0.24
	0.02	0.03	0.04	0.05	0.06	0.07	0.08	0.09	0.10	0.11	0.12

Table 22 Feasible combinations by fixing price of natural gas and spark spread rate

KEY: Non-feasible scenarios (blue); Scenarios technically feasible, but non-existent at the European context (gray); Existent and feasible scenarios (white).

Figure 41 shows the isolines obtained after using DER-CAM to obtain the percentage of savings corresponding to each combination of prices.



Figure 41 Isolines for the price of natural gas

There are isolines for the price of natural gas in the diagram outlining the percentage of savings vs. the spark spread rate. In these isolines, the larger the spark spread, the larger the percentage of savings. And the isolines never touch each other, even if they become closer and closer.

In the feasibility assessment of a CCHP-TS system, there is a clear relationship between the percentage of savings and the spark spread rate. However, this

relationship can be described also by isolines for the price of electricity and natural gas. These isolines presents different slopes among them and specially between the two prices. That suggests that the price of electricity and natural gas are impacting differently. Therefore, it would be interesting to explore them as individual variables, rather than consolidate them into the spark spread rate.

4.6 Conclusions of the section

The work in this chapter demonstrates the importance of analyzing multiple scenarios of energy load size and spark spread rates to assess the techno-economic feasibility of a Trigeneration system with Thermal Storage (CCHP-TS). The methodology proposed combines a full factorial DoE, the energy system optimization with DER-CAM, the clustering method k-means, and the Multi-Criteria Decision-Making method ELECTRE 1S.

The results highlight the joined influence of spark spread and energy loads over the percentage of savings. Moreover, the analysis emphasizes the interest of using load dominance rates r_E , r_H , r_C . These quantify the relative weight of the loads for each energy vector. In other words, the results of this chapter strongly advise about the existing interaction effects between the variables of analysis.

Additionally, the work in this chapter gave some hints to suspect that the impact of the prices (electricity and natural gas) on the feasibility of a CCHP-TS system could be different in magnitude (section 4.5). Therefore, in the next section, the prices are analyzed separately, instead of consolidated into the spark spread rate.

In conclusion, the work in chapter 4 demonstrates that the CCHP-TS model used is relevant and sensitive to the variables of analysis (energy prices and annual size of the loads). The next part of the research will deepen the impact of these variables by implementing global sensitivity analysis methods and analyzing the prices separately.

5 PHASE II: Sensitivity analysis of the CCHP-TS feasibility

5.1 Introduction

This chapter consists in examining the impact of five variables - the price of electricity (pE), the price of natural gas (pNG), and the annual loads (E : electricity, H : heating, C : cooling) – on the feasibility of the Trigeneration-Thermal Storage systems considering two metrics: the amount of savings, and the percentage of savings. The first metric quantifies the absolute savings of using the CCHP-TS system, while the second measures the relative savings. Studying both aim to understand if the variables impact differently in each case.

The tool used for the energy system optimization is the adapted model explained in section 3.3.1, and the technological settings showed in Table 10 to Table 14. The methods used to perform the sensitivity analysis are Morris (derivative-based approach), Sobol (variance-based approach), and VARS (variogram-based approach). By using the three methods, we intend to compare the capacity of each, evaluating their computational cost, as well as precision and information given in an operational context of feasibility analysis.

We introduce in this chapter the use of isolines for each variable, to allow a deeper understanding of the impact of the different variables.

At the end of the chapter, we determine 1) the combination of energy prices (pE and pNG) and size of the annual energy loads (E , H , C) that make a Trigeneration – Thermal Storage feasible; 2) the impact of each price component, establishing the real relevance of using the Spark Spread rate as a common ratio to access the economic feasibility of a Trigeneration-Thermal Storage. Additionally, there is an overall comparison of the three sensitivity analysis methods studied.

5.2 Morris – Derivative based approach

As explained in subsection 3.3.3.1, Morris SA calculates the sensitivity analysis indexes based on r routes that change all the variables one by one. The generation of routes is based on the method of Latin Hypercube (LHS) proposed by Morris (1991). Afterwards, the sensitivity indexes are given and interpreted for different ranges of loads.

For this work, $r=20$ routes that allow varying each of the five variables (pE , pNG , E , H , and C). All of them use a $p=4$ levels, $\Delta=2/3$, and uniform distribution. Campolongo [119] suggests $r=10$ and $p=4$ to ensure a representative sample, ours is double the size, then it is reasonable to trust in ours. The prices are expressed in \$/kWh and their ranges are $R=\{0.10 ; 0.28\}$ for pE and $R=\{0.02 ; 0.10\}$ for pNG . The ranges of the prices are chosen to include the case of different European countries (Figure 16 and Eurostat [66]). On the other hand, the different loads (E , H , and C) vary in three ranges, all expressed in GWh/y: firstly, in the range from 0 to 10, when $E=\{0,3.3,6.6,10\}$, $H=\{0,3.3,6.6,10\}$, and $C=\{0,3.3,6.6,10\}$; secondly, the range from 0 to 100, when $E=\{0,33,66,100\}$, $H=\{0,33,66,100\}$, and $C=\{0,33,66,100\}$; and thirdly, the range from 0 to 1000, when $E=\{0,333,666,1000\}$, $H=\{0,333,666,1000\}$, and $C=\{0,333,666,1000\}$. These ranges aim to cover logarithmically the energy loads presented in the subsection 2.2.2. The computational cost of this method represents 120 simulations per each range of loads. Table 23 shows the first points of the $r=20$ routes, generated with LHS.

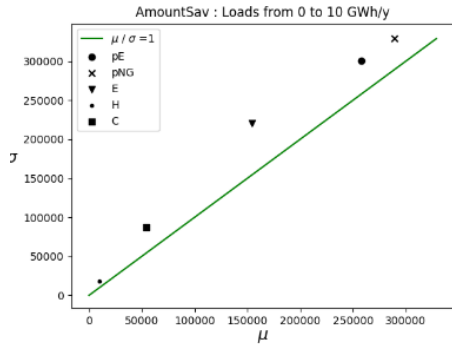
<i>1rs point of route...</i>	pE	pNG	E	H	C
1	0.28	0.100	100.00	33.33	100.00
2	0.16	0.020	0.00	100.00	100.00
3	0.10	0.073	100.00	33.33	0.00
4	0.22	0.020	33.33	66.67	33.33
5	0.28	0.020	100.00	0.00	66.67
6	0.22	0.047	0.00	100.00	0.00
7	0.16	0.047	66.67	0.00	33.33
8	0.28	0.100	66.67	33.33	0.00
9	0.22	0.073	66.67	66.67	66.67
10	0.10	0.073	33.33	100.00	66.67
11	0.22	0.020	0.00	66.67	66.67
12	0.28	0.047	33.33	0.00	100.00
13	0.16	0.073	100.00	100.00	100.00
14	0.22	0.100	66.67	0.00	33.33
15	0.10	0.100	33.33	33.33	0.00
16	0.28	0.020	0.00	66.67	33.33
17	0.16	0.073	66.67	100.00	33.33
18	0.10	0.047	0.00	33.33	66.67
19	0.10	0.047	33.33	66.67	0.00
20	0.16	0.100	100.00	0.00	100.00

Table 23 First point of the 20 routes for the Morris SA

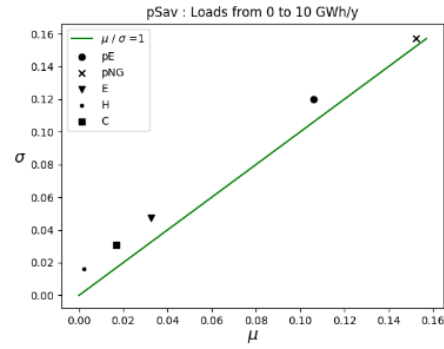
The results are given in planes (μ, σ) , following the proposal of Morris and Saltelli [119], [156]. For comparison purposes among the variables, the plane (μ, σ) uses the absolute value $|\mu|$, instead of μ . A the line $\mu = \sigma$ helps to identify three types of variables: 1) when $\sigma > \mu$, it is a variable with non-linear and/or interaction effects, 2) when $\sigma \approx \mu$, the non-linear and/or interaction effects are small, 3) when $\sigma < \mu$, the variable has strong additive effect (linear), without interactions. Additionally, the tables below each chart show the values of μ , to compare it with μ^* , giving information regarding the monotonic or non-monotonic behavior of variables.

The three charts and tables at the left part of Figure 42 analyze the amount of savings when E, H , and C range from 0 to 10, from 0 to 100, and from 0 to 1000 (top, middle, and bottom respectively).

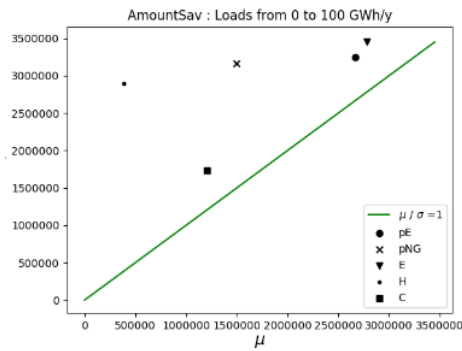
Similarly, the three charts and tables at the right part of Figure 42 give the information for the percentage of savings when E, H , and C range from 0 to 10, from 0 to 100, and from 0 to 1000 (top, middle, and bottom respectively).



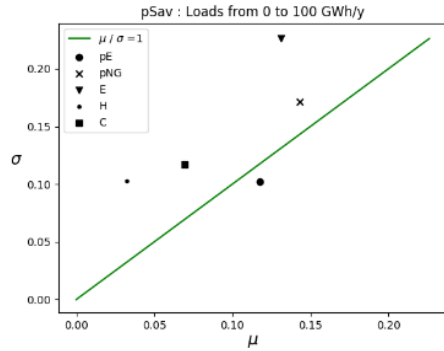
Parameter	μ^*	μ	σ
pE	257,595	257,595	301,104
pNG	289,411	-289,411	329,031
E	154,534	154,395	220,748
H	9,608	9,608	18,528
C	54,278	54,210	87,317



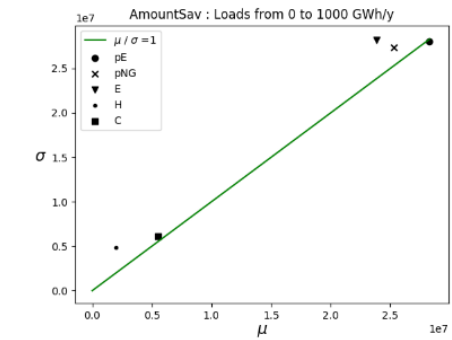
Parameter	μ^*	μ	σ
pE	0.11	0.11	0.12
pNG	0.15	-0.15	0.16
E	0.03	0.03	0.05
H	0.01	0.00	0.02
C	0.02	0.02	0.03



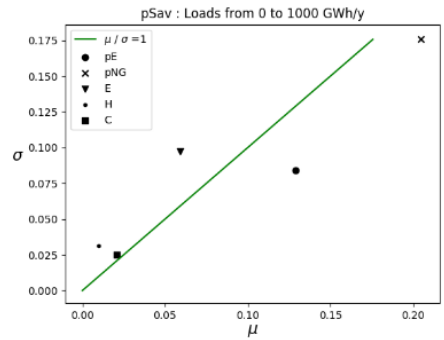
Parameter	μ^*	μ	σ
pE	2,669,796	2,669,796	3,250,379
pNG	2,136,661	-1,497,704	3,168,391
E	2,780,388	2,780,388	3,451,706
H	855,156	-384,349	2,896,074
C	1,205,430	1,205,430	1,730,378



Parameter	μ^*	μ	σ
pE	0.12	0.12	0.10
pNG	0.16	-0.14	0.17
E	0.13	0.13	0.23
H	0.05	-0.03	0.10
C	0.07	0.07	0.12



Parameter	μ^*	μ	σ
pE	28,290,128	28,290,128	28,012,717
pNG	25,260,280	-25,260,280	27,393,063
E	23,821,583	23,821,583	28,168,247
H	2,017,753	2,010,932	4,833,183
C	5,505,114	5,505,114	6,137,699



Parameter	μ^*	μ	σ
pE	0.13	0.13	0.08
pNG	0.21	-0.21	0.18
E	0.07	0.06	0.10
H	0.02	-0.01	0.03
C	0.02	0.02	0.03

Figure 42 Morris sensitivity indexes for the ranges 0 to 10 GWh/y (top), 0 to 100 GWh/y (middle), and 0 to 1000 GWh/y (bottom). Each range shows the analysis for the amount of savings (left) and the percentage of savings (right)

Regarding the amount of savings, Figure 42 (left) first shows that $\sigma \geq \mu$ for all the variables and all the ranges. That suggests that all these variables have interaction effects. Second, it describes the influence of the variables on the output. In general, the value μ is larger for pNG , pE and E than for H and C , therefore pNG , pE and E are more influential for all the cases. The order of relevance depends on the range. For the range 0 to 10, pNG and pE are highly influential variables; whilst for the range 0 to 100, it is pE and E ; and then for the range 0 to 1000, pNG , pE and E are nearly equivalent. It worth noticing that H and C became middling influential for the range 0 to 100, but never became as important as the other variables. Thirdly, the variables are completely monotonic ($|\mu| = \mu^*$), except for pNG and H in the range 0 to 100, and H for the range 0 to 1000. Finally, notice that in all the ranges pNG has a negative μ , meaning that the larger pNG , the lower the amount of savings. That also happens for H , but only in the range 0 to 100.

Regarding the percentage of savings, Figure 42 (right) first shows that pE and pNG have low or no interaction effects ($\sigma \approx < \mu$) for all the ranges, and E has the largest interaction effects. Second, it describes the influence of the variables on the output. It is quite clear that pNG is the most influential variable and pE is middling important. The relevance of loads varies depending on the range. E becomes a very relevant in the range of 0 to 100 but seems middling important on the other two. H and C are in general non-relevant. Third, variables are completely monotonic ($|\mu| = \mu^*$), except pNG and H in the range 0 to 100, and H and E in the range 0 to 1000. Finally, the pNG and H have a negative μ in all the ranges, therefore, the larger they are, the lower the percentage of savings.

From the description above, it is evident that the prices and electricity load are the most influential variables, either over the amount or the percentage of savings. The order of relevance depends on the resolution and range of analysis, but this relates with the fact that Morris method is mostly a qualitative way to identify the influential variables. Then, different resolutions and ranges are explored below, to corroborate the above-mentioned findings.

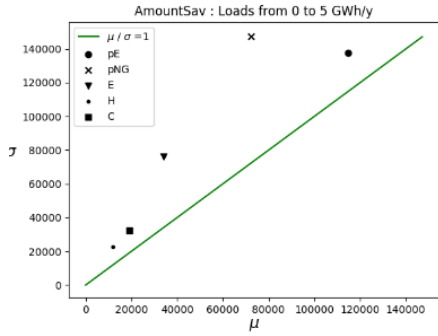
The range from 0 to 100 GWh/y is particularly relevant because the high energy intensity building presented in subsection 2.2.2 are within this range [44], [52],

[76], [77]. Therefore, the next part of the section intends to refine its analysis by studying it in smaller partitions and increasing the resolution, thereby complementing the findings above. The new ranges are 0 to 5, 5 to 10, 10 to 40, 40 to 70, and 70 to 100 GWh/y (Figure 43 and Figure 44).

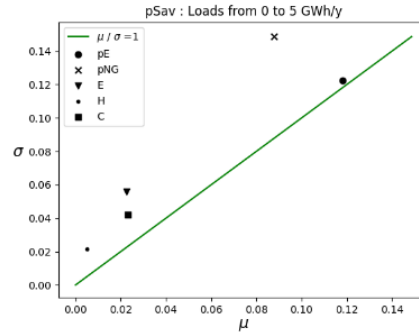
Regarding the amount of savings, Figure 43 (left) and Figure 44 (left) shows that pE is as influential or even more than pNG , because $\mu(pE) > \mu(pNG)$. The figure also displays that E is generally more relevant than H and C , but less than the prices. Regarding the interaction effects, all variables have them at the range 0 to 5. However, especially for the prices, the interaction effects gradually decrease while passing through the different ranges. On the other hand, all variables exhibit non-monotonic behavior in at least one of the ranges analyzed. And finally, pNG has a negative μ in all the ranges, therefore, the larger it is, the lower the amount of savings.

Regarding the percentage of savings, Figure 43 (right) and Figure 44 (right) shows that pNG is the most influential variable, except for the range 0 to 5, where pE is. For the loads, their relevance changes from range to range, but frequently E seems more relevant. Regarding the interaction effects for the prices, they gradually decrease while increasing the energy loads. As for the non-monotonic behavior, μ and μ^* indicate that all variables have it in at least one of the ranges. Finally, pNG has a negative μ in all the ranges, and H has it for three of them, therefore, the larger they are, the lower the percentage of savings.

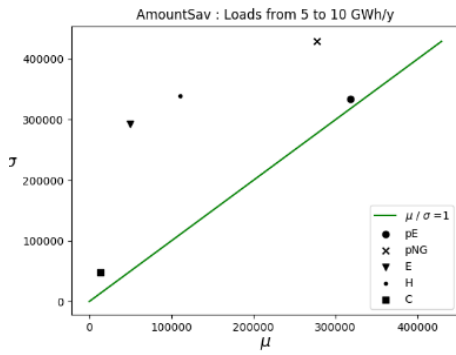
A way to explain why the ranges present different order in the relevance of the variables is that Morris is a method based on the derivative of the range (local slopes). But the derivatives differ across the function, even more if it is a multi-variable function.



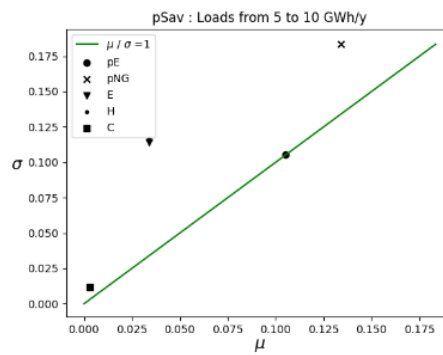
Parameter	μ^*	μ	σ
pE	114,893	114,892	137,885
pNG	72,264	-72,229	147,236
E	34,129	34,129	76,130
H	11,833	11,827	22,824
C	19,194	19,194	32,259



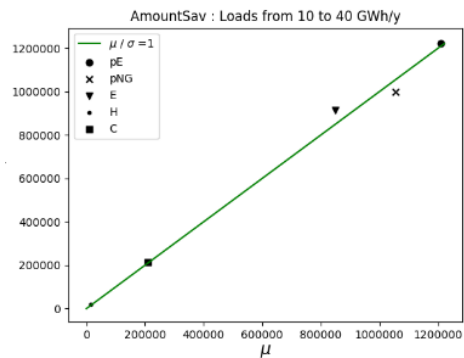
Parameter	μ^*	μ	σ
pE	0.12	0.12	0.12
pNG	0.09	-0.09	0.15
E	0.02	0.02	0.06
H	0.01	0.01	0.02
C	0.02	0.02	0.04



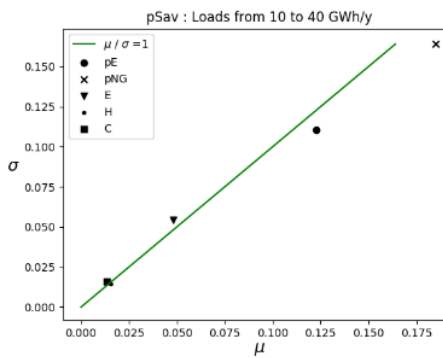
Parameter	μ^*	μ	σ
pE	331,241	317,769	333,833
pNG	332,582	-276,919	428,896
E	132,021	-50,347	292,705
H	110,460	110,460	339,229
C	29,992	13,929	48,440



Parameter	μ^*	μ	σ
pE	0.11	0.11	0.11
pNG	0.15	-0.13	0.18
E	0.04	-0.03	0.11
H	0.04	0.03	0.12
C	0.01	0.00	0.01



Parameter	μ^*	μ	σ
pE	1,209,486	1,209,486	1,221,216
pNG	1,055,926	-1,055,926	1,000,230
E	848,560	848,560	915,860
H	14,446	14,073	19,288
C	210,607	210,607	212,842



Parameter	μ^*	μ	σ
pE	0.12	0.12	0.11
pNG	0.19	-0.19	0.16
E	0.05	0.05	0.05
H	0.02	-0.02	0.02
C	0.01	0.01	0.02

Figure 43 Morris sensitivity indexes for the ranges 0 to 5 GWh/y, 5 to 10 GWh/y, and 10 to 40 GWh/y. Each range shows the analysis for the amount of savings (left) and the percentage of savings (right)

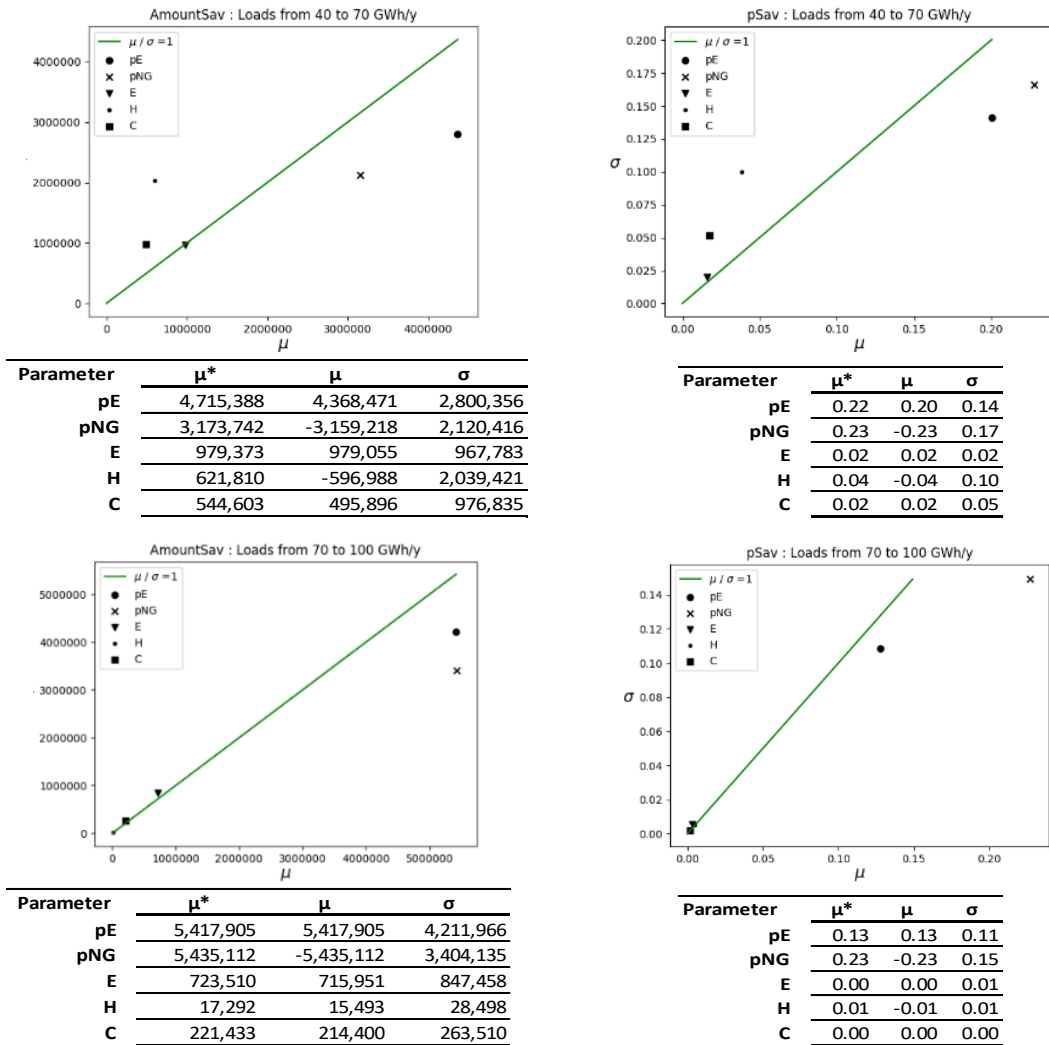


Figure 44 Morris sensitivity indexes for the ranges 40 to 70 GWh/y, and 70 to 100 GWh/y. Each range shows the analysis for the amount of savings (left) and the percentage of savings (right)

In general, the conclusions that the Morris SA reveal for this case study are:

- **For the amount of savings:** The most relevant variables are pE , pNG , and E . All variables have interaction effects, but the larger the energy loads, the lower the interaction effects. All variables present some non-monotonic behavior in at least one range, but it is more frequent for the case of H and pNG . Finally, an increase in pNG has always a negative impact on the amount of savings, and the case is similar for H at a few ranges (from example, with loads from 40 to 70 GWh/y).

- **For the percentage of savings:** The most relevant variables are pNG , pE , and E . This finding matches with the conclusion of chapter 4. The variables, especially the prices, seems to have less interaction effects than on the analysis of amount of savings. But E is the contrary. On the other hand, the variables that present non-monotonic behavior at some ranges are mostly H , and pNG . Finally, in all the cases, an increase in pNG and H has a negative impact on the percentage of savings.
- **Regarding the prices:** At a first glance, pE is in general more relevant than pNG when the analysis is in amount of savings. In contrast, when it is in percentage of savings, pNG is generally more influent.

For this case study, the Morris sensitivity analysis method has some limitations:

1. The calculation of the elementary effects and SA indexes are strongly affected by the choice of the sample, which in turn depends on
 - a. The resolution of the range
 - b. The point of the range where the sample is taken
2. It does not quantify the interaction effects of the variables

Therefore, the following two Sensitivity Analysis methods intend to solve these limitations. VARS is a method that outlines the importance of the variables across their whole range. And Sobol can quantify the interaction effects.

5.3 VARS – Variogram based approach

As explained in subsection 3.3.3.3, this method explores each variable along its range by fixing the other ones. It uses Latin Hypercube Sampling (LHS) to choose four seed points. Afterwards, the charts of distance and variograms are drawn for each variable to outline the relevance of each variable.

Similarly than in Morris method, the prices are expressed in \$/kWh and the loads in GWh/y, with ranges (R), increments (Δh) and number of levels ($'dim(h)'$) as

follows: for pE a $R=\{0.10 ; 0.28\}$, with $\Delta h=0.01$ and $dim(h)=17$, for pNG a $R=\{0.02 ; 0.10\}$ with $\Delta h =0.005$ and $dim(h)=15$, and for E, H and C a $R=\{0 ; 100\}$ with $\Delta h=5$ and $dim(h)=20$. All variables have uniform distribution. The computational cost of this method is 376 simulations, which is around three times more than Morris. Table 24 shows the $n=4$ seed points obtained with Latin Hypercube Sampling (LHS). Razavi [110] suggests $n=2$ to ensure a representative sample, ours is double the size, then it is reasonable to trust in ours. The values for $R, \Delta h$ and $dim(h)$ are chosen to explore the prices and loads presented in subsection 2.2 and have similar $dim(h)$ among all the variables.

	pE	pNG	E	H	C
seed 1	0.10	0.055	40	70	65
seed 2	0.15	0.075	95	85	75
seed 3	0.22	0.020	55	0	10
seed 4	0.24	0.095	10	40	25

Table 24 Seed point for VARS SA

Figure 45 shows the behavior of the variograms for the amount of savings. Firstly, it indicates that the most relevant variables are pE, pNG and E , which is in line with the Morris method results. The three have variogram curves with big slopes, compared with H and C . A large slope, for example in pE , means that the larger the difference in pE , the larger the difference in amount of savings. One of the advantages of VARS is that it outlines the relevance of variables across the range of analysis. With that said, notice that the order of relevance is the same along the whole range of analysis (pE, pNG, E, H , and C). See the zoom at the bottom of Figure 45, showing the first part of the curve.

Secondly, Figure 45 shows that all variables keep the same sign of the slope. This is contrary to Morris method, that identifies a non-monotonic behavior of the variables for some sampling points. What happens is that VARS method dilutes the non-monotonic behavior when it is found only in some specific spots of the range. That is possible because VARS consider a larger sample and is able to build a more general trend. From the operational conclusion (feasibility), it implies that VARS helps to identify general trends, instead of focusing on small differences.

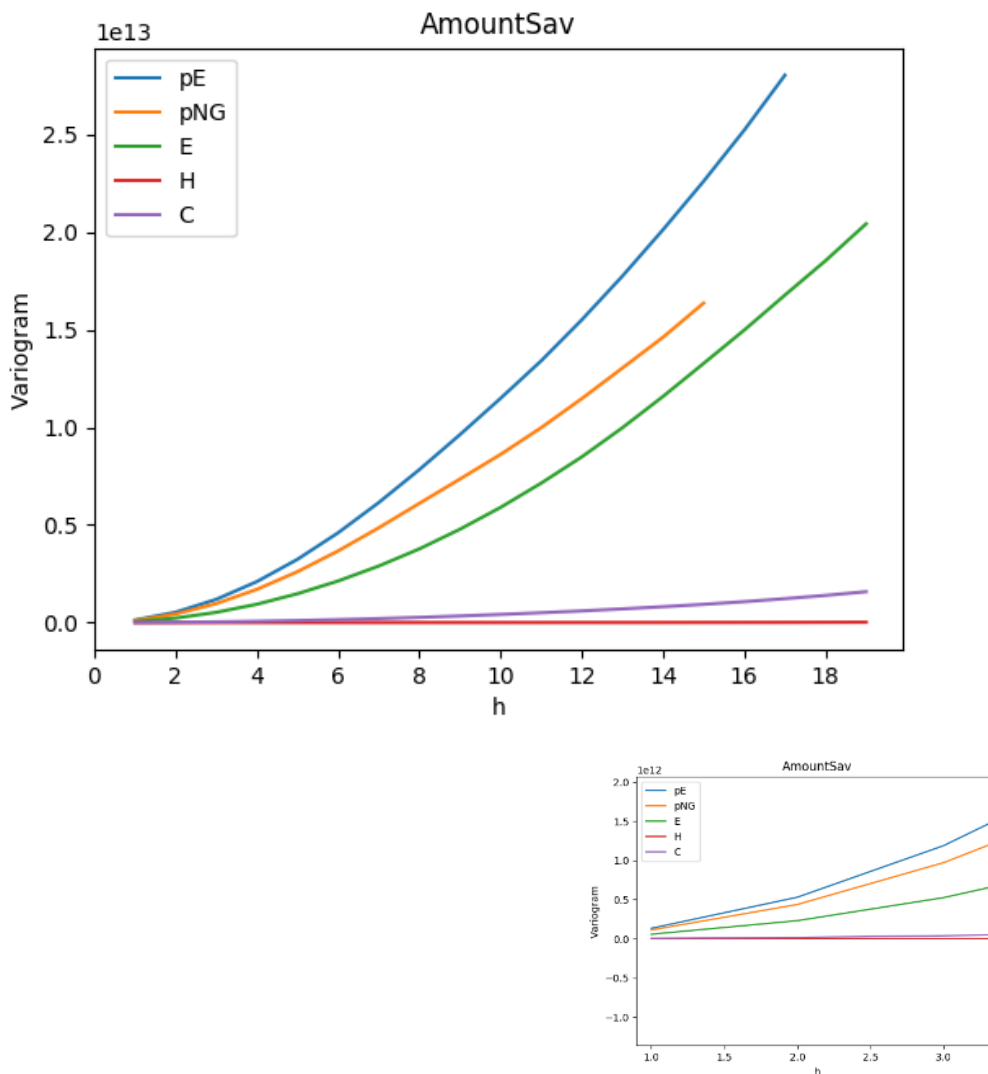


Figure 45 Variogram of variables for the amount of savings (top), zoom (bottom)

By design, the variogram of a variable is always in the first quadrant of the cartesian plane. Therefore, to clearly understand the influence for each variable on the output, it is necessary to observe the sign of its slope by plotting the raw data obtained from the four seed points (Figure 46). It is observed that a grow in pE , E , or C drives an increment of the amount of savings (positive slope). In contrast, when pNG grows, it decreases (negative slope). In the case of H : Morris SA detected that for some ranges, its increment has a negative impact on the amount of savings. But VARS, that has more sample points, shows instead that the behavior is quite asymptotic (slope ≈ 0).

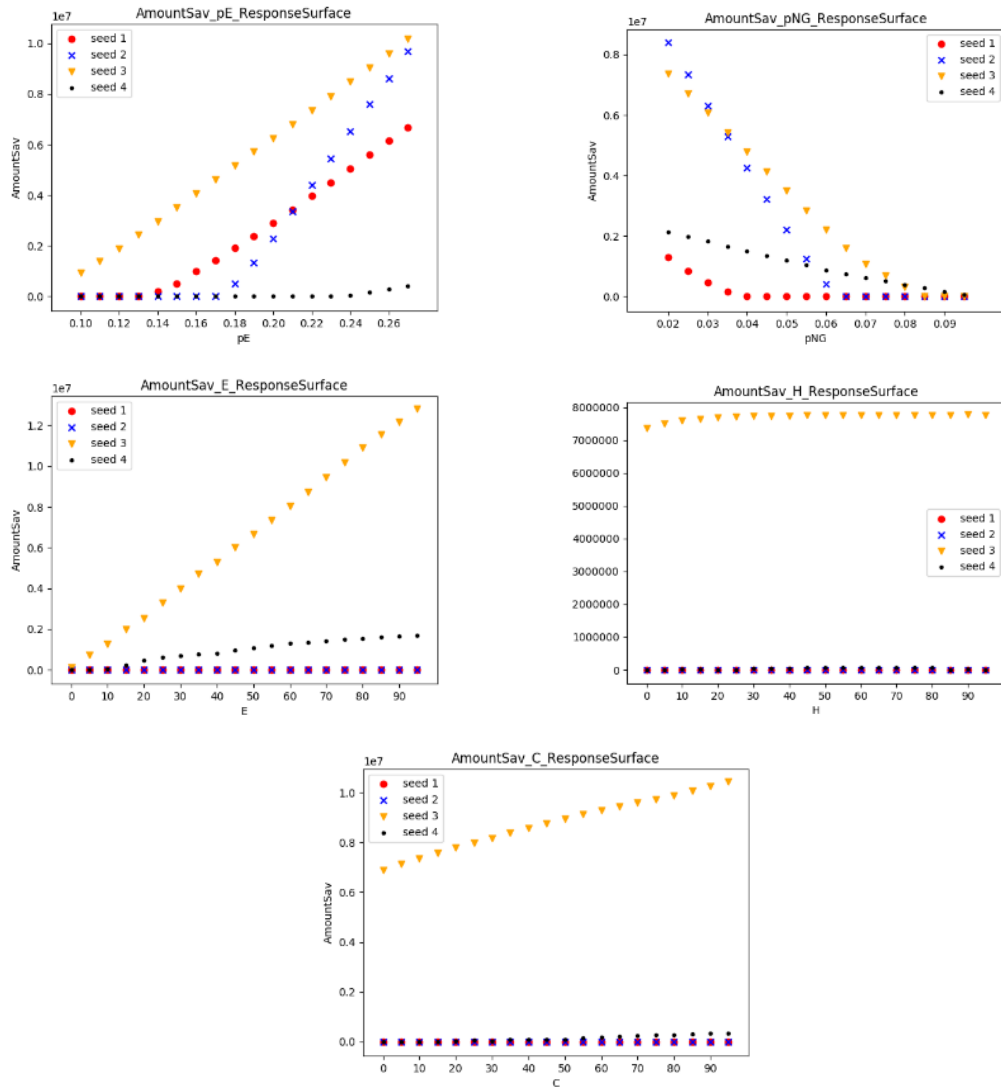


Figure 46 Response surface (amount of savings) vs. the raw data corresponding to the four seed points for variables pE , pNG , E , H , and C .

On the other hand, Figure 47 shows the behavior of the variograms for the percentage of savings. Similar than in Morris, it indicates that the most relevant variables are pNG , and pE . E is mediumly important and H and C are almost negligible. The order of relevance keeps, the same even along the whole range of analysis (see the zoom at the bottom of Figure 47), but the difference in relevance makes bigger, while h grows (bigger values of the variables). This matches with the analysis in subsections 4.4.3 and 4.4.4, showing that the prices are always the most important variables, afterwards the E loads display a

unfading relevance, but H and C show relevance only for small spark spread rates.

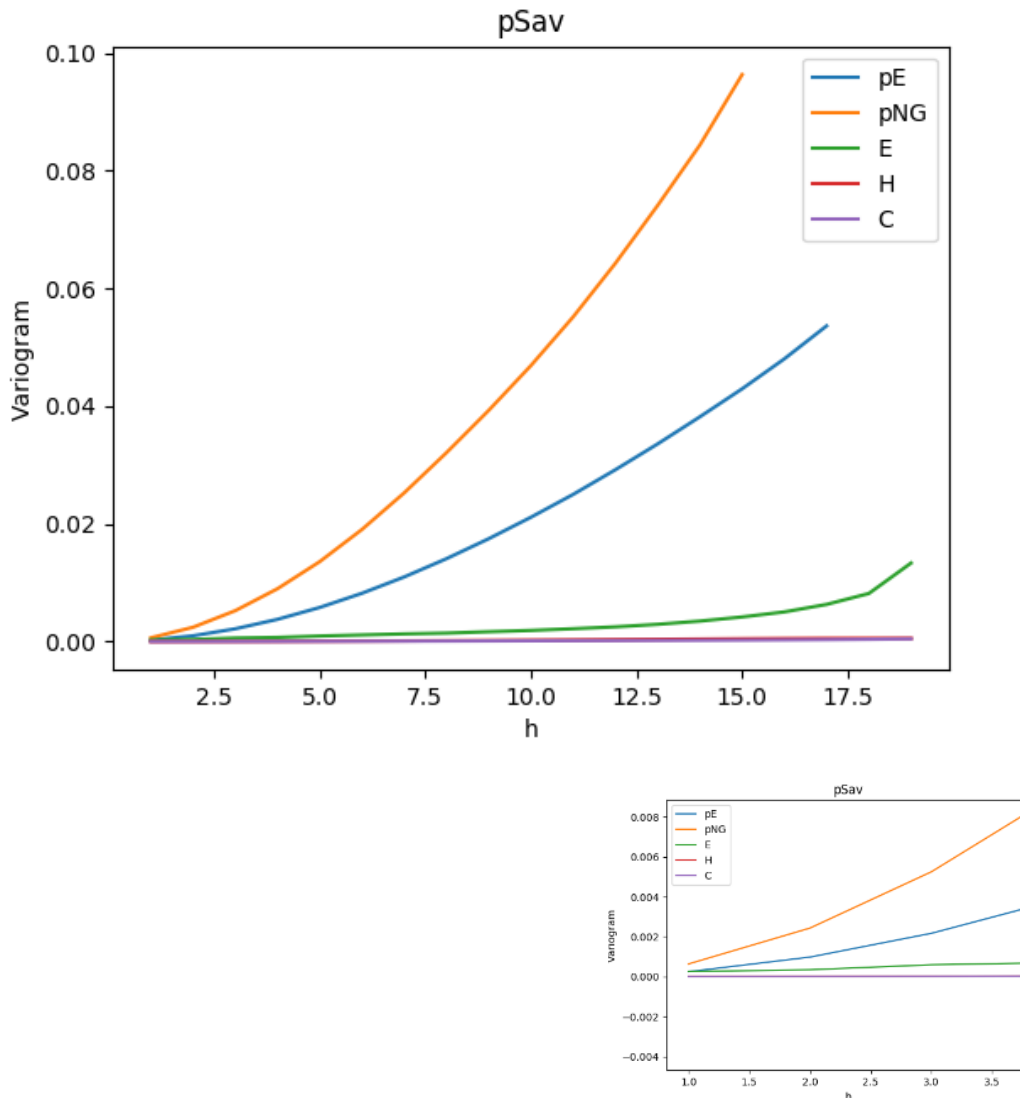


Figure 47 Variogram of variables for the percentage of savings (top), zoom (bottom)

The variograms of Figure 47 locate in the first quadrant of the cartesian plane. Therefore, to understand the influence for each variable on the output, Figure 48 plots the raw data obtained from the four seed points. It is observed that a grow in pE , E , or C increases the percentage of savings (positive slope). However, when pNG or H grow, the output decreases (negative slope). The latter analysis of H matches with the remark in subsections 4.4.1 and 4.4.4

stating that it is preferable to use the boiler when heating loads dominate. Also notice that although the slope of C is positive, it is close to zero. Therefore, it is not a surprise that sections 4.4.1 and 4.4.4 mentioned that the absorption chiller is feasible only in certain conditions.

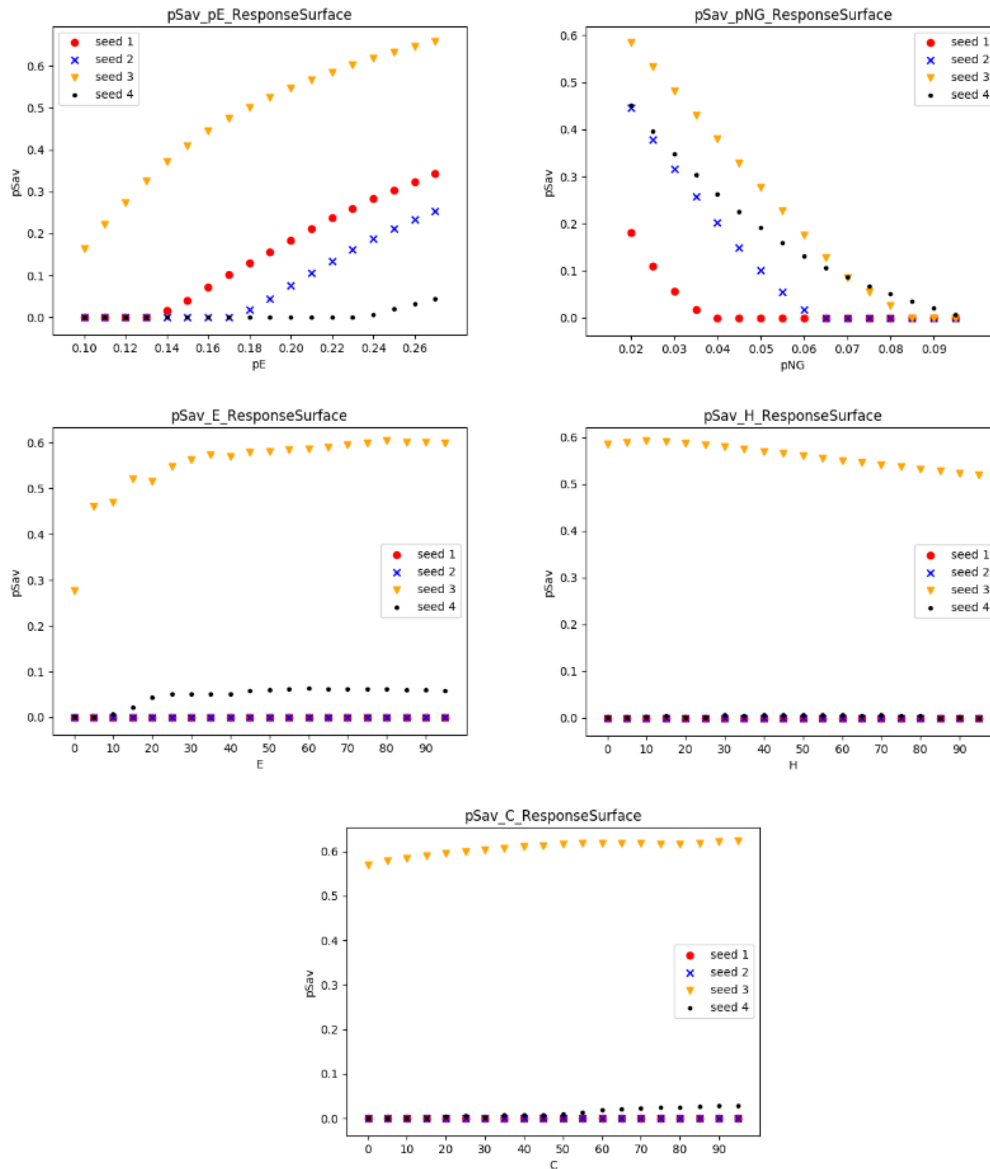


Figure 48 Response surface (percentage of savings) vs. the raw data corresponding to the four seed points for variables pE , pNG , E , H , and C .

Regarding the prices, both, VARS and Morris agree that pE is more relevant than pNG when the analysis is in amount of savings. And it is vice versa for the percentage of savings.

In general, the conclusions obtained with VARS and Morris are similar, except that VARS:

- It has a computational cost around three more times than Morris.
- It does not give any idea of the interaction effects.
- It provides a more holistic understanding of the direction of influence for each variable. For example, for the analysis of the amount of savings, it shows that the effect of H is quite asymptotic instead of focusing on its non-monotonic nature, as Morris did.

5.4 Sobol – Variance based approach

As explained in subsection 3.3.3.2, this method is a variance decomposition approach and it is based on a Monte-Carlo numerical procedure to generate random samples. It calculates the contribution of each variable, as well as the interaction among them.

Like VARS and Morris, the ranges of analysis are for pE a $R=\{0.10;0.28\}$, for pNG a $R=\{0.02;0.10\}$, and for E , H and C a $R=\{0;100\}$. All variables with uniform distribution. The prices are expressed in \$/kWh and the loads in GWh/y. The computational cost of this method is 12,000 simulations.

The Sobol SA indexes for the amount of savings are in Figure 49. The top part shows S_1 and S_T , the individual and total effects of the variables respectively. The difference between S_1 and S_T corresponds to the interaction effects. Just as Morris SA suggests, all the variables have interaction effects ($\sigma \geq \mu$). But different than Morris, Sobol does not identify if they exist at a specific part of the range. Additionally, just as Morris and VARS SA stated, the most influential variable for the amount of savings is pE , closely followed by pNG and E . Contrary, H and C are non-influential factors.

The bottom part of Figure 49 shows S_2 , the 2nd order SA index that describes the interaction effects of the variables per pair. The largest interaction effects

are between $E - pNG$ and $E - pE$. Then, it means that the relevance of E is highly tied to the value of pNG and pE . Other interesting observation is that pNG is the only variable that has interaction effects with all the others. This is an indication of its relevance, even though it does not have the largest individual and total index (S_1 and S_7).

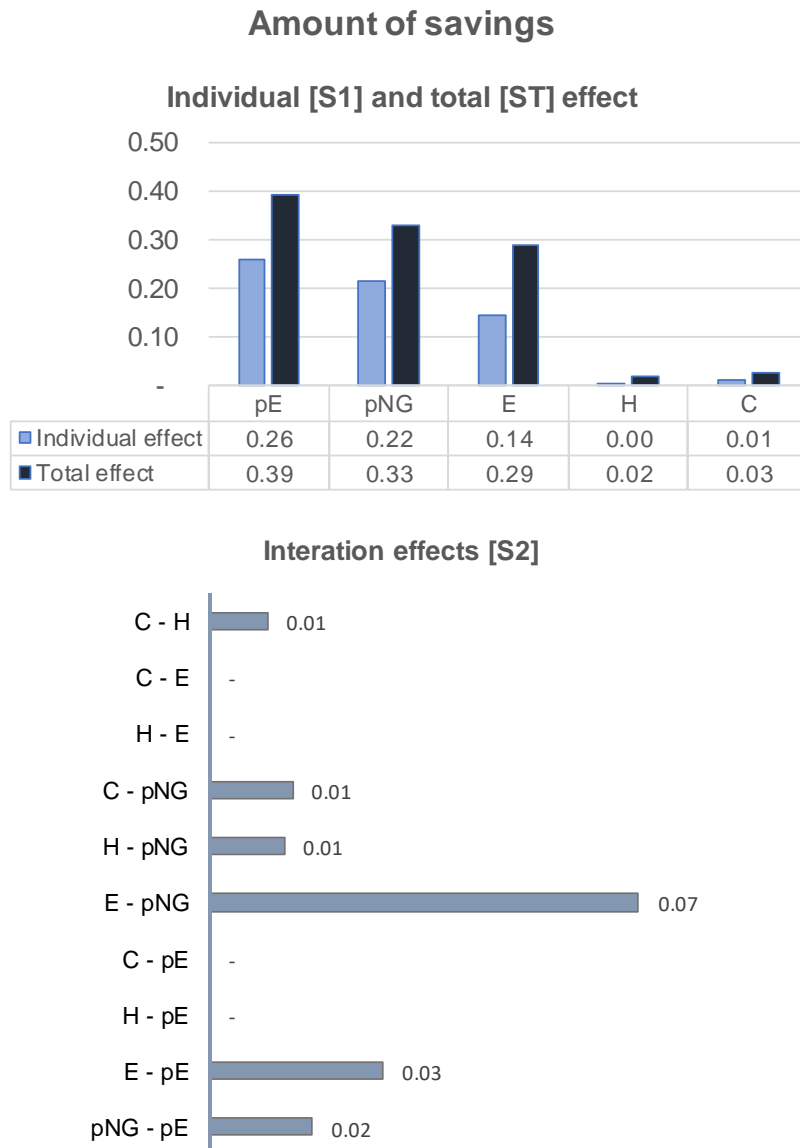


Figure 49 Sobol SA indexes for amount of savings

Some drawbacks of Sobol SA method in comparison with Morris and VARS, is that it does not give any information regarding: 1) the non-monotonic behavior of the variables; 2) the direction of influence for each variable on the output.

Figure 50 shows the Sobol SA indexes for the percentage of savings. Same than Morris and VARS, Sobol individual indexes indicate that the most influential variable is pNG , followed by pE . Here, E becomes less influential, compared with the analysis of the amount of savings. That is because, when measuring the amount of savings, there is a direct link between the money saved and the size of E . But when measuring percentage of savings, it considers the proportions, rather than the total amount. Still E is slightly more influential than H and C , just as Morris and VARS also point out.

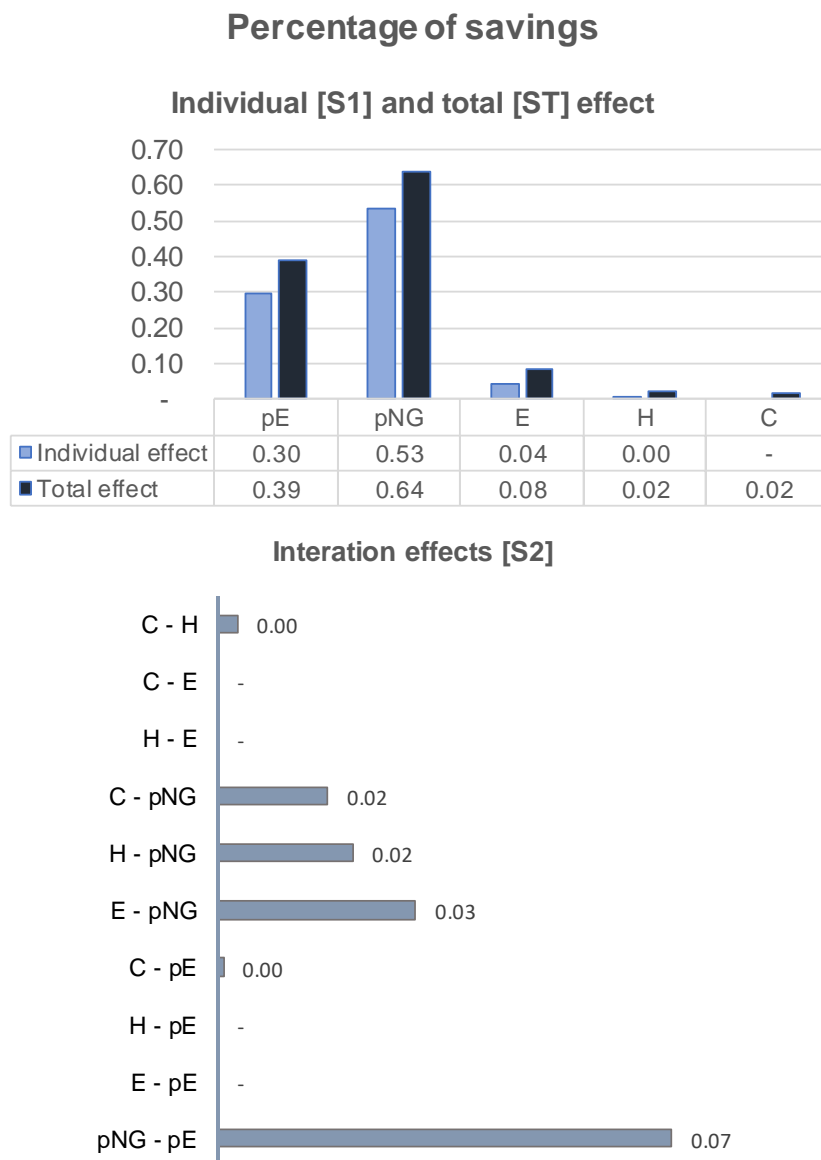


Figure 50 Sobol SA indexes for percentage of savings

The bottom part of Figure 50 displays the 2nd order SA indexes. Sobol suggests that all the variables have interaction effects, contrary to Morris SA where prices had several cases of $\sigma \leq \mu$ (no interaction effects) in Figure 42, Figure 43, and Figure 44.

Similar than with the analysis of the amount of savings above, pNG is the only variable that has interaction effects with all the others. The largest one is the index $pE - pNG$, which is notably bigger compared with its analogous in the amount of savings (Figure 49). This could suggest that the Spark Spread rate (SS) is more relevant in the case of the percentage of savings.

On the other hand, the interaction effect $pNG - E$ is lower for the percentage of savings than for the amount of savings, but the interaction $pNG - H$ and $pNG - C$ are slightly higher (see Figure 49 vs. Figure 50). This suggests two things: First, the influence of the three loads is more equilibrated when analyzing the percentage of savings, but it depends on the level of pNG . The last sentence matches with the analysis of Figure 37 and Figure 38, where the percentage of savings for the SS1 seems larger in the middle of the ternary diagram, corresponding to a balance among the loads. Second, the analysis in chapter 4 highlights the relevance of the spark spread. Although the interaction $pNG - pE$ is significant in this Sobol SA analysis, the variable that mostly interacts with the loads is the price of natural gas.

Finally, Figure 51 shows the data obtained with SOBOL, consolidating it by bins. They describe the general trend of the average amount and percentage of savings throughout the axis of pE , pNG , and E (the three most influential variables).

There are some important differences between the images shown in Figure 51: First, the number of cases with high feasibility (given by the red-yellow color scale) is larger when measuring in terms of percentage of savings. That is because the latter quantifies the relative savings. Then, a scenario with a small amount of savings could be shown blue in at the left image of Figure 51, but red in the right one because the relative savings (percentage of savings) is large. The second difference is that E is more influential in the amount than in the

percentage of savings (also discussed in Figure 50). For the percentage of savings (right in Figure 51), the highly feasible scenarios are found all along the edge of the cube where pNG is smaller and pE is larger. In contrast, the highly feasible scenarios for the amount of savings (left of Figure 51) are found at the corner of the cube where pNG is smaller, pE is larger, and E is higher. This matches with the interaction effects $E - pNG$ and $E - pE$ found and discussed in Figure 49.

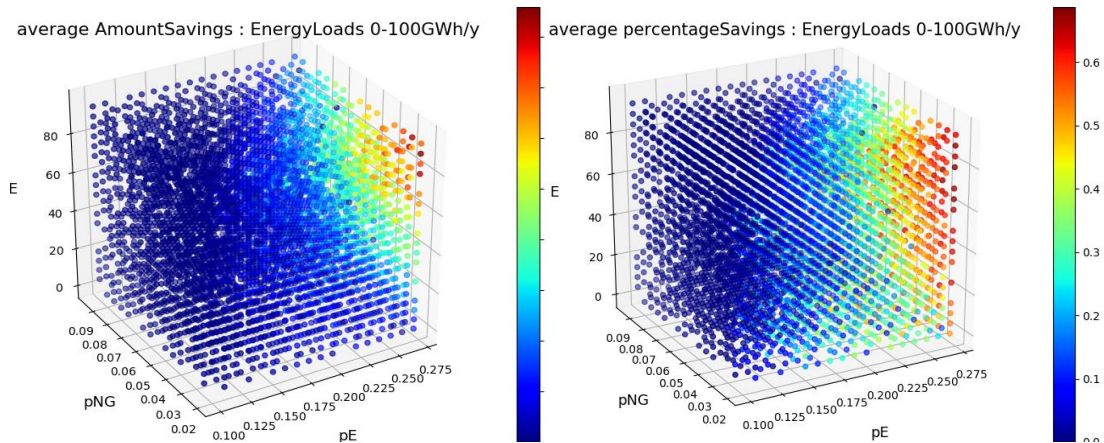


Figure 51 Three dimensional charts of the average amount and percentage of savings (left and right respectively), across pE , pNG , and E .

KEY: The units of the color scale for the average amount of savings (left) is M\$, while the average percentage of savings (right) is expressed in fraction.

Finally, it is good to highlight that 99% of the CCHP-TS scenarios analyzed in this section have better environmental performance than their reference scenario, where is considered a carbon intensity of electricity equal to 0.447 kg CO₂ eq. / kWh. This corresponds to the average in Europe [14].

5.5 General conclusion of the sensitivity analysis

The results stemming from the GSA method aim to establish the influence of energy prices and loads over the feasibility of Trigeneration-Thermal Storage systems. The analysis considers two metrics: the amount of savings, and the percentage of savings.

The **amounts of savings** quantify the nominal sum of money saved by using the CCHP-TS system. Here, the most relevant variables are pE , pNG , and E , in that order. Regarding the interaction effects, $E - pNG$ and $E - pE$ are the most significant. It is because, as observed in Figure 51 (left), the smaller pNG and larger pE , it is more relevant to have a high E . Another important remark is that pNG is the only variable having interaction effects with all the other.

The **percentage of savings** measures the relative savings regardless of its nominal value. Here, the most relevant variables are pNG , pE , and E , while H and C seem quite irrelevant. However, E becomes less influential, compared with the analysis of amount of savings. That is because, when measuring the amount of savings, there is a direct link between the money saved and the size of E . But when measuring percentage of savings, it considers the proportions, rather than the total amount. On the other hand, pNG and H have negative slopes, therefore, an increase in any of them leads to a decrease in the percentage of savings. Regarding the interaction effects, pNG is again the variable that has coupling effects with all the others. The largest interaction is between the two prices. The same does not happen with the amount of savings, which suggests that the SS is more relevant in the case of the percentage of savings.

Other interesting aspect is connecting the conclusions reached here, and the ones obtained in chapter 4. To start, regarding the lack of relevance of H and C , note that chapter 4 gave a grasp of this while concluding that it is more profitable to use boiler and vapor-compression chiller when heating or cooling loads dominate. In a similar vein, it concludes that the heat scrap does not affect the percentage of savings significantly. On the other hand, chapter 4 implements load dominance rates and ternary diagrams to show the results. It could be said that it was the first sign of existing interaction effects between the variables of analysis. Finally, the chapter also proposes a two-level characterization, firstly based on Spark Spread rate, and secondly on the annual loads. This is well explained by the results of the sensitivity analysis, indicating that the prices are more relevant than the loads. However, the sensitivity analysis quantifies the relevance and even separates the effect of each variable, including the prices.

It is interesting to see how chapter 4 and 5 match and complement each other. Because the first provides the physical explanation to the numerical results of the second.

Concerning the interest of studying the **energy prices** separately, it can be said that both, pE and pNG , are relevant individually regardless of the output measure (amount or percentage of savings). Also, they are clearly tied, either directly or indirectly. For the percentage of savings, the interaction effect between them is very strong. While for the amount of savings, each price has interaction effects with E , therefore, they have an indirect link. However, the main difference between both energy prices is that, in either output (amount or percentage of savings), pNG keeps interaction effects with all the other variables, indicating that its influence is wider. Moreover, when referring to the percentage of savings, the energy loads interact almost exclusively with pNG . Due to this, it is recommendable to analyze them separately, to clearly quantify their contribution to the feasibility of CCHP-TS systems.

5.6 Overall comparison of the three SA methods

Given the results across this chapter, it is possible to see some of the strengths and weaknesses of the different GSA methods.

Morris is computationally cheap and easy to implement. However, the method is more useful to differentiate between the influential and non-influential variables, rather than clearly ranking them [119]. This is because the rank of the variables is very sensitive to the range of analysis and its resolution. As observed in Figure 42, Figure 43, and Figure 44 where the output depends on the location of the different levels explored). Morris also gives an idea of the interaction effects present in each variable, but it does not measure them. Additionally, Morris identifies when a variable has a non-monotonic behavior, but its outcome is limited by the information acquired with the sampling points.

VARSA is a medium expensive method in computational terms. The method outlines the importance of the variables across their whole range quite precisely (its ranking matches with the Sobol method). However, it does not give an idea of the interaction effects among variables. Because, as mentioned in section 5.3, a directional variogram only assesses the sensitivity of the response surface Y in the direction of variable X_i . Another characteristic of VARSA is that it provides a more holistic understanding of the sign of the slope (direction of influence) for each variable and its monotonic or non-monotonic behavior. While Morris suggest that the effect of the heating demand, H , is non-monotonic for the amount of savings, VARSA shows that this effect in general is asymptotic (Figure 46). Therefore, VARSA provides a more integrated view thanks to the number of samples.

Sobol is an extremely expensive method in terms of computational resources. Its most important advantage is that it gives accurate information regarding the individual effect of a variable and its interaction effects with the other variables. However, this method does not give any information neither regarding the non-monotonic behavior of variables nor their sign of the slope (direction of influence on the output). The reason is simple. As mentioned in subsection 3.3.3.2, Sobol is a variance-based approach, contrary to Morris (a derivative-based approach) and VARSA that analyze sensitivity out of the slopes and derivatives of the variables.

Therefore, the decision to implement one method or the other depends on the interest of the analyst. Morris is a quick way to discard non-influential variables, identifies a non-monotonic behavior and gives an idea of the interaction effects. Crossing the analysis of the results given by Morris and VARSA, could provide a precise rank of the influential variables, an idea of the interaction effects, and a more holistic vision of the direction of influence for each variable (including non-monotonic behaviors). Otherwise, crossing the analysis of the results given by VARSA and Sobol would perfectly rank the influential variables, estimate their interaction effects, and provide a holistic vision of the direction of influence for each variable. However, the latter combination is computationally costly.

Another option yet to explore in future research is extending the Morris approach to calculate the second order sensitivity index, just as Garcia Sanchez does for the context of energy in buildings [113]. Although, this option is computationally expensive and removes one of the advantages of Morris method.

5.7 Isolines of the variables

This section presents isolines that deepen the impact of one variable depending on the values of the others. This analysis is especially important to verify or discard the hypothesis laid out in section 4.6: the impact of the energy prices might be different. Therefore, it aims to understand if using a spark spread rate is reasonable or the price of electricity and natural gas should be considered separately.

To exemplify how isolines are built, let us take Figure 52 (top). Each isoline corresponds to the optimized sequence of scenarios for the given values pNG , E , H , and C , while varying pE step by step (taking the seed points and samples generated for VARS SA). The optimization is conducted with the Python-PYOMO.CPLEX tool.

Figure 52 (top) shows especially the effect of pNG on the amount of savings. As expected, $pNG=0.020$ gives the largest amount of savings and $pNG=0.095$ gives the lowest. But the effect between the isolines $pNG=0.055$ (blue) and $pNG=0.075$ (orange) worth analyzing. At $pE=0.22$, the orange isoline of $pNG=0.075$ exceeds the blue one of $pNG=0.055$. In other words, a higher price of natural gas gives larger amount of savings. At a first glance, this sounds divergent from the normal trend, but the effect is due to the size of the loads (E , H , and C). The orange isoline $pNG=0.075$ exceeds in magnitude all the loads of the blue isoline $pNG=0.055$. Then, with the objective of separating the effect of pNG and the loads (E , H , and C), the Figure 52 (bottom) adds an extra isoline (light blue). The extra isoline has $pNG=0.075$, but the loads are equal to the blue isoline of $pNG=0.055$. The result is that, both, the blue and the light blue isolines

are perfectly parallel. Therefore, now it is clear that an increase of the loads drives a growth in the slope of the pNG isolines, rising the amount of savings.

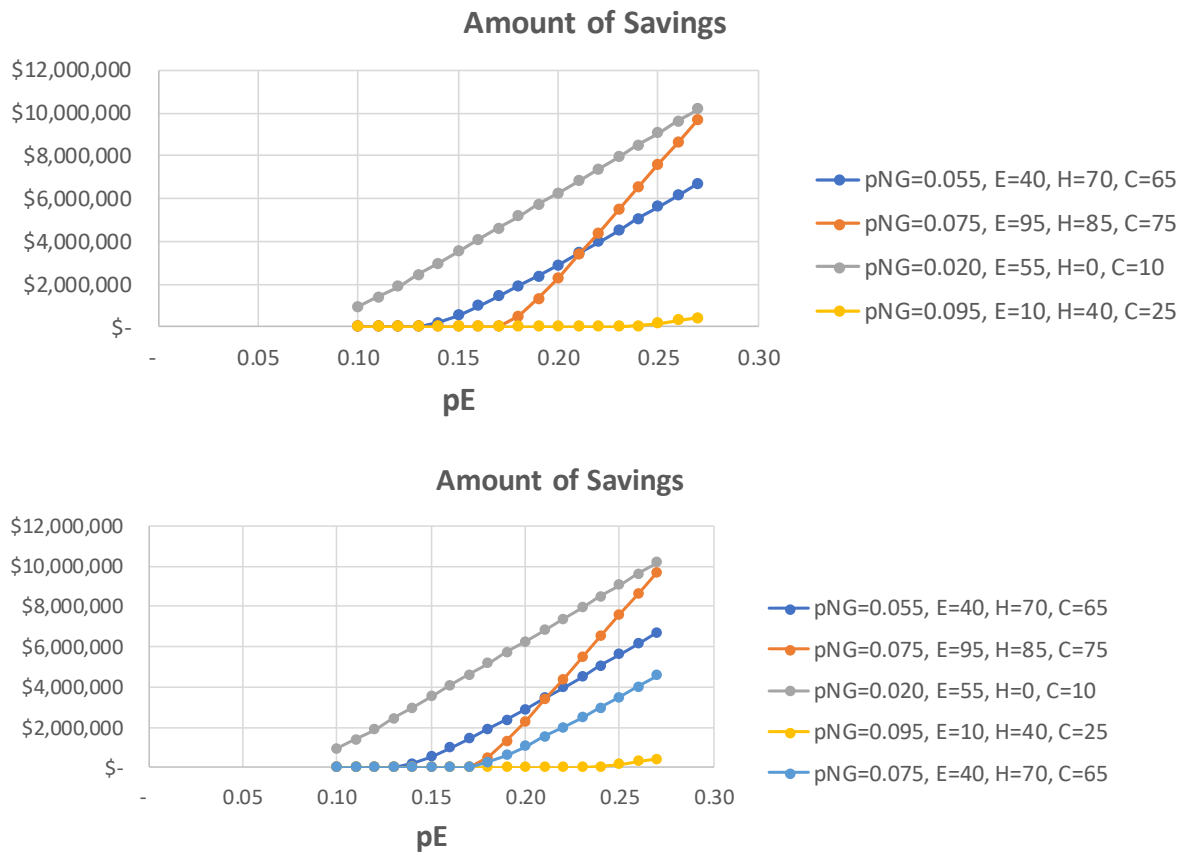


Figure 52 Isolines of $pNG-E-H-C$ across the electricity price [pE] for the amount of savings (top); and addition of the isoline $pNG=0.075, E=40, H=70, C=65$ (bottom)

Similarly, Figure 53 shows especially the effect of pNG on the percentage of savings. The latter increases while decreasing the price of natural gas and increasing the price of electricity. The threshold of spark spread rate when the scenarios start being feasible, is different for each isoline ($SS=2.52$ for $pNG=0.095$, $SS=2.26$ for $pNG=0.075$, $SS=2.36$ for $pNG=0.055$). Therefore, the spark spread threshold could be lower than 3, depending on the price of natural gas. This is a reason why the prices should be analyzed separately.

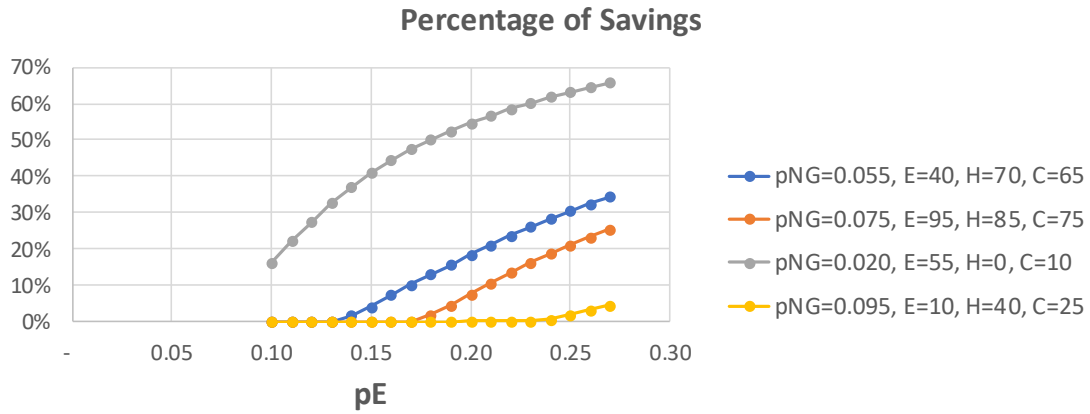


Figure 53 Isolines of $pNG-E-H-C$ across the electricity price [pE] for the percentage of savings

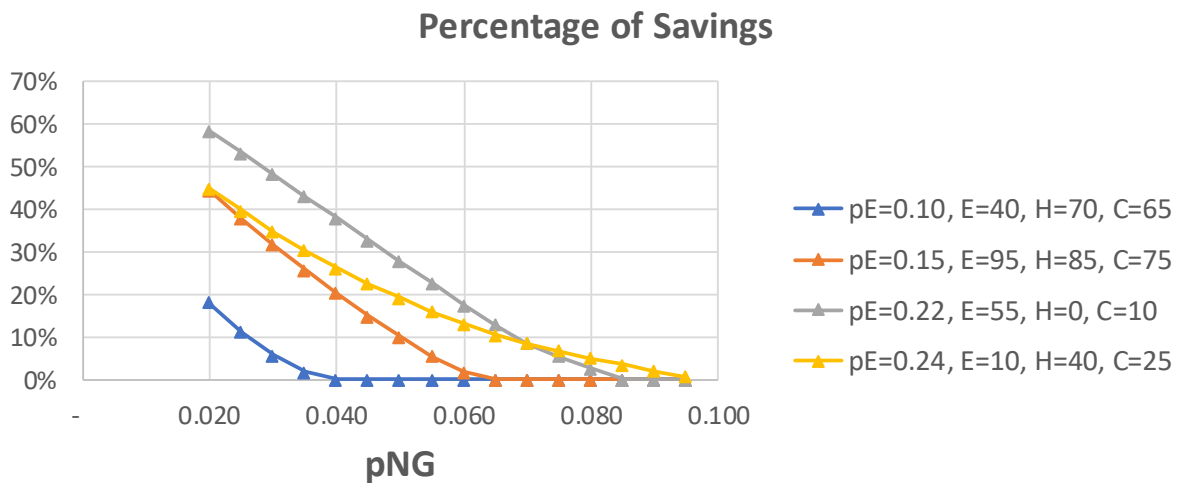
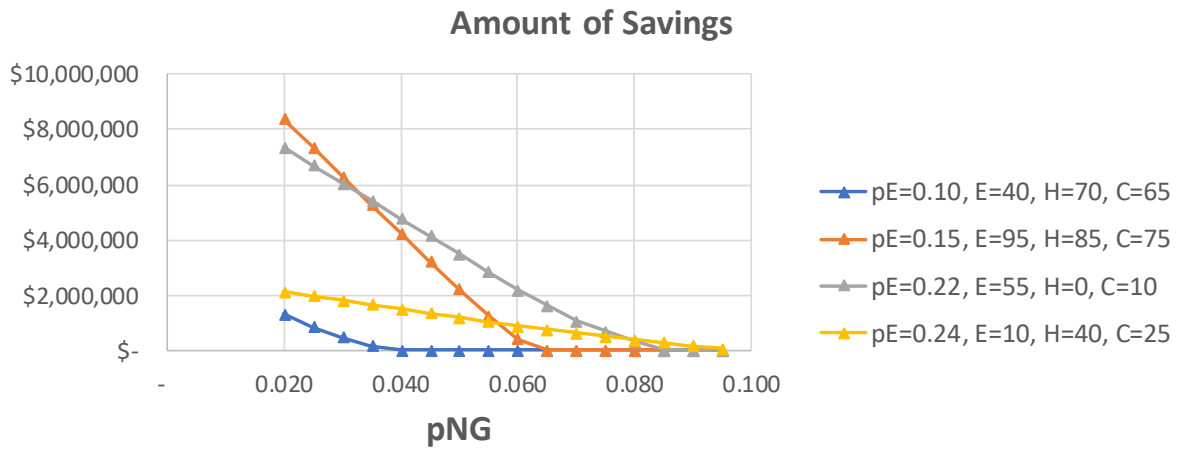


Figure 54 Isolines of $pE-E-H-C$ across the natural gas price [pNG] for the amount and percentage of savings (top and bottom respectively)

Similarly, Figure 54 shows that the larger pNG , the lower the amount and percentage of savings. Also, it presents that the threshold when each scenario is feasible depends on the combination of pE and pNG . And it is evident that the size of the loads makes a difference on the slope of each curve. For example, it is interesting that for small values of pNG , the amount and percentage of savings are higher for the isolines $pE=0.15$ and $pE=0.22$, than for $pE=0.24$. This is due to the size of the loads (E, H, C), that have larger impact when pNG is smaller. That is related with the 2nd order effects identified between pNG and the loads during the analysis with the Sobol SA method (section 5.4).

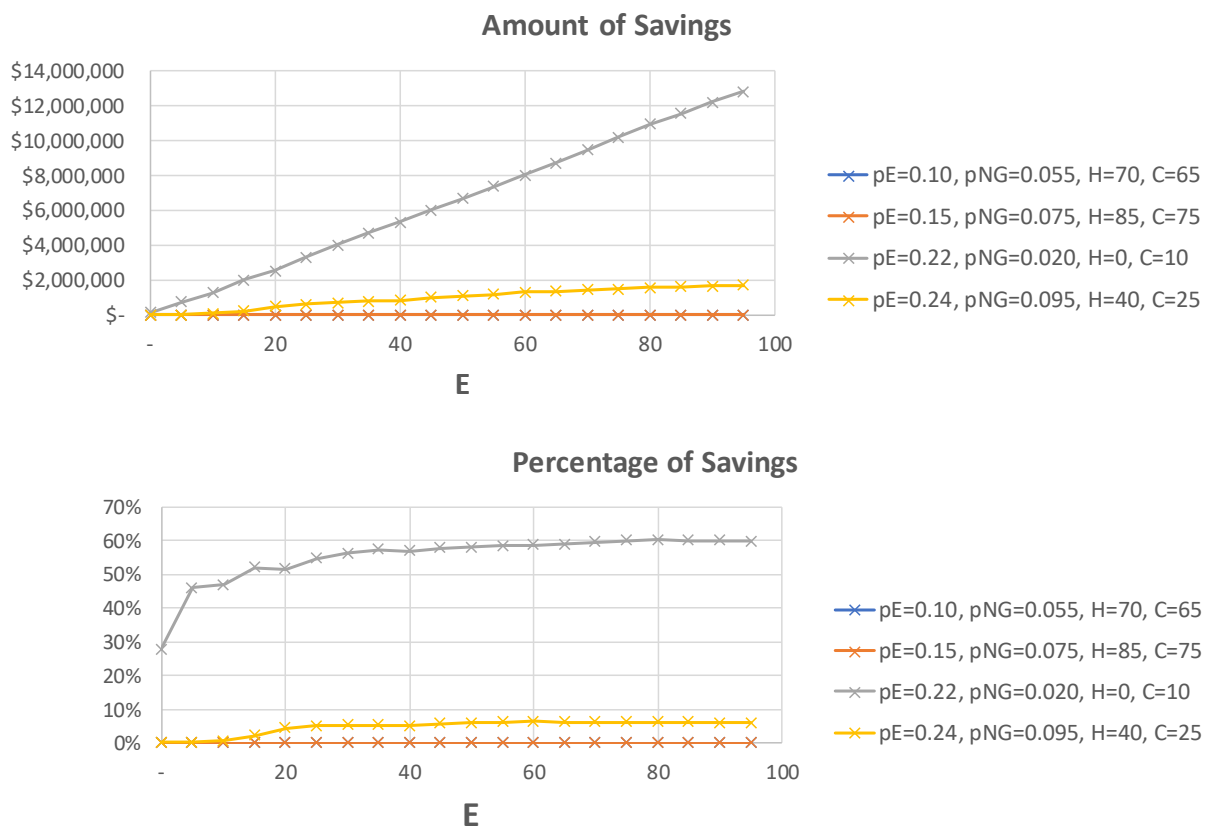


Figure 55 Isolines of pE - pNG - H - C across the annual electricity load [E] for the amount and percentage of savings (top and bottom respectively)

For the case of annual electricity load, Figure 55 top shows that the larger E , the higher the amount of savings. But notice that for two isolines ($pE=0.10, pNG=0.055$ and $pE=0.15, pNG=0.075$), none of the scenarios is feasible. It is because of the low spark spread ratio (two or less).

However, the percentage of savings has an asymptotic behavior (Figure 55 bottom). Each E isoline has a threshold where the percentage of savings reaches a stable point for any larger load. Then, for example in the isoline of $pE=0.22$ and $pNG=0.020$, it should not be a big difference in percentage of savings between having an $E=35$ or an $E=95$.

For the case of annual heating load, Figure 56 shows feasible scenarios only for the largest spark spread rate ($pE=0.22$, $pNG=0.020$, $SS=11$). Figure 56 top shows that the amount of savings behaves asymptotic after certain threshold of H , but in general almost constant. This behavior is different for the percentage of savings because the larger H , the larger the reference cost, while the amount of savings keep the same (asymptotic behavior). Therefore, the larger H , the lower the percentage of savings.

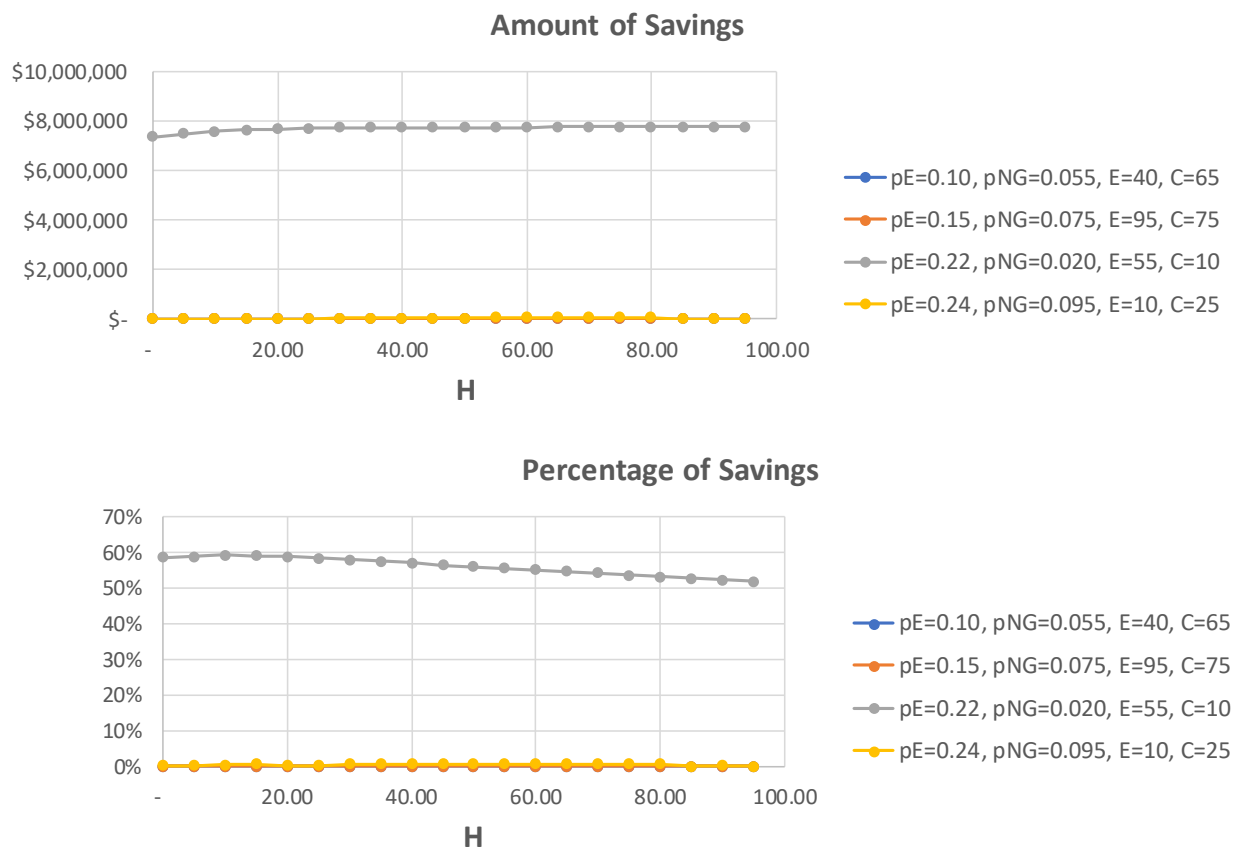


Figure 56 Isolines of pE - pNG - E - C across the annual heating load [H] for the amount and percentage of savings (top and bottom respectively)

For the case of annual cooling load, Figure 57 top shows that the amount of savings grows with C . While Figure 57 bottom presents an asymptotic behavior in the percentage of savings (almost constant).

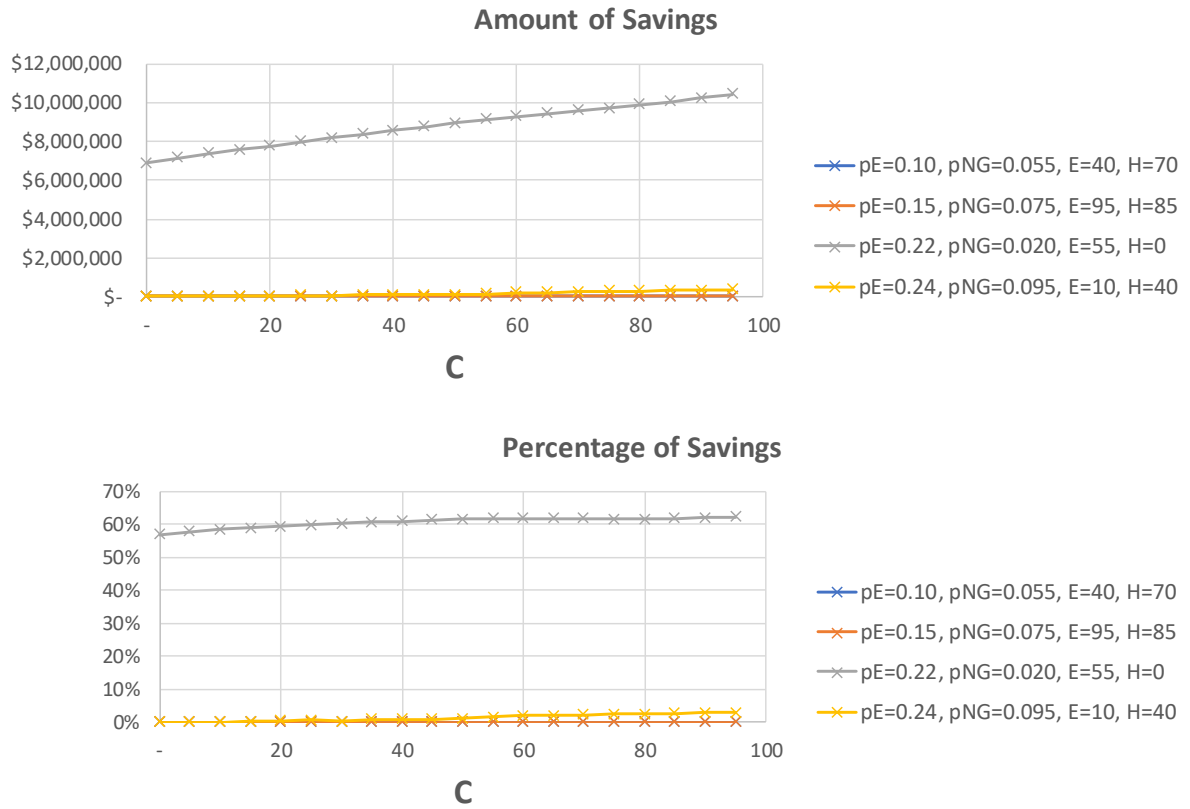


Figure 57 Isolines of pE - pNG - E - H across the annual cooling load [C] for the amount and percentage of savings (top and bottom respectively)

6 CONCLUSIONS AND FUTURE WORK

6.1 General conclusions

The trigeneration systems with thermal storage (CCHP-TS) are key technologies to reduce greenhouse gas emissions and improve the distributed generation of energy. The study of their feasibility has been crucial across the scientific community and governmental organizations. Therefore, this work aims to contribute by systematically identifying the most relevant variables to assess if CCHP-TS systems is techno-economically feasible.

It is worth mentioning that this work is conducted in hourly timestep. Not all the authors and computational tools do it, and its relevance is because the smaller the timestep, the higher the precision of the assessment. This is a must in context like the European, where the interest of buying fuel and selling electricity is not straight forward due to the large energy prices.

The study considers the relevance of five variables: the price of electricity [pE], the price of natural gas [pNG], the size of the annual loads of electricity [E], heating [H], and cooling [C]. In particular, the objective of this work is to proof (or discard) the following hypothesis:

1. There is a combination of energy prices (pE and pNG) and size of the energy loads (E , H , and C) that makes a Trigeneration – Thermal Storage feasible,
2. The energy prices should be considered separately, instead of consolidating them into the spark spread rate (SS).

The first part of this work assessed the techno-economic feasibility, measuring the percentage of savings obtained by using a CCHP-TS system instead of the reference scenario (Figure 3). Techniques of clustering and MCDM allowed to analyze the data and generate ternary diagrams.

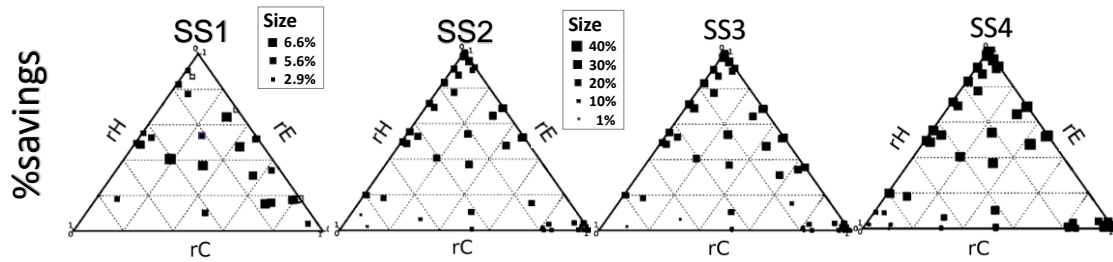


Figure 58 Ternary diagrams of SS1, SS2, SS3, and SS4 for the distribution of the percentage of savings across dominance rates (rE , rH , rC). Taken from subsection 4.4.3.

These diagrams (Figure 58) showed qualitatively that the percentage of savings is firstly driven by the spark spread rate (SS) and secondly by the size of energy loads. Specifically, the size of the electric annual load (E) proved to be relevant in all the cases.

The second part of the work had the objective to conduct a sensitivity analysis of five variables affecting the feasibility of CCHP-TS (the price of electricity pE , the price of natural gas pNG , and the annual loads E : electricity, H : heating, C : cooling). There was a special emphasis in analyzing the electricity and natural gas prices separately, instead of consolidating them into the spark spread rate. For that, three sensitivity analysis methods were used and compared: Morris (derivative-based approach), Sobol (variance-based approach), and VARS (variogram-based approach). The analysis was conducted considering two metrics: the amount of savings, and the percentage of savings. The first one quantifies the absolute savings of using the CCHP-TS system instead of the reference scenario, and the second measures the relative savings. The results of this part gave answer to the two hypotheses raised.

HYPOTHESIS 1

Yes, there are combination of energy prices and size of the energy loads that make a Trigeration – Thermal Storage feasible. The optimal combination depends on the metric considered.

When talking about the **amount of savings**, pE , pNG , and E are, by far, the most relevant variables. While H and C seem comparatively unimportant. The

main interaction effects are between the electricity load and the energy prices ($E - p_{NG}$ and $E - pE$). In other words, having a large E is good, but it should be along with a small p_{NG} and high pE (see Figure 51 left). Vice versa it is also true. The discussion of Figure 52 shows that, for determined pE and p_{NG} , an increase of the loads rises the amount of savings. Finally, it is good to mention that p_{NG} is a singular variable that has interaction effects with all the others.

When talking about the **percentage of savings**, the energy prices pE , and p_{NG} are the most relevant variables. E is still more influential than H and C , but it becomes less influential compared with its analysis for the amount of savings. That is because, when measuring the amount of savings, there is a direct link between the money saved and the size of E . But when measuring percentage of savings, it considers the proportions, rather than the total amount. Nevertheless, an important remark is that in the percentage of savings, the influence of the three loads (E , H , and C) is slightly more equilibrated than in the amount of savings (individually and in terms of interaction effects). All this fit with the analysis of chapter 4. On the other hand, p_{NG} is again the only variable that has interaction effects with all the others, but some aspects draw attention. The index $p_{NG} - pE$ is notably bigger compared with its analogous in the amount of savings, suggesting that the Spark Spread rate (SS) could be relevant for the relative savings. However, that resolution becomes weak when noticing that the energy loads have interaction effects almost exclusively with p_{NG} . Therefore, the relevance of E , H , and C is strongly linked only to the price of natural gas.

HYPOTHESIS 2

Concerning the interest of studying the **energy prices** separately, it can be said that both, pE and p_{NG} , are relevant individually regardless of the output measure (amount or percentage of savings). Also, they are clearly tied, either directly or indirectly. For the percentage of savings, the interaction effect between them is very strong. While for the amount of savings, each price has interaction effects with E , therefore, they have an indirect link. However, the main difference between them is that, in either output (amount or percentage of

savings), p_{NG} keeps interaction effects with all the other variables, indicating that its influence is wider. Specifically talking about the percentage of savings, the energy loads interact almost exclusively with p_{NG} . Moreover, although p_E also has a strong interaction effects with p_{NG} , section 5.7 shows that, contrary to the general rule established by international governmental organisms [13] and explained in section 2.2, the spark spread threshold could be lower than three depending on the price of natural gas. Therefore, it is recommendable to analyze separately the energy prices while assessing the feasibility of Trigeneration systems with Thermal Storage.

Some pertinent final remarks regarding the nature of this work include the following:

First, the thesis provides a grasp on the flexibility of the CCHP-TS system by presenting the different combinations of the variables that fluctuate across their range. Then, it is possible to determine at what extend the CCHP-TS system keeps being economically feasible.

Second, all the analysis in this thesis is conducted without considering any regulatory incentive. Therefore, when the analysis shows that a scenario is feasible, it means that the characteristics of the technology and the market are enough.

Third, the work exhibits that electricity loads have a larger influence than heating and cooling in the techno-economic feasibility of CCHP-TS system. However, note that the presence (not dominance) of heating and cooling potentially fosters the environmental performance, because it takes advantage of the residual heat. Then, a recommendation for policy makers is to identify facilities that have a large electric load and incentivize, through pricing mechanisms, the aggregation of thermal loads and the use of CCHP-TS. This would encompass the heating and cooling infrastructure with the urban planning.

Finally, the conclusions of the work are quite aligned with the hypothesis proposed by Knizley et. al. when analyzing CHP systems [47]. However, this work goes a step further by 1) analyzing the CCHP-TS system, 2) analyzing

many combinations of energy prices and loads, 3) getting conclusive results, by using many tools, regarding the impact of each variable for the case study of a University campus.

6.2 Conclusions from the methodology

Aside from the technical results discussed above, the objective of this work is to analyze and contrast the different steps taken at the methodology of the thesis.

The general methodology is presented in section 3.1 and starts with a division in two phases. Each of them with a clear purpose. The first examines the relevance of the CCHP-TS model (feasibility and sensitivity to four selected variables). The second conduct a global sensitivity analysis of the feasibility studying five selected variables.

These two phases are complementary in two way. To start, developing the work in phase one helped to get familiarized with the model, the variables, and their synergy. As an example, one of the hypotheses proposed in this thesis is an outcome of the first phase. To continue, while the second phase (developed in chapter 5) clearly estimates the relevance of each variable, the first phase (in chapter 4) helps to understand the physical behavior of the technology. For example, while chapter 5 finds that H and C are not relevant variables, chapter 4 explains that the reason is that it is more profitable to use boiler and vapor-compression chiller when heating or cooling loads dominate.

Other valuable remark of the methodology is regarding the energy system optimization. DER-CAM model was a good way to get the first general approach. But eventually, the level of automatization required in the simulation process obliged us to move forward (see subsection 3.3.1). Then, we adapted an hourly time-step model of the CCHP-TS systems into the programming language Python. This allowed to run thousands of simulations in a very agile way.

Finally, the sensitivity analysis is another key part of the methodology. The first approach was using a full factorial DoE as an exploratory analysis. It is

computationally cheap and easy to implement; therefore, we were able to use DER-CAM for the energy system optimization. Later on, we needed a more robust way to assess the influence of variables (see subsection 3.3.5). Then, using the model adapted into Python, we used and compared three global sensitivity analysis methods. This allowed identifying their advantages and limitations (detailed in section 5.6), but more important, this complementarity thereby reinforced the techno-economic feasibility analysis of the Trigeneration systems with Thermal Storage.

6.3 Future work

Across the literature there are several works using modeling and data analysis to study the feasibility of Trigeneration and Thermal Storage system. Nevertheless, there is still room for research and innovation.

Some opportunities for future work include the study of different hourly load profiles, and price schemes.

Regarding the price schemes, we recommend performing a similar analysis to this work, but now considering variable pE and pNG , that could differ across the days of the week and even along the same day. Including this into the model, intuitively, will foster the use of thermal storage during the hours of the day when the prices of electricity and natural gas are lower.

Regarding the hourly load profile, an option is to characterize it through the study of load duration curves, taking as references works as Poulin et. al. and Ueckerdt et al. [177], [178]. Similarly, it is pertinent to measure the interdependence between E, H, and C in different case studies. This would give the opportunity to create more reasonable scenarios while conducting sensitivity analysis. Following the same line of thought, it is also relevant to deepen the study for the flexibility of the CCHP-TS system. It includes analyzing the impact in the optimal solution due to climate change, considering extreme peaks of heating and cooling.

Another interesting study would be to perform a sensitivity analysis to know how the different regulatory incentives could affect positively (or negatively) the feasibility of the CCHP-TS system. A valuable extend of the model could even include other technologies such as PV, fuel cells, solar collectors, heat pumps, etc. Then, it would be possible to verify how their current price and governmental incentives could affect the feasibility of CCHP-TS systems.

Specifically, we recommend continue working with pE and pNG separated, instead of consolidating them into the spark spread.

REFERENCES

- [1] H. Hajabdollahi, "Investigating the effects of load demands on selection of optimum CCHP-ORC plant," *Appl. Therm. Eng.*, vol. 87, pp. 547–558, 2015.
- [2] E. Cardona, P. Sannino, A. Piacentino, and F. Cardona, "Energy saving in airports by trigeneration. Part II: Short and long term planning for the Malpensa 2000 CHCP plant," *Appl. Therm. Eng.*, vol. 26, no. 14–15, pp. 1437–1447, 2006.
- [3] U. Al-Mulali and C. N. Binti Che Sab, "The impact of energy consumption and CO 2 emission on the economic and financial development in 19 selected countries," *Renew. Sustain. Energy Rev.*, vol. 16, no. 7, pp. 4365–4369, 2012.
- [4] A. N. Rezitis and S. M. Ahammad, "Energy consumption and economic growth in South and Southeast Asian countries: Evidence from a dynamic panel data approach," *Int. Energy J.*, vol. 15, no. 3, pp. 103–116, 2015.
- [5] S. Stjepanović, "Relationship between energy consumption and economic growth in 30 countries in Europe – panel," *Ekon. Pregl.*, vol. 69, no. 1, pp. 43–57, 2018.
- [6] N. S. Ouedraogo, "Energy consumption and economic growth: Evidence from the economic community of West African States (ECOWAS)," *Energy Econ.*, vol. 36, pp. 637–647, 2013.
- [7] F. Faisal, T. Tursoy, and O. Ercantan, "The relationship between energy consumption and economic growth: Evidence from non-Granger causality test," *Procedia Comput. Sci.*, vol. 120, no. 2017, pp. 671–675, 2017.
- [8] K. Pinzón, "Dynamics between energy consumption and economic growth in Ecuador: A granger causality analysis," *Econ. Anal. Policy*, vol. 57, pp. 88–101, 2018.
- [9] IPCC 2014, "Climate Change 2014: Synthesis Report. Contribution of Working Groups I, II and III to the Fifth Assessment Report of the

- Intergovernmental Panel on Climate Change [Core Writing Team, R.K. Pachauri and L.A. Meyer (eds.)],” 2014.
- [10] International Energy Agency, “Total final energy consumption, by sector.” [Online]. Available: <https://www.iea.org/subscribe-to-data-services/world-energy-balances-and-statistics>. [Accessed: 12-Feb-2020].
- [11] M. GALINDO FERNÁNDEZ, C. ROGER-LACAN, U. GÄHRS, and V. AUMAITRE, *Efficient district heating and cooling markets in the EU: Case studies analysis, replicable key success factors and potential policy implications*, no. December. 2016.
- [12] US International Energy Agency, “Cogeneration and District Energy,” OECD, Oct. 2009.
- [13] CODE2 - Cogeneration Observatory and Dissemination Europe, “European cogeneration roadmap,” no. January, 2015.
- [14] A. Moro and L. Lonza, “Electricity carbon intensity in European Member States: Impacts on GHG emissions of electric vehicles,” *Transp. Res. Part D Transp. Environ.*, vol. 64, no. November 2016, pp. 5–14, 2018.
- [15] Ministry of the Economy of Luxembourg, “Assessment of the National and Regional Potential for the Application of High-Efficiency Cogeneration and Efficient District Heating,” *Wildl. Soc. Bull.*, no. August, 2016.
- [16] G. Angrisani, A. Akisawa, E. Marrasso, C. Roselli, and M. Sasso, “Performance assessment of cogeneration and trigeneration systems for small scale applications,” *Energy Convers. Manag.*, vol. 125, pp. 194–208, 2016.
- [17] The European Parliament and the Council of the European Union, “Directive 2012/27/EU of the European Parliament and of the Council of 25 October 2012 on Energy Efficiency,” *Official Journal of the European Union*, no. L 315/1. pp. 1–56, 2012.
- [18] COGEN Portugal, “Cogeração na Indústria. A cogeração como medida de eficiência energética na indústria: vantagens, enquadramento regulatório e situação em Portugal.” Batalha, Portugal, 2015.

- [19] COGEN Portugal, “A Cogeração em Portugal - Desafios e Oportunidades.” 2011.
- [20] C. E. Sopas, “Auditoria Energética e Aplicação de Medidas de Eficiência Energética a uma Instalação Industrial do Sector Farmacêutico,” Faculdade de Ciências e Tecnologia - Universidade Nova de Lisboa, 2015.
- [21] L. Fu, X. L. Zhao, S. G. Zhang, Y. Jiang, H. Li, and W. W. Yang, “Laboratory research on combined cooling, heating and power (CCHP) systems,” *Energy Convers. Manag.*, vol. 50, no. 4, pp. 977–982, 2009.
- [22] X. Song, L. Liu, T. Zhu, T. Zhang, and Z. Wu, “Comparative analysis on operation strategies of CCHP system with cool thermal storage for a data center,” *Appl. Therm. Eng.*, vol. 108, pp. 680–688, 2016.
- [23] W. Liu, G. Chen, B. Yan, Z. Zhou, H. Du, and J. Zuo, “Hourly operation strategy of a CCHP system with GSHP and thermal energy storage (TES) under variable loads: A case study,” *Energy Build.*, vol. 93, pp. 143–153, 2015.
- [24] A. D. Smith, P. J. Mago, and N. Fumo, “Benefits of thermal energy storage option combined with CHP system for different commercial building types,” *Sustain. Energy Technol. Assessments*, vol. 1, no. 1, pp. 3–12, 2013.
- [25] G. Pagliarini and S. Rainieri, “Modeling of a thermal energy storage system coupled with combined heat and power generation for the heating requirements of a University Campus,” *Appl. Therm. Eng.*, vol. 30, no. 10, pp. 1255–1261, 2010.
- [26] U. Persson and S. Werner, “STRATEGO: Quantifying the Heating and Cooling Demand in Europe,” 2015.
- [27] P. G. Nicolas, V. Konstaninos, K.-R. Anna, M. R. J. Antonio, and P. L. Alicia, *Heat and Cooling Demand and Market Perspective, Report EUR 25381 EN*. 2012.
- [28] International Energy Agency, “The Future of Cooling in China sustainable air conditioning,” no. June, 2019.

- [29] US Department of Energy, “Combined Heat and Power Technology Fact Sheet Series: Reciprocating Engines,” 2016.
- [30] US International Energy Agency, “Combined Heat and Power: Evaluating the benefits of greater global investment,” *OECD / IEA*, 2008.
- [31] Eurostat, “Combined Heat and Power (CHP) data 2005-2017,” 2017.
- [32] UN-ESCAP, *Low carbon green growth roadmap for Asia and the Pacific*. 2012.
- [33] UN-ESCAP, “Low carbon green growth roadmap for Asia and the Pacific: CHP fact sheet,” 2012.
- [34] Euroheat & Power, “District Energy in China,” 2017. [Online]. Available: <https://www.euroheat.org/knowledge-hub/district-energy-china/>. [Accessed: 13-Nov-2019].
- [35] Euroheat & Power, “District Energy Explained,” *Knowledge Hub*. [Online]. Available: <https://www.euroheat.org/knowledge-hub/district-energy-explained/>. [Accessed: 11-Nov-2019].
- [36] Department for Business Energy & Industrial Strategy, “Evidence Gathering: Thermal Energy Storage (TES) Technologies,” *Renew. Sustain. Energy Rev.*, vol. 80, pp. 1–85, 2016.
- [37] A. Arteconi, C. Brandoni, and F. Polonara, “Distributed generation and trigeneration: Energy saving opportunities in Italian supermarket sector,” *Appl. Therm. Eng.*, vol. 29, no. 8–9, pp. 1735–1743, 2009.
- [38] G. Streckiene, V. Martinaitis, A. N. Andersen, and J. Katz, “Feasibility of CHP-plants with thermal stores in the German spot market,” *Appl. Energy*, vol. 86, no. 11, pp. 2308–2316, 2009.
- [39] Encyclopaedia Britannica, “Tropical and subtropical desert climate.” [Online]. Available: <https://www.britannica.com/science/tropical-and-subtropical-desert-climate>. [Accessed: 13-Nov-2019].
- [40] Solargis & the World Bank Group, “Global Solar Atlas 2.0,” 2019. [Online]. Available: <https://globalsolaratlas.info>. [Accessed: 13-Nov-2019].

- [41] P. J. Mago, N. Fumo, and L. M. Chamra, "Methodology to perform a non-conventional evaluation of cooling, heating, and power systems," *Proc. Inst. Mech. Eng. Part A J. Power Energy*, vol. 221, no. 8, pp. 1075–1087, 2007.
- [42] N. Fumo and L. M. Chamra, "Analysis of combined cooling, heating, and power systems based on source primary energy consumption," *Appl. Energy*, vol. 87, no. 6, pp. 2023–2030, 2010.
- [43] N. Fumo, P. J. Mago, and L. M. Chamra, "Energy and economic evaluation of cooling, heating, and power systems based on primary energy," *Appl. Therm. Eng.*, vol. 29, no. 13, pp. 2665–2671, 2009.
- [44] J. J. Wang, Y. Y. Jing, C. F. Zhang, and Z. J. Zhai, "Performance comparison of combined cooling heating and power system in different operation modes," *Appl. Energy*, vol. 88, no. 12, pp. 4621–4631, 2011.
- [45] C. Z. Li, Y. M. Shi, and X. H. Huang, "Sensitivity analysis of energy demands on performance of CCHP system," *Energy Convers. Manag.*, vol. 49, no. 12, pp. 3491–3497, 2008.
- [46] J. Y. Wu, J. L. Wang, and S. Li, "Multi-objective optimal operation strategy study of micro-CCHP system," *Energy*, vol. 48, no. 1, pp. 472–483, 2012.
- [47] A. Knizley *et al.*, "Evaluation of the operational cost savings potential from a D-CHP system based on a monthly power-to-heat ratio analysis," *Cogent Eng.*, vol. 2, no. 1, pp. 1–13, 2015.
- [48] M. Li, H. Mu, N. Li, and B. Ma, "Optimal design and operation strategy for integrated evaluation of CCHP (combined cooling heating and power) system," *Energy*, vol. 99, pp. 202–220, 2016.
- [49] G. Sundberg, "Ranking factors of an investment in cogeneration: Sensitivity analysis ranking the technical and economical factors," *Int. J. Energy Res.*, vol. 25, no. 3, pp. 223–238, 2001.
- [50] H. Hajabdollahi, A. Ganjehkaviri, and M. N. M. Jaafar, "Assessment of new operational strategy in optimization of CCHP plant for different climates using evolutionary algorithms," *Appl. Therm. Eng.*, vol. 75, pp. 468–480,

2015.

- [51] A. G. Memon and R. A. Memon, "Parametric based economic analysis of a trigeneration system proposed for residential buildings," *Sustain. Cities Soc.*, vol. 34, no. February, pp. 144–158, 2017.
- [52] E. Cardona, A. Piacentino, and F. Cardona, "Energy saving in airports by trigeneration. Part I: Assessing economic and technical potential," *Appl. Therm. Eng.*, vol. 26, no. 14–15, pp. 1427–1436, 2006.
- [53] A. D. Smith, N. Fumo, and P. J. Mago, "Spark spread - A screening parameter for combined heating and power systems," *Appl. Energy*, vol. 88, no. 5, pp. 1494–1499, 2011.
- [54] K. C. Kavvadias, "Energy price spread as a driving force for combined generation investments: A view on Europe," *Energy*, vol. 115, pp. 1632–1639, 2016.
- [55] P. Fonseca, G. Markogiannakis, A. de Almeida, C. Kofod, and N. Feilberg, "Characterization of the household electricity consumption in the EU , potential energy savings and specific policy recommendations," pp. 781–793, 2009.
- [56] M. B. Tookanlou, M. M. Ardehali, and M. E. Nazari, "Combined cooling, heating, and power system optimal pricing for electricity and natural gas using particle swarm optimization based on bi-level programming approach: Case study of Canadian energy sector," *J. Nat. Gas Sci. Eng.*, vol. 23, pp. 417–430, 2015.
- [57] D. Chan, M. Cameron, and Y. Yoon, "Key success factors for global application of micro energy grid model," *Sustain. Cities Soc.*, vol. 28, pp. 209–224, 2017.
- [58] B. Afework, J. Hanania, K. Stenhouse, and J. Donev, "Thermal power," *Energy Education - University of Calgary*, 2018. .
- [59] L. Neves, "Q&A session during the oral dissertation of Mexitli Eva Sandoval Reyes to obtain the PhD degree." Lisbon, Portugal, 2020.

- [60] Midwest CHP Application Center and Avalon Consulting Inc., “Combined Heat and Power Resource Guide,” p. 59, 2005.
- [61] G. Dillingham, C. Gamarra, and L. Rao, “Microgrids with CHP - Improving campus and community resilience,” in *Webinar MRC - Microgrids Resources Coalition* -, 2017.
- [62] S. Blumsack, “Lesson 10.1 Risk in Electricity Markets: Temporal, Locational and the Spark Spread,” *PennState College of Earth and Mineral Science*, 2019. [Online]. Available: <https://www.e-education.psu.edu/ebf483/node/699>. [Accessed: 17-Dec-2019].
- [63] A. Alli, “African governments ’ quest for cheap electricity has kept millions of us in the dark,” *Quartz Africa*, pp. 1–6, 2018.
- [64] Statista Research Department, “Household electricity price worldwide in 2016, by region,” 2016. [Online]. Available: <https://www.statista.com/statistics/497410/worldwide-electricity-price-by-region/>. [Accessed: 17-Dec-2019].
- [65] International Gas Union, “Wholesale gas price survey - 2019 edition,” 2019.
- [66] Eurostat, “Eurostat,” *Electricity and natural gas prices charged to final consumers (2017)*, 2018. [Online]. Available: <https://ec.europa.eu/eurostat/tgm/table.do?tab=table&init=1&plugin=1&language=en&pcode=ten00117>. [Accessed: 31-Oct-2018].
- [67] E. Ronn, *Real Options and Energy Management: Using Options Methodology to Enhance Capital Budgeting Decisions*. Risk Books, 2002.
- [68] R. S. Elias, M. I. M. Wahab, and L. Fang, “The spark spread and clean spark spread option based valuation of a power plant with multiple turbines,” *Energy Econ.*, vol. 59, pp. 314–327, 2016.
- [69] Invest Northern Ireland, “Combined Heat & Power Guide A best practice guide for businesses in Northern Ireland.”
- [70] H. D. Vignesh Gowrishankar, Christina Angelides, “Combined Heat and

- Power Systems : Improving the Energy Efficiency of Our Manufacturing Plants , Buildings , and Other Facilities,” *Nat. Resour. Def. Counc.*, 2013.
- [71] Carbon Trust, “Good practices guide 388: Combined heat and power for buildings,” 2004.
- [72] U.S. EPA (Environmental Protection Agency), “Combined Heat and Power - A guide to developing and implementing greenhouse gas reduction programs,” 2014.
- [73] The World Bank, “Electric power consumption (kWh per capita),” *IEA Statistics*, 2014. [Online]. Available: <https://data.worldbank.org/indicator/eg.use.elec.kh.pc>. [Accessed: 17-Sep-2018].
- [74] United Nations, “Household Size and Composition Around the World 2017,” p. 36, 2017.
- [75] School of Engineering and Applied Science at Columbia University, “Estimated Total Annual Building Energy Consumption at the Block and Lot Level for NYC.” [Online]. Available: <http://qsel.columbia.edu/nycenergy/>. [Accessed: 17-Sep-2018].
- [76] Instituto Superior Técnico, “Campus Sustentável.” [Online]. Available: <http://sustentavel.unidades.tecnico.ulisboa.pt/quem-somos/683-2/>. [Accessed: 01-Jun-2018].
- [77] U.S. DOE, “Combined Heat and Power Installation Database.” [Online]. Available: <https://doe.icfwebservices.com/chpdb/state/IL>. [Accessed: 18-Sep-2018].
- [78] D. W. Wu and R. Z. Wang, “Combined cooling, heating and power: A review,” *Prog. Energy Combust. Sci.*, vol. 32, no. 5–6, pp. 459–495, 2006.
- [79] Stockholm Environment Institute, “Modeling tools.” [Online]. Available: <https://www.energycommunity.org/default.asp?action=tools>. [Accessed: 02-Dec-2019].
- [80] D. Connolly, H. Lund, B. V. Mathiesen, and M. Leahy, “A review of

- computer tools for analysing the integration of renewable energy into various energy systems,” *Appl. Energy*, vol. 87, no. 4, pp. 1059–1082, 2010.
- [81] A. U. Department of Development and Planning, “Other Tools.” [Online]. Available: <https://www.energyplan.eu/othertools/>. [Accessed: 02-Dec-2019].
- [82] A. Lyden, R. Pepper, and P. G. Tuohy, “A modelling tool selection process for planning of community scale energy systems including storage and demand side management,” *Sustain. Cities Soc.*, vol. 39, no. August 2017, pp. 674–688, 2018.
- [83] ENERGIANALYSE.DK, “Download COMPOSE.” [Online]. Available: <http://energianalyse.dk/index.php/software>.
- [84] RETScreen eLearning, *Feasibility Analysis with RETScreen Expert*. 2017.
- [85] HOMER Energy LLC, “HOMER pricing.” [Online]. Available: <https://www.homerenergy.com/products/pro/pricing/index.html>. [Accessed: 02-Dec-2019].
- [86] Lawrence Berkeley National Laboratory - University of California, “DER-CAM Web Optimization tool.” [Online]. Available: <https://microgrids2.lbl.gov>.
- [87] H. Ravn, “The Balmorel Model Structure. Version of the document: 3.03,” 2016.
- [88] US Department of Energy, “How Microgrids Work.” [Online]. Available: <https://www.energy.gov/articles/how-microgrids-work>. [Accessed: 16-Dec-2019].
- [89] E. Cardona and A. Piacentino, “A measurement methodology for monitoring a CHCP pilot plant for an office building,” *Energy Build.*, vol. 35, no. 9, pp. 919–925, 2003.
- [90] G. Angrisani, A. Rosato, C. Roselli, M. Sasso, and S. Sibilio, “Experimental results of a micro-trigeneration installation,” *Appl. Therm.*

Eng., vol. 38, pp. 78–90, 2012.

- [91] B. Li, P. Hu, N. Zhu, F. Lei, and L. Xing, “Performance analysis and optimization of a CCHP-GSHP coupling system based on quantum genetic algorithm,” *Sustain. Cities Soc.*, vol. 46, no. January, p. 101408, 2019.
- [92] H. Li, R. Nalim, and P. A. Haldi, “Thermal-economic optimization of a distributed multi-generation energy system - A case study of Beijing,” *Appl. Therm. Eng.*, vol. 26, no. 7, pp. 709–719, 2006.
- [93] B. Pickering, S. Ikeda, and R. Ooka, “Comparison of Metaheuristic and Linear Programming Models for the Purpose of Optimising Building Energy Supply Operation Schedule Comparison of Metaheuristic and Linear Programming Models for the Purpose of Optimising Building Energy Supply Operation Sche,” no. May, 2016.
- [94] S. Ikeda and R. Ooka, “Metaheuristic optimization methods for a comprehensive operating schedule of battery, thermal energy storage, and heat source in a building energy system,” *Appl. Energy*, vol. 151, pp. 192–205, 2015.
- [95] A. Fügenschuh and ResearchGate, “What is the advantages of MIP model over metaheuristics?,” 2016. [Online]. Available: https://www.researchgate.net/post/what_is_the_advantages_of_MIP_model_Why_the_MIP_model_are_proposed_for_the_problems. [Accessed: 16-Dec-2019].
- [96] M. Fischetti and A. Lodi, “Local branching,” *Math. Program.*, vol. 98, no. 1, pp. 23–47, 2003.
- [97] GAMS Development Corp., “About the Company.” [Online]. Available: <https://www.gams.com/about-the-company/>. [Accessed: 04-Dec-2019].
- [98] Sandia National Laboratories, “About Pyomo.” [Online]. Available: <http://www.pyomo.org/about>. [Accessed: 28-Oct-2019].
- [99] Sandia National Laboratories, “Pyomo Documentation 5.6.6.” [Online]. Available: <https://pyomo.readthedocs.io/en/stable/>. [Accessed: 28-Oct-

- 2019].
- [100] R. Fourer, D. M. Gay, and B. W. Kernighan, "A Modeling Language for Mathematical Programming," *Manage. Sci.*, vol. 36, no. 5, pp. 519–554, 1990.
- [101] IBM Corporation, "CPLEX Optimizer." [Online]. Available: <https://www.ibm.com/analytics/cplex-optimizer>. [Accessed: 04-Dec-2019].
- [102] IBM Corporation, "CPLEX Performance Tuning for Mixed Integer Programs." [Online]. Available: <https://www.ibm.com/support/pages/cplex-performance-tuning-mixed-integer-programs>. [Accessed: 16-Dec-2019].
- [103] IBM Corporation, "relative MIP gap tolerance: CPLEX." [Online]. Available: https://www.ibm.com/support/knowledgecenter/SSSA5P_12.9.0/ilog.odms.cplex.help/CPLEX/Parameters/topics/EpGap.html. [Accessed: 22-Apr-2020].
- [104] M. Jaxa-Rozen and J. Kwakkel, "Tree-based ensemble methods for sensitivity analysis of environmental models: A performance comparison with Sobol and Morris techniques," *Environ. Model. Softw.*, vol. 107, no. May, pp. 245–266, 2018.
- [105] A. Saltelli and P. Annoni, "How to avoid a perfunctory sensitivity analysis," *Environ. Model. Softw.*, vol. 25, no. 12, pp. 1508–1517, 2010.
- [106] C. Vidal, *The beginning and the end: The meaning of life in a cosmological perspective*. 2014.
- [107] A. Saltelli *et al.*, "Why so many published sensitivity analyses are false: A systematic review of sensitivity analysis practices," *Environ. Model. Softw.*, vol. 114, no. March 2018, pp. 29–39, 2019.
- [108] T. Wei, "A review of sensitivity analysis methods in building energy analysis," *Renew. Sustain. Energy Rev.*, vol. 20, pp. 411–419, 2013.

- [109] X. Song, J. Zhang, C. Zhan, Y. Xuan, M. Ye, and C. Xu, "Global sensitivity analysis in hydrological modeling: Review of concepts, methods, theoretical framework, and applications," *J. Hydrol.*, vol. 523, no. 225, pp. 739–757, 2015.
- [110] S. Razavi and H. V Gupta, "A new framework for comprehensive, robust, and efficient global sensitivity analysis:2. Application," *Water Resour. Res.*, vol. 52, pp. 440–455, 2016.
- [111] S. Razavi and H. Gupta, "A new framework for comprehensive, robust, and efficient global sensitivity analysis: 1. Theory," *Water Resour. Res.*, vol. 52, pp. 423–439, 2016.
- [112] F. Sarrazin, F. Pianosi, and T. Wagener, "Global Sensitivity Analysis of environmental models: Convergence and validation," *Environ. Model. Softw.*, vol. 79, pp. 135–152, 2016.
- [113] D. Garcia Sanchez, B. Lacarrière, M. Musy, and B. Bourges, "Application of sensitivity analysis in building energy simulations: Combining first- and second-order elementary effects methods," *Energy Build.*, vol. 68, no. PART C, pp. 741–750, 2014.
- [114] C. Spitz, L. Mora, E. Wurtz, and A. Jay, "Practical application of uncertainty analysis and sensitivity analysis on an experimental house," *Energy Build.*, vol. 55, pp. 459–470, 2012.
- [115] H. Shen and A. Tzempelikos, "Sensitivity analysis on daylighting and energy performance of perimeter offices with automated shading," *Build. Environ.*, vol. 59, pp. 303–314, 2013.
- [116] Cross Validated, "Difference between Sensitivity analysis and Design of Experiments." [Online]. Available: <https://stats.stackexchange.com/questions/333857/difference-between-sensitivity-analysis-and-design-of-experiments>. [Accessed: 24-Nov-2019].
- [117] T. Rakić, I. Kasagić-Vujanović, M. Jovanović, B. Jančić-Stojanović, and D. Ivanović, "Comparison of Full Factorial Design, Central Composite

- Design, and Box-Behnken Design in Chromatographic Method Development for the Determination of Fluconazole and Its Impurities,” *Anal. Lett.*, vol. 47, no. 8, pp. 1334–1347, 2014.
- [118] NIST - National Institute of Standards and Technology, “How do you select an experimental design?,” *NIST/SEMATECH e-Handbook of Statistical Methods*, 2013. [Online]. Available: <https://www.itl.nist.gov/div898/handbook/pri/section3/pri33.htm>. [Accessed: 22-Mar-2020].
- [119] A. Saltelli, M. Ratto, T. Andres, F. Campolongo, J. Cariboni, and M. Saisana, *Global Sensitivity Analysis: The Primer*. 2008.
- [120] A. Saltelli, S. Tarantola, and K. P. S. Chan, “A quantitative model-independent method for global sensitivity analysis of model output,” *Technometrics*, vol. 41, no. 1, pp. 39–56, 1999.
- [121] D. R. Anderson, D. J. Sweeney, and T. A. Williams, “Experimental Design,” *ENCYCLOPEDIA BRITANNICA*. [Online]. Available: <https://www.britannica.com/science/statistics/Experimental-design>. [Accessed: 06-Dec-2019].
- [122] M. Shivhare and G. McCreath, “Practical considerations for DoE implementation in quality by design,” *Bioprocess Int.*, vol. 8, no. 6, pp. 22–30, 2010.
- [123] A. Capetillo and F. Ibarra, “Multiphase injector modelling for automotive SCR systems: A full factorial design of experiment and optimization,” *Comput. Math. with Appl.*, vol. 74, no. 1, pp. 188–200, 2017.
- [124] M. Stadler, M. Groissböck, G. Cardoso, and C. Marnay, “Optimizing Distributed Energy Resources and building retrofits with the strategic DER-CAModel,” *Appl. Energy*, vol. 132, pp. 557–567, 2014.
- [125] M. Stadler *et al.*, “DER - CAM User Manual,” pp. 1–55, 2016.
- [126] D. Steen, M. Stadler, G. Cardoso, M. Groissböck, N. DeForest, and C. Marnay, “Modeling of thermal storage systems in MILP distributed energy resource models,” *Appl. Energy*, vol. 137, pp. 782–792, 2015.

- [127] G. Cardoso, M. Stadler, S. Mashayekh, and E. Hartvigsson, "The impact of ancillary services in optimal DER investment decisions," *Energy*, vol. 130, pp. 99–112, 2017.
- [128] S. Mashayekh, M. Stadler, G. Cardoso, and M. Heleno, "A mixed integer linear programming approach for optimal DER portfolio, sizing, and placement in multi-energy microgrids," *Appl. Energy*, vol. 187, no. C1, pp. 154–168, 2017.
- [129] E. R. Morgan, S. Valentine, C. A. Blomberg, E. R. Limpaecher, and E. V. Dydek, "Boston Community Energy Study – Zonal Analysis for Urban Microgrids," *Massachusetts Inst. Technol. Lincoln Lab.*, 2016.
- [130] Grid Integration Group - LBNL, "California CHP Potential In 2030," 2016.
- [131] E. S. Lee, C. Gehbauer, B. E. Coffey, A. McNeil, M. Stadler, and C. Marnay, "Integrated control of dynamic facades and distributed energy resources for energy cost minimization in commercial buildings," *Sol. Energy*, vol. 122, pp. 1384–1397, 2015.
- [132] J. Jung and M. Villaran, "Optimal planning and design of hybrid renewable energy systems for microgrids," *Renew. Sustain. Energy Rev.*, vol. 75, no. August 2015, pp. 180–191, 2017.
- [133] G. Ghatikar, S. Mashayekh, M. Stadler, R. Yin, and Z. Liu, "Distributed energy systems integration and demand optimization for autonomous operations and electric grid transactions," *Appl. Energy*, vol. 167, no. 2016, pp. 432–448, 2016.
- [134] H. J. Adèr and G. J. Mellenbergh, "Advising on Research Methods: a consultant's companion," p. 574, 2008.
- [135] S. Ramos, J. M. Duarte, F. J. Duarte, and Z. Vale, "A data-mining-based methodology to support MV electricity customers' characterization," *Energy Build.*, vol. 91, pp. 16–25, 2015.
- [136] R. García Ochoa and B. Graizbord Ed, "Privation of energy services in Mexican households: An alternative measure of energy poverty," *Energy Res. Soc. Sci.*, vol. 18, pp. 36–49, 2016.

- [137] G. Grigoras and F. Scarlatache, “An assessment of the renewable energy potential using a clustering based data mining method. Case study in Romania,” *Energy*, vol. 81, pp. 416–429, 2015.
- [138] P. A. Sánchez-Pérez, M. Robles, and O. A. Jaramillo, “Real time Markov chains: Wind states in anemometric data,” *J. Renew. Sustain. Energy*, vol. 8, no. 2, 2016.
- [139] Decisive Data, “4 Types of Cluster Analysis Techniques Used in Data Science.” [Online]. Available: <https://www.decisivedata.net/blog/4-types-of-cluster-analysis-techniques-used-in-data-science>. [Accessed: 09-Dec-2019].
- [140] Scikit Learn, “2.3. Clustering.” [Online]. Available: <https://scikit-learn.org/stable/modules/clustering.html#k-means>. [Accessed: 23-Oct-2019].
- [141] N. Oskolkov and Towards data science, “How to cluster in High Dimensions.” [Online]. Available: <https://towardsdatascience.com/how-to-cluster-in-high-dimensions-4ef693bacc6>. [Accessed: 09-Dec-2019].
- [142] V. Molchanov and L. Linsen, “Overcoming the curse of dimensionality when clustering multivariate volume data,” *VISIGRAPP 2018 - Proc. 13th Int. Jt. Conf. Comput. Vision, Imaging Comput. Graph. Theory Appl.*, vol. 3, no. Visigrapp, pp. 29–39, 2018.
- [143] L. Morissette and S. Chartier, “The k-means clustering technique: General considerations and implementation in Mathematica,” *Tutor. Quant. Methods Psychol.*, vol. 9, no. 1, pp. 15–24, 2013.
- [144] M. A. Hartigan and M. A. Wong, “Algorithm AS 136 : A K-Means Clustering Algorithm,” *J. R. Stat. Soc.*, vol. 28, no. 1, pp. 100–108, 1979.
- [145] F. McLoughlin, A. Duffy, and M. Conlon, “A clustering approach to domestic electricity load profile characterisation using smart metering data,” *Appl. Energy*, vol. 141, pp. 190–199, 2015.
- [146] J. Kogan, C. Nicholas, and M. Teboulle, *Grouping multidimensional data: Recent advances in clustering*. 2006.

- [147] E. Estrada, R. Maciel, A. Ochoa, B. Bernabe-Loranca, D. Oliva, and V. Larios, "Smart City Visualization Tool for the Open Data Georeferenced Analysis Utilizing Machine Learning," *Int. J. Comb. Optim. Probl. Informatics*, vol. 9, no. 2, pp. 25–40, 2018.
- [148] G. Cruz-Cárdenas, J. T. Silva, S. Ochoa-Estrada, F. Estrada-Godoy, and J. Nava-Velázquez, "Delineation of Environmental Units by Multivariate Techniques in the Duero River Watershed, Michoacán, Mexico," *Environ. Model. Assess.*, vol. 22, no. 3, pp. 257–266, 2017.
- [149] R. Silva-Flores, J. C. Hernández-Díaz, and C. Wehenkel, "Does community-based forest ownership favour conservation of tree species diversity? A comparison of forest ownership regimes in the Sierra Madre Occidental, Mexico," *For. Ecol. Manage.*, vol. 363, pp. 218–228, 2016.
- [150] A. Saltelli, S. Tarantola, F. Campolongo, and M. Ratto, *Sensitivity analysis in practice: a guide to assessing scientific models*. 2004.
- [151] E. Fabrizio and V. Monetti, "Methodologies and advancements in the calibration of building energy models," *Energies*, vol. 8, no. 4, pp. 2548–2574, 2015.
- [152] J. C. Lam, K. K. W. Wan, and L. Yang, "Sensitivity analysis and energy conservation measures implications," *Energy Convers. Manag.*, vol. 49, no. 11, pp. 3170–3177, 2008.
- [153] N. H. Sandberg, I. Sartori, and H. Brattebø, "Sensitivity analysis in long-term dynamic building stock modeling - Exploring the importance of uncertainty of input parameters in Norwegian segmented dwelling stock model," *Energy Build.*, vol. 85, pp. 136–144, 2014.
- [154] W. Tian and P. De Wilde, "Uncertainty and sensitivity analysis of building performance using probabilistic climate projections: A UK case study," *Autom. Constr.*, vol. 20, no. 8, pp. 1096–1109, 2011.
- [155] S. Razavi, "VARS-Tool: A Comprehensive, Efficient, and Robust Toolbox for Global sensitivity analysis," no. June, pp. 1–10, 2016.
- [156] M. D. Morris, "Factorial Sampling Plans for Preliminary Computational

- Experiments,” *Technometrics*, vol. 33, no. 2, pp. 161–174, May 1991.
- [157] F. Campolongo, J. Cariboni, and A. Saltelli, “An effective screening design for sensitivity analysis of large models,” *Environ. Model. Softw.*, vol. 22, no. 10, pp. 1509–1518, 2007.
- [158] R. M. Anacleto Gomes, “A multidisciplinary approach for building retrofit driven by thermal comfort,” Instituto Superior Técnico - Universidade de Lisboa, 2018.
- [159] H. Sohier, J. L. Farges, and H. Piet-Lahanier, *Improvement of the representativity of the morris method for air-launch-to-orbit separation*, vol. 19, no. 3. IFAC, 2014.
- [160] A. Saltelli, “Making best use of model evaluations to compute sensitivity indices,” *Comput. Phys. Commun.*, vol. 145, no. 2, pp. 280–297, 2002.
- [161] S. Razavi, “Seminar ‘A New Framework for Comprehensive, Efficient, and Robust Global Sensitivity Analysis’, by Saman Razavi, University of Saskatchewan,” 2017. [Online]. Available: <https://www.youtube.com/watch?v=BfVCYx0O4e4>.
- [162] F. A. C. Viana, “A Tutorial on Latin Hypercube Design of Experiments,” *Qual. Reliab. Eng. Int.*, vol. 32, no. 5, pp. 1975–1985, 2016.
- [163] R. Sheikholeslami and S. Razavi, “Progressive Latin Hypercube Sampling: An efficient approach for robust sampling-based analysis of environmental models,” *Environ. Model. Softw.*, vol. 93, pp. 109–126, 2017.
- [164] J. L. Vujic, “Monte Carlo Sampling Methods.” .
- [165] “Monte Carlo method.” [Online]. Available: https://en.wikipedia.org/wiki/Monte_Carlo_method#Definitions. [Accessed: 06-Dec-2019].
- [166] V. Schwieger, “Sensitivity analysis as a general tool for model optimisation – examples for trajectory estimation,” *J. Appl. Geod.*, vol. 1, no. 1, 2007.
- [167] W. E. Becker, S. Tarantola, and G. Deman, “Sensitivity analysis

- approaches to high-dimensional screening problems at low sample size,” *J. Stat. Comput. Simul.*, vol. 88, no. 11, pp. 2089–2110, 2018.
- [168] A. Wang and D. P. Solomatine, “Practical experience and framework for sensitivity analysis of hydrological models: six methods, three models, three criteria,” *Hydrol. Earth Syst. Sci. Discuss.*, no. February, pp. 1–34, 2018.
- [169] A. Thaler and D. Watzenig, *Automotive Battery Technology*. Springer Science & Business Media, 2014.
- [170] V. R. Joseph, L. Gu, S. Ba, and W. R. Myers, “Space-Filling Designs for Robustness Experiments,” *Technometrics*, vol. 61, no. 1, pp. 24–37, 2019.
- [171] Datadvance, “Generic Tool for Design of Experiments (GT DoE),” 2020. [Online]. Available: <https://www.datadvance.net/product/pseven-core/generic-tool-for-design-of-experiments/>. [Accessed: 31-Mar-2020].
- [172] Eurostat, “Electricity and gas prices, 2013–15,” 2016. [Online]. Available: [https://ec.europa.eu/eurostat/statistics-explained/index.php/File:Electricity_and_gas_prices,_second_half_of_year,_2013–15_\(EUR_per_kWh\)_YB16-fr.png](https://ec.europa.eu/eurostat/statistics-explained/index.php/File:Electricity_and_gas_prices,_second_half_of_year,_2013–15_(EUR_per_kWh)_YB16-fr.png).
- [173] B. Roy, “Classement et choix en présence de points de vue multiples,” *RAIRO - Oper. Res. - Rech. Opérationnelle*, vol. 2, no. V1, pp. 57–75, 1968.
- [174] P. Haurant, P. Oberti, and M. Muselli, “Multicriteria selection aiding related to photovoltaic plants on farming fields on Corsica island: A real case study using the ELECTRE outranking framework,” *Energy Policy*, vol. 39, no. 2, pp. 676–688, 2011.
- [175] M. A. Alzoubi and T. Zhang, “Characterization of Energy Efficient Vapor Compression Cycle Prototype with a Linear Compressor,” *Energy Procedia*, vol. 75, no. 2, pp. 3253–3258, 2015.
- [176] M. A. Abd Majid, S. A. Sulaiman, T. Fujii, and Naono, “Studies on Steam Absorption Chillers Performance at a Cogeneration Plant,” *MATEC Web Conf.*, vol. 13, p. 05003, 2014.

- [177] A. Poulin, M. Dostie, M. Fournier, and S. Sansregret, "Load duration curve: A tool for technico-economic analysis of energy solutions," *Energy Build.*, vol. 40, no. 1, pp. 29–35, 2008.
- [178] F. Ueckerdt *et al.*, "Representing power sector variability and the integration of variable renewables in long-term energy-economy models using residual load duration curves," *Energy*, vol. 90, pp. 1799–1814, 2015.
- [179] D. Bouyssou and B. Roy, "La notion de seuils de discrimination en analyse multicritère," *INFOR Inf. Syst. Oper. Res.*, vol. 25, no. 4, pp. 302–313, 1987.
- [180] B. Roy, "Classement et choix en présence de points de vue multiples," *Rev. française d'informatique Rech. opérationnelle*, vol. 2, no. V.1, pp. 57–75, 1968.
- [181] D. Bouyssou and B. Roy, "La Notion De Seuils De Discrimination En Analyse Multicritère," *Inf. Syst. Oper. Res.*, vol. 25, no. 4, pp. 302–313, 1987.
- [182] B. Roy, "The outranking foundations approach and the methods," *Theory Decis.*, vol. 31, pp. 49–73, 1991.

ANNEX I. Consolidated output data from DERCAM

This annex presents the output data from DERCAM, once it was automatically extracted from the individual reports. All this, using the code in Annex II.

Data from SS=3.0

<i>Segregation parameters</i>													% CO ₂	% Heat
E	H	C	E4E	E4C	E4CS	H4H	H4C	H4CS	Grid	Boiler	Abs	%sav	reduction	scrap
100	0.1	10	62%	4%	0%	0%	30%	3%	62%	0%	29%	4%	9%	37%
100	0.1	100	29%	27%	0%	0%	44%	0%	66%	0%	8%	4%	10%	1%
100	0.1	500	9%	47%	0%	0%	44%	0%	82%	0%	3%	3%	6%	1%
100	1	10	61%	4%	1%	2%	29%	4%	63%	0%	29%	4%	9%	36%
100	1	100	29%	27%	0%	1%	43%	0%	66%	0%	8%	5%	10%	0%
100	1	500	9%	47%	0%	1%	43%	0%	82%	0%	2%	3%	6%	5%
100	10	0.1	87%	0%	0%	12%	0%	0%	60%	45%	69%	4%	9%	81%
100	10	1	78%	0%	0%	14%	6%	2%	60%	30%	82%	4%	10%	65%
100	10	10	60%	3%	1%	10%	22%	4%	37%	4%	42%	6%	16%	29%
100	10	100	28%	27%	0%	8%	36%	0%	64%	3%	7%	6%	11%	1%
100	10	500	9%	46%	0%	5%	39%	0%	82%	0%	2%	3%	6%	0%
100	100	0.1	81%	0%	0%	19%	0%	0%	34%	85%	90%	5%	12%	70%
100	100	1	75%	0%	0%	24%	1%	1%	35%	80%	90%	5%	12%	58%
100	100	10	58%	3%	1%	30%	7%	2%	22%	61%	45%	7%	17%	20%
100	100	100	29%	27%	1%	29%	15%	0%	46%	48%	8%	6%	15%	1%
100	100	500	9%	46%	0%	25%	19%	0%	77%	39%	2%	4%	8%	0%
100	400	0.1	77%	0%	0%	23%	0%	0%	19%	94%	84%	4%	9%	62%
100	400	1	72%	0%	0%	27%	0%	0%	21%	93%	84%	4%	9%	52%
100	400	10	57%	3%	1%	36%	2%	0%	24%	88%	40%	4%	10%	20%
100	400	100	29%	27%	0%	39%	5%	0%	48%	83%	8%	5%	10%	1%
100	400	500	9%	46%	0%	38%	7%	0%	77%	77%	2%	4%	7%	0%
1000	0.1	400	40%	16%	0%	0%	44%	0%	85%	0%	6%	3%	5%	0%
1000	1	400	40%	15%	0%	0%	44%	1%	70%	0%	12%	3%	7%	12%
1000	10	100	56%	5%	0%	3%	34%	2%	81%	0%	18%	3%	6%	66%
1000	10	400	40%	14%	0%	1%	43%	1%	71%	0%	12%	3%	7%	10%
1000	100	10	71%	0%	0%	20%	7%	3%	80%	46%	69%	3%	6%	78%
1000	100	100	55%	4%	1%	13%	24%	4%	62%	13%	31%	4%	9%	26%
1000	100	400	40%	13%	1%	9%	36%	2%	57%	4%	16%	5%	10%	10%
1000	400	0.1	82%	0%	0%	18%	0%	0%	42%	70%	91%	3%	9%	77%
1000	400	1	81%	0%	0%	18%	0%	0%	42%	69%	91%	3%	9%	76%
1000	400	10	75%	0%	0%	22%	2%	2%	42%	60%	90%	3%	9%	65%
1000	400	100	55%	3%	1%	23%	14%	4%	34%	34%	47%	5%	13%	28%
1000	400	400	39%	12%	1%	22%	25%	1%	42%	24%	19%	6%	13%	7%
500	0.1	100	54%	9%	0%	0%	35%	2%	65%	0%	18%	4%	9%	68%
500	0.1	500	28%	28%	0%	0%	44%	0%	80%	0%	5%	4%	6%	57%
500	1	100	53%	9%	0%	0%	35%	2%	65%	0%	18%	4%	9%	68%
500	1	500	28%	28%	0%	0%	44%	0%	80%	0%	5%	4%	6%	57%
500	10	10	76%	0%	0%	4%	15%	5%	60%	0%	74%	3%	9%	83%
500	10	100	52%	9%	0%	3%	34%	2%	65%	0%	18%	5%	9%	66%
500	10	500	28%	28%	0%	3%	41%	0%	80%	0%	5%	4%	7%	57%
500	100	0.1	85%	0%	0%	15%	0%	0%	59%	67%	87%	4%	9%	91%
500	100	1	83%	0%	0%	16%	1%	0%	59%	63%	88%	4%	9%	89%
500	100	10	68%	0%	0%	20%	7%	5%	60%	43%	78%	5%	10%	75%
500	100	100	49%	7%	1%	15%	25%	3%	41%	13%	29%	6%	14%	15%
500	100	500	27%	26%	0%	14%	33%	0%	66%	12%	7%	5%	10%	0%
500	400	0.1	80%	0%	0%	20%	0%	0%	34%	80%	90%	4%	11%	72%
500	400	1	79%	0%	0%	21%	0%	0%	34%	79%	90%	4%	11%	70%
500	400	10	68%	0%	0%	27%	2%	2%	33%	69%	90%	5%	12%	49%
500	400	100	48%	6%	1%	30%	14%	2%	28%	46%	32%	6%	16%	10%
500	400	500	27%	25%	0%	30%	19%	0%	57%	43%	8%	5%	12%	0%

Data from SS=3.9

Segregation parameters

														% CO ₂	%Heat
E	H	C	E4E	E4C	E4CS	H4H	H4C	H4CS	Grid	Boiler	Abs	%sav	reduction	scrap	
0.1	0.1	100	0%	53%	2%	0%	42%	2%	65%	0%	4%	4%	9%	0%	
0.1	0.1	1000	0%	52%	0%	0%	48%	0%	66%	0%	5%	6%	8%	0%	
0.1	0.1	500	0%	53%	0%	0%	47%	0%	73%	0%	4%	5%	7%	0%	
0.1	1	10	0%	33%	0%	35%	32%	0%	94%	39%	1%	1%	1%	0%	
0.1	1	100	0%	54%	2%	2%	40%	2%	66%	2%	4%	4%	9%	2%	
0.1	1	500	0%	53%	0%	0%	47%	0%	73%	0%	4%	5%	7%	0%	
0.1	10	10	0%	33%	0%	62%	5%	0%	94%	89%	1%	1%	1%	0%	
0.1	10	100	0%	54%	2%	14%	30%	1%	66%	20%	3%	4%	10%	0%	
0.1	10	500	0%	53%	0%	4%	43%	0%	73%	3%	3%	6%	8%	0%	
0.1	100	100	0%	54%	2%	37%	7%	0%	67%	78%	3%	4%	8%	0%	
0.1	100	500	0%	52%	1%	24%	23%	0%	71%	39%	3%	6%	8%	0%	
0.1	400	100	0%	53%	2%	43%	2%	0%	65%	94%	3%	3%	5%	0%	
0.1	400	500	0%	51%	1%	37%	11%	0%	63%	69%	4%	6%	8%	0%	
1	0.1	100	1%	53%	2%	0%	42%	2%	65%	0%	4%	4%	9%	1%	
1	0.1	500	0%	53%	0%	0%	47%	0%	73%	0%	4%	5%	7%	0%	
1	1	10	3%	30%	0%	35%	32%	0%	95%	39%	1%	1%	1%	0%	
1	1	100	1%	52%	3%	2%	40%	3%	62%	1%	4%	5%	10%	0%	
1	1	500	0%	53%	0%	0%	47%	0%	73%	0%	4%	6%	7%	0%	
1	10	100	1%	52%	3%	13%	30%	2%	63%	16%	4%	5%	11%	0%	
1	10	500	0%	53%	0%	4%	43%	0%	73%	3%	3%	6%	8%	0%	
1	100	100	1%	54%	2%	37%	7%	0%	67%	78%	3%	4%	8%	0%	
1	100	500	0%	52%	1%	24%	23%	0%	71%	39%	3%	6%	8%	0%	
1	400	100	0%	52%	1%	24%	23%	0%	71%	39%	3%	6%	8%	0%	
1	400	100	1%	53%	2%	43%	2%	0%	66%	94%	3%	3%	5%	0%	
1	400	500	0%	52%	0%	37%	11%	0%	63%	69%	4%	6%	8%	0%	
10	0.1	1	62%	3%	1%	1%	23%	10%	41%	0%	43%	3%	7%	49%	
10	0.1	10	27%	24%	1%	1%	46%	2%	65%	0%	9%	5%	7%	9%	
10	0.1	100	5%	50%	1%	0%	42%	1%	65%	0%	4%	5%	10%	2%	
10	0.1	500	1%	52%	0%	0%	47%	0%	73%	0%	4%	6%	7%	0%	
10	1	1	57%	3%	1%	10%	21%	9%	41%	2%	42%	6%	10%	36%	
10	1	10	26%	24%	1%	8%	40%	2%	65%	1%	8%	6%	8%	4%	
10	1	100	5%	49%	2%	1%	41%	1%	64%	0%	5%	6%	10%	0%	
10	1	500	1%	52%	0%	0%	47%	0%	73%	0%	4%	6%	7%	0%	
10	10	0.1	70%	0%	0%	28%	0%	1%	45%	79%	48%	4%	8%	59%	
10	10	1	53%	2%	1%	34%	6%	3%	42%	64%	40%	6%	10%	24%	
10	10	10	26%	23%	1%	31%	19%	1%	48%	41%	10%	6%	12%	0%	
10	10	100	5%	48%	3%	12%	31%	2%	61%	12%	4%	7%	11%	0%	
10	10	500	1%	52%	0%	4%	43%	0%	72%	2%	4%	6%	8%	0%	
10	100	1	52%	3%	1%	43%	1%	0%	42%	95%	36%	3%	4%	21%	
10	100	10	28%	22%	6%	41%	2%	0%	36%	91%	8%	4%	7%	3%	
10	100	100	5%	49%	2%	36%	8%	0%	58%	71%	4%	6%	11%	0%	
10	100	500	1%	51%	1%	23%	23%	0%	71%	37%	3%	6%	8%	0%	
10	400	10	28%	22%	6%	44%	0%	0%	35%	98%	7%	2%	3%	1%	
10	400	100	5%	49%	2%	42%	2%	0%	64%	93%	3%	4%	6%	0%	
10	400	500	1%	50%	1%	36%	11%	0%	63%	68%	4%	6%	9%	0%	
100	0.1	0.1	99%	0%	0%	0%	1%	0%	19%	0%	88%	17%	13%	99%	
100	0.1	1	93%	0%	0%	0%	6%	2%	21%	0%	88%	17%	13%	90%	
100	0.1	10	68%	3%	1%	0%	23%	6%	11%	0%	55%	20%	18%	49%	
100	0.1	100	30%	27%	0%	0%	42%	1%	41%	0%	13%	16%	15%	6%	
100	0.1	500	9%	44%	0%	0%	47%	0%	59%	0%	6%	9%	10%	0%	
100	1	0.1	98%	0%	0%	1%	1%	0%	19%	0%	87%	18%	13%	97%	
100	1	1	92%	0%	0%	1%	6%	1%	19%	0%	84%	18%	14%	89%	
100	1	10	67%	3%	1%	1%	23%	6%	10%	0%	55%	20%	18%	47%	
100	1	100	30%	27%	0%	1%	42%	1%	41%	0%	12%	16%	15%	5%	
100	1	500	9%	44%	0%	0%	47%	0%	59%	0%	6%	9%	10%	0%	
100	10	0.1	88%	0%	0%	11%	0%	0%	19%	3%	77%	20%	16%	83%	
100	10	1	83%	0%	0%	11%	5%	1%	21%	2%	88%	20%	17%	74%	
100	10	10	63%	3%	0%	8%	23%	4%	13%	0%	54%	22%	21%	35%	
100	10	100	29%	26%	1%	5%	38%	1%	41%	0%	12%	17%	17%	0%	
100	10	500	9%	44%	0%	2%	45%	0%	59%	0%	6%	9%	10%	0%	
100	100	0.1	77%	0%	0%	22%	0%	0%	11%	75%	84%	19%	17%	64%	

continue...

continue...

Segregation parameters

E	H	C	E4E	E4C	E4CS	H4H	H4C	H4CS	Grid	Boiler	Abs	%sav	% CO ₂ reduction	%Heat scrap
100	100	1	74%	0%	0%	25%	1%	1%	11%	72%	84%	19%	18%	56%
100	100	10	58%	2%	1%	29%	7%	2%	10%	57%	49%	21%	20%	20%
100	100	100	29%	26%	1%	28%	16%	1%	40%	44%	9%	17%	17%	0%
100	100	500	9%	43%	1%	18%	30%	0%	57%	19%	5%	10%	12%	0%
100	400	0.1	75%	0%	0%	25%	0%	0%	10%	93%	82%	12%	10%	59%
100	400	1	72%	0%	0%	28%	0%	0%	9%	92%	84%	12%	10%	51%
100	400	10	57%	3%	1%	37%	2%	1%	10%	86%	47%	13%	11%	18%
100	400	100	28%	26%	1%	39%	5%	0%	40%	80%	9%	12%	12%	0%
100	400	500	9%	43%	0%	35%	13%	0%	58%	60%	5%	10%	10%	0%
1000	0.1	0.1	100%	0%	0%	0%	0%	0%	16%	0%	87%	14%	5%	100%
1000	0.1	1	99%	0%	0%	0%	1%	0%	16%	0%	87%	14%	5%	99%
1000	0.1	10	93%	0%	0%	0%	5%	1%	16%	0%	89%	14%	5%	93%
1000	0.1	100	64%	2%	1%	0%	27%	6%	19%	0%	58%	17%	10%	51%
1000	0.1	400	45%	13%	1%	0%	39%	2%	19%	0%	28%	17%	12%	28%
1000	1	0.1	100%	0%	0%	0%	0%	0%	16%	0%	87%	14%	5%	100%
1000	1	1	99%	0%	0%	0%	1%	0%	16%	0%	87%	14%	5%	99%
1000	1	10	93%	0%	0%	0%	6%	1%	16%	0%	89%	14%	6%	92%
1000	1	100	64%	2%	1%	0%	27%	6%	19%	0%	58%	17%	10%	51%
1000	1	400	45%	13%	1%	0%	39%	2%	19%	0%	28%	17%	12%	28%
1000	10	0.1	99%	0%	0%	1%	0%	0%	16%	0%	87%	14%	5%	99%
1000	10	1	98%	0%	0%	1%	1%	0%	16%	0%	87%	14%	5%	98%
1000	10	10	92%	0%	0%	1%	6%	1%	17%	0%	89%	15%	6%	91%
1000	10	100	64%	2%	1%	1%	26%	6%	19%	0%	58%	17%	10%	50%
1000	10	400	45%	13%	1%	1%	39%	2%	19%	0%	28%	17%	12%	28%
1000	100	0.1	89%	0%	0%	11%	0%	0%	16%	0%	89%	17%	9%	87%
1000	100	1	88%	0%	0%	11%	1%	0%	16%	0%	89%	17%	9%	87%
1000	100	10	83%	0%	0%	10%	5%	1%	17%	0%	89%	17%	10%	80%
1000	100	100	60%	2%	1%	8%	24%	6%	19%	0%	58%	19%	13%	39%
1000	100	400	43%	12%	1%	5%	37%	2%	19%	0%	28%	19%	14%	20%
1000	400	0.1	78%	0%	0%	22%	0%	0%	7%	36%	85%	19%	14%	71%
1000	400	1	77%	0%	0%	22%	0%	0%	7%	36%	85%	19%	14%	71%
1000	400	10	74%	0%	0%	23%	3%	1%	7%	32%	87%	19%	15%	65%
1000	400	100	56%	2%	0%	21%	17%	4%	8%	18%	61%	21%	18%	27%
1000	400	400	40%	11%	1%	17%	29%	2%	15%	11%	28%	21%	19%	6%
500	0.1	0.1	100%	0%	0%	0%	0%	0%	17%	0%	85%	15%	7%	100%
500	0.1	1	99%	0%	0%	0%	1%	0%	17%	0%	86%	15%	7%	98%
500	0.1	10	87%	0%	0%	0%	10%	3%	17%	0%	87%	16%	8%	84%
500	0.1	100	55%	6%	1%	0%	34%	4%	17%	0%	42%	18%	13%	35%
500	0.1	500	28%	25%	0%	0%	46%	1%	36%	0%	16%	15%	12%	9%
500	1	0.1	100%	0%	0%	0%	0%	0%	17%	0%	86%	15%	7%	100%
500	1	1	98%	0%	0%	0%	1%	0%	17%	0%	86%	15%	7%	98%
500	1	10	87%	0%	0%	0%	10%	3%	17%	0%	87%	16%	8%	84%
500	1	100	56%	6%	1%	0%	34%	3%	17%	0%	41%	18%	13%	37%
500	1	500	28%	24%	0%	0%	46%	1%	36%	0%	16%	15%	12%	9%
500	10	0.1	97%	0%	0%	3%	0%	0%	19%	0%	87%	15%	8%	97%
500	10	1	96%	0%	0%	2%	1%	0%	17%	0%	86%	16%	8%	96%
500	10	10	85%	0%	0%	2%	10%	3%	17%	0%	87%	16%	9%	81%
500	10	100	55%	6%	1%	1%	33%	4%	13%	0%	42%	19%	14%	36%
500	10	500	28%	24%	0%	1%	46%	0%	36%	0%	16%	15%	13%	8%
500	100	0.1	83%	0%	0%	17%	0%	0%	17%	20%	90%	19%	13%	79%
500	100	1	82%	0%	0%	17%	1%	0%	17%	19%	88%	19%	13%	77%
500	100	10	74%	0%	0%	16%	6%	3%	7%	6%	85%	19%	15%	65%
500	100	100	50%	6%	1%	12%	28%	4%	13%	3%	41%	22%	18%	20%
500	100	500	27%	24%	0%	9%	40%	0%	36%	0%	14%	17%	15%	0%
500	400	0.1	75%	0%	0%	25%	0%	0%	7%	63%	87%	19%	15%	65%
500	400	1	74%	0%	0%	26%	0%	0%	10%	62%	88%	19%	16%	62%
500	400	10	67%	0%	0%	28%	3%	1%	11%	55%	85%	19%	16%	49%
500	400	100	48%	5%	1%	28%	16%	2%	6%	35%	41%	21%	20%	11%
500	400	500	27%	24%	1%	25%	24%	1%	34%	26%	12%	17%	16%	0%

Data from SS=5.4

Segregation parameters

														% CO ₂	%Heat
E	H	C	E4E	E4C	E4CS	H4H	H4C	H4CS	Grid	Boiler	Abs	%sav	reduction	scrap	
0.1	0.1	100	0%	53%	3%	0%	42%	2%	83%	0%	2%	4%	5%	2%	
0.1	0.1	500	0%	51%	0%	0%	49%	0%	72%	0%	4%	5%	6%	1%	
0.1	1	10	0%	33%	0%	35%	32%	0%	94%	39%	1%	1%	1%	0%	
0.1	1	100	0%	54%	3%	3%	38%	2%	82%	3%	2%	4%	5%	3%	
0.1	1	500	0%	51%	0%	0%	49%	0%	72%	0%	4%	5%	7%	1%	
0.1	10	10	0%	33%	0%	62%	5%	0%	94%	89%	1%	1%	1%	0%	
0.1	10	100	0%	53%	3%	22%	21%	1%	82%	32%	2%	4%	6%	2%	
0.1	10	500	0%	50%	0%	4%	46%	0%	72%	5%	4%	5%	7%	0%	
0.1	100	100	0%	54%	2%	41%	3%	0%	84%	88%	1%	3%	5%	0%	
0.1	100	500	0%	51%	0%	29%	20%	0%	81%	48%	2%	5%	6%	0%	
0.1	400	100	0%	53%	2%	44%	1%	0%	84%	97%	1%	2%	3%	0%	
0.1	400	500	0%	50%	0%	40%	10%	0%	72%	74%	3%	4%	6%	0%	
1	0.1	100	1%	52%	3%	0%	42%	2%	83%	0%	2%	4%	5%	0%	
1	0.1	500	0%	51%	0%	0%	49%	0%	72%	0%	4%	5%	6%	1%	
1	1	10	3%	30%	0%	35%	32%	0%	95%	40%	1%	1%	1%	0%	
1	1	100	1%	52%	3%	3%	39%	2%	82%	3%	2%	4%	5%	1%	
1	1	500	0%	50%	0%	0%	49%	0%	72%	0%	4%	5%	7%	1%	
1	10	10	3%	30%	0%	57%	9%	0%	90%	81%	3%	1%	2%	0%	
1	10	100	1%	53%	3%	22%	21%	1%	82%	30%	2%	4%	6%	0%	
1	10	500	0%	50%	0%	4%	46%	0%	71%	4%	4%	5%	7%	1%	
1	100	100	1%	53%	2%	41%	3%	0%	84%	88%	1%	3%	5%	0%	
1	100	500	0%	50%	1%	29%	19%	0%	81%	46%	2%	4%	6%	0%	
1	400	100	1%	54%	1%	44%	1%	0%	85%	97%	1%	2%	3%	0%	
1	400	500	0%	50%	0%	40%	10%	0%	72%	74%	3%	4%	6%	0%	
10	0.1	1	62%	3%	1%	1%	23%	10%	41%	0%	42%	3%	7%	50%	
10	0.1	10	28%	26%	1%	1%	43%	1%	63%	0%	9%	6%	6%	20%	
10	0.1	100	5%	48%	3%	0%	41%	2%	78%	0%	3%	7%	6%	4%	
10	0.1	500	1%	50%	0%	0%	49%	0%	72%	0%	4%	5%	6%	1%	
10	1	1	57%	3%	1%	10%	20%	9%	41%	2%	41%	5%	10%	38%	
10	1	10	25%	23%	1%	8%	41%	2%	67%	1%	8%	6%	8%	1%	
10	1	100	5%	48%	3%	2%	39%	2%	78%	0%	3%	7%	6%	2%	
10	1	500	1%	50%	0%	0%	49%	0%	72%	0%	4%	5%	7%	1%	
10	10	0.1	72%	0%	1%	26%	0%	1%	42%	80%	28%	3%	8%	63%	
10	10	1	54%	3%	1%	34%	6%	3%	41%	65%	38%	6%	10%	28%	
10	10	10	28%	27%	1%	33%	12%	0%	64%	60%	6%	6%	7%	20%	
10	10	100	5%	48%	3%	14%	28%	2%	69%	15%	3%	7%	10%	0%	
10	10	500	1%	50%	0%	4%	46%	0%	72%	4%	4%	5%	7%	1%	
10	100	10	28%	23%	5%	42%	2%	0%	45%	92%	7%	3%	6%	1%	
10	100	100	5%	49%	2%	39%	5%	0%	72%	79%	2%	5%	8%	0%	
10	100	500	1%	49%	1%	27%	21%	0%	77%	41%	2%	5%	6%	0%	
10	400	10	28%	23%	6%	42%	0%	0%	37%	98%	6%	1%	3%	6%	
10	400	100	5%	49%	2%	43%	1%	0%	72%	94%	2%	4%	5%	0%	
10	400	500	1%	49%	1%	41%	7%	0%	77%	78%	2%	5%	6%	0%	
100	0.1	0.1	99%	0%	0%	0%	1%	0%	19%	0%	62%	22%	13%	99%	
100	0.1	1	95%	0%	0%	0%	5%	0%	19%	0%	62%	23%	13%	93%	
100	0.1	10	68%	3%	1%	0%	23%	5%	21%	0%	47%	24%	16%	51%	
100	0.1	100	30%	27%	0%	0%	42%	0%	42%	0%	12%	18%	15%	6%	
100	0.1	500	9%	43%	0%	0%	47%	0%	61%	0%	6%	10%	9%	2%	
100	1	0.1	98%	0%	0%	1%	0%	0%	19%	0%	62%	23%	13%	98%	
100	1	1	94%	0%	0%	1%	5%	0%	19%	0%	62%	23%	14%	92%	
100	1	10	68%	3%	1%	1%	22%	5%	21%	0%	45%	24%	16%	51%	
100	1	100	30%	27%	0%	1%	42%	0%	42%	0%	12%	18%	15%	6%	
100	1	500	9%	43%	0%	0%	47%	0%	62%	0%	6%	10%	9%	2%	
100	10	0.1	88%	0%	0%	11%	0%	1%	20%	3%	74%	24%	16%	83%	
100	10	1	84%	0%	0%	11%	4%	0%	21%	2%	65%	24%	17%	77%	
100	10	10	64%	3%	1%	8%	21%	4%	13%	0%	48%	24%	21%	40%	
100	10	100	29%	26%	0%	5%	39%	1%	41%	0%	12%	19%	17%	0%	
100	10	500	9%	43%	0%	2%	46%	0%	62%	0%	6%	10%	9%	0%	
100	100	0.1	78%	0%	0%	22%	0%	0%	10%	75%	48%	22%	18%	64%	

continue...

continue...

Segregation parameters

E	H	C	E4E	E4C	E4CS	H4H	H4C	H4CS	Grid	Boiler	Abs	%sav	% CO ₂ reduction	%Heat scrap
100	100	1	75%	0%	0%	24%	1%	0%	11%	73%	52%	22%	18%	60%
100	100	10	59%	3%	1%	29%	6%	2%	21%	63%	41%	23%	17%	26%
100	100	100	27%	24%	1%	27%	21%	1%	30%	34%	12%	19%	17%	1%
100	100	500	9%	42%	0%	20%	29%	0%	65%	22%	5%	10%	10%	0%
100	400	0.1	77%	0%	0%	23%	0%	0%	21%	94%	60%	14%	9%	62%
100	400	1	74%	0%	0%	25%	0%	0%	8%	92%	34%	15%	10%	57%
100	400	10	59%	3%	1%	34%	2%	1%	10%	87%	37%	16%	11%	28%
100	400	100	27%	24%	1%	40%	7%	0%	29%	75%	12%	15%	12%	1%
100	400	500	9%	42%	0%	37%	12%	0%	65%	63%	4%	9%	9%	0%
1000	0.1	0.1	100%	0%	0%	0%	0%	0%	16%	0%	63%	22%	5%	100%
1000	0.1	1	99%	0%	0%	0%	0%	0%	16%	0%	63%	22%	5%	99%
1000	0.1	10	95%	0%	0%	0%	5%	0%	16%	0%	66%	22%	5%	95%
1000	0.1	100	67%	3%	0%	0%	26%	4%	19%	0%	53%	23%	9%	57%
1000	0.1	400	45%	13%	1%	0%	39%	3%	19%	0%	28%	23%	12%	28%
1000	1	0.1	100%	0%	0%	0%	0%	0%	16%	0%	59%	22%	5%	100%
1000	1	1	99%	0%	0%	0%	0%	0%	16%	0%	63%	22%	5%	99%
1000	1	10	95%	0%	0%	0%	5%	0%	16%	0%	66%	22%	5%	95%
1000	1	100	67%	3%	0%	0%	26%	4%	19%	0%	53%	23%	9%	57%
1000	1	400	45%	13%	1%	0%	39%	2%	19%	0%	28%	23%	12%	29%
1000	10	0.1	99%	0%	0%	1%	0%	0%	16%	0%	63%	22%	5%	99%
1000	10	1	98%	0%	0%	1%	0%	0%	16%	0%	63%	22%	5%	98%
1000	10	10	94%	0%	0%	1%	5%	0%	16%	0%	66%	22%	6%	93%
1000	10	100	66%	3%	0%	1%	26%	4%	19%	0%	52%	23%	9%	56%
1000	10	400	45%	13%	1%	1%	39%	2%	19%	0%	28%	23%	12%	28%
1000	100	0.1	89%	0%	0%	11%	0%	0%	16%	0%	64%	24%	9%	87%
1000	100	1	89%	0%	0%	11%	0%	0%	16%	0%	63%	24%	9%	87%
1000	100	10	85%	0%	0%	11%	4%	0%	16%	0%	66%	24%	9%	82%
1000	100	100	61%	3%	0%	8%	24%	4%	19%	0%	55%	25%	13%	43%
1000	100	400	43%	12%	1%	5%	37%	2%	19%	0%	28%	24%	14%	20%
1000	400	0.1	78%	0%	0%	22%	0%	0%	11%	41%	66%	25%	13%	72%
1000	400	1	78%	0%	0%	22%	0%	0%	11%	40%	65%	25%	13%	72%
1000	400	10	75%	0%	0%	22%	2%	0%	11%	37%	64%	25%	14%	67%
1000	400	100	57%	3%	0%	22%	16%	3%	15%	22%	51%	25%	16%	32%
1000	400	400	39%	11%	1%	18%	29%	2%	16%	11%	28%	25%	18%	6%
500	0.1	0.1	100%	0%	0%	0%	0%	0%	16%	0%	64%	22%	7%	100%
500	0.1	1	99%	0%	0%	0%	1%	0%	17%	0%	64%	22%	7%	99%
500	0.1	10	90%	1%	0%	0%	10%	0%	17%	0%	66%	23%	8%	89%
500	0.1	100	56%	6%	1%	0%	34%	4%	17%	0%	41%	23%	13%	37%
500	0.1	500	28%	25%	0%	0%	46%	0%	36%	0%	16%	18%	12%	9%
500	1	0.1	100%	0%	0%	0%	0%	0%	20%	0%	65%	21%	7%	100%
500	1	1	99%	0%	0%	0%	1%	0%	16%	0%	68%	23%	7%	98%
500	1	10	89%	1%	0%	0%	10%	0%	21%	0%	66%	21%	9%	88%
500	1	100	56%	6%	1%	0%	34%	3%	17%	0%	41%	23%	13%	37%
500	1	500	28%	25%	0%	0%	46%	0%	36%	0%	16%	18%	12%	9%
500	10	0.1	97%	0%	0%	2%	0%	0%	16%	0%	62%	23%	7%	97%
500	10	1	97%	0%	0%	2%	1%	0%	17%	0%	63%	23%	8%	96%
500	10	10	88%	1%	0%	2%	9%	0%	17%	0%	66%	23%	9%	86%
500	10	100	55%	6%	1%	1%	33%	3%	17%	0%	41%	23%	14%	35%
500	10	500	28%	25%	0%	1%	46%	0%	42%	0%	14%	18%	12%	8%
500	100	0.1	83%	0%	0%	17%	0%	0%	16%	20%	63%	25%	13%	79%
500	100	1	83%	0%	0%	17%	1%	0%	17%	20%	71%	25%	13%	78%
500	100	10	76%	0%	0%	16%	7%	1%	17%	14%	67%	25%	14%	68%
500	100	100	50%	6%	1%	12%	29%	3%	17%	3%	40%	25%	18%	18%
500	100	500	27%	24%	0%	9%	40%	0%	36%	1%	14%	19%	15%	0%
500	400	0.1	74%	0%	0%	26%	0%	0%	11%	63%	60%	23%	15%	63%
500	400	1	74%	0%	0%	26%	0%	0%	11%	63%	57%	23%	15%	62%
500	400	10	70%	0%	0%	27%	2%	1%	7%	57%	63%	24%	16%	56%
500	400	100	48%	6%	1%	29%	15%	2%	17%	40%	36%	24%	18%	10%
500	400	500	27%	24%	0%	25%	24%	0%	35%	27%	12%	19%	16%	0%

Data from SS=6.6

Segregation parameters

E	H	C	E4E	E4C	E4CS	H4H	H4C	H4CS	Grid	Boiler	Abs	%sav	% CO ₂ reduction	%Heat scrap
0.1	1	10	1%	41%	15%	6%	27%	10%	15%	12%	9%	10%	17%	7%
0.1	10	100	0%	47%	4%	8%	38%	3%	42%	11%	8%	16%	11%	0%
0.1	10	500	0%	50%	1%	2%	47%	1%	44%	1%	8%	17%	12%	0%
0.1	100	10	1%	42%	15%	41%	1%	0%	15%	94%	6%	5%	5%	7%
0.1	100	100	0%	46%	5%	34%	13%	1%	41%	63%	7%	14%	10%	0%
0.1	100	500	0%	48%	2%	15%	33%	1%	45%	21%	7%	16%	11%	0%
0.1	0.1	10	1%	41%	16%	1%	30%	12%	15%	1%	9%	9%	17%	10%
0.1	0.1	100	0%	46%	5%	0%	45%	4%	41%	0%	8%	16%	11%	1%
0.1	0.1	500	0%	50%	0%	0%	49%	0%	46%	0%	8%	16%	11%	0%
0.1	1	1	3%	26%	4%	46%	18%	3%	69%	55%	7%	2%	2%	0%
0.1	1	100	0%	47%	4%	1%	44%	4%	42%	1%	8%	15%	11%	0%
0.1	1	500	0%	50%	0%	0%	49%	0%	46%	0%	8%	16%	11%	0%
0.1	10	11	1%	41%	14%	28%	12%	4%	19%	57%	8%	11%	15%	1%
0.1	400	100	0%	41%	7%	47%	4%	1%	44%	87%	6%	9%	5%	0%
0.1	400	500	0%	48%	2%	33%	16%	1%	44%	57%	6%	15%	10%	0%
1	0.1	10	5%	38%	14%	1%	30%	12%	20%	1%	9%	10%	16%	8%
1	0.1	100	1%	46%	4%	0%	45%	4%	42%	0%	8%	16%	11%	0%
1	0.1	500	0%	50%	0%	0%	49%	0%	45%	0%	8%	17%	11%	0%
1	1	1	19%	14%	2%	30%	31%	4%	51%	25%	18%	9%	3%	6%
1	1	10	5%	38%	13%	6%	28%	10%	16%	8%	10%	11%	16%	9%
1	1	100	1%	46%	5%	1%	44%	4%	41%	0%	8%	17%	11%	1%
1	1	500	0%	50%	0%	0%	49%	0%	46%	0%	8%	17%	11%	0%
1	10	0.1	41%	1%	1%	55%	1%	1%	47%	93%	58%	4%	1%	33%
1	10	1	18%	14%	2%	59%	6%	1%	52%	85%	16%	6%	2%	6%
1	10	10	5%	38%	13%	28%	12%	4%	16%	56%	8%	10%	14%	11%
1	10	100	1%	46%	4%	8%	37%	3%	42%	11%	8%	16%	11%	1%
1	10	500	0%	50%	1%	2%	47%	1%	45%	1%	7%	16%	11%	0%
1	100	10	5%	39%	13%	42%	1%	0%	21%	94%	7%	5%	5%	3%
1	100	100	1%	46%	5%	34%	14%	1%	42%	63%	7%	14%	10%	0%
1	100	500	0%	48%	2%	15%	33%	1%	45%	21%	7%	16%	11%	0%
1	400	10	5%	37%	14%	44%	0%	0%	20%	98%	6%	2%	2%	0%
1	400	100	0%	39%	9%	46%	4%	1%	40%	86%	6%	10%	5%	2%
1	400	500	0%	48%	2%	33%	16%	1%	44%	57%	6%	15%	10%	0%
10	0.1	0.1	92%	0%	0%	1%	2%	4%	12%	0%	60%	19%	2%	93%
10	0.1	1	64%	2%	1%	1%	21%	11%	13%	0%	58%	21%	7%	55%
10	0.1	10	33%	26%	6%	0%	29%	7%	13%	0%	13%	23%	14%	36%
10	0.1	100	5%	43%	5%	0%	42%	5%	39%	0%	9%	18%	11%	5%
10	0.1	500	1%	49%	0%	0%	49%	0%	46%	0%	8%	17%	11%	1%
10	1	0.1	84%	0%	0%	10%	2%	3%	12%	0%	60%	20%	6%	83%
10	1	1	60%	2%	1%	7%	22%	7%	13%	0%	59%	23%	10%	46%
10	1	10	30%	23%	5%	4%	30%	7%	13%	0%	15%	24%	16%	21%
10	1	100	5%	42%	4%	1%	44%	4%	41%	0%	9%	18%	12%	0%
10	1	500	1%	49%	0%	0%	49%	0%	46%	0%	8%	17%	11%	1%
10	10	0.1	70%	0%	0%	28%	0%	1%	12%	66%	59%	20%	11%	61%
10	10	1	53%	2%	1%	32%	8%	4%	13%	51%	55%	23%	13%	28%
10	10	10	28%	21%	7%	22%	16%	5%	11%	33%	14%	24%	18%	10%
10	10	100	5%	42%	4%	8%	37%	4%	40%	8%	8%	18%	12%	0%
10	10	500	1%	49%	1%	2%	47%	1%	46%	0%	8%	17%	11%	0%
10	100	0.1	67%	0%	0%	33%	0%	0%	12%	96%	51%	9%	4%	55%
10	100	1	52%	2%	1%	44%	1%	0%	14%	93%	50%	10%	5%	24%
10	100	10	29%	23%	6%	40%	3%	1%	12%	88%	12%	14%	8%	13%
10	100	100	5%	42%	4%	34%	14%	1%	40%	59%	7%	17%	11%	0%
10	100	500	1%	48%	1%	15%	34%	1%	45%	22%	7%	17%	11%	0%
10	400	0.1	65%	0%	1%	34%	0%	0%	21%	99%	10%	2%	2%	42%
10	400	1	50%	2%	2%	46%	0%	0%	19%	98%	38%	4%	2%	15%
10	400	10	27%	20%	8%	43%	0%	0%	31%	97%	8%	5%	3%	2%
10	400	100	5%	42%	4%	44%	4%	0%	37%	86%	7%	12%	7%	1%
10	400	500	1%	47%	2%	33%	16%	1%	46%	58%	6%	15%	10%	0%
100	0.1	0.1	99%	0%	0%	0%	0%	0%	9%	0%	18%	39%	14%	99%
100	0.1	1	94%	0%	0%	0%	3%	2%	9%	0%	62%	40%	15%	93%
100	0.1	10	68%	3%	1%	0%	22%	6%	10%	0%	52%	41%	18%	51%
100	0.1	100	30%	24%	2%	0%	42%	3%	22%	0%	18%	33%	17%	7%
100	0.1	500	9%	42%	0%	0%	48%	1%	39%	0%	10%	22%	13%	0%
100	1	0.1	98%	0%	0%	1%	0%	0%	10%	0%	74%	40%	14%	98%
100	1	1	94%	0%	0%	1%	2%	2%	9%	0%	50%	40%	15%	93%
100	1	10	69%	3%	1%	1%	22%	4%	10%	0%	51%	41%	18%	53%
100	1	100	29%	24%	2%	0%	42%	3%	22%	0%	18%	33%	17%	6%

continue...

continue...

Segregation parameters

E	H	C	E4E	E4C	E4CS	H4H	H4C	H4CS	Grid	Boiler	Abs	%sav	% CO ₂ reduction	%Heat scrap
100	1	500	9%	42%	0%	0%	48%	1%	39%	0%	10%	22%	13%	0%
100	10	0.1	89%	0%	1%	10%	0%	0%	8%	0%	1%	40%	17%	86%
100	10	1	86%	0%	0%	10%	3%	1%	6%	0%	67%	41%	18%	80%
100	10	10	65%	3%	1%	7%	21%	4%	6%	0%	52%	42%	22%	41%
100	10	100	29%	23%	2%	4%	40%	3%	22%	0%	17%	33%	19%	1%
100	10	500	9%	42%	0%	2%	47%	0%	39%	0%	10%	23%	13%	0%
100	100	0.1	77%	0%	0%	23%	0%	0%	6%	73%	56%	37%	19%	62%
100	100	1	74%	0%	0%	24%	1%	0%	9%	72%	69%	37%	18%	58%
100	100	10	59%	3%	1%	29%	7%	2%	5%	56%	43%	39%	21%	26%
100	100	100	27%	23%	1%	26%	21%	1%	23%	32%	13%	33%	18%	1%
100	100	500	9%	41%	1%	13%	35%	1%	39%	13%	8%	22%	14%	0%
100	400	0.1	76%	0%	0%	24%	0%	0%	4%	93%	51%	26%	11%	60%
100	400	1	72%	0%	0%	28%	0%	0%	5%	91%	62%	25%	11%	52%
100	400	10	58%	3%	1%	36%	2%	0%	7%	86%	45%	27%	12%	20%
100	400	100	28%	24%	2%	39%	7%	0%	24%	74%	12%	26%	13%	3%
100	400	500	9%	41%	1%	30%	18%	1%	38%	48%	8%	21%	13%	0%
1000	0.1	0.1	100%	0%	0%	0%	0%	0%	4%	0%	58%	39%	5%	100%
1000	0.1	1	100%	0%	0%	0%	0%	0%	4%	0%	58%	39%	5%	100%
1000	0.1	10	95%	0%	0%	0%	4%	1%	4%	0%	70%	39%	5%	95%
1000	0.1	100	67%	2%	1%	0%	25%	6%	5%	0%	63%	41%	10%	56%
1000	0.1	400	45%	12%	1%	0%	39%	2%	12%	0%	30%	39%	12%	29%
1000	1	0.1	100%	0%	0%	0%	0%	0%	4%	0%	58%	39%	5%	100%
1000	1	1	99%	0%	0%	0%	0%	0%	4%	0%	58%	39%	5%	99%
1000	1	10	95%	0%	0%	0%	4%	1%	4%	0%	70%	39%	5%	95%
1000	1	100	67%	2%	1%	0%	25%	6%	5%	0%	63%	41%	10%	56%
1000	1	400	45%	12%	1%	0%	40%	2%	12%	0%	31%	39%	13%	28%
1000	10	0.1	99%	0%	0%	1%	0%	0%	4%	0%	58%	39%	5%	99%
1000	10	1	98%	0%	0%	1%	0%	0%	4%	0%	58%	39%	5%	99%
1000	10	10	94%	0%	0%	1%	4%	0%	4%	0%	67%	39%	6%	94%
1000	10	100	66%	2%	1%	1%	24%	6%	5%	0%	63%	41%	10%	55%
1000	10	400	45%	12%	1%	1%	39%	2%	12%	0%	30%	39%	13%	28%
1000	100	0.1	90%	0%	0%	10%	0%	0%	4%	0%	58%	40%	9%	89%
1000	100	1	90%	0%	0%	10%	0%	0%	4%	0%	58%	40%	9%	89%
1000	100	10	86%	0%	0%	9%	4%	0%	4%	0%	68%	40%	10%	84%
1000	100	100	62%	2%	1%	7%	23%	6%	5%	0%	63%	42%	14%	45%
1000	100	400	43%	12%	1%	5%	37%	2%	12%	0%	30%	40%	15%	21%
1000	400	0.1	77%	0%	0%	23%	0%	0%	4%	33%	58%	41%	15%	71%
1000	400	1	77%	0%	0%	23%	0%	0%	4%	32%	58%	41%	15%	70%
1000	400	10	74%	0%	0%	23%	2%	0%	4%	29%	68%	41%	15%	66%
1000	400	100	57%	2%	1%	21%	16%	4%	2%	15%	58%	42%	18%	32%
1000	400	400	39%	11%	1%	17%	30%	2%	12%	10%	29%	41%	19%	5%
500	0.1	0.1	100%	0%	0%	0%	0%	0%	7%	0%	76%	39%	7%	100%
500	0.1	1	99%	0%	0%	0%	1%	0%	7%	0%	76%	39%	7%	99%
500	0.1	10	89%	0%	0%	0%	8%	3%	7%	0%	76%	40%	8%	88%
500	0.1	100	57%	6%	1%	0%	33%	4%	5%	0%	45%	41%	13%	40%
500	0.1	500	29%	23%	0%	0%	47%	1%	22%	0%	19%	33%	14%	8%
500	1	0.1	100%	0%	0%	0%	0%	0%	3%	0%	58%	39%	7%	100%
500	1	1	99%	0%	0%	0%	1%	0%	9%	0%	76%	38%	7%	99%
500	1	10	89%	0%	0%	0%	8%	2%	7%	0%	74%	39%	9%	88%
500	1	100	57%	6%	1%	0%	33%	3%	5%	0%	45%	41%	13%	41%
500	1	500	29%	23%	0%	0%	47%	1%	22%	0%	20%	33%	14%	8%
500	10	0.1	98%	0%	0%	2%	0%	0%	4%	0%	78%	39%	7%	98%
500	10	1	97%	0%	0%	2%	1%	1%	3%	0%	82%	39%	8%	96%
500	10	10	88%	0%	0%	2%	8%	2%	6%	0%	74%	40%	10%	86%
500	10	100	56%	6%	1%	1%	33%	3%	5%	0%	45%	41%	14%	39%
500	10	500	28%	23%	0%	1%	46%	1%	22%	0%	19%	33%	14%	7%
500	100	0.1	83%	0%	0%	17%	0%	0%	7%	9%	76%	41%	14%	79%
500	100	1	82%	0%	0%	17%	1%	0%	7%	9%	76%	41%	14%	77%
500	100	10	76%	0%	0%	16%	6%	2%	3%	4%	72%	41%	15%	68%
500	100	100	51%	6%	1%	11%	29%	3%	5%	1%	43%	43%	19%	23%
500	100	500	27%	23%	0%	7%	42%	1%	22%	0%	18%	34%	17%	0%
500	400	0.1	74%	0%	0%	26%	0%	0%	4%	60%	59%	39%	16%	63%
500	400	1	73%	0%	0%	26%	0%	0%	4%	59%	72%	39%	16%	62%
500	400	10	69%	1%	0%	28%	2%	0%	3%	53%	55%	39%	17%	55%
500	400	100	48%	5%	1%	28%	16%	2%	6%	34%	41%	41%	20%	10%
500	400	500	27%	23%	1%	22%	27%	1%	21%	22%	16%	34%	18%	0%

ANNEX II. Equation used in MATLAB to extract information from DER-CAM reports

This annex presents the code used in Matlab to automatically extract the data from the reports of DER-CAM. The information obtained from here was used in section 4.3.

From DER CAM report, it is obtained the following information:

Name of the variable at the code	Units	Description
Fuel_Consump_CHP	kWh	Total annual Natural Gas consumption of CHP system
Fuel_Consump_Boiler	kWh	Total annual Natural Gas consumption of boiler
COP_Abs	-	COP of the Absorption chiller
COP_Elect	-	COP of the Electric chiller
Price_ElectGrid	EUR / kWh	Electricity price at the grid
Price_Fuel	EUR / kWh	Natural Gas price
Elect_Load	kWh	Total annual Electricity load
Heat_Load	kWh	Total annual Heat load
Cool_Load	kWh	Total annual Cooling load
Elect_CHP	kWh	Total annual Electricity produced by all the CHP system
Elect_Grid	kWh	Total annual Electricity imported from the Grid
Heat_CHP	kWh	Total annual Heat produced by the CHP
Heat_Boiler	kWh	Total annual Heat produced by the boiler
Cool_Absorption	kWh	Total annual Cooling produced by Absorption chiller
Cool_Electric	kWh	Total annual Cooling produced by Electric chiller

Table 25 Raw data obtained from DER-CAM report (part 1)

Name of the variable at the code	Units	Description
Cool_Storage_Out	kWh	Total annual Cooling output of the Cooling Storage
Cool_Storage_In	kWh	Total annual Cooling input of the Cooling Storage
Offset	kWh	Total annual Electricity consumption that is avoided through the usage of Absorption chiller (compared with the reference scenario)
CHP_InstCap	kW or MW	Installed capacity of CHP units for each technology type (ICE, CT, MT, FC) at the selected optimal scenario
CHP_Nunits	units	Number of CHP units for each technology type and installed capacity (ICE, CT, MT, FC) at the selected optimal scenario
CHP_TS or Discrete Technologies (i)	kWh	Total annual Electricity production by the CHP units technology i, where $i = 1, 2, \dots, n$
%savings	-	Percentage of economic savings of the system, compared with the reference scenario
%CO ₂ ^{reduc}	-	Percentage of CO ₂ reduction of the system, compared with the reference scenario

Table 26 Raw data obtained from DER-CAM report (part 2)

Now, with this information, the following indexes are calculated.

- ❖ Amount of Electricity / Heat scrapped (reported per year, but calculated in hourly basis)

Name of the variable at the code	Nomenclature at the paper	Units	Description
propElectScrapped	$E_{\text{scrap}}^{\text{CHP}}$	-	Portion of Electricity produced by the CHP that is being scrapped
propHeatScrapped	$H_{\text{scrap}}^{\text{CHP}}$	-	Portion of Heat produced by the CHP that is being scrapped

Table 27 Electricity and Heat produced by the CHP and scrapped

$$\text{propElectScrapped} = \text{Elect_CHP_scrap} / [\text{Elect_CHP} + \text{Elect_CHP_scrap}]$$

$$\text{propHeatScrapped} = \text{Heat_CHP_scrap} / [\text{Heat_CHP} + \text{Heat_CHP_scrap}]$$

where Elect_CHP_scrap and Heat_CHP_scrap are calculated as follows,

It is known that the average Heat-to-Power ratio at the CHP units is $\text{HtP}=1.4$, therefore, for each unit of electricity produced, 1.4 units of heat are produced.

Then, the following analysis is conducted for each hour of the year,

<p>If $(\text{HtP} * \text{Elect_CHP}) < (\text{Heat_CHP})$</p> <p>Elect_CHP_scrap = $(\text{Heat_CHP}/\text{HtP}) - (\text{Elect_CHP})$</p>
<p>If $(\text{HtP} * \text{Elect_CHP}) > (\text{Heat_CHP})$</p> <p>Heat_CHP_scrap = $(\text{HtP} * \text{Elect_CHP}) - (\text{Heat_CHP})$</p>

Table 28 Energy scrap produced by the CHP

❖ Source proportion per energy type (calculated per year)

Name of the variable at the code	Nomenclature at the paper	Units	Description
prop_Elect_CHP	$E_{\text{cons}}^{\text{CHP}}$	-	Portion of Electricity consumed coming from the CHP
prop_Elect_Grid	$E_{\text{cons}}^{\text{Grid}}$	-	Portion of Electricity consumed coming from the Grid
prop_Heat_CHP	$H_{\text{cons}}^{\text{CHP}}$	-	Portion of Heat consumed coming from the CHP
prop_Heat_Boiler	$H_{\text{cons}}^{\text{Boiler}}$	-	Portion of Heat consumed coming from the Boiler
prop_Cool_Absorption	C^{Absorp}	-	Portion of Cooling produced with Absorption chiller
prop_Cool_Electric	-	-	Portion of Cooling produced with Electric chiller

Table 29 Source proportion per type of energy

$$\text{prop_Elect_CHP} = \text{Elect_CHP} / [\text{Elect_CHP} + \text{Elect_Grid}]$$

$$\text{prop_Elect_Grid} = 1 - \text{prop_Elect_CHP}$$

$$\text{prop_Heat_CHP} = \text{Heat_CHP} / [\text{Heat_CHP} + \text{Heat_Boiler}]$$

$$\text{prop_Heat_Boiler} = 1 - \text{prop_Heat_CHP}$$

$$\text{prop_Cool_Absorption} = \text{Cool_Absorption} / [\text{Cool_Absorption} + \text{Cool_Electric}]$$

$$\text{prop_Cool_Electric} = 1 - \text{prop_Cool_Absorption}$$

❖ Proportion of energy source for the system (for all the year)

Name of the variable at the code	Nomenclature at the paper	Units	Description
prop_Elec_Grid_Sys	E_{GRID}	-	Portion of total energy at the system coming from Electricity of the Grid
prop_Elec_CHP_used_Sys	E_{CHPused}	-	Portion of total energy at the system coming from Electricity produced by the CHP that is being used
prop_Elect_CHP_scrap_Sys	E_{CHPscrap}	-	Portion of total energy at the system coming from Electricity produced by the CHP that is being scrapped
prop_Heat_Boiler_Sys	H_{BOILER}	-	Portion of total energy at the system coming from Heat produced by Boiler
prop_Heat_CHP_used_Sys	H_{CHPused}	-	Portion of total energy at the system coming from Heat produced by the CHP that is being used
prop_Heat_CHP_scrap_Sys	H_{CHPscrap}	-	Portion of total energy at the system coming from Heat produced by the CHP that is being scrapped

Table 30 Source proportion for the whole system

$$\text{prop_Elec_Grid_Sys} = \text{Elect_Grid} / [\text{Elect_Grid} + \text{Elect_CHP_Used} + \text{Elect_CHP_scrap} + \text{Heat_Boiler} + \text{Heat_CHP_Used} + \text{Heat_CHP_scrap}]$$

where, Elect_Grid , Elect_CHP_scrap , Heat_Boiler and Heat_CHP_scrap are given in Table 25 and Table 27. And, the following equalities are established,

$$\text{Elect_CHP_Used} = \text{Elect_CHP}$$

$$\text{Heat_CHP_Used} = \text{Heat_CHP}$$

$$\text{prop_Elec_CHP_used_Sys} = \text{Elect_CHP_Used} / [\text{Elect_Grid} + \text{Elect_CHP_Used} + \text{Elect_CHP_scrap} + \text{Heat_Boiler} + \text{Heat_CHP_Used} + \text{Heat_CHP_scrap}]$$

$$\text{prop_Elect_CHP_scrap_Sys} = \text{Elect_CHP_scrap} / [\text{Elect_Grid} + \text{Elect_CHP_Used} + \text{Elect_CHP_scrap} + \text{Heat_Boiler} + \text{Heat_CHP_Used} + \text{Heat_CHP_scrap}]$$

$$\text{prop_Heat_Boiler_Sys} = \text{Heat_Boiler} / [\text{Elect_Grid} + \text{Elect_CHP_Used} + \text{Elect_CHP_scrap} + \text{Heat_Boiler} + \text{Heat_CHP_Used} + \text{Heat_CHP_scrap}]$$

$$\text{prop_Heat_CHP_used_Sys} = \text{Heat_CHP_Used} / [\text{Elect_Grid} + \text{Elect_CHP_Used} + \text{Elect_CHP_scrap} + \text{Heat_Boiler} + \text{Heat_CHP_Used} + \text{Heat_CHP_scrap}]$$

$$\text{prop_Heat_CHP_scrap_Sys} = \text{Heat_CHP_scrap} / [\text{Elect_Grid} + \text{Elect_CHP_Used} + \text{Elect_CHP_scrap} + \text{Heat_Boiler} + \text{Heat_CHP_Used} + \text{Heat_CHP_scrap}]$$

❖ Flow shares at the CCHP-Thermal Storage system (for all the year)

Name of the variable at the code	Nomenclature at the paper	Units	Description
prop_Elect4Elect	E4E	-	Proportion of Electricity produced by CHP and used to supply Electric Demand compared with the total energy produced by the CHP
prop_Elect4Cool	E4C	-	Proportion of Electricity produced by CHP and used to supply Cooling Demand compared with the total energy produced by the CHP
prop_Elect4CoolStg	E4CS	-	Proportion of Electricity produced by CHP and used for Cooling Storage compared with the total energy produced by the CHP
prop_Heat4Heat	H4H	-	Proportion of Heat produced by CHP and used to supply Heat Demand compared with the total energy produced by the CHP
prop_Heat4Cool	H4C	-	Proportion of Heat produced by CHP and used to supply Cooling Demand compared with the total energy produced by the CHP
prop_Heat4CoolStg	H4CS	-	Proportion of Heat produced by CHP and used for Cooling Storage compared with the total energy produced by the CHP

Table 31 Source proportion for the whole system

$$\text{prop_Elect4Elect} = \text{Elect4Elect} / [\text{Elect4Elect} + \text{Elect4Cool} + \text{Elect4CoolStg} + \text{Heat4Heat} + \text{Heat4Cool} + \text{Heat4CoolStg}]$$

where,

$$\text{Heat4Heat} = \text{Heat_Load} * \text{prop_Heat_CHP}$$

$$\text{Heat4Cool} = \{ [\text{Cool_Load} - \text{Cool_Storage_Out}] * \text{COP_Elect} \} / \{ _ _ \text{COP_Abs_} * _ \text{prop_Cool_Absorption_} * _ \text{prop_Heat_CHP_} \}$$

$$\text{Heat4CoolStg} = [\text{Cool_Storage_In} * \text{COP_Elect}] / [_ _ \text{COP_Abs_} * _ \text{prop_Cool_Absorption_} * _ \text{prop_Heat_CHP_}]$$

The reason for the formulas of Heat4Cool and Heat4CoolStg are described in the following diagram:

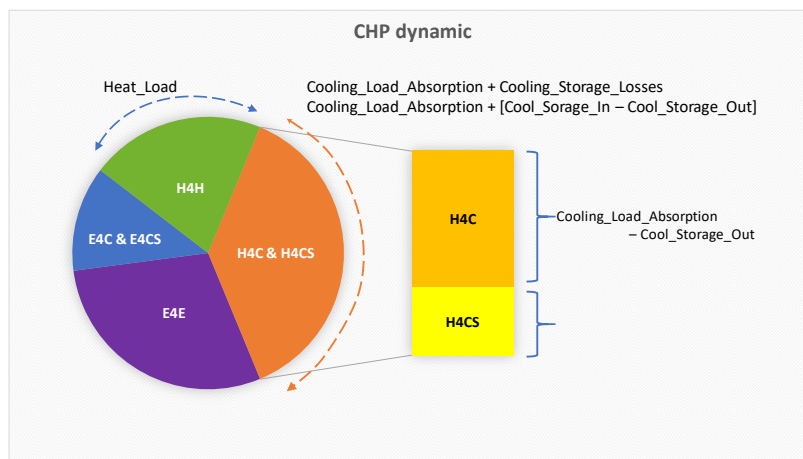


Figure 59 Graphical explanation of Heat for Cooling (H4C) and Heat for Cooling Storage (H4CS)

similarly,

$$\text{Elect4Elect} = \text{Elect_Load} * \text{prop_Elect_CHP}$$

$$\text{Elect4Cool} = \{ [\text{Cool_Load} - \text{Cool_Storage_Out}] * \text{COP_Elect} \} / \{ _ _ \text{COP_Elect_} * _ \text{prop_Cool_Electric_} * _ \text{prop_Elect_CHP_} \}$$

$$\text{Elect4CoolStg} = [\text{Cool_Storage_In} * \text{COP_Elect}] / [_ _ \text{COP_Elect_} * _ \text{prop_Cool_Electric_} * _ \text{prop_Elect_CHP_}]$$

$$\text{prop_Elect4Cool} = \text{Elect4Cool} / [\text{Elect4Elect} + \text{Elect4Cool} + \text{Elect4CoolStg} + \text{Heat4Heat} + \text{Heat4Cool} + \text{Heat4CoolStg}]$$

$$\text{prop_Elect4CoolStg} = \text{Elect4CoolStg} / [\text{Elect4Elect} + \text{Elect4Cool} + \text{Elect4CoolStg} + \text{Heat4Heat} + \text{Heat4Cool} + \text{Heat4CoolStg}]$$

$$\text{prop_Heat4Heat} = \text{Heat4Heat} / [\text{Elect4Elect} + \text{Elect4Cool} + \text{Elect4CoolStg} + \text{Heat4Heat} + \text{Heat4Cool} + \text{Heat4CoolStg}]$$

$$\text{prop_Heat4Cool} = \text{Heat4Cool} / [\text{Elect4Elect} + \text{Elect4Cool} + \text{Elect4CoolStg} + \text{Heat4Heat} + \text{Heat4Cool} + \text{Heat4CoolStg}]$$

$$\text{prop_Heat4CoolStg} = \text{Heat4CoolStg} / [\text{Elect4Elect} + \text{Elect4Cool} + \text{Elect4CoolStg} + \text{Heat4Heat} + \text{Heat4Cool} + \text{Heat4CoolStg}]$$

❖ Demand and consumption rates

Name of the variable at the code	Nomenclature at the paper	Units	Description
Elect2Heat_Consumed	E(consumption)/C(consumption)	-	Rate of total electricity to heat consumption
Elect2Cool_Load	E(load) / C(load)	-	Rate of total electricity to cooling load
propFuelBoiler2CHP		-	Rate of Boiler to CHP natural gas consumption

Table 32 Source proportion for the whole system

$$\text{Elect2Heat_Consumed} = \text{ElectConsumed} / \text{HeatConsumed}$$

where,

$$\text{ElectConsumed} = \text{Elect_CHP} + \text{Elect_Grid}$$

$$\text{propElectConsumedCoveredCHP} = \text{Elect_CHP} / \text{ElectConsumed} = \text{prop_Elect_CHP}$$

$$\text{HeatConsumed} = \text{Heat_CHP} + \text{Heat_Boiler}$$

$$\text{propHeatConsumedCoveredCHP} = \text{Heat_CHP} / \text{HeatConsumed} = \text{prop_Heat_CHP}$$

$$\text{Elect2Cool_Load} = \text{Elect_Load} / \text{Cool_Load}$$

$$\text{propFuelBoiler2CHP} = \text{Fuel_Consump_Boiler} / \text{Fuel_Consump_CHP}$$

_ _

Relations that were already verified:

$$\mathbf{ElectConsumed} = \text{Elect_CHP} + \text{Elect_Grid}$$

$$\mathbf{HeatConsumed} = \text{Heat_CHP} + \text{Heat_Boiler}$$

$$\text{Cool_Absorption} + \text{Cool_Electric} = \text{Cool_Load}$$

The assumption made:

$$\text{Elect_CHP} + \text{Elect_Grid} - \text{Elect_Load} = \mathbf{Elect_Cool}$$

$$\text{Heat_CHP} + \text{Heat_Boiler} - \text{Heat_Load} = \mathbf{Heat_Cool}$$

ANNEX III. Multi-criteria Decision Making ELECTRE 1S

This annex presents the theoretical background of the Multi-criteria Decision Making ELECTRE 1S, that is used to determine the k number of clusters within the methodology k -Means. This reference is used in subsection 3.2.3.3 and section 4.3.

Multicriterial Decision Making (MCDM) [174] is a modern decisional and mathematical tool from operational research that treats complex problems with conflicting targets. It allows the comparison between different a alternatives based on f “conflicting” decision criteria, in order to lead to the more judicious choice [173], [179].

Total aggregations such as summatory or arithmetic mean are widely diffused tools despite their significant drawbacks such as the fact that a single common scale is evaluating all the criteria or that there are losses of information due to the synthesis and compensations. The outranking approach is relevant to avoid these limitations, since its aggregation process allows different evaluation scales while compensation is eluded thanks to thresholds.

ELECTRE 1S is an outranking approach of MCDM, used to state the relation between two alternatives. It is a binary relation meaning *Alternative A is at least as good as alternative B*. The relation is verified [180], if:

1. the concordance condition is verified, following the majority principle according to which a sufficient level of criteria is concordant with the outranking hypothesis,
2. The non-veto condition is verified: none criterion in the set of criteria that are discordant with the outranking hypothesis is in a veto situation.

To provide a clearer explanation, consider a set of alternatives $A = \{a_1, \dots, a_i, \dots, a_k\}$ and a family of r criteria $G = \{g_1 \dots g_j \dots g_r\}$. Each criterion g_j has a corresponding weight to define priorities $w_j \in [0,1]$. The values of a_i and a_k

on criterion g_j are $g_j(a_i)$ and $g_j(a_k)$ respectively. And $\Omega_j(a_k, a_i)$ defines the advantage of a_k over a_i for criterion g_j in Eq. 45 [174].

$$\Omega_j(a_k, a_i) = \begin{cases} g_j(a_k) - g_j(a_i) & \text{if } g_j \text{ has to be maximized} \\ g_j(a_i) - g_j(a_k) & \text{if } g_j \text{ has to be minimized} \end{cases} \quad \text{Eq. 45}$$

For each criterion, there are thresholds of indifference q_j and strict preference p_j , which allow drawing preferences between alternatives for driving decision. When $\Omega_j(a_k, a_i)$ is lower than q_j or larger than p_j , this leads to a situation of indifference or strict preference of one of the alternative over another, from criterion g_j point of view [181]. Then the partial concordance index for the criterion g_j (Eq. 46) quantifies the preference relation between the alternatives and the level of agreement of the criterion with the outranking relation (Figure 60).

$$c_j(a_i, a_k) = \begin{cases} 0 & \text{if } \Omega_j(a_k, a_i) \geq p_j \text{ (} a_k \text{ strictly preferred to } a_i \text{)} \\ \frac{p_j - \Omega_j(a_k, a_i)}{p_j - q_j} & \text{if } p_j > \Omega_j(a_k, a_i) > q_j \text{ (} a_k \text{ weakly preferred to } a_i \text{)} \\ 1 & \text{if } \Omega_j(a_k, a_i) \leq q_j \text{ (} a_i \text{ at least as good as } a_k \text{)} \end{cases} \quad \text{Eq. 46}$$

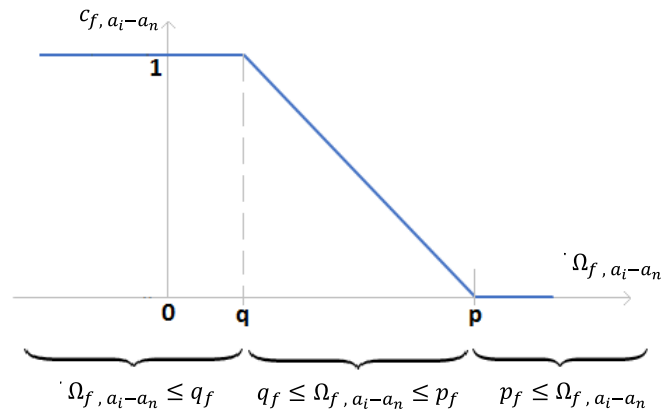


Figure 60 Behavior of partial concordance Index $[c_j(a_i, a_k)]$, depending on the value of q_i , p_i and Ω_i .

We deduce then $c(a_k, a_i)$ the global concordance index calculated per pair of alternatives in Eq. 47:

$$c(a_k, a_i) = \sum_{j=1}^r w_j c_j(a_k, a_i) \quad \text{Eq. 47}$$

where,

$$\sum_{j=1}^r w_j = 1 \quad \text{Eq. 48}$$

Then $c(a_k, a_i)$ is compared to a level of majority $s \in [0.5; 1 - \min(w_j)]$ to verify the concordance condition in Eq. 49:

$$c(a_k, a_i) \geq s \quad \text{Eq. 49}$$

The reader should recall that the relation *Alternative A is at least as good as alternative B* is verified if the concordance and non-veto conditions are fulfilled for each pair of alternatives.

The first, the concordance condition, requires building the concordance matrix by applying Eq. 49 to each pair of alternatives. The concordance condition expresses that the coalition of criteria supporting that one alternative outranks the other, surpasses a minimum level of agreement, which is called the majority principle.

The second, the non-veto condition, requires building the discordance matrix by applying Eq. 50 to each pair of alternatives.

$$\Omega_j(a_k, a_i) \geq v_j \quad \text{Eq. 50}$$

The non-veto condition for each criterion (Eq. 50), is a maximum limit on the predilection of an alternative: if alternative B is better than A for a given criterion and surpasses its veto condition, B will be better than A no matter the value of the other criteria. In other words, if an alternative is extremely worse in a specific criterion, it does not matter how good it is in the others, it will be discarded. The veto threshold is established by the analyst. Therefore, $\Omega_j(a_k, a_i)$ must be on the interval $[p_j, v_j]$ [182]. The veto effect works on the principle of all or nothing.

ANNEX IV. Adaptation of DER-CAM model into Python

This annex the mathematical model adapted from DER-CAM and coded in the programming language Python. This process is deeply described in subsection 3.3.1.

CONSTANTS

Annual loads and energy prices

E_t	Annual electricity load at time t [kWh _E]
H_t	Annual heating load at time t [kWh _H]
C_t	Annual cooling load at time t [kWh _C]
p_E	Price of electricity from the grid $\left[\frac{\$}{\text{kWh}_E} \right]$
p_{NG}	Price of natural gas $\left[\frac{\$}{\text{kWh}_{NG}} \right]$

Costs per technology

CC_{Fix_u}	Fixed capital cost of CHP type u [\$/CHP unit installed]
CC_{Fix_v}	Fixed capital cost of technology v [\$] $\forall v=\{\text{Boiler, Abs, VCchiller, CStg, HStg}\}$
CC_{Var_u}	Variable capital cost of CHP type u [\$/kW installed]
CC_{Var_v}	Variable capital cost of technology v [\$/kW or kWh installed] $\forall v=\{\text{Boiler: [$/kW}_H\text{], Abs: [$/kW}_E\text{], VCchiller: [$/kW}_E\text{], CStg: [$/kWh}_E\text{], HStg: [$/kWh}_H\text{]}\}$
OM_{Fix_u}	Fix O&M cost of CHP type u [\$/kW installed]
OM_{Fix_v}	Fix O&M cost of technology v [\$/kW or kWh installed] $\forall v=\{\text{Boiler: [$/kW}_H\text{], Abs: [$/kW}_E\text{], VCchiller: [$/kW}_E\text{], CStg: [$/kWh}_E\text{], HStg: [$/kWh}_H\text{]}\}$
OM_{Var_u}	Variable O&M cost of CHP type u [\$/kWh _E produced]

OMVar _v	Variable O&M cost of technology v [\$ / kWh produced] $\forall v = \{\text{Boiler: } [\$ / \text{kWh}_H], \text{ Abs: } [\$ / \text{kWh}_E], \text{ VCchiller: } [\$ / \text{kWh}_E], \text{ CStg: } [\$ / \text{kWh}_E], \text{ HStg: } [\$ / \text{kWh}_H]\}$
Lifetime _v	Lifetime of technology u or v [years]
<u><i>Interest rate and factor to annualize capital costs</i></u>	
IR	Discount rate [-]
	$B = \frac{IR}{(1 - (1 + IR)^{-\text{Lifetime}_s})}$
<u><i>Others</i></u>	
$\varphi_{\text{charge}}^s$	Charge efficiency of the storage unit s [-] $\forall s = \{\text{HStg: Heat Storage, CStg: Cold Storage}\}$
$\varphi_{\text{discharge}}^s$	Discharge efficiency of the storage unit s [-] $\forall s = \{\text{HStg: Heat Storage, CStg: Cold Storage}\}$
φ_{decay}^s	Decay of the storage unit s [-] $\forall s = \{\text{HStg: Heat Storage, CStg: Cold Storage}\}$
η_{Boiler}	Efficiency of the boiler [-]
chpIC _u	Installed capacity of the CHP type u [kW _E]
CHPminLoad _u	Minimum load of the CHP type u [% of the chpIC _u]
COP _{VCchiller}	COP of the vapor compression chiller for space cooling $\left[\frac{\text{kWh}_C}{\text{kWh}_E} \right]$
COP _{Abs}	COP of the absorption chiller for space cooling $\left[\frac{\text{kWh}_C}{\text{kWh}_H} \right]$
HtE _u	Heat to electricity rate of the CHP type u $\left[\frac{\text{kWh}_H}{\text{kWh}_E} \right]$
M = 10000000	Big constant used at the constraints involving binary variables [-]
MinState ^s	Minimum state of charge of the storage unit s [% of the Installed capacity]

	$\forall s=\{\text{HStg: Heat Storage, CStg: Cold Storage}\}$
MaxCharge ^s	Maximum charge rate of the storage unit s [% of the Installed capacity]
	$\forall s=\{\text{HStg: Heat Storage, CStg: Cold Storage}\}$
MaxDischarge ^s	Maximum discharge rate of the storage unit s [% of the Installed capacity]
	$\forall s=\{\text{HStg: Heat Storage, CStg: Cold Storage}\}$
<p><i>*The COP is a unitless measure of performance that expresses the ratio of output and input energy. The list above expresses the units just to specify the kind of output and input energy { E:electricity, H:heating, C:cooling }.</i></p>	

SETS to count iterations

firstHours = [0,24,...,840]	List containing the row of the 1st hour of each characteristic day {Jan-week-Hour0, Jan-weekend-Hour0, ... , Dec-peak-Hour0}
HoursDay = {0,23}	Set to loop the 24 hours of each characteristic day
NchpTech = {0,9}	Set to loop the types of CHP technology available
Ndays _t	List containing the number of characteristic days per month { Jan: week=22days, weekend=8days, peak=1day ; ... ; Dec: week=21days, weekend=9days, peak=1day }
Nhours = {0,863}	Set to loop the characteristic hours of the year { Jan: week (1,24), weekend (1,24), peak (1,24) ; ... ; Dec: week (1,24), weekend (1,24), peak (1,24)}

VARIABLES

Non-negative integer variables

CStgI	Installed capacity of the Cold Storage, expressed as the electricity consumed by the vapor-compression chiller [kWh _E]
HStgIC [kWh _H]	Installed capacity of the Heat Storage
mCHP _{u,t} $\forall u \in N_{chpTech}, t \in N_{Hours}$	Number of active units of CHP type u at time t [no. of units]
nCHP _u $\forall u \in N_{chpTech}$	Number of installed units of CHP type u [no. of units]

Binary variables

w ^v	Binary variable to activate the fixed capital cost of the unit v $\forall v = \{\text{Boiler, Abs, VCchiller, CStg, HStg}\}$
y ^s	Binary variable making input and output mutually exclusive in the storage $\forall s = \{\text{HStg: Heat Storage, CStg: Cold Storage}\}$

NON-NEGATIVE REAL VARIABLES

Grid

eGrid_t $\forall t \in N_{Hours}$ Electricity imported from the grid at time t [kWh_e]

CHP units

eCHP_{u,t} $\forall u \in N_{chpTech}, t \in N_{Hours}$ Electricity produced by the CHP type u at time t [kWh_E]

$H_{CHP_{u,t}} \forall u \in N_{chpTech}, t \in N_{Hours}$	Heat produced by the CHP type u at time t [kWh _H]
$H_{scrapCHP_{u,t}} \forall u \in N_{chpTech}, t \in N_{Hours}$	Heat scrap from the production of the CHP type u at time t [kWh _H]
 <i><u>Boiler</u></i>	
BoilerIC	Installed capacity of boiler [kW _H]
$H_{boiler_t} \forall t \in N_{Hours}$	Heat produced by the boiler at time t [kWh _H]
 <i><u>Absorption chiller</u></i>	
AbsIC	Installed capacity of absorption chiller, expressed as the electricity consumed by the vapor-compression chiller [kW _E]
$H_{abs_t} \forall t \in N_{Hours}$	Heat consumed by the absorption chiller at time t [kWh _H]
 <i><u>Vapor-compression chiller</u></i>	
VCchillerIC	Installed capacity of vapor-compression chiller, expressed as the electricity consumed by the vapor-compression chiller [kW _E]
$e_{VCchiller_t} \forall t \in N_{Hours}$	Electricity consumed by the vapor-compression chiller at time t [kWh _E]
 <i><u>Cold Storage</u></i>	
$e_{CStgState_t} \forall t \in N_{Hours}$	Charging state of the Cold Storage at time t , expressed as the electricity

	consumed by the vapor-compression chiller [kWh _E]
$eCStgIn_t \quad \forall t \in NHours$	Input to the Cold Storage at time t, expressed as the electricity consumed by the vapor-compression chiller [kWh _E]
$eCStgOut_t \quad \forall t \in NHours$	Output to the Cold Storage at time t, expressed as the electricity consumed
by the	vapor-compression chiller [kWh _E]
<u>Heat Storage</u>	
$HStgState_t \quad \forall t \in NHours$	Charging state of the Heat Storage at time t [kWh _H]
$hHStgIn_{u,t} \quad \forall t \in NHours$	Input to the Heat Storage at time t [kWh _H]
$hHStgOut_t \quad \forall t \in NHours$ [kWh _H]	Output to the Heat Storage at time t

OBJECTIVE FUNCTION: MINIMIZING TOTAL ANNUAL COST

$$\text{MIN Cost} \quad \text{Eq. 51}$$

$$= \text{Grid}(\text{Cost}) + \text{CHP}(\text{Cost}) + \text{Boiler}(\text{Cost}) + \text{Abs}(\text{Cost}) \\ + \text{VCchiller}(\text{Cost}) + \text{CStg}(\text{Cost}) + \text{HStg}(\text{Cost})$$

where,

$$\text{Cost related to the grid} \quad \text{Eq. 52}$$

$$\text{Grid}(\text{Cost}) = \sum_{t=0}^{863} Ndays_t \cdot p_E \cdot eGrid_t$$

Cost related to the CHP unit

Eq. 53

$$\text{CHP}(\text{Cost}) = \sum_{u=0}^9 a_{1,u} \cdot n\text{CHP}_u + \sum_{u=0}^9 \sum_{t=0}^{863} \text{Ndays}_t \cdot a_{2,u} \cdot e\text{CHP}_{u,t}$$

with,

$$a_{1,u} = B[\text{CCFix}_u + (\text{chpIC}_u)\text{CCVar}_u] + (\text{chpIC}_u)\text{OMFix}_u$$

$$a_{2,u} = \text{OMVar}_u + \frac{\text{PNG}}{\eta_{\text{Boiler}}}$$

Cost related to the boiler

Eq. 54

$$\text{Boiler}(\text{Cost}) = b_0 \cdot w^{\text{Boiler}} + b_1 \cdot \text{BoilerIC} + \sum_{t=0}^{863} \text{Ndays}_t \cdot b_2 \cdot \text{Hboiler}_t$$

with,

$$b_0 = B \cdot \text{CCFix}_{\text{Boiler}}$$

$$b_1 = B \cdot \text{CCVar}_{\text{Boiler}} + \text{OMFix}_{\text{Boiler}}$$

$$b_2 = \text{OMVar}_{\text{Boiler}} + \frac{\text{PNG}}{\eta_{\text{Boiler}}}$$

Cost related to the absorption chiller

Eq. 55

$$\text{Abs}(\text{Cost}) = c_0 \cdot w^{\text{Abs}} + c_1 \cdot \text{AbsIC} + \sum_{t=0}^{863} \text{Ndays}_t \cdot c_2 \cdot \text{Habs}_t \cdot c_3$$

with,

$$c_0 = B \cdot \text{CCFix}_{\text{Abs}}$$

$$c_1 = B \cdot \text{CCVar}_{\text{Abs}} + \text{OMFix}_{\text{Abs}}$$

$$c_2 = \text{OMVar}_{\text{Abs}}$$

$$c_3 = \frac{\text{COP}_{\text{Abs}}}{\text{COP}_{\text{VCchiller}}}$$

Cost related to the vapor-compression chiller

Eq. 56

VCchiller(Cost)

$$= d_0 \cdot w^{VCchiller} + d_1 \cdot VCchillerIC + \sum_{t=0}^{863} Ndays_t \cdot d_2 \cdot eVCchiller_t \cdot d_3$$

with,

$$d_0 = B \cdot CCFix_{VCchiller}$$

$$d_1 = B \cdot CCVar_{VCchiller} + OMFix_{VCchiller}$$

$$d_2 = OMVar_{VCchiller}$$

$$d_3 = 1$$

Cost related to the Cold Storage

Eq. 57

$$CStg(Cost) = e_0 \cdot w^{CStg} + e_1 \cdot CStgIC + \sum_{t=0}^{863} Ndays_t \cdot e_2 \cdot eCStgState_t$$

with,

$$e_0 = B \cdot CCFix_{CStg}$$

$$e_1 = B \cdot CCVar_{CStg} + OMFix_{CStg}$$

$$e_2 = OMVar_{CStg}$$

Cost related to the Heat Storage

Eq. 58

$$HStg(Cost) = f_0 \cdot w^{HStg} + f_1 \cdot HStgIC + \sum_{t=0}^{863} Ndays_t \cdot f_2 \cdot eHStgState_t$$

with,

$$f_0 = B \cdot CCFix_{HStg}$$

$$f_1 = B \cdot CCVar_{HStg} + OMFix_{HStg}$$

$$f_2 = OMVar_{HStg}$$

CONSTRAINTS RELATED TO ENERGY BALANCES

Covering Electric demand (1 restriction/h) Eq. 59

$$eGrid_t + \sum_u eCHP_{u,t} - eVCchiller_t = E_t$$

Covering Heat demand (1 restriction/h) Eq. 60

$$Hboiler_t + \sum_u HCHP_{u,t} - Habs_t - hHStgIn_t + \left(\varphi_{discharge}^{HStg} \right) hHStgOut_t = H_t$$

Covering Cooling demand (1 restriction/h) Eq. 61

$$\left(\frac{COP_{Abs}}{COP_{VCchiller}} \right) Habs_t + eVCchiller_t - eCStgIn_t + \left(\varphi_{discharge}^{CStg} \right) eCStgOut_t = \frac{C_t}{COP_{VCchiller}}$$

CONSTRAINT RELATED TO CHP UNITS

Electricity production of CHP does not exceed the installed capacity of the CHP units (10 restrictions/h, one per each CHP type) Eq. 62

$$chpIC_u \cdot mCHP_{u,t} \geq eCHP_{u,t}$$

Electricity prod of CHP is minimum the MinLoad
(10 restrictions/h, one per each CHP type) Eq. 63

$$\text{CHPminLoad}_u \cdot \text{chpIC}_u \cdot \text{mCHP}_{u,t} \leq \text{eCHP}_{u,t}$$

The amount of active CHP units each hour, does not exceed the CHP
units installed (10 restrictions/h, one per each CHP type) Eq. 64

$$\text{nCHP}_u \geq \text{mCHP}_{u,t}$$

Heat produced and scrap by each CHP units, is tied to its Electricity
production (10 restrictions/h, one per each CHP type) Eq. 65

$$\text{HtE}_u \cdot \text{eCHP}_{u,t} = \text{HCHP}_{u,t} + \text{HscrapCHP}_{u,t}$$

CONSTRAINT RELATED TO BOILER

Installed capacity of boiler is not exceed (1 restriction/h) Eq. 66

$$\text{BoilerIC} \geq \text{Hboiler}_t$$

Binary variable that activates the fixed capital cost of Boiler Eq. 67

The binary variable is zero if the installed capacity is larger than one.
In contrast it is one if the installed capacity is zero.

$$\text{BoilerIC} \geq 0.001 - M(1 - w^{\text{Boiler}})$$

*A strict inequality constraint $\text{BoilerIC} > 0 - M(1 - w^{\text{Boiler}})$ would make the optimization not well-defined. Because it would always be possible to make the objective value better by moving closer and closer to the value of the inequality, without reaching the optimum.

$$\text{BoilerIC} \leq 0 + M \cdot w^{\text{Boiler}}$$

CONSTRAINT RELATED TO VAPOR – COMPRESSION CHILLER

Installed capacity of vapor-compression chiller is not exceed (1 restriction/h) Eq. 68

$$\text{VCchillerIC} \geq e\text{VCchiller}_t$$

Binary variable that activates the fixed capital cost of VCchiller Eq. 69

The binary variable is zero if the installed capacity is larger than one. In contrast it is one if the installed capacity is zero.

$$\text{VCchillerIC} \geq 0.001 - M(1 - w^{\text{VCchiller}})$$

*A strict inequality constraint $\text{VCchillerIC} > 0 - M(1 - w^{\text{VCchiller}})$ would make the optimization not well-defined. Because it would always be possible to make the objective value better by moving closer and closer to the value of the inequality, without reaching the optimum.

$$\text{VCchillerIC} \leq 0 + M \cdot w^{\text{VCchiller}}$$

CONSTRAINT RELATED TO ABSORPTION CHILLER

Installed capacity of absorption chiller is not exceed (1 restriction/h) Eq. 70

$$\text{AbsIC} \geq \left(\frac{\text{COP}_{\text{Abs}}}{\text{COP}_{\text{VCchiller}}} \right) \text{Habs}_t$$

Binary variable that activates the fixed capital cost of Abs Eq. 71

The binary variable is zero if the installed capacity is larger than one.
In contrast it is one if the installed capacity is zero.

$$\text{AbsIC} \geq 0.001 - M(1 - w^{\text{Abs}})$$

*A strict inequality constraint $\text{AbsIC} > 0 - M(1 - w^{\text{Abs}})$ would make the optimization not well-defined. Because it would always be possible to make the objective value better by moving closer and closer to the value of the inequality, without reaching the optimum.

$$\text{AbsIC} \leq 0 + M \cdot w^{\text{Abs}}$$

CONSTRAINTS RELATED TO COLD STORAGE

Charging state of the Cold storage (1 restriction/h) Eq. 72

$$e\text{CStgState}_t = \begin{cases} \left(\varphi_{\text{charge}}^{\text{CStg}} \right) e\text{CStgIn}_t - e\text{CStgOut}_t, & \text{if } t \in \text{firstHours} \\ \left(1 - \varphi_{\text{decay}}^{\text{CStg}} \right) e\text{CStgState}_{t-1} + \left(\varphi_{\text{charge}}^{\text{CStg}} \right) e\text{CStgIn}_t - e\text{CStgOut}_t, & \text{otherwise} \end{cases}$$

Cold Storage level ends the day as it started (1 restriction/day = 36) Eq. 73

$$e\text{CStgState}_t = \begin{cases} e\text{CStgState}_{t+(24-1)}, & \text{if } t \in \text{firstHours} \\ \text{none}, & \text{otherwise} \end{cases}$$

Min state of charge of the Cold Storage (1 restriction/h) Eq. 74

$$eCStgState_t \geq MinState^{CStg} \cdot CStgIC$$

Max state of charge of the Cold Storage (1 restriction/h) Eq. 75

$$eCStgState_t \leq CStgIC$$

Max charge rate of the Cold Storage (1 restriction/h) Eq. 76

$$\left(\varphi_{charge}^{CStg} \right) eCStgIn_t \leq MaxCharge^{CStg} \cdot CStgIC$$

Max discharge rate of the Cold Storage (1 restriction/h) Eq. 77

$$eCStgOut_t \leq MaxDischarge^{CStg} \cdot CStgIC$$

$eCStgIn_t$ and $eCStgOut_t$ are mutually exclusive Eq. 78

The two following constraints express that the Cold storage input and output are mutually exclusive. A binary value of 0, enables output from the Cold storage. When it is 1, input is active.

$$\left(\varphi_{charge}^{CStg} \right) eCStgIn_t \leq M \cdot y^{CStg}$$

$$eCStgOut_t \leq M(1 - y^{CStg})$$

Binary variable that activates the fixed capital cost of Cold Storage. Eq. 79

These constraints use a binary variable to activates the fixed capital cost of Cold Storage. It values one if the installed capacity of the Cold storage is larger than zero. In contrast it is zero if the installed capacity is 0.

$$CStgIC \geq 0.001 - M(1 - w^{CStg})$$

*Note that a strict inequality constraint $CStgIC > 0 - M(1 - w^{CStg})$ would make the optimization not well-defined. Because it would always be possible to make the objective value better by moving closer and closer to the value of the inequality, without reaching the optimum.

$$CStgIC \leq 0 + M \cdot w^{CStg}$$

CONSTRAINTS RELATED TO HEAT STORAGE

Charging state of the Heat storage (1 restriction/h) Eq. 80

$$HStgState_t = \begin{cases} (\varphi_{charge}^{HStg}) hHStgIn_t - hHStgOut_t, & \text{if } t \in \text{firstHours} \\ (1 - \varphi_{decay}^{HStg}) HStgState_{t-1} + (\varphi_{charge}^{HStg}) hHStgIn_t - hHStgOut_t, & \text{otherwise} \end{cases}$$

Heat Storage level ends the day as it started (1 restriction/day = 36) Eq. 81

$$HStgState_t = \begin{cases} HStgState_{t+(24-1)}, & \text{if } t \in \text{firstHours} \\ \text{none}, & \text{otherwise} \end{cases}$$

Min state of charge of the Heat Storage (1 restriction/h) Eq. 82

$$HStgState_t \geq \text{MinState}^{HStg} \cdot HStgIC$$

Max state of charge of the Heat Storage (1 restriction/h) Eq. 83

$$\text{HStgState}_t \leq \text{HStgIC}$$

Max charge rate of the Heat Storage (1 restriction/h) Eq. 84

$$\left(\varphi_{\text{charge}}^{\text{HStg}}\right) \text{hHCStgIn}_t \leq \text{MaxCharge}^{\text{HStg}} \cdot \text{HStgIC}$$

Max discharge rate of the Heat Storage (1 restriction/h) Eq. 85

$$\text{hHStgOut}_t \leq \text{MaxDischarge}^{\text{HStg}} \cdot \text{HStgIC}$$

hHStgIn_t and hHStgOut_t are mutually exclusive Eq. 86

The two following constraints express that the Heat storage input and output are mutually exclusive. A binary value of 0, enables output from the Heat storage. When it is 1, input is active.

$$\left(\varphi_{\text{charge}}^{\text{HStg}}\right) \text{hHStgIn}_t \leq M \cdot y^{\text{HStg}}$$

$$\text{hHStgOut}_t \leq M(1 - y^{\text{HStg}})$$

Binary variable that activates the fixed capital cost of Heat Storage Eq. 87

These constraints use a binary variable to activates the fixed capital cost of Heat Storage. It values one if the installed capacity of the

Heat storage is larger than zero. In contrast it is zero if the installed capacity is 0.

$$\text{HStgIC} \geq 0.001 - M(1 - w^{\text{HStg}})$$

*Note that a strict inequality constraint $\text{HStgIC} > 0 - M(1 - w^{\text{HStg}})$ would make the optimization not well-defined. Because it would always be possible to make the objective value better by moving closer and closer to the value of the inequality, without reaching the optimum.

$$\text{HStgIC} \leq 0 + M \cdot w^{\text{HStg}}$$

Titre : Méthodologie pour identifier les variables clés conduisant à la faisabilité technico-économique de la trigénération - systèmes de stockage thermique

Mots clés : Systèmes de trigénération couplés à du stockage thermique, faisabilité technico-économique, demandes en énergies, prix de l'énergie, analyse de sensibilité .

Résumé : Les systèmes de trigénération couplés à du stockage thermique (CCHP-TS) contribuent à la production distribuée d'énergie et à la réduction des émissions de gaz à effet de serre. Néanmoins, il est important d'évaluer leur faisabilité technico-économique pour assurer une mise en œuvre à long terme. Par ailleurs, la détermination et la caractérisation des variables influentes sont essentielles pour identifier les domaines d'application les plus viables. Potentiellement, cela peut stimuler l'intérêt des chefs de projet, des investisseurs et des décideurs politiques, encourageant ainsi l'adoption de cette technologie.

Plusieurs auteurs suggèrent que les prix et les demandes en énergies (électricité, chaleur et froid) sont des variables importantes de la faisabilité technico-économique des systèmes CCHP-TS. Ils ont notamment utilisé le ratio Spark Spread (SS) qui est le rapport entre le coût de l'électricité du réseau et le combustible de cogénération. Cependant, seules quelques études évaluent l'influence combinée des prix et de la demande en énergies, avec certaines limites dans leur modèle, la technologie analysée ou même la résolution temporelle de la demande.

Comme la littérature révèle que les prix de l'énergie et les niveaux de demandes sont des variables importantes, cette étude propose et analyse deux hypothèses : 1) Il existe un couplage entre les prix de l'énergie et la variabilité des demandes en énergies qui influence techniquement et économiquement sur la faisabilité des systèmes CCHP-TS; 2) Les prix de l'énergie (électricité et gaz naturel) doivent être considérés séparément plutôt que d'utiliser le ratio Spark Spread.

Le travail est divisé en deux phases. La première est une analyse exploratoire visant à démontrer que le modèle utilisé de CCHP-TS est pertinent et sensible aux variables d'analyse (prix et demandes énergétiques). La seconde est une analyse de sensibilité rigoureuse qui permet de plus une comparaison de trois «approches»: Morris, Sobol et VARS.

Les résultats indiquent que les prix de l'énergie et l'importance de la demande électrique sont les variables les plus importantes pour garantir la faisabilité d'un système CCHP-TS. L'ordre d'importance entre les prix de l'énergie diffère selon que l'indicateur de performance économique utilisé soit absolu (montant d'économies réalisées [\$]) ou relatif (pourcentage d'économies réalisées [%]). Dans les deux cas, le prix du carburant est la variable ayant un effet d'interaction avec les autres variables les plus importants.

La méthodologie de la première phase intègre des outils tels que le plan d'expériences factoriel complet, l'outil de simulation et d'optimisation DER-CAM et une nouvelle combinaison de la méthode de clustering k-Means et d'une méthode d'aide à la décision multicritère (MCDM). Pour la deuxième phase, il s'agit principalement de l'utilisation des méthodes globales d'analyse de sensibilité et de l'adaptation d'un modèle CCHP-TS programmée en langage Python qui utilise la bibliothèque d'optimisation PYOMO et le solveur CPLEX. Dans cette deuxième phase, la mise en œuvre des trois méthodes d'analyse de sensibilité a permis une identification des avantages et limites de chacune. L'analyse de la faisabilité techno-économique s'en trouve renforcée en utilisant leurs complémentarités.

Title : Methodology to identify the key variables driving the techno-economic feasibility of Trigereneration – Thermal Storage systems

Keywords : Trigereneration systems with thermal storage, techno-economic feasibility, energy loads, energy prices, sensitivity analysis.

Abstract : Trigereneration systems with thermal storage (CCHP-TS) contribute to the distributed generation of energy and the reduction of greenhouse gas emissions. Nevertheless, it is important to assess their techno-economic feasibility to ensure long-term implementation. Moreover, determining and characterizing the influential variables is essential to identify the most viable application fields. Potentially, this could foster the interest of project managers, investors, and policymakers, therefore encouraging the adoption of this technology.

Several authors suggest that energy prices and loads are important variables for the techno-economic feasibility of CCHP-TS systems. Particularly they have explored the Spark Spread rate, a ratio between the cost of electricity from the grid and the CHP fuel. However, just a few studies are assessing the prices and loads together, with some limitations in their model, the technology analyzed, or even the resolution of the loads.

As the literature reveals that energy prices and loads size are important variables, this study aims to analyze two hypotheses proposed: 1) There is a combination of energy prices and the size of the annual energy loads that makes techno-economically feasible a CCHP-TS system; 2) The energy prices (electricity and natural gas) should be considered separately instead of consolidating them into the spark spread rate (SS).

The analysis is divided into two phases. The first one is an exploratory analysis aiming to demonstrate that the model for CCHP-TS is relevant and sensitive to the variables of analysis (energy prices and loads). The second is a rigorous sensitivity analysis and the comparison of three approaches: Morris, Sobol, and VARS.

The results state that energy prices and the annual size of the electric load are the most relevant variables on the feasibility of a CCHP-TS system. The order of relevance between the energy prices relies on the measure used for the economic performance: either absolute (expressed in the amount of savings [\$]) or relative (expressed in the percentage of savings [%]). But in both cases, the price of the fuel is the variable with the largest interaction effects.

The methodology of the first phase incorporates tools such as full factorial design of experiments (DoE), DER-CAM simulation and optimization tool, and a novel combination of k-Means clustering and multicriteria decision making (MCDM). For the second phase, it is mainly the use of global sensitivity analysis methods and the adaptation of a CCHP-TS model into the programming language Python, using the optimization library PYOMO and the solver CPLEX. In this second phase, the implementation of the three sensitivity analysis methods allowed identifying their advantages and limitations. Moreover, this complementarity thereby reinforced the techno-economic feasibility analysis.
